2012

Parasitic nematode ion channels: improving understanding of pharmacology and genetic composition

Samuel Buxton
Iowa State University

Parasitic nematode ion channels: improving understanding of pharmacology and genetic composition

by

Samuel Buxton

A dissertation submitted to the graduate faculty

in partial fulfillment of the requirements for the degree of

DOCTOR OF PHILOSOPHY

Major: Toxicology

Program of Study Committee:
Richard J. Martin, Major Professor
Alan P. Robertson, Major Professor
Anumantha G. Kanthasamy
Heather M. W. Greenlee
Jeffrey K. Beetham
Jacques Cabaret

Iowa State University

Ames, Iowa

2012

TABLE OF CONTENTS

ABSTRACT

Parasitic nematode infections of humans, plants and animals are of major economic impact. These parasites cause losses of billions of dollars per year in crop damage and through livestock infection; the infections to humans are equally debilitating. Anthelmintics are the main chemotherapeutic agents used for treatment and prophylaxis of nematode infections because there is presently no effective vaccine on the market. Most of the anthelmintics presently used in treating nematode infections in humans were first developed for use in animals. In most cases, these anthelmintics have been used in humans without changing the properties of the drugs at all. However, resistance has been reported to the mainstay anthelmintics, namely AChR agonists (levamisole, pyrantel), benzimidazoles (albendazole) and macrocyclic lactones (ivermectin). There is therefore the urgent need to understand the genetics of the receptors targeted by these anthelmintics and the mechanisms of resistance, with the view to improving efficacy of the presently used drugs. In addition, there is the need to find alternative targets for developing new anthelmintics as well as fully studying the mechanism of action of any new anthelmintic.

We have demonstrated the effects of the new novel-acting cyclooctadepsipeptide anthelmintic, emodepside, on the membrane potential and voltage-activated currents in the pig parasite *Ascaris suum*. Emodepside hyperpolarized the membrane in a slow, time-dependent manner without changing the input conductance. We show that the purported emodepside target receptors in *C. elegans*, SLO-1 and LAT-1 are expressed in the muscle flap of *A. suum* (*Asu-slo-1* and *Asu-lat-1*). Emodepside potentiated the voltage-activated Ca^{2+}-dependent K^+ channel currents in a time- and voltage-dependent manner. We have demonstrated that emodepside effect on the K^+ channel currents is inhibited by iberiotoxin, a

selective SLO-1 channel inhibitor. The effects of emodepside on the membrane potential and K^+ channel currents were modulated by NO and protein kinase activators/inhibitors. Last but not least, we demonstrate that diethylcarbamazine (DEC), a filarial anthelmintic, potentiates the effects of emodepside on the membrane potential and SLO-1-like currents. Our results clearly demonstrate effects of emodepside in a parasitic nematode and the modulation of emodepside effects by second messengers like protein kinases. We also show that a formulation of emodepside and DEC could be used for treating filarial parasites, slowing the development of resistance to emodepside.

Finally, we show the cloning of four acetylcholine receptor subunit genes from another pig parasite, *Oesophagostomum dentatum* and the expression and characterization of these receptor subunits in *Xenopus laevis* oocytes. By employing the three ancillary factors of *Haemonchus contortus, Hc-ric-3.1, Hc-unc-50* and *Hc-unc-74,* we have characterized four levamisole receptor subtypes of *O. dentatum* with different pharmacological properties. First, the receptor subtype we have termed Pyr-nAChR, was composed of *Ode-unc-29* and *Ode-unc-63* and responded to pyrantel as the most potent agonist. The second receptor subtype, Pyr/Tbd-nAChR, responded to pyrantel and tribendimidine as the most potent agonists and was composed of *Ode-unc-29, Ode-unc-63* and *Ode-unc-38*. The third receptor subtype, nAChR, responded to ACh as the most potent agonist and was composed of *Ode-unc-29, Ode-unc-63* and *Ode-acr-8*. The last receptor subtype, Lev-nAChR, responded to levamisole as the most potent agonist and was composed of *Ode-unc-29, Ode-unc-63, Ode-acr-8* and *Ode-unc-38*. In the Lev-nAChR, derquantel distinguished receptor subtypes with pA2 values of 6.8 and 8.4 for levamisole and pyrantel, respectively. The calcium permeability (P_{Ca}/P_{Na}) of three receptor subtypes differed. We measured P_{Ca}/P_{Na} of 10.3, 0.38 and 0.38 for the Lev-

nAChR, Pyr/Tbd-nAChR and nAChR subtypes, respectively. Unlike the receptors in *Caenorhabditis elegans* and *Haemonchus contortus*, all three ancillary factors were not absolutely required to reconstitute *O. dentatum* functional levamisole receptors. We reconstituted receptors with robust responses to the agonists when we sequentially removed these ancillary factors. However, removal of all three factors did not reconstitute any receptors, demonstrating the need for at least one of these ancillary factors. Our results demonstrate the plasticity in the levamisole receptors of *O. dentatum* and suggest that the subtypes may have different physiological roles and/or expressed in different tissues of the parasite.

CHAPTER 1 General Introduction

1.1 Introduction

Ion channels in parasitic nematode are important targets for the drugs used in the treatment of these worms. These drugs (anthelmintics) are grouped according to the target sites; the cholinergic agonists (cholinomimetics) and antagonists act on nicotinic acetylcholine receptors (nAChRs) located on the nematode somatic muscle; the macrocyclic lactones (avermectins and milbemycins) act on glutamate-gated chloride channels; the benzimidazoles act on beta-tubulin to inhibit polymerization; and the more recently marketed emodepside, a cyclooctadepsipeptide that reportedly acts on the voltage-activated calcium-dependent potassium channels (SLO-1) and latrophilin-like receptors (LAT) in the free-living nematode *Caenorhabditis elegans*. These anthelmintics, among other effects, interfere with the movement, feeding, egg laying and growth of nematodes. The nematode nicotinic acetylcholine receptors, which are the targets of cholinergic anthelmintics like levamisole, pyrantel, morantel, tribendimidine and derquantel, are different from the vertebrate nicotinic acetylcholine receptors in some respects. The importance of these nicotinic receptors in nematodes and their attractiveness as anthelmintic target site(s) is underscored by the recent introduction of a new class of anthelmintics, the amino-acetonitrile derivatives (AADs, such as monepantel) which act on nAChRs. On the flip side, voltage-activated channels in nematodes are under-utilized as drug target sites. Such a voltage-activated channel, the voltage-activated calcium-dependent potassium channel (SLO-1, or BK channel) has been

hailed as the main or one of the main target sites of the recently introduced emodepside. As with other drugs used to treat parasites, there is a growing problem of anthelmintic resistance to all the major classes of anthelmintics, except emodepside. Therefore these PhD studies were undertaken to address two main concerns. First was to ascertain the mechanism of action of emodepside in the pig parasite *Ascaris suum.* It is important to clearly define the mechanism of emodepsides action in parasitic nematodes so as to curtail any problems of resistance. The second main aim of this PhD studies was to characterize, at the genetic level, the nicotinic acetylcholine receptors of another pig parasite, *Oesophagostomum dentatum* as drug target site(s) and understand some possible mechanisms of anthelmintic resistance.

1.2 Thesis Organization

In this thesis, a general introduction is presented about parasitic nematodes and the ion channels of these nematodes as anthelmintic target sites. A brief emphasis is placed on the cyclooctadepsipeptide emodepside, the calcium-activated potassium channel SLO-1 and the nicotinic acetylcholine receptors. In chapter 2, I have reviewed the literature relating to soil transmitted helminths, the pig parasitic nematodes *Ascaris suum* and *Oesophagostomum dentatum*, the voltage-activated calcium-dependent potassium channels (SLO-1) and nicotinic acetylcholine receptors of parasitic nematodes. In the two subsequent chapters, I present work done by myself and our collaborators that have either been published or submitted for publication. Chapter 3 deals with the "resistance-busting" anthelmintic emodepside and its effect on the voltage-activated currents in *Ascaris suum*. All the work outlined in this paper was done by me, except the *Asu-slo-1* and *Asu-lat-1* clonings which

were done by our collaborators at Institut National de la Recherche Agronomique (INRA-Nouzilly) in France. Chapter 4 describes the cloning of *O. dentatum* levamisole-sensitive acetylcholine receptor subunit genes and their expression in oocytes of the South African frog, *Xenopus laevis*. The gene clonings in this chapter was done by me and our collaborators during my 6-month stay in France (INRA-Nouzilly). All the electrophysiological studies were done by me at ISU. In chapter 5, I give a general discussion and conclusions of this PhD research work and suggestions for future work. Appendix A contains a review paper on emodepside written as a follow-up to our emodepside publication; appendix B is an invited paper on the electrophysiology techniques we use in the laboratory. Last but not least, appendix C contains a review on levamisole as an anthelmintic and the renewed interest in studying the genetics of the levamisole receptor, the nicotinic acetylcholine receptor.

CHAPTER 2 Literature Review

2.1 Soil Transmitted Helminths

Parasites are organisms that live inside or outside another organism mostly of a different species, such that the parasites benefit at the expense of the host (Wall and Shearer, 2001). Some parasites cause the death of their hosts whilst other parasites do not cause death of the hosts but poor growth, weight loss, compromised immune system, anemia and in humans, impaired cognitive skills. Depending on where the parasites reside, they can be classified as ectoparasites or endoparasites. Ectoparasites, such as ticks, live on the host body surface whilst endoparasites, such as parasitic worms, live inside the host. Parasites that feed off another parasite are known as epiparasites (Leake, 2004). Such an epiparasite is a protozoan living in the digestive tract of a dog flea. Unlike free-living organisms, parasites face the problem of living in an environment that actively seeks to destroy or repel them. The hosts of parasites secrete proteins and other factors in an attempt to dislodge these parasites from their habitat. These parasites must therefore evade the host immune system in order to establish a habitat, as well as produce offspring. For zoonotic parasites or parasites with more than one host at different life stages of the parasite, another problem is the ability to live in different hosts or different tissues of a host. Not all parasites are strictly parasitic at all life stages, so the ability to move from a free-living, non-infective stage to a parasitic stage is a specialty of some parasites.

Helminths (Greek: *helmins*) are simply worm-like organisms. Parasitic helminths have been recognized since ancient times with early cures dating as far back as the 16th century (Kliks, 1990). Human helminth infections can be traced as far back as the pre-ice age migration of

Homo sapiens from East Africa to all parts of the world (Cox, 2002). There have been reports of intestinal helminthes in old World human archaeological samples, for example, *Dicrocoelium dentriticum* in 11th century AD England (Pike and Biddle, 1966). Parasite species like *Trichuris trichiuria* and *Enterobius vermicularis* have been described as "heirloom parasites" associated with transberingeal immigrants and their dogs. These endoparasitic helminths ("worms") are divided into two phyla, namely the Platyhelminths (tapeworms and trematodes) and the roundworms or nematodes (Wang *et al*., 2008). Soil-transmitted helminths (STH) are part of the so-called Neglected Tropical Diseases (NTD). The three main STHs that are of worldwide concern are the roundworms (*Ascaris lumbricoides*), the whipworms (*Trichuris trichiura*) and the hookworms (*Necator americanus* or *Ancylostoma duodenale*); the estimated human population affected by these three alone is over 1.5 billion (Bethony *et al*., 2006; Hotez *et al*., 2007; 2008). A large number of these infections occur in children (de Silva *et al*., 2003), especially infections with *Ascaris lumbricoides* and *Trichuris trichiura* which generally reach peak infection intensity in school-aged children. The majority of infections occur in the tropic regions of Africa, Latin America, the Caribbean's, Middle East and Asia where the combination of warm, moist and insanitary conditions creates the right environment for the eggs or larvae of these parasites to thrive. According to Hotez and Kamath (2009) for example, almost half of Sub-Saharan Africa's poorest people have hookworm infections with 40 to 50 million children of school going age and 7 million pregnant women infected by these hookworms. In fact, the burden of NTDs may be underestimated in Sub-Saharan Africa. These STH infections cause stunted growth, cognitive deficits, intellectual and educational retardation, distended abdomen and in severe cases, death. It is estimated that 12000 to 135000 annual deaths result

from these helminth infections (WHO, 2002, 2004). The disease burden attributed to soil-transmitted helminthiasis is assessed by disability-adjusted life years (DALYs) because these infections cause more disability than mortality (WHO, 2002). Not of least concern in veterinary medicine is the number of infections in livestock and companion animals by these parasitic helminthes.

Nematodes are very abundant helminthes, probably second only to arthropods in terms of numbers and species (Blaxter, 1998). Nematodes are very diverse and can be found in very different habitats. Parasitic nematodes, such as *Ascaris lumbricoides*, *Brugia malayi*, and *Onchocerca volvulus* produce disease burdens in humans that exceed malaria, tuberculosis and other better known conditions (Hotez and Kamath, 2009). Livestock parasites like *Oesophagostomum dentatum*, *Ascaris suum*, *Haemonchus contortus*, *Teladorsagia circumcincta*, and *Trichostrongylus colubriformis* depress agricultural production and food supply. Parasitic nematodes cause more than US$100 billion each year in crop damage and US$11 billion in economic loss through livestock and domestic animal infections (Brown *et al.*, 2006).

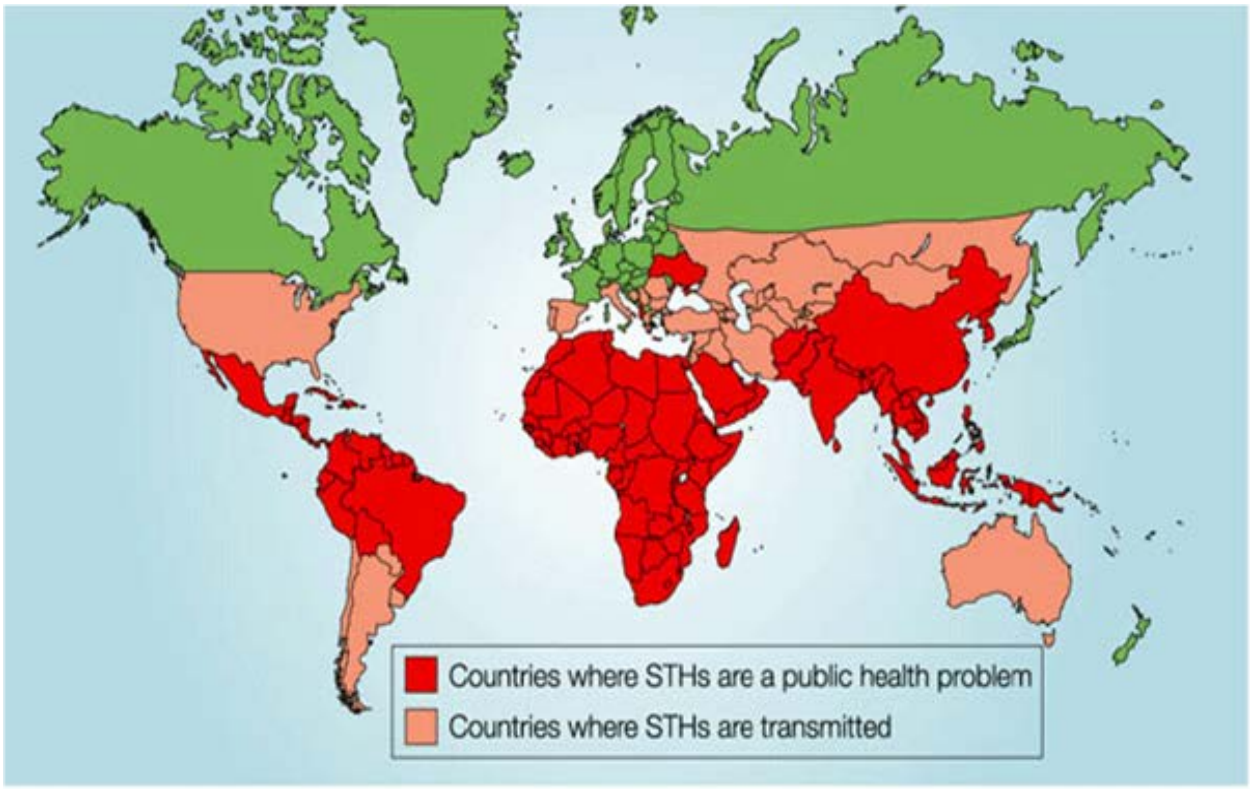

Figure 2 Global distribution of soil-transmitted helminth infections

These STHs are a public health concern in Latin America, Africa, Middle East and Asia. There are still infections and transmissions of the STHs in Australia and a few countries in Europe, although these are of limited public health concern. Modified from Savioli & Albonico (2004).

2.1.1 *Ascaris spp.* and Ascariasis

The genus *Ascaris* has two species, *Ascaris lumbricoides* and *Ascaris suum*. *A. lumbricoides* is a parasitic nematode of humans whilst the closely related *A. suum* parasitizes pigs. Female worms are generally larger than male worms; adult worms are 15 – 35 cm in length. Both

roundworms reside in the small intestine of their hosts and have a direct life-cycle. When humans consume food contaminated with *Ascaris spp.* eggs, the eggs reach the small intestine where they undergo one or two moults and hatch into larvae (Bradley and Jackson, 2004). The larvae penetrate the intestinal mucosa, enter the blood stream and are carried to the liver and then the lungs. Studies with *Ascaris suum* suggest liver invasion occurs 1 – 2 days post-infection and lungs invasion 5 – 6 days post-infection (Anderson, 2000). The larvae grow and molt in the alveoli. After about 3 weeks, L3 larvae are coughed up or migrate up the trachea, swallowed and re-enter the gastrointestinal tract. They mature to egg-laying adult female and male worms in the small intestine after 9 – 11 weeks of egg ingestion. The female worms can lay as many as 200,000 eggs per day which when fertilized can become infective after about 20 days. The infective eggs can persist in the soil and maintain their viability for a year or more under the right warm, moist and insanitary conditions. A number of studies have demonstrated the viability of *Ascaris spp.* eggs under different conditions like alkaline pH and temperature (Ghiglietti *et al*., 1995), H_2SO_4 (Cruz *et al*., 2011), and sewage treatment (Johnson *et al*., 1998).

Infection with *A. lumbricoides* results in Ascariasis. The most intense *A. lumbricoides* infection is in children. Large numbers of adult *Ascaris* worms can cause abdominal distension (Bethony *et al*., 2006), temporary lactose intolerance (Carrera *et al*., 1984), impaired fat digestion, reduced vitamin absorption (Taren *et al*., 1987). These might in turn lead to nutritional and growth deficits, especially in children (Stephenson *et al*., 1980). In that regard, some studies have found a positive correlation between weight gain in children and treatment with anthelmintics (Stephenson et al., 1989; Stephenson et al., 1993a, b) or Vitamin A supplementation (Donnen *et al*., 1998). Aggregation of adult worms in the ileum

of children can cause its obstruction (Villamizar *et al*., 1996) with attendant complications like volvulus, intussusception, bowel infarction and intestinal obstruction (Khuroo *et al*., 1990). Because adult *Ascaris* move in children with high fever, they may appear in the nasopharynx or anus of these children. Migration of *Ascaris spp.* larvae may cause localized reactions in various organs. Penetration of lungs by these larvae can cause Loeffler's pneumonia, in which pools of blood and dead epithelial cells clog air spaces in the lungs (Gutierrez, 2000).

Over 800 million people are estimated to be infected with *A. lumbricoides* in the tropics and subtropics (Hotez *et al*., 2007; Hotez, 2008). In Ghana, for instance, some vegetable growers use wastewater to irrigate their farms, putting themselves and consumers of vegetables from those farms at risk of *Ascaris* and other nematode infections (Seidu *et al*., 2008). It is estimated that about 200,000 people per day in Accra consume lettuce grown on such farms, an indication of the number of people at risk of *Ascaris* infections (Amoah *et al*., 2007). Mass drug chemotherapy programs in Ghana for STHs is only focused on children of school-going age, leaving those who are not in this category as a reservoir for *Ascaris lumbricoides* (and other parasitic nematode) reinfections (Tay *et al*., 2010).

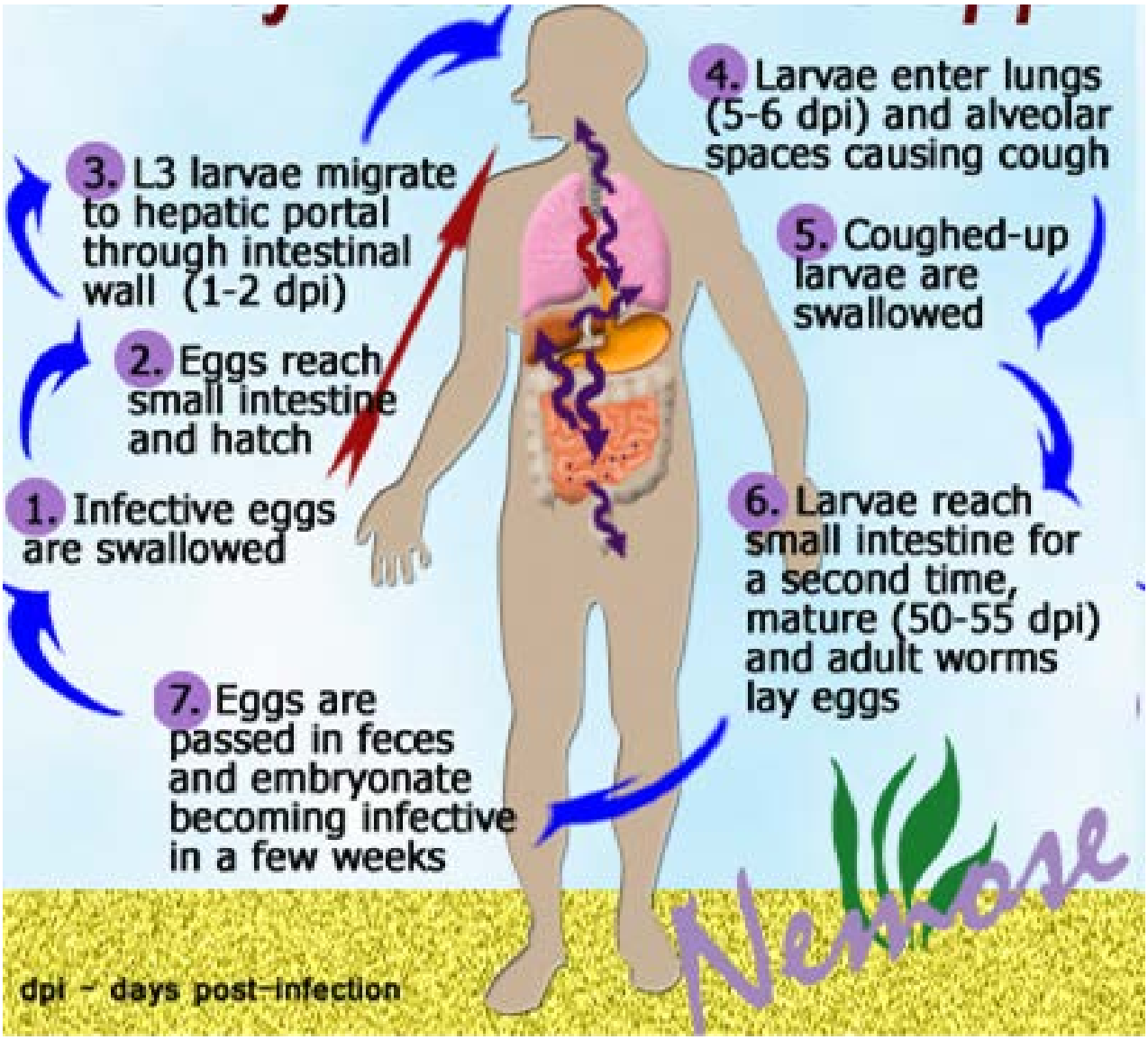

Figure 2.1 Life cycle of *Ascaris spp*.

Modified from www.metapathogen.com/roundworm/ (Accessed on 01-18-12 at 10:38AM CST)

2.1.2 *Oesophagostomum spp.* and Oesophagostomiasis

Oesophagostomum spp. are helminthes that belong to the family Strongyloidea. The subfamily Oesophagostominae is rich in species that parasitize pigs, ruminants, primates, and rodents. These parasites cause Oesophagostomiasis in the host, which is characterized by the formation of nodular lesions mostly in the small intestines of these hosts. Therefore, members in this genus of parasitic nematodes are also known as nodular worms. There are a number of reports of *Oesophagostomum bifurcum* infections of man, although these infections are mostly localized to the northern parts of Ghana and Togo, West Africa (Pit *et al.*, 1999; Storey *et al.*, 2001; Yelifari *et al.*, 2005; Ziem *et al.*, 2005; 2006). *O. bifurcum* infection of humans causes uninodular and multinodular lesion formation in the entire colon wall, resulting in general abdominal pain, persistent diarrhea, and severe wasting, as well as accounting for about 1 % of major acute surgical procedures in northern Ghana (Storey *et al.*, 2000). Adult worms are about 7-15 mm long.

The oval *Oesophagostomum spp.* eggs are passed in feces and develop rapidly into first-stage larvae as early as 24-hours at optimum temperatures. First-stage larvae (L1) feed on bacteria in the environment and develop into second-stage larvae (L2) 24-hours after hatching. The second-stage larvae subsequently moult to infective larvae (L3). The host is infected by ingesting third-stage larvae. The infective larvae then invade the intestinal mucosa, develop to the fourth stage and re-enter the lumen of the large intestine. Most larvae moult to the adult stage in 20-30 days. The adult worms live in the large intestine where they lay eggs (Anderson, 1992). Figure 2.2 shows the life cycle of *Oesophagostomum spp.*

The different *Oesophagostomum spp.* parasites that infect livestock are *O. radiatum* (infect cattle), *O. asperum* (parasitize caecum and colon of goats), *O. columbianum* (parasitize large intestines of sheep, goats, alpaca), *O. venulosum* (parasitize sheep and goats), *O. quadrispinulatum* and *O. dentatum* (parasitize pigs). The two *Oesophagostomum* parasites of pigs usually coexist in the same host and appear to be less pathogenic than the species that parasitize other animals (Steward and Gasbarre, 1989). They cause nodular lesions most obvious in the caecum and mid-colon. These parasites can maintain high worm burdens in the pig without eliciting immune responses (Roepstorff and Nansen, 1994). *O. dentatum* are cosmopolitan parasites found in the large intestine of pigs. *O. dentatum* and *Ascaris suum* usually infect pigs concurrently (Helwigh *et al*., 1999). Although there are little to no estimates on the impact of *O. dentatum* infections of pigs, these parasites are economically important, but less so when compared with *A. suum* and other more pathogenic parasites of livestock.

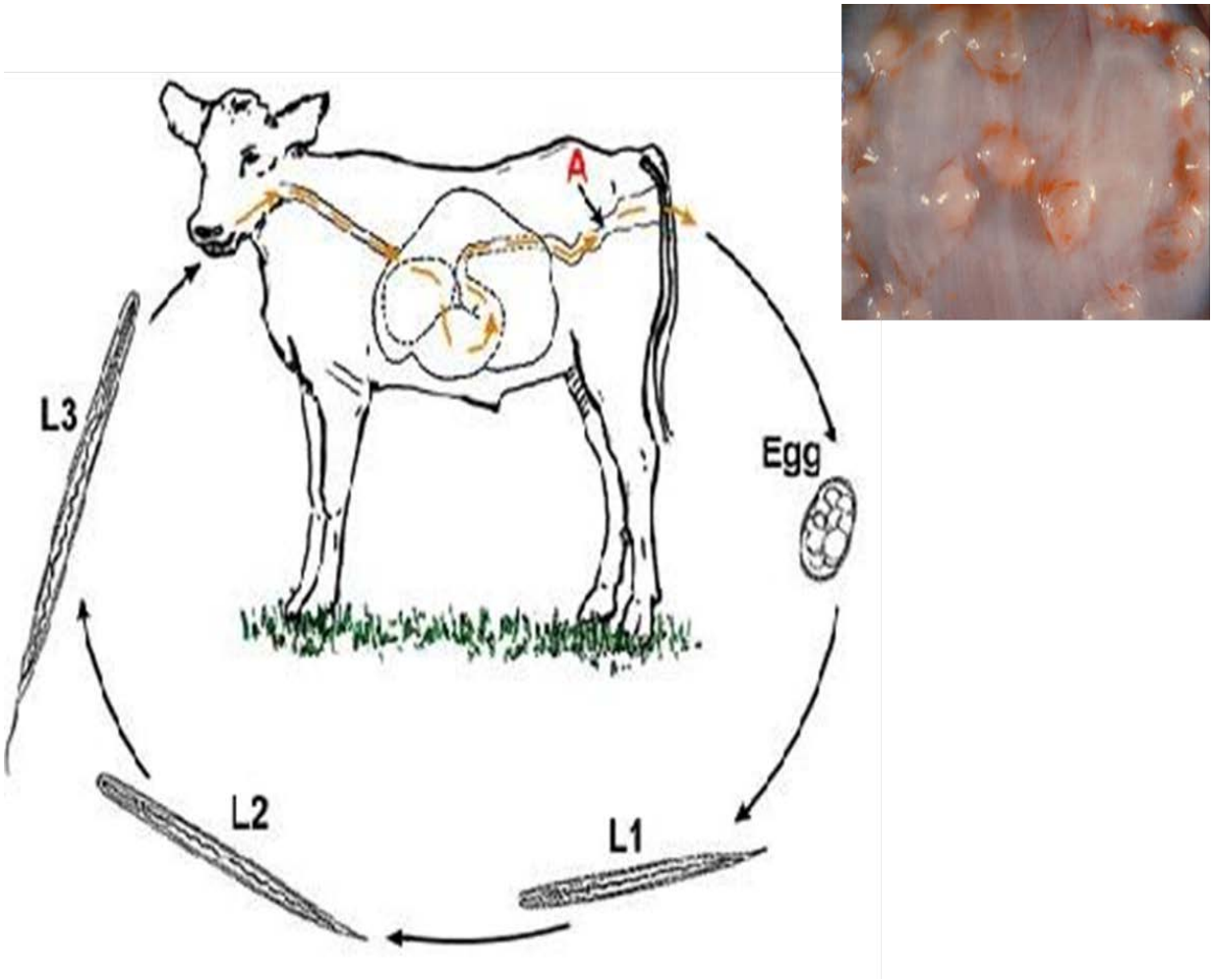

Figure 2.2 Life-cycle of *Oesophagostomum spp.*

Insert shows the nodular lesions caused by these parasites. The life-cycle of the animal parasites are not significantly different from the life-cycle of the human parasite, *O. bifurcum*. Modified from Gasser *et al.* (2007) and http://en.wikipedia.org/wiki/File:Life_cyc.jpg (Accessed on 01-27-12 at 6:08PM CST)

2.2 Nematode Muscular and Nervous Systems

The neuromuscular system of *Ascaris spp.* is perhaps the earliest well-characterised neuromuscular system of nematodes. The body muscle anatomy was described as early as 1866 (Schneider, 1866). It is unique and different from the neuromuscular system of vertebrates, in that the muscle cells send projections to the nerves instead of the other way round in vertebrates. *Ascaris spp.*, as well as other nematodes have a fixed number of cells and cell divisions (del Castillo *et al*., 1989). Another unique feature about this nematode is the small and constant number of neurons (ca 250) and the large cells which make up its musculature. The literature review on nematode neuromuscular system below follows that of *Ascaris lumbricoides* and *Ascaris suum*.

2.2.1 Nematode Muscular System

The anatomy of nematode body muscle, as previously stated, is unique because the muscles send projections to the nervous system. From the outside, a transverse section of *Ascaris* body is composed of three concentric rings of cuticle, hypodermis and somatic muscle layer, Figure 2.3A (Martin *et al*., 1991). The somatic muscle layer surrounds the perienteric cavity which contains the gut. The mononucleated muscle cells are separated into the dorsal and ventral fields by the two lateral lines (del Castillo *et al*., 1989) and they contract in opposition to produce motion (Weisblat and Russel, 1976). The muscle cells are about 5×10^4 in number, which are kept reasonably constant (Stretton, 1976). Anchored below the hypodermis is the obliquely striated contractile substance, known as the spindle or fibre

(Rosenbluth, 1965a, 1967, 1969). The thin and thick filaments are arranged in an acute angle, permitting the smooth muscle to be greatly extensible whilst maintaining the velocity of contraction (Robertson and Martin, 1993a).

According to Martin and Donahue (1987), the excitatory neurotransmitter ACh produces fast contraction of the muscle through Ca^{2+} fixation by the actin whilst a change in the light chain myosin phosphorylation state is associated with relaxation produced by the inhibitory neurotransmitter GABA. Close to the mid-section of the spindle, the muscle cell forms a balloon-like, 200 µm structure known now as the bag or belly. The muscle bag, Figure 2.3B, lies in the perienteric space and contains the single nucleus of the muscle cell, submembrane mitochondria and particulate glycogen (Rosenbluth, 1965b). Each muscle cell sends processes known as muscle arms which arise from the base of the bag and cross transversely to the syncytium over the nerve cord. Most muscle cells possess a mean of 2.7 muscle arms (Stretton, 1976). The arms at the nerve cord branch into thin, finer terminal processes known as 'fingers' which form tight, intertwined junctions with the 'fingers' of adjacent arms at the syncytium. These tight 'fingers' extend longitudinally apposed to the nerve cord and are responsible for the electrical coupling between adjacent muscle cells (DeBell *et al*., 1963). The syncytium and nerve cord fibers form neuromuscular junctions in *Ascaris*.

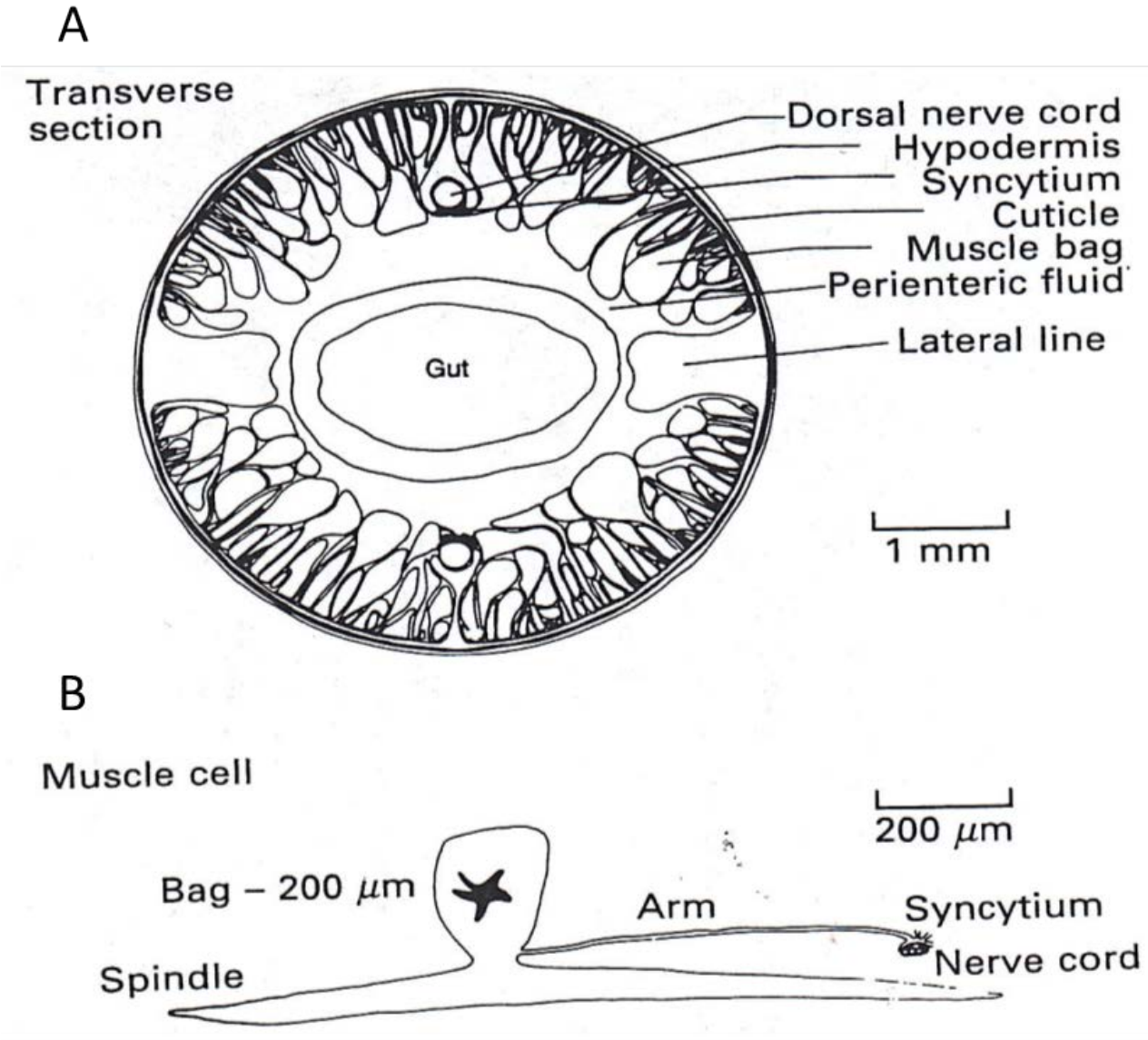

Figure 2.3 *Ascaris* body section and muscle structure

(A) Transverse section of anterior portion of *Ascaris* body showing arrangement and position of the nerve cords, lateral line, hypodermis, syncytium, cuticle, muscle bag, gut and perienteric fluid. (B) Structure of the muscle of *Ascaris* showing the 200 μm muscle bag, the spindle, muscle arm and location of syncytium and nerve cord. From Martin *et al*. (1991).

2.2.2 Nematode Nervous System

At the head region of *Ascaris* is the circumferential nerve ring and associated ganglia that surrounds the pharynx. The ganglia associated with the anterior nerve ring are 5 in number, namely a dorsal ganglion and a ventral ganglion, two lateral ganglia and a retrovesicular ganglion. The retrovesicular ganglion contains 13 neurons (Angstadt *et al*., 1989). At the posterior region of the worm is another smaller set of ganglia. Arising from the nerve ring are the dorsal and ventral nerve cords that pass caudally along the length of the *Ascaris* body (Stretton *et al*., 1978; Stretton *et al*., 1985). The motor nervous system of *Ascaris* (the remaining nervous system in a decapitated worm that controls movement) is divided into 5 repeating segments. Each segment contains 11 motorneurones with their somata in the ventral nerve cord (Stretton *et al*., 1978).

Based on their morphology (distribution of axons and dendrites), the 11 motorneurones were divided into 7 types. Three (DI, DE2, DE3) of the seven types occur only once in each segment whilst the other four types (DE1, VI, V1 and V2) occur twice in each segment. Two types (V1 and V2) are contained only in the ventral nerve cord but the remaining five have processes in both dorsal and ventral nerve cords. The processes of these motorneurones in both dorsal and ventral nerve cords are linked by processes known as commissures (Hesse, 1892). According to Davis and Stretton (1989), all-or-none action potentials have never been observed in the commissural motorneurones of *Ascaris*; the all-or-none action potential is commonly used by nerve cells in the animal kingdom. However, synaptic transmission in this nematode is graded and mediated without spikes. Inhibitory potentials recorded in DI and VI motorneurones (Stretton *et al*., 1978) correlate with GABA-immunoreactivity identified in DI and VI motorneurones (Johnson and Stretton, 1985; Sithigorngul *et al*., 1989) and the

suggestion that these two motorneurones are inhibitory. ACh is the excitatory neurotransmitter in these nematodes, a suggestion supported by histochemical studies that identified choline acetyltransferase in DE1, DE2 and DE3 motorneurones (Johnson and Stretton, 1985). Also in each segment are 6 non-segmental interneurones, 3 right-hand commissures and one left-hand commissure, Figure 2.4. The 6 non-segmental interneurones which are located in the ventral cord have their somata either in the head or tail segments. In addition to the two major nerve cords, there is the dorsal lateral, dorsal sublateral, ventral lateral and ventral sublateral minor nerve cords (Johnson and Stretton, 1987).

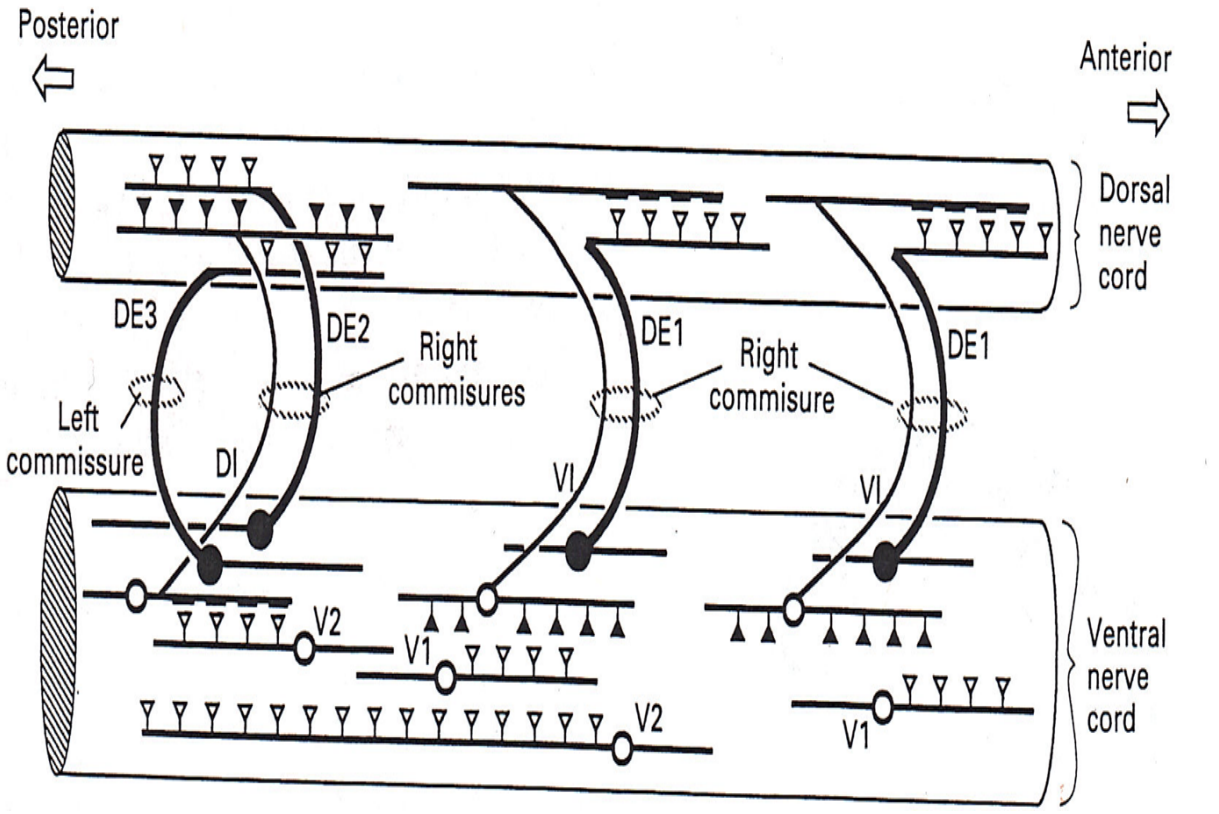

Figure 2.4 Organization of the motor nervous system of *Ascaris suum* in one segment. Present in each segment are 11 motorneurones, six non-segmental interneurones running the length of the ventral cord. Seven morphological types of the motorneurones are found in each segment, all with cell bodies in the ventral cord; DI = dorsal inhibitory, VI = ventral inhibitory, DE1 = dorsal excitatory 1, DE2 = dorsal excitatory 2, DE3 = dorsal excitatory 3, V1 and V2 = ventral excitatory. Modified from Martin *et al*., (1991).

2.2.3 Electrophysiology of Somatic Muscle

The resting membrane potential of *Ascaris* somatic muscle range from -30 mV to -40 mV. DeBell *et al.* (1963) measured the membrane potential in the nuclear bags of *Ascaris lumbricoides* in 30 % diluted sea water to be -29.86 mV. However, membrane potential of -34.5 mV was recorded for somatic muscle cells in the presence of the perienteric fluid from *Ascaris* (del Castillo *et al*., 1964a). The membrane potential of *Ascaris* is largely determined by membrane conductance to anions, such as extracellular Cl^- ions but less so by conductance to cations, such as K^+ (Brading and Caldwell, 1971). Sodium ions (Na^+) also contribute to the membrane potential, although to a lesser extent as demonstrated by permeability ratios of 1:4:7 for K^+, Na^+ and Cl^- (Caldwell and Ellory, 1968). The composition of the perienteric fluid significantly influences the membrane potential of *Ascaris*. It contains low concentrations of Cl- and high concentrations of the carboxylic acids acetate, propionate, succinate, 2-methylbutyrate and 2-methylvalerate produced from anaerobic metabolism of glucose (Hobson *et al*., 1952a; Saz and Weil, 1962; Tsang and Saz, 1973). According to Thorn and Martin (1987), high conductance Ca^{2+}-dependent Cl^- channels present in *A. suum* muscle is permeable to these carboxylic acids. Caldwell (1974) suggested that an active electrogenic pump moving these carboxylic acids may account for the state of the membrane potential.

Intracellular recordings (Jarman, 1959) from *A. suum* muscle cells demonstrated the presence of regular, spontaneous spike-like depolarizations (up to 10 mV in amplitude) superimposed on the resting potential. Three types of spontaneous electrical activity are observable in the muscle of *Ascaris*, namely (i) spikes of varying amplitude up to 30 – 40 mV lasting 5 – 50

msec; slow wave depolarizations of 100 – 1000 msec duration and amplitudes up to 20 mV; and long lasting waves (3 – 20 sec), about 5 mV in amplitude, that modulate the level of spontaneous activity (DeBell *et al*., 1963; Weisblat and Russel, 1976). Figure 2.5 below illustrates the three types of electrical activity. Spikes of larger amplitude are usually observed when recording from muscles near or directly over the nerve cord. Slow waves are not artifacts with recordings or movements because under conditions where contractions and spike potentials are abolished, they still persist. The depolarization phase of these spikes is caused by Ca^{2+} currents (Weisblat *et al*., 1976) whilst K^{+} currents are responsible for the repolarization phase (Martin, 1982).

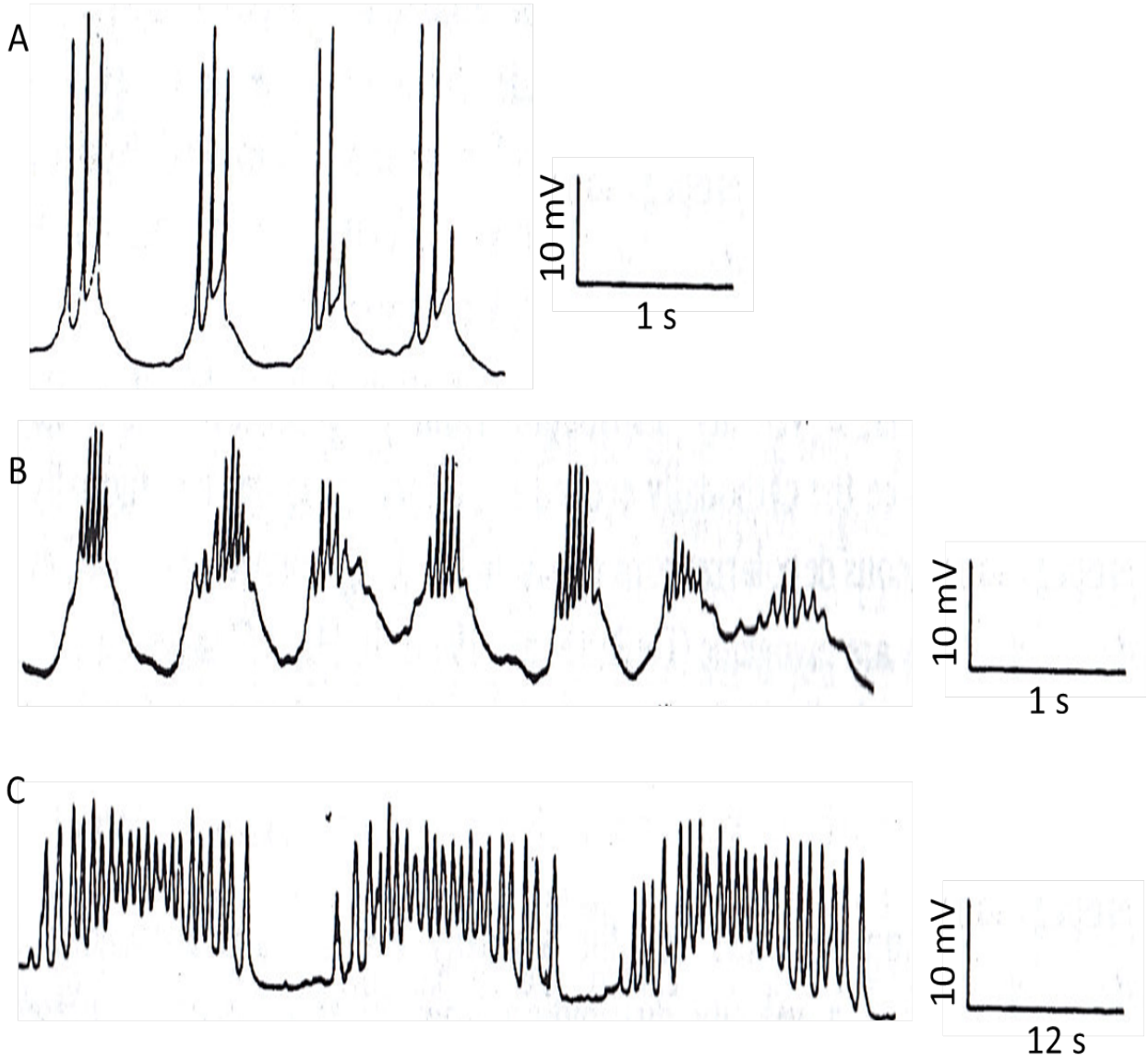

Figure 2.5 Sample traces of spontaneous electrical activity in *Ascaris* muscle cells.

(A and B) Slow waves with spike potentials, showing the smaller slow waves and larger spike potentials. Multiple spike potentials superimposed on a single slow wave. Visible muscle contractions usually correlated with the electrical activity. (C) Long lasting, modulating potentials with ~20 sec periods. Modified from Weisblat and Russel (1976).

2.3 Nicotinic Acetylcholine Receptors, nAChR

Acetylcholine receptors are transmembrane proteins that respond to the neurotransmitter acetylcholine. Early studies on the acetylcholine receptors (AChR) resulted in the classification of these receptors into two classes based on their pharmacology, namely muscarinic AChRs and nicotinic AChRs. Both cholinergic receptor classes belong to different and distinct protein superfamilies; the muscarinic AChRs are metabotropic and the nicotinic AChRs are ionotropic. The nicotinic acetylcholine receptors are large transmembrane proteins (290 kDa) and members of the cys-loop ligand-gated ion channel (LGIC) superfamily of receptors (Unwin, 2005). They have an N-terminal extracellular ligand-binding domain, a membrane-spanning domain and an intracellular domain. The cys-loop LGIC superfamily of receptors also includes the γ-aminobutyric acid receptor ($GABA_A$), the glycine receptor and the serotonin (5-HT) receptor. The characterizing features of receptors of the cys-loop LGIC superfamily are: (i) a cysteine loop in the α-subunit separated by 13 amino acids (Gruhn *et al*., 2002); (ii) four transmembrane domains (Touroutine *et al*., 2005); amino acid sequence homology and (iv) similar arrangement of subunits. Unlike the muscarinic AChRs, the nicotinic ACh receptors are not coupled to second messenger cascades but are directly coupled to ion channels. These nAChR are pentameric transmembrane receptors. The importance of nAChRs is underscored by their involvement in autoimmune and genetic disorders, such as Myasthenia gravis, Rasmussen's encephalitis, Alzheimer's disease, Parkinson's disease, and Schizophrenia.

2.3.1 Vertebrate nAChR

Earlier characterizations of vertebrate nicotinic AChR used the electric tissue of *Torpedo californica* and/or *T. marmorata*. Cloning (Ballivet *et al*., 1982; Giraudat *et al*., 1982; Sumikawa *et al*., 1982), sequencing (Noda *et al*., 1982; Devillers-Thiery *et al*., 1983; Noda *et al*., 1983) and heterologous expression of the subunits of the *Torpedo* nAChR has tremendously increased our understanding about these receptors and the cys-loop LGIC superfamily of receptors. Resolution of the *Torpedo* electric organ nAChR at 4.0 Å and 4.6 Å has provided useful insights into the three-dimensional structure of cys-loop LGIC (Miyazawa *et al*., 1999; Unwin, 2005). Vertebrate muscle nAChR is perhaps the best characterized of the family of LGIC. It is composed of 4 different subunits assembled in a stoichiometry of α2βγδ (Karlin, 1980; Karlin *et al*., 1983). In adult muscle nAChRs, the γ subunit is replaced by ε subunit; the γ subunit is expressed in embryonic muscle nAChRs. The circular order of subunit arrangement is established as αγαδβ (Karlin and Akabas, 1995). Unlike the muscle nAChRs, the neuronal nAChRs are far more diverse, with different subunit combinations based on reports of eight alpha subunit genes (α2 - α9) and three beta subunit genes (β2 – β4) (Millar, 2003). In addition, the neuronal nAChRs differ from the muscle nAChRs in sensitivities to nicotinic antagonists and single-channel properties (Colquhoun *et al*., 1987; Steinbach and Ifune, 1989). Table 2.0 below illustrates the subunit diversity of the neuronal nAChR compared with the muscle nAChRs. The five subunits are arranged like staves with an opening in the middle. The subunits are classified as alpha (α) or non-alpha (β, δ, ε, ϒ); the distinction is the presence of vicinal dicysteines in the α-subunits. Each subunit is composed of ~400-520 amino acids. In vertebrates, 16 subunit encoding

genes have been identified so far, with an extra subunit identified in chickens (Millar, 2003). The largest vertebrate nAChR subunits is found in the pufferfish, which possesses 28 subunits (Jones *et al*., 2003). These nAChRs can be homopentameric (all 5 α-subunits, such as in vertebrate neuronal nAChRs) or heteropentameric (2 α-subunits and 3 non- α-subunits, such as in vertebrate muscle nAChRs).

Each subunit has four transmembrane domains, TM1-TM4 and each transmembrane domain consists of approximately 20 amino acids. Available evidence suggests that TM2 in each subunit forms the lining of the channel pore (Hung *et al*., 2005; Bafna *et al*., 2008; Cymes and Grosman, 2008). The ACh binding site is at the interface of 2 adjacent subunits formed by 6 distinct regions of loops in the N-terminal extracellular side. Loops A, B, C are contributed by α-subunits and loops D, E, F contributed by either α- or non- α-subunits, figure 2.6C (Corringer *et al*., 2000). Available electrophysiological evidence suggests there are two non-equivalent ACh binding sites, between α1 – γ and α1 – δ subunits for the muscle nAChR (Kreienkamp *et al*., 1995). Based on the proposed binding position by Unwin (1993), the canonical ACh binding site is thought to be between the positive face of the α-subunit and the negative face of the non- α-subunit.

According to Blount and Merlie (1989), the γ and δ subunits associate efficiently with the α subunit, modifying its binding characteristics. The authors observed no association between the α subunit and the β subunit. In agreement with that, Kreienkamp *et al.* (1995) reported that the β subunit does not contribute to the formation of a binding site but promotes surface expression of the assembled pentamer. However, the β subunits in neuronal nAChRs contribute to the formation of ligand binding sites (Luetje and Patrick, 1991; Drenan *et al*., 2008). Blount and Merlie (1989) also observed that the αγ and αδ complexes formed

different high affinity binding sites for *d*-tubocurarine, accounting for the two nonequivalent binding sites of nAChRs. The association and oligomerization of subunits to form a functional receptor is governed by a number of factors.

During the assembly process, the subunits are inserted in the endoplasmic reticulum where they undergo folding and post-translational modifications. Any unassembled subunits show little accumulation in cells and are most susceptible to degradation (Blount and Merlie, 1990). Chaperone protein association with the subunits as well as subunit-subunit associations promotes the assembly process and stability of the assembled complexes. There are several reports of association between chaperone proteins and nAChR subunits. For example, the chaperone protein RIC-3 has been reported to enhance α7 and other nAChR subunits in attaining their correct conformational states (Ben-Ami *et al*., 2005a; Castillo *et al*., 2005; Treinin, 2008; Ben-Ami *et al*., 2009a).

Other such proteins include the ER-residents BiP (immunoglobulin heavy chain binding protein) (Blount and Merlie, 1991; Paulson *et al*., 1991) and calnexin (Gelman *et al*., 1995; Keller *et al*., 1996), as well as rapsyn (43K protein) which is important in clustering of nAChRs at the post-synapse of the neuromuscular junction (Froehner *et al*., 1990; Phillips *et al*., 1991). Calnexin, according to Keller and Taylor (1998) associates with unassembled subunits and stabilizes them but dissociates when the subunits assemble. They also demonstrated that dissociating calnexin from the subunits enhanced their polyubiquitination and degradation in the proteasome. Inherent properties of the subunits also govern the assembly of nAChRs. Sequence elements in the N-terminal domain of the subunits affect ligand recognition and subunit-subunit interactions and arrangements, as revealed by mutated and chimeric subunits (Blount and Merlie, 1989; Sine and Claudio, 1991; Yu and Hall, 1991;

Sumikawa, 1992). Formation of the correct ligand binding sites is partly dictated by the specificity of subunit associations.

Using the temperature sensitivity of *T. californica* nAChRs, Green and Claudio (1993) observed that αβγ trimers were the earliest identifiable assembly intermediates. The next assembly intermediates identified were αβγδ tetramers. The pentameric product is formed by the addition of a second α subunit to the αβγδ tetramers. A transfection study suggested that αγ and αδ dimers were formed first with the oligomerization of these dimers and addition of a β subunit to form the pentamer (Keller and Taylor, 1999).

Table 1 Subunit diversity of vertebrate neuronal nAChRs compared with muscle nAChRs

Receptor subtype	Subunits	Subunit combinations
Muscle-type	α1, β1, γ, δ, ε	α1,β1,γ,δ‡
		α1,β1,ε,δ‡
Neuronal (αBTX-insensitive)	α2–α6, β2–β4	α2β2
		α2β4
		α3β2
		α3β4
		α4β2
		α4β4
		α6β2§
		α6β4
		α2α5β2
		α3α5β2
		α3α5β4
		α3α6β2
		α3α6β4
		α3β3β4
		α4α5β2
		α5α6β2
		α6β3β4
		α3α5β2β4
		α3α6β3β4
		α4α5α6β2
		α4β2β3β4
Neuronal (αBTX-sensitive)	α7, α8¶	α7
		α8
		α7β2
		α7β3
		α7α8
		α5α7β2
		α5α7β4
Sensory epithelia	α9, α10	α9
		α9α10

Modified from Millar (2003)

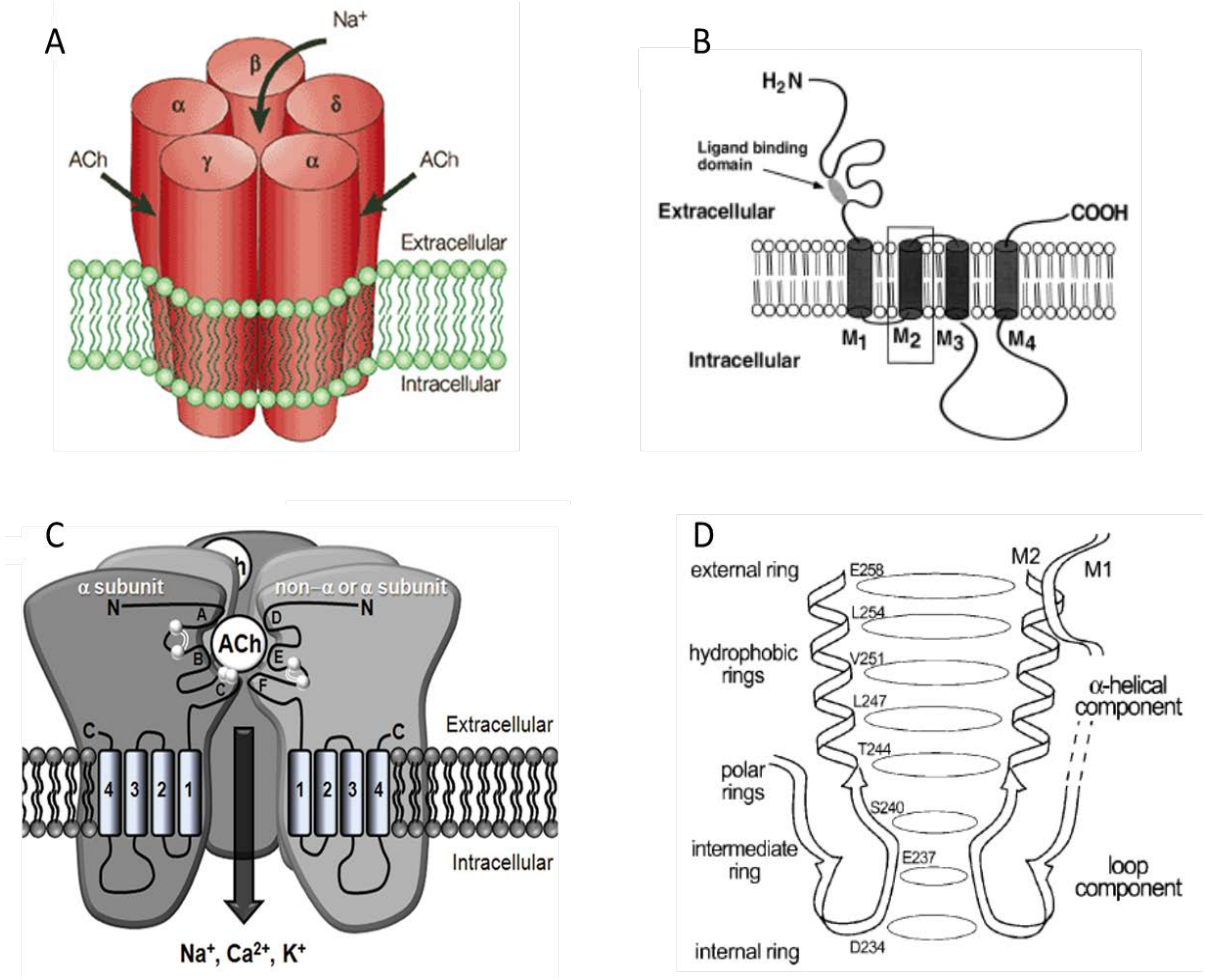

Figure 2.6 Structure of the vertebrate nicotinic acetylcholine receptor.

(A) View of the nAChR from top, showing the subunits, channel pore and ACh binding sites. Modified from Karlin (2002). (B) View of the extracellular ligand-binding site, 4 TM domains and predicted pore liner (highlighted TM2) of the nAChR. From Paterson and Nordberg (2000) (C) Side view of the nAChR showing the loops that contribute to the ACh binding pocket. From Jones & Sattelle (2010). (D) Structural and functional model of the nAChR showing the pore-lining M2 helix, the water pore (upper part of channel) and selectivity filter (lower loop). From Corringer *et al*. (2000).

2.3.2 *Caenorhabditis elegans* AChR

The free-living nonparasitic nematode *Caenorhabditis elegans* possess the most diverse and extensive nAChR subunit gene families currently known. Completion of the *C. elegans* genome sequencing project paved the way for the identification of the nAChR gene family. However before completion of the sequencing project, investigation of resistance to levamisole led to the identification of the subunits *unc-38* (α-subunit), *lev-1* and *unc-29* (both non-α-subunits) (Fleming *et al*., 1997). Lewis *et al*. (1980) observed that mutation of *C. elegans* genes like *unc-29, unc-38, unc-63, lev-1, unc-50,* and *unc-74* leads to levamisole resistance. The nAChR of *C. elegans* fall into levamisole-sensitive and levamisole-insensitive groups, figure 2.7B. Investigation of subunit mutations that caused neuronal degeneration led to the identification of *deg-3* (Treinin and Chalfie, 1995) and *des-2* (Treinin *et al*., 1998; Yassin *et al*., 2001) subunits, both α-subunits. The subunit genes *acr-2* (Squire *et al*., 1995), *acr-3* (Baylis *et al*., 1997) and *acr-16* (identified as Ce21) (Ballivet *et al*., 1996) were cloned with a probe derived from *Drosophila melagonaster* nAChR cDNA cross-hybridized with either a vertebrate nAChR cDNA or already identified *C. elegans* nAChR cDNA. The genes *acr-2* and *acr-3* are located in the same orientation, the former only 281 upstream of the latter. ACR-16 is closely related to the homomeric vertebrate α7. It forms a homomeric, levamisole-insensitive receptor at the *C. elegans* neuromuscular junction (NMJ), and together with ACR-8 accounts for all levamisole-insensitive nAChR signaling at the NMJ (Touroutine *et al*., 2005).

Up to 29 subunits have been identified and divided into five groups based on homology of the sequences, figure 2.7A. These are the ACR-16 group, the ACR-8 group, the UNC-38

group, the UNC-29 group and the DEG-3 group. Each group is named after the first member identified. A set of subunits which are highly homologous to the other subunits but do not fall into any of the five groups are put into the 'Orphan' group of receptors. According to Jones and Sattelle (2004), the ACR-8 and DEG-3 groups represent nematode-specific family of receptor subunits. The *C. elegans* DEG-3/DES-2 receptor is localized to nonsynaptic regions, the sensory endings of chemosensory neurons and expression in *Xenopus* oocytes shows that it is activated by choline (Yassin *et al*., 2001). UNC-38, UNC-63 and ACR-6 are in the UNC-38 group whilst UNC-29, LEV-1, ACR-2 and ACR-3 are in the UNC-29 group. UNC-38, UNC-29, LEV-1 and UNC-63 are expressed in the body wall muscles, showing that these subunits may combine into the same receptor (Culetto *et al*., 2004). UNC-63 is additionally expressed in neurons and vulval muscles. The *lev-8* subunit gene, previously designated as *acr-13*, is expressed in body wall and uterine muscles (Towers *et al*., 2005). It encodes an α-subunit in the ACR-8 group. Five subunits make up the *C. elegans* levamisole-sensitive receptor. Three of these subunits (UNC-29, UNC-38 and UNC-63) are designated as essential subunits and the other two (LEV-1 and LEV-8) as non-essential subunits.

Although all the *C. elegans* nAChR subunits possess the characterizing features common to all nAChRs, some of the subunits have some modifications. In the pore-lining TM2 domain, the members of the ACR-8 group (ACR-8, ACR-12, ACR-13) possess a histidine residue (basic) in place of the well-conserved glutamate residue (acidic), figure 2.7C. Additionally, ACR-5 from the DEG-3 group contains FxCC in the C loop instead of the highly-conserved YxCC motif (Jones and Sattelle, 2004). The YxCC motif is important for ACh binding and studies suggest that mutating this motif in α7 receptors to FxCC results in significant reduction in affinities for ACh and nicotine (Galzi *et al*., 1991).

Furthermore, some molecular components (genes/proteins) are known to be associated upstream or downstream with nAChR assembly and function. The genes, *unc-50* and *unc-74* discovered in mutagenesis screens for levamisole resistance are important in nAChR assembly. UNC-50 is a conserved transmembrane protein localized to the Golgi apparatus. Eimer *et al.* (2007) observed that *C. elegans unc-50* was required for subtype-specific trafficking of assembled nAChRs such that the absence of *unc-50* resulted in sorting of a subset of the nAChRs in the body wall muscle to the lysosomal system for degradation. UNC-74 seems to be required solely for the expression of levamisole-sensitive nAChRs. It is predicted that *unc-74* encodes a thioredoxin protein. Another gene, *ric-3*, identified in screens for resistance to inhibitors for cholinesterase is also important in *C. elegans* nAChR function. It encodes an endoplasmic reticulum transmembrane protein that acts as a chaperone in folding, maturation and assembly of multiple nAChRs (Ben-Ami *et al*., 2005a; Castillo *et al*., 2005; Lansdell *et al*., 2005; Millar, 2008). RIC-3, UNC-50 and UNC-74 are three important ancillary proteins that affect *C. elegans* nAChR assembly and function. These three ancillary proteins, together with UNC-29, UNC-38, UNC-63, LEV-1 and LEV-8 are required to reconstitute functional, levamisole-sensitive *C. elegans* nAChR in *Xenopus* oocytes (Boulin *et al*., 2008). Injection of the 8 genes for these proteins reconstitutes a receptor that responds robustly to ACh, followed by levamisole with the least response to nicotine.

In addition to these three ancillary proteins, there are other proteins that affect *C. elegans* nAChR. *lev-10* was identified on the basis of mutants being weakly resistant to levamisole (Gally *et al*., 2004). It encodes a protein, LEV-10, that is required for clustering AChRs in body wall muscle. In the *lev-10* mutants, the density of levamisole-sensitive AChRs at the

NMJ but not the number of functional AChRs, is significantly reduced. The levamisole-sensitive receptors in these *lev-10* mutants are distributed extrasynaptically (Qian *et al*., 2008). Using these extrasynaptic levamisole-sensitive receptors in *lev-10* mutants, Qian *et al.* (2008) demonstrated that *lev-8* knockouts had longer single channel closed times whilst *lev-1* knockouts had smaller single-channel conductance and fewer expressed channels. LEV-10 is part of a physical complex with LEV-9 and the L-nAChR localized at the NMJ. In another screen for *C. elegans* mutants weakly resistant to levamisole, *oig-4* was identified. It encodes the OIG-4 protein that contains a single immunoglobulin domain. OIG-4 interacts with the L-nAChR/LEV-9/LEV-10 physical complex such that its removal results in a loss of L-nAChR clusters mainly by destabilizing the complex (Rapti *et al*., 2011).

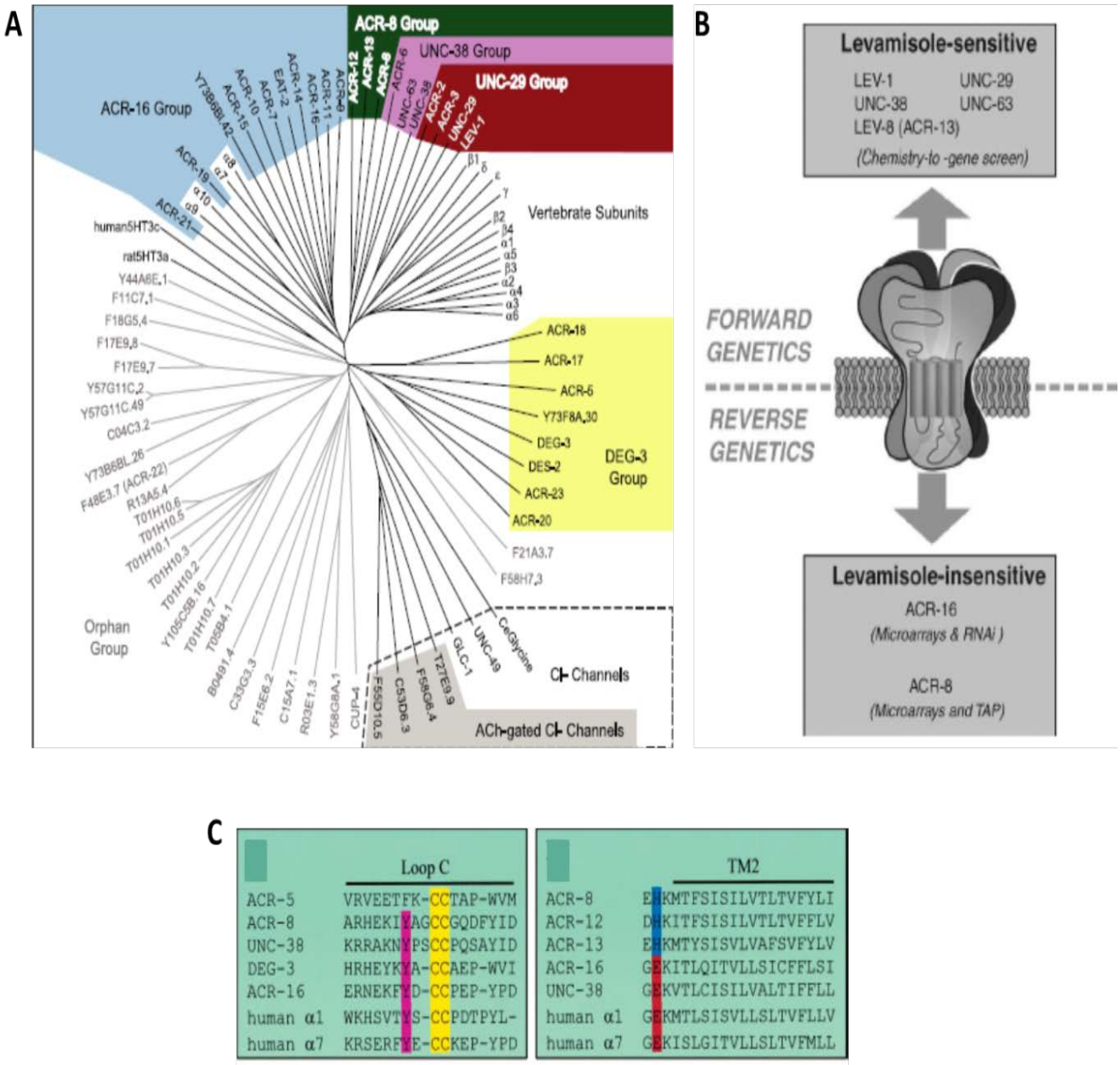

Figure 2.7 *Caenorhabditis elegans* nicotinic acetylcholine receptor diversity. (A) The nAChR of *C. elegans* are put into five groups (colored regions), with a set of 26 subunits not belonging to any of these groups put under 'orphan' group. (B) The two levamisole-sensitive and levamisole-insensitive groups of *C. elegans* NMJ nAChRs showing the subunits in these groups. (C) The modified sequence features in some *C. elegans* subunits, mainly in the

YxCC motif of loop C and the glutamate residue of TM2. Modified from Brown *et al.* (2006); Jones and Sattelle (2004).

Table 2 Characterization of *C. elegans* nAChR by heterologous expression

Receptor	Pharmacology	Reference
DEG-3/DES-2	Preferentially activated by choline; sensitive to dTC and strychnine	(Treinin *et al*., 1998; Yassin *et al*., 2001)
ACR-16	Homomeric channel. Nic is partial agonist; lev, butamisole, mor & pyr antagonists. Sensitive to DHβE & dTC; poorly sensitive to MLA & BTX. Insensitive to oxantel & ivermectin	(Ballivet *et al*., 1996; Raymond *et al*., 2000)
UNC-38/UNC-29/LEV-1	Levamisole is agonist. Sensitive to dTC, Mec, neosurugatoxin. Insensitive to BTX	(Fleming *et al*., 1997)
UNC-63/UNC-29/LEV-1	Levamisole is agonist. Sensitive to Mec	(Culetto *et al*., 2004)
UNC-38/ACR-2	Levamisole is agonist. Sensitive to Mec	(Squire *et al*., 1995)
UNC-38/ACR-3	Levamisole is agonist. Sensitive to dTC & Mec	(Baylis *et al*., 1997)

Modified from Jones and Sattelle (2004)
Abbreviations: Nic = Nicotine; Lev = Levamisole; Mor = Morantel; Pyr = Pyrantel; DHβE = Dihydro-β-erythroidine; dTC = d-tubocurarine; MLA = Methyllcaconitine; BTX = Bungarotoxin; Mec = Mecamylamine

2.3.3 Parasitic nematodes AChR

The nAChR of parasitic nematodes differ from the nAChR of *C. elegans* in their electrophysiological properties and subunit compositions. The presence of more than one subtype of nAChR, in terms of conductance states and pharmacological differences, has been well reported in some parasitic nematodes. Single channel recordings in *Ascaris suum* by Robertson and Martin (1993b) suggested the presence of at least two open states and three closed states of the levamisole-activated single-channel currents. Robertson and colleagues used the natural anthelmintic paraherquamide and its semisynthetic derivative, 2-deoxy-paraherquamide to distinguish cholinergic receptor subtypes in *A. suum* muscle (Robertson *et al*., 2002). They used the antagonist effects of these two compounds on muscle contractions elicited by nicotine, levamisole, pyrantel and bephenium to show the subtype selectivity. These authors showed that paraherquamide was able to select for a nicotine receptor subtype whilst 2-deoxy-paraherquamide selected for a bephenium receptor subtype.

Similarly, Martin and colleagues used the nAChR agonists methyridine and levamisole to show the subtype selectivity of cholinergic agonists and antagonists for nAChR in *A. suum* and *O. dentatum* (Martin *et al*., 2003). Methyridine had a selective action on the nicotine subtype (N-subtype) of receptors in these two parasites. In these preparations, methyridine caused membrane depolarizations, conductance increase and inhibition of larval migration. A previous paper reported that methyridine (10 nM – 1 mM) has no effects on chick α7 or *C. elegans* ACR-16 expressed in *Xenopus* oocytes (Raymond *et al*., 2000), suggesting that this compound has subtype-selective effects. Another demonstration of the presence of different pharmacological subytpes of nAChR in *A. suum* and the selectivity of cholinomimetics was

reported by Martin *et al.* (2004). These authors showed that oxantel was selective for the N-subtype receptors (nicotine, methyridine) but thenium selectivity was between L- and B-subtype receptor agonists. Single-channel recordings in *A. suum* demonstrated the presence of three conductance states, G25, G35 and G45 which respectively corresponds to the N-subtype, the L-subtype and the B-subtype of receptors, figure 2.8 (Qian et al., 2006).

Further, single-channel recordings of nAChR from *O. dentatum* demonstrated the presence of a heterogenous population of levamisole-sensitive receptors with the conductance states G25, G35, G45 and G55 (Martin *et al*., 1997). Robertson *et al.* (Robertson *et al.*, 1999) expanded on these observations and demonstrated that the conductance states G25, G35, G40 and G45 are found in the levamisole-sensitive strain of *O. dentatum* (SENS) but the G35 conductance state was absent in the levamisole-resistant strain (LEVR), figure 2.9. In pyrantel-resistant *O. dentatum*, four conductance states of the nicotinic receptors were still observed but the percentage of active patches and probability of channel opening (P_o) were reduced when compared with anthelmintic sensitive worms, figure 2.9 (Robertson *et al*., 2000). These single-channel records amply demonstrate the heterogeneity of nAChRs in parasitic nematodes.

Indeed, the diversity of levamisole receptors in parasitic nematodes has been reported by Neveu *et al.* (2010) at the genetic level. These authors reported identification of the *C. elegans* homologs of *unc-38, unc-29, unc-63* and *lev-1* in the trichostrongylid parasites *Haemonchus contortus, Trichostrongylus colubriformis* and *Teladorsagia circumcincta*. Most importantly, they identified up to four paralogs of the *unc-29* gene in each trichostrongylid parasite, showing the diversity of these receptors in parasitic nematodes. These authors also reported the identification of abbreviated transcripts of *unc-63* in the

resistant isolates of all three trichostrongylid parasites. Reconstitution experiments in *Xenopus* oocytes showed that a levamisole-sensitive nAChR is formed with the *H. contortus* gene products ACR-8, UNC-29, UNC-38 and UNC-63 but ommission of ACR-8 reconstitutes a pyrantel-sensitive nAChR (Boulin *et al*., 2011). In *A. suum* however, only two genes, *Asu-unc-29* and *Asu-unc-38* were used to reconstitute nAChR in oocytes (Williamson *et al*., 2009). Injecting 1:1 ratio of these two genes led to reconstitution of a receptor that responded to levamisole, ACh and nicotine and is antagonized by mecamylamine. Varying the amount of the two subunit genes injected into the oocytes reconstituted receptors with different pharmacologies. 1:5 *Asu-unc-38*:*Asu-unc-29* reconstituted a receptor that responded robustly to pyrantel but not to oxantel, a receptor with levamisole as the full agonist and nicotine as the partial agonist. When 5:1 *Asu-unc-38*:*Asu-unc-29* was injected, the receptor responded robustly to oxantel but not to pyrantel and nicotine was the full agonist whilst levamisole was the partial agonist.

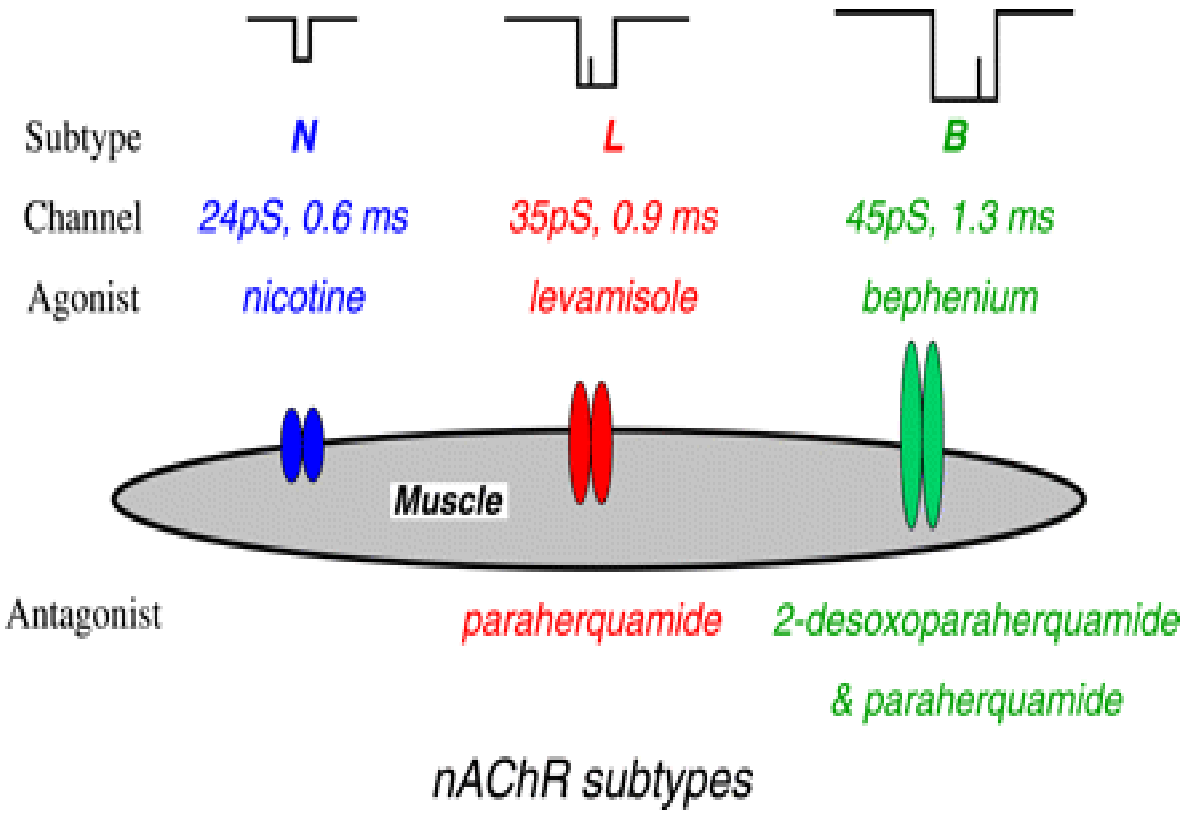

Figure 2.8 Three subtypes of nicotinic acetylcholine receptors in *A. suum* revealed by single-channel records.

The subtypes N, L and B are preferentially activated by nicotine, levamisole and bephenium respectively and correspond to the single-channel conductances 24pS, 35pS and 45pS respectively. From Qian *et al.* (2006).

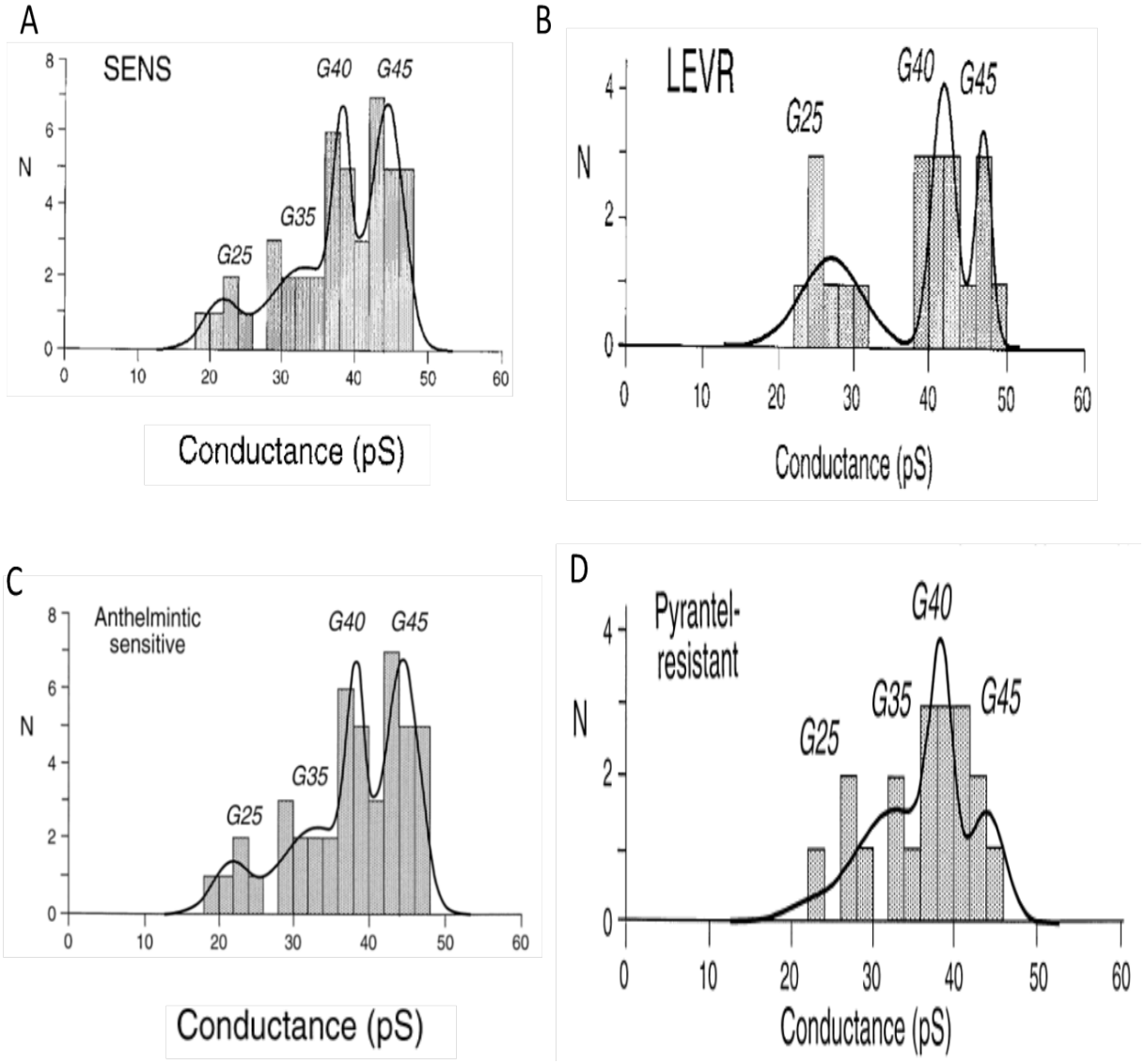

Figure 2.9 Diversity of *O. dentatum* levamisole receptors revealed by single-channel conductances.

(A) Frequency histogram of levamisole-activated conductance states in SENS worms. (B) Frequency histogram of levamisole-activated conductance states in LEVR worms. Note the absence of the G35 conductance state in the LEVR worms. (C) Frequency histogram of the conductance states in the levamisole-sensitive worms in (A). (D) Frequency histogram of the conductance states in pyrantel-resistant worms. From Robertson *et al*. (1999, 2000).

2.4 Voltage-activated calcium-dependent potassium channels

Voltage-activated potassium channels (K_v) are a family of potassium-selective ion channels with multiple members. Some members of the voltage-activated K^+ channel family have 6 transmembrane domains (6 TM; S1 – S6) (Kim *et al*., 1995; Yellen, 2002), such as the small conductance and intermediate conductance Ca^{2+}-activated K^+ channels. Other members have 2 TM domains; examples include the inward rectifiers and K_{ATP}. The voltage-activated calcium-dependent K^+ channels have 7 TM domains, an S0 domain in addition to the S1 – S6 domains of the standard voltage-activated K^+ channels. The gene that codes for these voltage-activated channels is referred to as KCN (Gutman *et al*., 2003; 2005). Figure 2.10A below illustrates the standard structure of the voltage-dependent K^+ channels.

Elkins *et al.* (1986) observed that voltage-clamp recordings of currents in the dorsal longitudinal flight muscles of mutant *Drosophila* with the *slowpoke* (*slo*) phenotype showed the absence of a Ca^{2+}-dependent K^+ current. This suggested that the *slo* gene codes for the Ca^{2+}-dependent K^+ channel. These channels are thus known as SLO-1, big conductance (Dworetzky *et al*., 1996) or maxi-K channels. They have an unusually large single-channel conductance, ~250 – 300 pS and are uniquely different in their requirement for depolarization and Ca^{2+} (Wei et al., 1994a; Kaczorowski et al., 1996). These 7 TM channels are distributed in excitable and non-excitable cells and are involved in maintaining the membrane potential of cells, tuning of cochlear hair cells, innate immunity, hormone secretion, and neurotransmitter release (Ghatta *et al*., 2006; Salkoff *et al*., 2006).

SLO-1/BK channels are homotetrameric or heterotetrameric, composed of four α-subunits alone or in association with the regulatory β-subunit (Knaus *et al*., 1994b). These channels

are localized on both the pre- and post-synapse in the nervous system. The regulatory β-subunit is composed of 2 putative TM domains, TM1 and TM2, connected by a large extracellular loop with intracellular N- and C-termini. Four conserved cysteines in the extracellular loop form disulfide linkages which induce conformational changes in the α-subunit that promotes binding of charybdotoxin (Knaus *et al*., 1994a; Hanner *et al*., 1998). Over four putative β-subunits have been identified, namely β1 from bovine tracheal smooth muscle (Garcia-Calvo *et al*., 1994; Knaus *et al*., 1994b), β2 from rat chromaffin cells (Wallner *et al*., 1999), β3 from testis (Brenner *et al*., 2000), rat insulinoma tumor cells and adrenal chromaffin cells (Xia *et al*., 1999), and β4 from brain (Brenner et al., 2000; Meera et al., 2000a). These β-subunits in different tissues regulate the properties of the α-subunits to meet the needs of the cells; these regulations include altering the pharmacological properties (McManus *et al*., 1995; Dworetzky *et al*., 1996), voltage dependence and gating of the channel (Brenner *et al*., 2000; Weiger *et al*., 2000; Ha *et al*., 2004), and the channels apparent calcium sensitivity (Wallner *et al*., 1995). The human BK channel β-subunit gene is designated KCNMB1.

The α-subunit is made up of a core and a tail; the 7 TM domains and intracellular domains S7 and S8 make up the core whilst intracellular domains S9 and S10 make up the tail (Magleby, 2003). A nonconserved linker connects the core and tail regions (Wei et al., 1994b). Both core and tail domains are separable and can be expressed independent of each other to form functional channels in *Xenopus* oocytes. The tail region contains the highly conserved aspartate residues forming the 'Ca^{2+} bowl' between S9 – S10 intracellular domains. In addition to the 'Ca^{2+} bowl' that confers the Ca^{2+} sensitivity to these channels, it has been demonstrated that Ca^{2+} can bind to other regions, such as the regulator of conductance for K^{+}

(Ludwig *et al*., 1999) between S7 and S8 (Xia *et al*., 2002). The Ca^{2+} for channel activation comes from either extracellular sources through voltage-activated Ca^{2+} channels or from intracellular stores, such as IP3 signaling pathway. Beside the 'Ca^{2+} bowl' at the C-terminus, there are other regulatory sites like leucines zipper domains for protein kinase A associations (Tian *et al*., 2003), phosphorylation sites for protein kinase C, tyrosine kinase (Wang *et al*., 1999a; Ling *et al*., 2000), cAMP- and cGMP-dependent protein kinases (Schubert and Nelson, 2001; Zhou *et al*., 2001; Ghatta *et al*., 2006).

Site-directed mutagenesis experiments suggest that arginine residues at every third position in the S4 domain confer voltage sensitivity to the channel (Papazian *et al*., 1991). Other reports suggest that the voltage sensitivity is also conferred by acidic residues in the S2 (Seoh *et al*., 1996) and S3 domains (Papazian *et al*., 1995; Ma *et al*., 2006). Residues like D153, E293, and R167 in the S2 domain and D186 in the S3 domain contribute to the voltage sensitivity of these channels. Located between S5 and S6 domains is the P-loop. This P-loop together with the S5 and S6 domains constitute the pore-forming motif. The receptors for the BK channel pore blockers iberiotoxin and charybdotoxin is in the P-loop (Ghatta *et al*., 2006). The channel pore opens in response to depolarizations that causes displacement of the charged residues in the S4 domain (Stefani *et al*., 1997; Horrigan and Aldrich, 2002).

In the nematode *C. elegans*, *slo-1* is expressed in body wall muscles and motorneurones (Wang *et al*., 2001; Carre-Pierrat *et al*., 2006). Two splice variants, *slo-1b* and *slo-1c*, that arise from alternative splicing have been identified in this model free-living nematode. The gene(s) that encode the mammalian BK channel β-subunit orthologue have not been identified in *C. elegans* or in any other nematode (Holden-Dye *et al*., 2007). *C. elegans* SLO-1 is involved in locomotion, feeding and reproduction. *C. elegans slo-1* loss of function

mutants has a jerky movement with increased reversals when compared to wild-type animals (Wang *et al*., 2001; Guest *et al*., 2007). SLO-1 in these nematodes appears to have an inhibitory role on neurotransmission. The presence of tetraethylammonium (TEA) and 4-aminopyridine (4-AP) sensitive potassium channels in *A. suum* was demonstrated by Martin *et al.* (1992). Subsequently, Verma *et al.* (2009) reported that these voltage-activated K^+ currents were Ca^{2+}-dependent, demonstrating the presence of SLO-1/BK channels in *A. suum*.

A

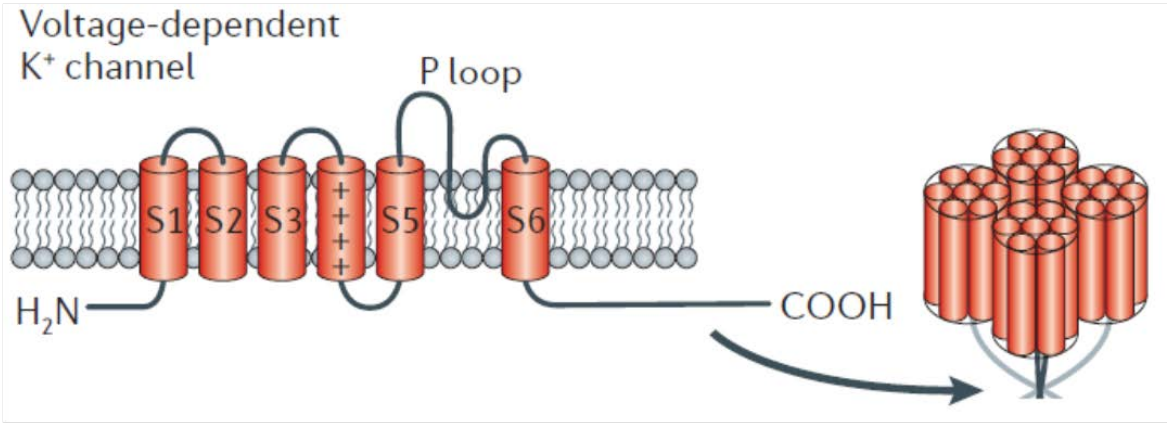

B

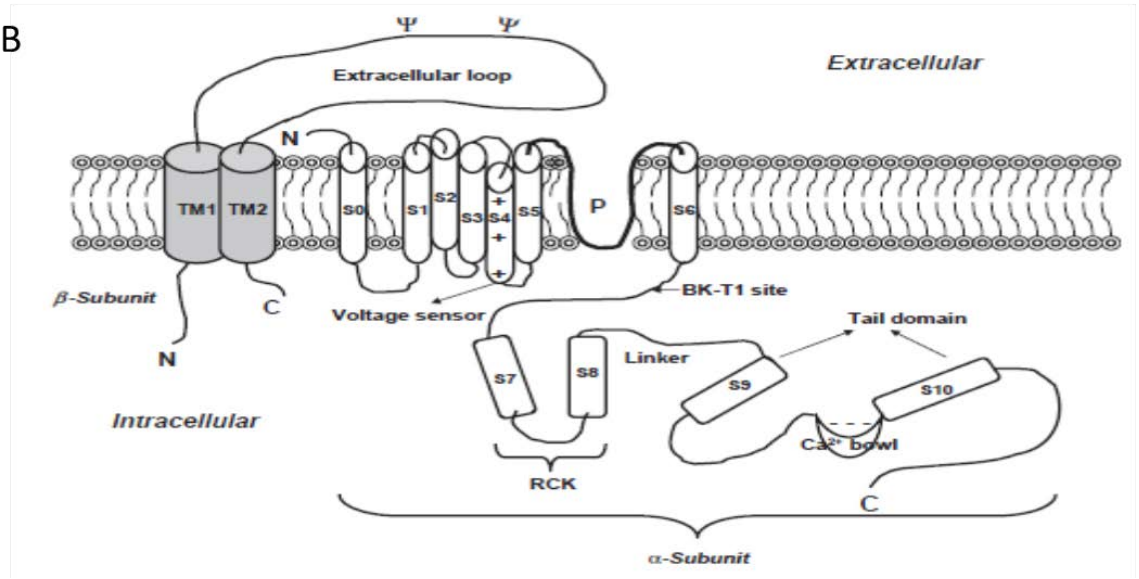

Figure 2.10 Schematic representation of the structure of voltage-activated K^+ channels.

(A) The standard voltage-activated K^+ channels have 6 TM domains, S1 – S6, and intracellular NH2 and COOH termini. (B) The voltage-activated Ca^{2+}-dependent K^+ channels have an S0 domain in addition to the 6 TM domains, a large intracellular C-loop, an extracellular N-termini and/or a regulatory β-subunit. From Salkoff *et al.* (2006) and Ghatta *et al.* (2006).

2.5 Anthelmintics and anthelmintic resistance

Most of the currently marketed anthelmintics act on the neurons and muscles of nematodes. The ion channels in these nematodes are attractive targets for these anthelmintics because of the quick onset of effects and the relatively selective action on the parasites (Wolstenholme, 2011). Some important differences between these ion channels in the parasites and the vertebrate hosts partly accounts for the selective effects of these anthelmintics. These anthelmintics are the main bastions of defense in the treatment of parasitic nematode infections.

2.5.1 Emodepside

Whilst screening for new anthelmintics with the poultry parasitic nematode *Ascaridia galli* as a test organism, Sasaki *et al.* (1992) discovered the cyclooctadepsipeptide PF1022A. This cyclooctadepsipeptide is isolated from the cultured fungus *Mycelia sterilia* that grows on the leaves of the shrub *Camellia japonica*. This shrub grows mainly in Japan and is sometimes known as the rose of winter; figure 2.11A. PF1022A is a neutral, colorless compound with the molecular formula $C_{52}H_{76}N_4O_{12}$ that melts between 104 – 106^{o}C. IR spectra of PF1022A showed the presence of amide and ester functions, figure 2.11B. It consists of two D-phenyl lactic acids, two D-lactic acids and four N-methyl-L-leucines in L-D-L configuration of cyclic octadepsipeptide (Harder *et al.*, 2005). At 2 mg/kg, PF1022A was effective against *Ascaridia galli* without exhibiting any toxic effects in the hosts. Additionally, no acute toxicity effects were observed when 1 g/Kg or 2 g/Kg (po) PF1022A was administered to

mice. It showed no activity against yeasts, fungi, Gram-positive and Gram-negative bacteria when tested at 100 µg/ml. Conder *et al.* (1995) observed that PF1022A was more potent at inhibiting motility of *Haemonchus contortus* than albendazole (a benzimidazole), ivermectin (a macrocyclic lactone) and levamisole (a cholinomimetic). Measurement of ATP levels indicated PF1022A inhibited *H. contortus* motility without causing parasite death. In addition to *H. contortus,* PF1022A showed activity against *Ostertagia ostertagi* and *Trichostrongylus colubriformis*, (Conder *et al*., 1995), *Heligmosomoides polygyrus*, *Trichinella spiralis*, *Heterakis spumosa*, and *Nippostrongylus brasiliensis* (Martin *et al.*, 1996a). Administration of PF1022A by routes other than oral (that is, parenteral) reduced its efficacy against *O. ostertagi* and *T. colubriformis*. PF1022A did not antagonize levamisole effects in current-clamp recordings in *Ascaris suum*, suggesting PF1022A may not exert its effects on nicotinic acetylcholine receptors.

To overcome the reduced activity when PF1022A was administered parenterally rather than orally and to increase other pharmacokinetic properties, two morpholine rings were attached to PF1022A at the phenyllactic acid position to synthesize emodepside (Bay 44-4400). Emodepside is therefore a semisynthetic derivative of PF1022A, figure 2.11C. Emodepside is currently available on the market as a formulation with praziquantel (Profender®) and toltrazuril (Procox®) for use in cats and dogs to treat parasitic helminthes, figure 2.11D. According to von Samson-Himmelstjerna *et al.* (2005), both PF1022A and emodepside are effective against benzimidazole-, ivermectin- and levamisole-resistant *H. contortus* in sheep and against ivermectin-resistant *Cooperia oncophora* in cattle, demonstrating the 'resistance-overcoming' property of both cyclooctadepsipeptides. Both cyclooctadepsipeptides were effective at reducing fecal egg counts and/or worm counts in both populations of parasites.

Schurmann *et al.* (2007) further demonstrated the inhibitory effects of emodepside and PF1022A on egg hatching and larval motility of several species of parasitic nematodes. In the free-living nonparasitic nematode, *Caenorhabditis elegans*, emodepside has been demonstrated to inhibit egg-laying, locomotion, and feeding by paralyzing body wall muscles and pharyngeal muscles (Harder *et al*., 2003; Willson *et al*., 2004; Bull *et al*., 2007). In *Ascaris suum*, emodepside caused a calcium-dependent membrane hyperpolarization, muscle relaxation, and inhibition of muscle contraction elicited by ACh and AF2 (Willson *et al*., 2003). Furthermore, emodepside has shown promise as an alternative drug for treating Onchocerciasis (Hudson and Nwaka, 2007; Boussinesq, 2008).

Available evidence suggests that the cyclooctadepsipeptides PF1022A and emodepside do not act at the same target site as the mainstay anthelmintics. Early investigation into the target site for PF1022A by Saeger *et al.* (2001) led to the identification of a *Haemonchus contortus* 3539 bp cDNA that encodes an orphan heptahelical transmembrane 110 kDa-receptor. The receptor, HC110-R is bound at the extracellular N-terminal side by alpha-latrotoxin, causing Ca^{2+} influx through Ca^{2+} channels. Alpha latrotoxin is the ligand of the latrophilin receptor. PF1022A binding to the N-terminal region of this receptor antagonizes latrotoxin signaling. Welz *et al.* (2005) reported identification of homologs of HC110-R in *Cooperia onchophora* and *Ostertagia ostertagi* which these authors termed depsiphilins. These depsiphilins and HC110-R are putative G protein-coupled receptors (GPCR) related to the mammalian latrophilin receptor. According to Willson *et al.* (2004), emodepside causes paralysis of the pharynx of *C. elegans* primarily by targeting neuronal latrophilin-like receptors (*lat-1*). Worms with a *lat-1* gene knock-out were found to be resistant to

emodepside. These authors also reported that pharynxes of worms with reduction or loss-of-function mutation in Gq, UNC-13 and phospholipase C-β (PLC-β) are resistant to emodepside. A latrophilin-like receptor in nematodes therefore appears to be an effector for emodepside and PF1022A (Harder *et al*., 2003). Binding of emodepside to a presynaptic latrophilin-like receptor may result in activation of Gqα and PLC-β. Diacylglyerol (DAG), a cleavage product of PLC-β action activates UNC-13 and synaptobrevin, leading to the release of a neurotransmitter that exerts its effects at the post-synaptic terminal (Harder *et al*., 2005).

However, Guest *et al.* (2007) observed that whilst a *C. elegans lat-1* null mutant is less sensitive to the inhibitory effects of emodepside on the pharynx, it was sensitive to the inhibitory effects of emodepside on locomotion. This led to the search for another effector or target molecule for emodepside. These authors reported recovery of nine alleles of a Ca^{2+}-activated K^+ channel gene, *slo-1*. Mutants of the *slo-1* were resistant to the inhibitory effects of emodepside on locomotion and pharyngeal pumping, strongly suggesting that the Ca^{2+}-activated K^+ channel is another and perhaps the main effector of emodepside effects.

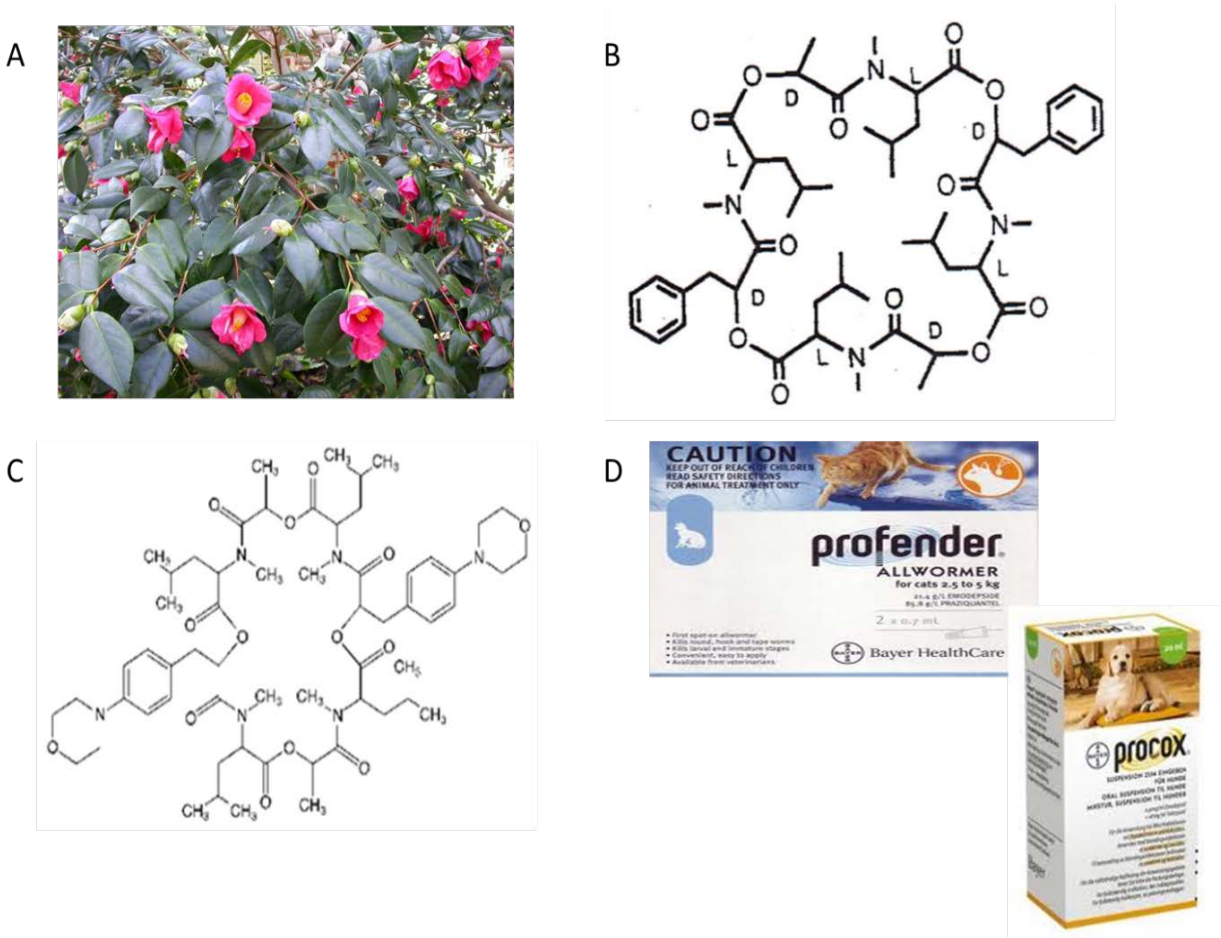

Figure 2.11 The Cyclooctadepsipeptide, PF1022A and the semisynthetic analog, emodepside. (A) *Camellia japonica*, the 'winter rose' shrub on which grows *Mycelia sterilia* from which PF1022A was extracted. Accessed from Missouri Botanical Garden, www.missouribotanicalgarden.org/gardens-gardening/your-garden/plant-finder/plant-details/kc/b546/camellia-japonica.aspx on 02-10-12 at 2:55pm CST. (B) Structure of PF1022A, the parent compound for emodepside. From Sasaki *et al.* (1992). (C) Structure of emodepside, showing the two morpholine rings attached at the phenyllactic acid positions of PF1022A. Accessed from Bayer HealthCare:Science for a better life, www.animalhealth.bayerhealthcare.com/3519.0.html?&tx_bahprdmx_pi[showUid]=81&cHash=44b75885b7 on 02-09-12 at 3:00pm CST. (D) Profender ® and Procox ®, emodepside

formulations approved for use in cats and dogs, respectively. Accessed on VET-MAGAZIN.de at 3:00pm CST on 02-09-12.

2.5.2 Levamisole, pyrantel, tribendimidine

Levamisole, pyrantel and tribendimidine are anthelmintics that act as agonists of the nicotinic receptors located on parasitic nematode somatic muscles (Harrow and Gration, 1985b; Martin, 1997; Martin and Robertson, 2007). Levamisole was introduced in the 1960s to treat parasitic nematode infections in humans and livestock animals. Levamisole is effective in treating Ascariasis in children (Lionel *et al*., 1969). It is the L-isomer of tetramisole, a synthetic compound. According to Aceves *et al.* (1970), tetramisole paralyzes live *Ascaris* in 3 min, causes sustained contraction of and depolarizes *Ascaris* somatic muscle. Pyrantel is used to treat roundworms, pinworms, and hookworms. Levamisole is an imidazothiazole whilst pyrantel is a tetrahydropyrimidine.

Both of these anthelmintics increases the input conductance and depolarizes *A. suum* muscle bags. Dose-conductance relationships suggested that pyrantel is more potent than levamisole (Harrow and Gration, 1985b). The reversal potential determined for pyrantel and levamisole were similar to the reversal potential for ACh, suggesting that both anthelmintics acted on the same cation channels as ACh. Levamisole and pyrantel act on synaptic and extrasynaptic nicotinic acetylcholine receptors. Because these drugs are not degraded by acetyl cholinesterase, they cause spastic paralysis of the parasitic worm. Levamisole and pyrantel are open-channel blockers at high concentrations and hyperpolarized potentials (Robertson and Martin, 1993a; Robertson et al., 1994). Contraction assays and larval migration studies

suggest that levamisole and pyrantel are selective for the L-type receptor (Robertson *et al*., 2002; Martin *et al*., 2003).

According to Hu *et al.* (2009), tribendimidine also acts on the L-type acetylcholine receptor. Tribendimidine was developed by the Chinese National Institute of Parasitic Diseases in the 1980s and is already approved for human use (Xiao *et al*., 2005). Laboratory studies have demonstrated the broad-spectrum anthelmintic efficacy of tribendimidine (Li et al., 2011; Sripa and Hong, 2011; Tritten et al., 2012).

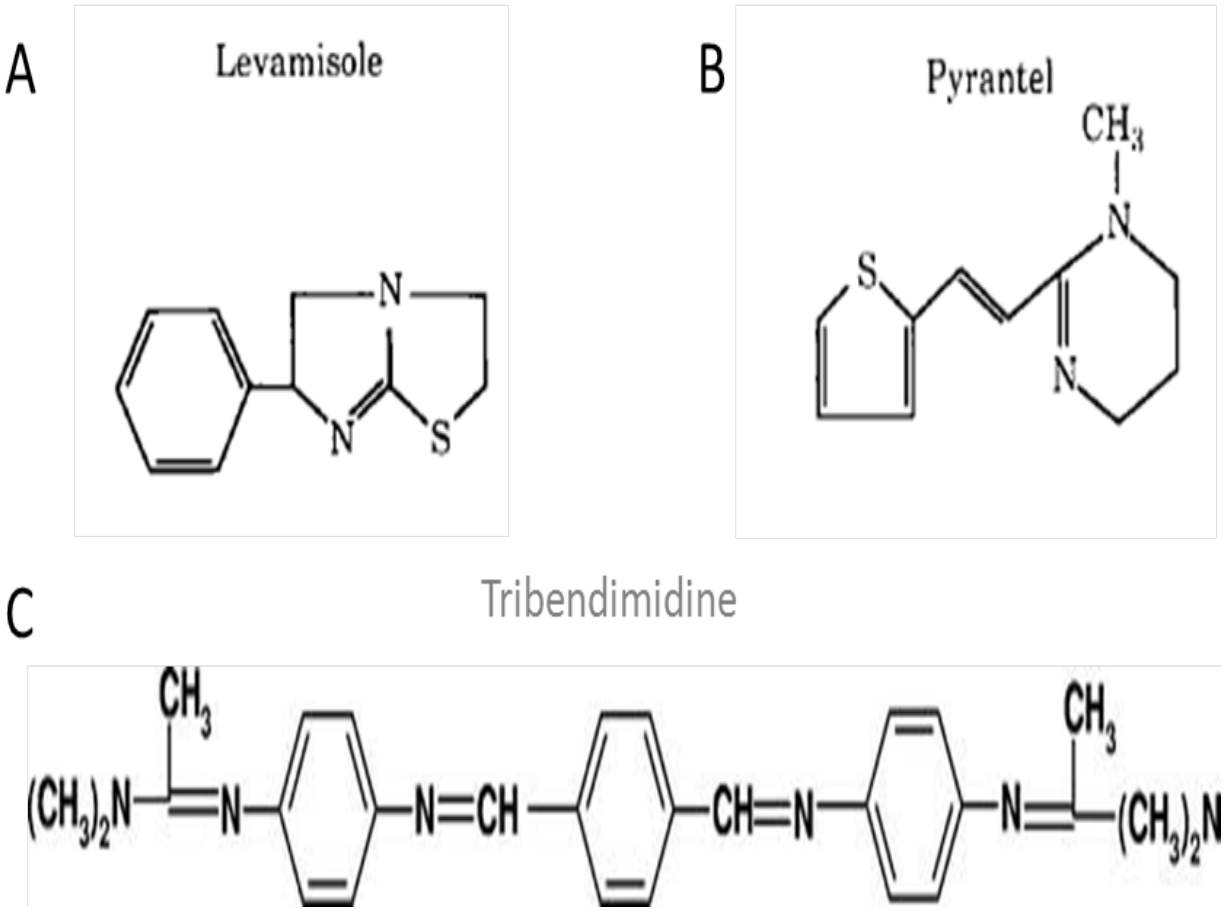

Figure 2.12 Chemical structures of levamisole (A), pyrantel (B) and tribendimidine (C). From Hu *et al*. (2009) and Martin & Robertson (2007).

2.5.3 Anthelmintic resistance

Resistance to drugs is a not a new phenomenon. Generally, a reduction in the effectiveness of a drug to cure a disease or kill parasites is referred to as drug resistance. According to Sangster and Gill (1999) and Prichard *et al.* (1980), anthelmintic resistance develops when more individuals in a parasite population that were hitherto affected by a given drug dose/concentration become unaffected or when there is a decline in the efficiency of a drug against a hitherto susceptible parasite population. This definition does not however suggest what causes the decline in the efficiency of a drug. An alternative definition of anthelmintic resistance that points to an origin states that anthelmintic resistance is "the genetically transmitted loss of sensitivity in worm populations that were previously sensitive to the same drug" (Köhler, 2001). This definition underscores the importance of genetics to drug resistance. Resistance to the anthelmintics used to treat parasitic helminth infections in livestock and companion animals is a well-documented problem. There are also reports of anthelmintic resistance in some human parasitic helminthes. For example, there are reports of praziquantel resistance in human Schistosomes (Cioli *et al*., 1995; Liang *et al*., 2000) and tetrahydropyrimidine resistance in human hookworms (Reynoldson *et al*., 1997). Resistance to most of these anthelmintics was reported as early as 3 – 10 years after their introduction. Figure 2.13 below illustrates the time after introduction of some anthelmintics till the first report of resistance. For example, resistance to thiabendazole, a benzimidazole was reported in 1964, about 3 years after its introduction. Because anthelmintic resistance is an economic

problem of tremendous importance, detecting resistance at the early stage is necessary in preventing an "endemic" problem. Usually, the first sign of resistance is treatment failure.

According to Wolstenholme *et al.* (2004), anthelmintic resistance arises through a limited number of ways, namely: (i) drug target modification; (ii) increase or change in drug metabolism, resulting in inactivation, removal or prevention of drug activation; modification in drug distribution, reducing accessibility to target tissues; and/or (iv) target gene amplification in order to overcome drug action. Receptor loss or decrease in target site affinity for anthelmintics appears to be major mechanisms helminthes use to acquire resistance (Köhler, 2001). Worth noting here is the distinction between drug resistance and intrinsic variations in drug sensitivity that is the result of: (i) variation in sensitivity at different stages of the parasites life cycle; (ii) variation in drug sensitivity between male and female parasites; variation in sensitivity by the same parasite species in different hosts; and (iv) variation in sensitivity between different species of a parasite (Sangster and Gill, 1999).

There are biochemical and electrophysiological basis for anthelmintic resistance. Some Single Nucleotide Polymorphisms (SNP) has been associated with anthelmintic resistance. A single nucleotide change usually leads to a change in the amino acid of the target site protein that alters the drug affinity. An example of SNP is found in benzimidazole (BZ) resistance. In *Haemonchus contortus, Teladorsagia circumcincta, Trichostrogylus colubriformis* and cyathostomins from horses, phenylalanine – tyrosine polymorphism at codon 167 of β-tubulin isotype 1 (F167Y) reduces affinity for BZ. Phenylalanine – tyrosine polymorphism at codon 167 of β-tubulin isotype 2 and at codon 200 of β-tubulin isotype 2 (F200Y) also reduces affinity for BZ in *H. contortus* (Kwa *et al*., 1994; Prichard, 2001; Silvestre and Cabaret, 2002). Increase in transport proteins that increases efflux of anthelmintics also lead

to resistance. P-glycoprotein (Pgp), a large, 170 kDa integral membrane protein that belongs to the ATP-binding cassette (ABC) transporter superfamily has been associated with multidrug resistance (MDR) in humans (Zhou, 2008) and helminthes (Blackhall *et al*., 1998; Xu *et al*., 1998; Sangster *et al*., 1999; Le Jambre *et al*., 2000; Kerboeuf *et al*., 2003). Several Pgps have been linked to BZ resistance in *H. contortus*.

Changes in the electrophysiological properties of nAChRs and mutations in nAChR subunit genes have been associated with resistance to levamisole and pyrantel. Robertson *et al.* (1999) demonstrated although levamisole-sensitive (SENS) and levamisole-resistant (LEVR) strains of *O. dentatum* contained the same number of receptors in muscle patches, the LEVR strain contained lower active patches. Furthermore, the mean open time for these channels and the probability of channel opening were reduced in the LEVR patches. Another striking distinguishing feature was the absence of one of the channel conductance states in the LEVR worms. In a related study, it was demonstrated that pyrantel-resistant *O. dentatum* had reduced probability of channel opening and percentage of active patches when compared with drug sensitive worms (Robertson *et al*., 2000). These results demonstrate that these parasites can change their receptor populations and/or properties to reduce the response to cholinergic anthelmintics. Indeed, a loss in nicotinic receptor aggregation due to mutation in *lev-10* plays a role in levamisole resistance (Qian *et al*., 2008).

Table 3 Examples of resistance mechanisms to the mainstay anthelmintic classes

Anthelmintic family	Resistance mechanism	Examples of parasites
Benzimidazoles	β-tubulin isotype 1 mutations: F200Y, F167Y β-tubulin isotype 2 mutations: F200Y, F167Y, deletion. Altered metabolism and or uptake.	*H. contortus, T. colubriformis, T. circumcincta, Fasciola hepatica*
Avermectins and milbemycins	Mutations in GluCl and/or GABA-R genes. Overexpression of P-glycoproteins	*Oesophagostomum spp,* sheep & cattle trichostrongyloids
nAChR agonists	Changes in nicotinic acetylcholine receptors	*H. contortus, O, dentatum,* small strongyles of horses

Modified from Wolstenholme *et al* (2004) and Sangster & Gill (1999)

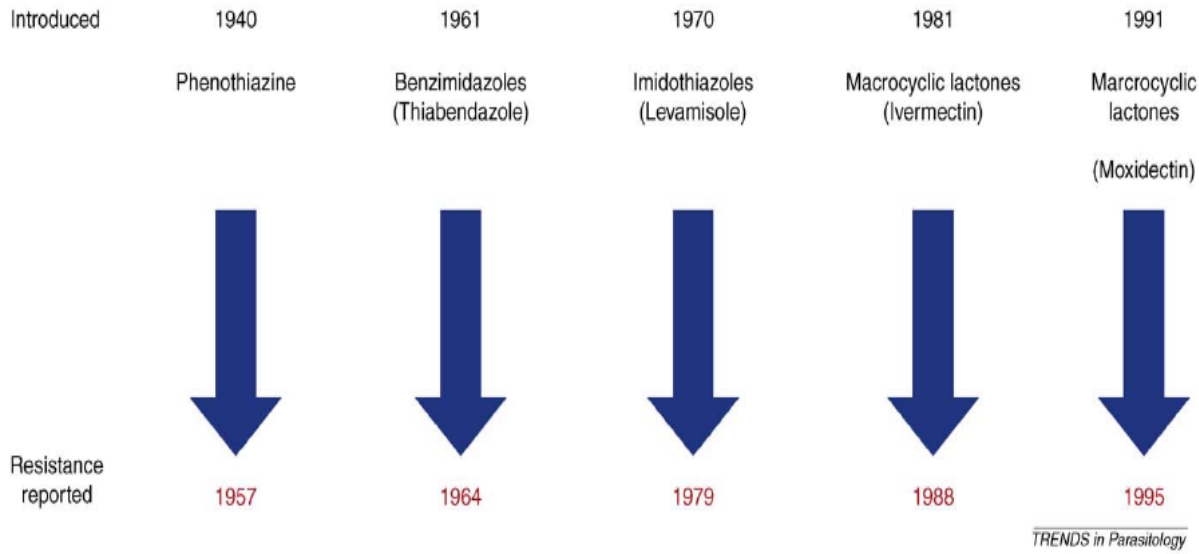

Figure 2.13 Timeline of introduction to first report of anthelmintic resistance.

From James *et al.* (2009)

2.6 Heterologous expression systems: *Xenopus laevis* oocytes

Heterologous (another 'organism') expression is the identification and expression of genes (DNA) in hosts/organisms different from the source of the genetic material. Heterologous expression has been used for a long time to study proteins and characterize ion channels and receptors. There are different types of expression systems, from yeast, *Escherichia coli*, and mammalian cell lines to *Xenopus laevis* oocytes. Certain factors determine the choice of an expression system, principal among them is the outcome of a study; whether the outcome is production of large quantities of protein or characterization of a receptor in the plasma membrane (Yesilirmak and Sayers, 2009). One of the most widely used expression systems is *Xenopus laevis* oocytes. *Xenopus laevis* oocytes have 6 growth stages, stages I to VI (Dumont, 1972). These oocytes are stored in the frog abdominal membrane with connective tissues, follicular cells and blood vessels. All growth stages of the oocytes are found in the ovary at any time. The size of oocytes at the different growth stages is a distinguishing factor, as well as the level of pigmentation (Weber, 1999). The stage V or VI oocytes are 1 to 1.2 mm in diameter with a clear difference between the dark animal pole and the white, non-pigmented vegetal pole. Stage V and VI oocytes are used for most electrophysiological studies but to study currents with fast kinetics, the smaller stage IV oocytes are preferable. The shape of oocytes is maintained by the vitelline membrane, which surrounds the plasma membrane. The vitelline membrane is devoid of ion channels and therefore does not affect electrophysiological experiments. However, it must be removed before patch-clamp recordings of oocytes because it prevents the formation of high resistance gigaseal between the oocyte and patch electrode. On the other hand, the follicular layer which surrounds the

vitelline membrane expresses ion channels, transporters (Miledi and Woodland, 1989a, 1989b) and is coupled to the oocytes by gap junctions (Browne and Werner, 1984). This must therefore be removed before conducting electrophysiological recordings.

The first observation that foreign RNA injected into oocytes from the South African frog, *Xenopus laevis*, can be translated into proteins was made by Gurdon and colleagues (1971). *X. laevis* oocytes are probably the simplest system for expressing receptors/ion channels (Buckingham *et al*., 2006). Early studies that used *X. laevis* oocytes dealt with proteins like globin, interferon and viral proteins that are of little interest to electrophysiologists (Laskey *et al*., 1972; Laskey and Gurdon, 1973; Gurdon *et al*., 1974; Laskey and Gurdon, 1974; Woodland *et al*., 1974). The first use of oocytes for expression of receptors and ion channels can be traced to the 1980s when these oocytes were used to express acetylcholine receptors, serotonin receptors and GABA receptors (Miledi *et al*., 1982a, 1982b; Gundersen *et al*., 1983; Miledi *et al*., 1983). Following these earlier studies, oocytes from the South African clawed-frog have been used to express and study different ligand-gated ion channels (LGIC). These oocytes are a very convenient expression system for LGIC following mRNA injection and for studying the effects of candidate ligands or drugs. Oocytes can efficiently translate exogenous mRNA microinjected into them because they contain stores of enzymes, organelles and proteins normally used after fertilization (Gurdon *et al*., 1971; Gurdon, 1973; Gurdon *et al*., 1973). The large size of these oocytes makes microinjection of complementary RNA or DNA and subsequent electrophysiological recordings relatively easy. Injection of cDNA into oocytes is technically more difficult because it requires locating the nucleus and the risk of damaging the nuclear membrane during microinjection is a concern. Different electrophysiological techniques can be employed to record from *X. laevis* oocytes but the

most commonly used and simplest method is perhaps the two-electrode voltage-clamp (Stuhmer and Parekh, 1995). Beside these, other advantages like the fact that *X. laevis* is a low-cost laboratory animal easily maintained in captivity and the possible simultaneous injection of different cRNAs or cDNAs makes them even more attractive as expression systems for studying ion channels and receptors.

As an expression system, *Xenopus* oocytes are not without their limitations. *Xenopus* oocytes are best kept at 19^{o}C or 20^{o}C, although they can be kept at lower temperatures (like 4^{o}C) but not at higher temperatures because they die quickly. This limitation must be considered when using these oocytes to study temperature-sensitive mutant proteins. *Xenopus* oocytes endogenously express a number of anionic and cationic channels, such as Ca^{2+}-activated Cl^{-} channels (Gomez-Hernandez *et al*., 1997; Callamaras and Parker, 2000), K^{+} channels (Lu *et al*., 1990; Parker and Ivorra, 1990; Brochiero *et al*., 2001), Na^{+} channels (Krafte and Volberg, 1992; Bossie *et al*., 1998), non-selective cation channels (Ludwig *et al*., 1999), and last but not least, hyperpolarization-activated Cl^{-} channels. These endogenous ion channels may interfere with the expression and studies of certain ion channels or proteins either by being upregulated by the expression of exogenous proteins or by forming heteromultimers with exogenous proteins expressed by the oocytes. Reports of seasonal variations in the quality of oocytes (Lafaire and Schwarz, 1986), a phenomenon that we have also observed in our laboratory, plus seasonal variation in the membrane potential of oocytes (Sigel, 1990) must be considered when performing experiments with this expression system.

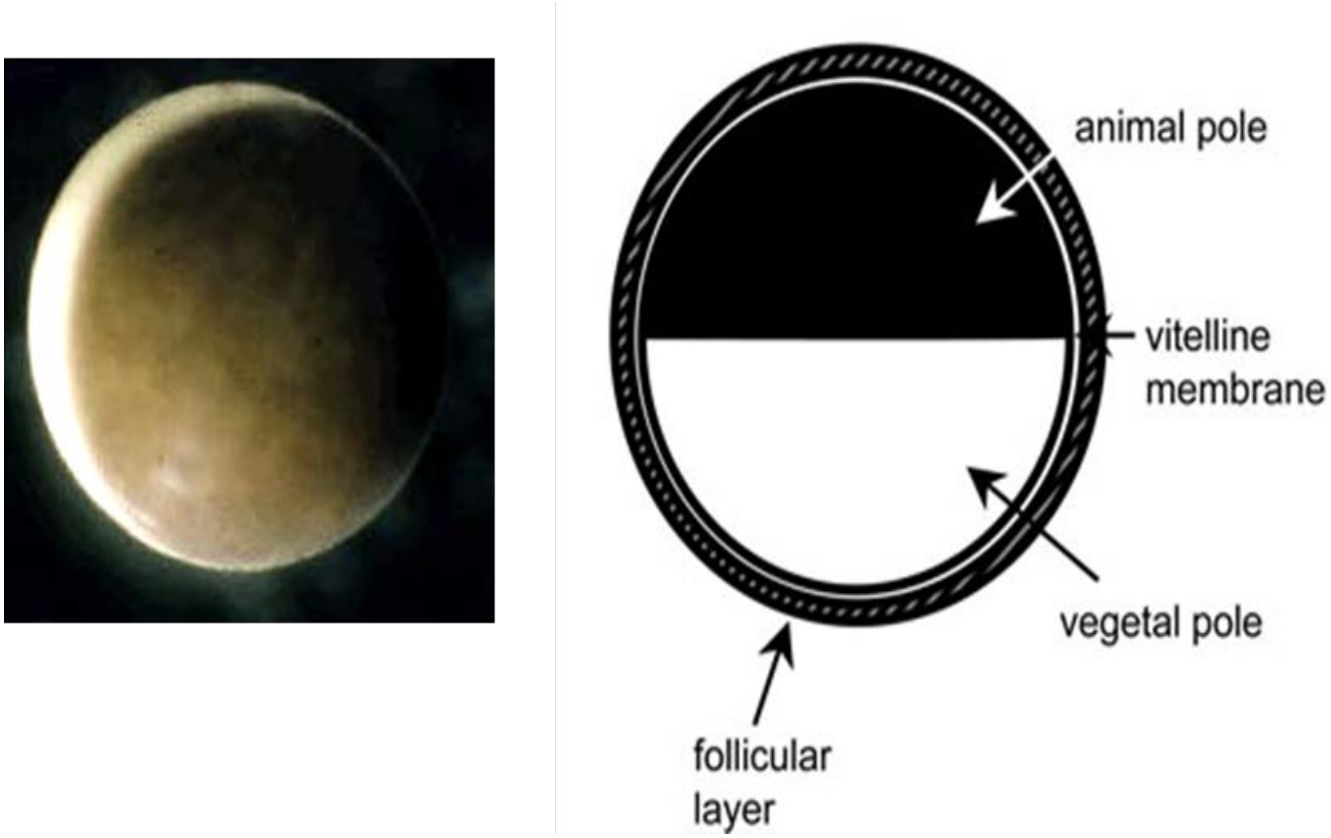

Figure 2.14 Structure of *Xenopus laevis* oocyte.

Right: defolliculated single oocyte, left: diagram showing the two poles, vitelline membrane and folliulcar layer of *X. laevis* oocytes. Modified from (Bianchi and Driscoll, 2006).

CHAPTER 3 On the mode of action of emodepside: slow effects on membrane potential and voltage-activated currents in *Ascaris suum*

Modified from paper published in the *British Journal of Pharmacology* (2011)

SK Buxton[2, 4], C Neveu[3, 4], CL Charvet[3, 4], AP Robertson[4] & RJ Martin[4, 5]

3.1 Abstract

Anthelmintics are required for treatment and prophylaxis of nematode parasites of humans and domestic animals. Emodepside, a cyclooctadepsipeptide, is a modern anthelmintic that has a novel mode of action involving a Ca^{2+}-activated K^+ channel (SLO-1) in *Caenorhabditis elegans*, sometimes mediated by a latrophilin (LAT) receptor. We examined mechanisms of action of emodepside in a parasitic nematode, *Ascaris suum*. RT-PCR was used to investigate expression of *slo-1* and *lat-1* in *A. suum* muscle flaps, and two-micropipette current-clamp and voltage-clamp techniques were used to record electrophysiological effects of emodepside. Expression of *slo-1* and *lat-1* were detected. Emodepside produced a slow time-dependent (20 min), 4-aminopyridine sensitive, concentration-dependent hyperpolarization and increase in voltage-activated K^+ currents. Sodium nitroprusside increased the hyperpolarizations and K^+ currents. N-nitro-L-arginine inhibited the hyperpolarizations and K^+ currents. Phorbol-12-myristate-13 acetate increased the K^+ currents, while staurosporine inhibited the hyperpolarizations and K^+ currents. Iberiotoxin reduced these emodepside K^+ currents. The effect of emodepside was reduced in Ca^{2+}-free solutions. Emodepside had no effect on voltage-activated Ca^{2+} currents. *Asu-slo-1* and *Asu-lat-1* are expressed in adult *A. suum* muscle flaps and emodepside produces slow activation of voltage-activated Ca^{2+}-dependent SLO-1-like K^+ channels. The effect of emodepside was enhanced by stimulation

of protein kinase C and NO pathways. The data are consistent with a model in which NO, PKC and emodepside signaling pathways are separate and converge on the K^+ channels, or in which emodepside activates NO and PKC signaling pathways to increase opening of the K^+ channels.

---

[1] Reprinted with permission of *British Journal of Pharmacology* (2011), **164**, 453-470
[2] Graduate student and primary researcher
[3] Assisted with the molecular biology aspect
[4] Contributed equally in writing the manuscript
[5] Corresponding author and Professor, Dept. Biomedical Sciences, Iowa State University

3.2 Introduction

Parasitic nematode infections, classed as neglected tropical diseases, remain a problem in both human and veterinary medicine. The estimated global prevalence of parasitic nematode infections in humans is over two billion and the global prevalence of ascariasis alone is over 800 million (Hotez et al., 2007; 2008). These parasites are debilitating to humans, causing lost work days, cognitive impairment and poor growth; they also depress agricultural production and food supply. Ascariasis is caused by *Ascaris lumbricoides* in humans: this parasite is nearly identical to the parasite, *Ascaris suum* of pigs which is a good model of the human parasite *A. lumbricoides*. In the absence of effective vaccines and adequate hygiene, anthelmintic drugs are used for treatment and prophylaxis. However, there have been reports of growing resistance to the classic anthelmintic drugs: benzimidazoles (albendazole), nicotinic agonists (levamisole/pyrantel) and macrocyclic lactones (ivermectin) (Prichard, 1990; 1994; Sangster and Gill, 1999; Sangster, 2001; Kaplan, 2002; Wolstenholme *et al*., 2004; Martin and Robertson, 2007; James *et al*., 2009). More recently, novel 'resistance-busting' anthelmintics (emodepside, a cyclooctadepsipeptide; monepantel, an amino-

acetonitrile derivative, and derquantel, a paraherquamide derivative) have been released onto the market. The need for the new anthelmintics and ways to combat resistance to the currently available anthelmintics cannot be overstated.

Sasaki *et al.* (1992) reported the isolation of the cyclooctadepsipeptide PF1022A from cultured *Mycelia sterilia*, a fungus found on the leaves of *Camellia japonica*. Emodepside is a semisynthetic analogue of PF1022A made by attaching two morpholine rings at the para position of the two phenyllactic acids (Harder *et al*., 2005) in order to enhance pharmacokinetic properties. Both emodepside and PF1022A have been shown to be effective against benzimidazole-, levamisole- and ivermectin-resistant nematode parasite isolates (Samson-Himmelstjerna von *et al*., 2005), and to be effective against a wide range of nematode parasites (Schurmann *et al*., 2007).

Wilson *et al. (2003)* reported that in *A. suum*, emodepside caused muscle relaxation and a 4-aminopyridine sensitive, calcium-dependent hyperpolarization of body wall muscle cells. The similarity of this response to that of the inhibitory neuropeptides PF1/PF2 led to the suggestion that emodepside may be acting at the neuromuscular junction to release an inhibitory neuropeptide with similar action to the neuropeptide PF1/PF2.

Two molecular effectors have been implicated in the mode of action of emodepside. The first, a latrophilin-like receptor, HC110-R, co-precipitated with PF1022A and was cloned from *Haemonchus contortus* (Saeger *et al*., 2001). Here it is interesting to note that FMRFamide-like neuropeptides like PF2 have been tested and found to act as ligands of HC110-R (Muhlfeld *et al*., 2009). However observations using latrophilin gene knockouts in *C. elegans*, found that emodepside still depressed locomotion but that in the pharyngeal muscle inhibitory effects were reduced (Willson et al., 2003; Guest et al., 2007). The

observations suggest that a latrophilin receptor is involved in the response to emodepside in the pharyngeal feeding circuit, but that other molecular effectors are also involved in the inhibition of locomotion. The second emodepside effector was identified in mutagenesis screens in *C. elegans*. These delivered multiple alleles of the voltage-gated calcium-sensitive potassium channel gene, *slo-1*, such that *slo-1* loss-of-function mutants were discovered to be resistant to the pleiotropic effects of emodepside on reproduction, locomotion and feeding. Effects of emodepside on the voltage-activated currents in a parasitic nematode have not been studied. Here, we find evidence of the expression of SLO-1 and LAT-1; we use current- and voltage-clamp electrophysiological techniques to investigate the mode of action of emodepside on membrane potential and voltage-activated currents in *Ascaris suum* as an example of a parasitic nematode. We find that emodepside activates K currents with SLO-1-like properties with effects being enhanced by PKC and NO signaling pathways.

3.3 Materials and Methods

3.3.1 Collection and Maintenance of worms

A. suum were collected weekly from Tyson Foods Inc. pork packing plant, Flindt Drive, Storm Lake, IA and from JBS Swift and Co. pork processing plant, Marshalltown, IA, USA. The adult worms were kept in Locke's solution (NaCl 155 mM, KCl 5 mM, $CaCl_2$ 2 mM, $NaHCO_3$ 1.5 mM, glucose 5 mM) at 32^{o}C. The solution was changed twice a day and the worms were used within 4 days of collection.

3.3.2 Sequence and gene expression analysis

Database searches were performed with the BLAST Network Service (NCBI), using the tBLASTn algorithm (Altschul *et al*., 1997). Signal peptide predictions were carried out using the Signal P 3.0 server (Bendtsen *et al*., 2004). Conserved protein domains as well as membrane-spanning regions were predicted using the SMART program (Schultz *et al*., 1998). Total RNA was prepared from body muscle flaps (see below) from *A. suum* adult worms using Trizol reagent (Invitrogen) by following the manufacturer's recommendations. RNA pellets were dissolved in 100 µl of RNAsecure resuspension solution (Ambion) and were DNase treated with the TURBO DNA-free kit (Ambion). The RNA concentration was measured using a nanodrop spectrophotometer (Thermo Scientific, Waltham, Massachusetts, USA). First strand cDNA synthesis was performed on 5 µg of total RNA using the oligo (dT) RACER primer (Invitrogen) and the superscript III reverse transcriptase (Invitrogen) according to the manufacturer's instructions. Reverse transcription-PCR experiments were carried out on first strand cDNA using two rounds of nested PCR, in a final volume of 20 µl, containing 200 ng of first-strand cDNA (or 1 µl of 1/100 dilution of amplification product from the first round of PCR), 1U of GoTaq polymerase (Promega), 0.25mmol/l dNTPs each and 0.3 µmol/l of each primer. Primer sequences used for RT-PCR experiments are provided in supplemental table 1. The reaction mixture was denatured by heating at 94°C for 5 min, followed by 33 cycles at 94°C for 45 s, 56°C for 45 s and 72°C for 45 s. A final extension step was performed at 72°C for 5 min. Amplification products were cloned in pGEM vector (Promega) and sequenced by GATC biotech (Konstanz, Germany).

3.3.3 Somatic muscle preparation

The anterior portion of the worm about 4 cm away from the head was used in all recordings. About 1 cm of this part of the worm was cut-out and the resulting cylindrical worm piece was cut open along a lateral line to form a muscle flap. The gut was removed to expose the muscle cells and the muscle flap was pinned onto a 35 x 10 mm Petri-dish lined with Sylgard and containing the perfusion solution. The preparation was placed in the experimental chamber and perfused with low-potassium *Ascaris* Perienteric Fluid (APF-ringer) solution (in mM: NaCl 23, Na acetate 110, KCl 3, $CaCl_2$ 6, $MgCl_2$ 5, Glucose 11, HEPES 5, pH adjusted to 7.6 with NaOH), unless otherwise stated, at a rate of 4 ml/min through a 20 gauge needle. The needle was placed directly above the muscle bag being recorded from. The preparation in the experimental chamber was kept at 34^{o}C by using a Warner heating collar (DH 35) and heating the perfusate with a Warner SH-27B inline heater (Hamden, CT, USA).

3.3.4 Electrophysiology of Somatic Muscle

Two micropipette voltage- and current-clamp techniques were used in examining the electrophysiological effects of emodepside on the muscle bag of *A. suum* (Figure 3.0A). The micropipettes, made of Borosilicate capillary glass with internal diameter 0.86 mm and external diameter 1.50 mm (Harvard Apparatus, Holliston, MA, USA) were pulled on a Flaming Brown micropipette puller (Sutter Instrument Co, Novato, CA, USA). The micropipettes were filled with 3 M potassium acetate to study the membrane potential and potassium current effects. The current-clamp and the voltage-sensing micropipettes had

resistances of 20 – 30 MΩ but the tip of the current-injecting micropipette for the voltage-clamp was broken to have resistance of 3 – 6 MΩ. The muscle bag was impaled with both micropipettes for all recordings. Axoclamp 2B amplifier, a 1320A Digidata interface and pCLAMP 8.2 software (Molecular Devices, Sunnyvale, CA, USA) were used in all recordings. In all current- and voltage-clamp recordings, the experiment sets were repeated on different worms to obtain the desired number of observations. In the current-clamp experiments, 40 nA hyperpolarizing pulses were injected for 500 ms at 0.30 Hz through the current-injecting micropipette and the change in membrane potential recorded with the voltage-sensing micropipette (Figure 3.0B).

In both current- and voltage-clamp experiments, cells close to the nerve cord were used. We kept the amplifier gain high (~100) and the phase lag low (~0.15 - 0.5 ms) to limit oscillations but adjusted these in some recordings. For activation of the potassium currents, the muscle bags were held at -35 mV and stepped up to 0, 5, 10, 15, 20, 25 and 30 mV (Figure 3.0C); the currents lasted 40 ms. For activation of the calcium currents, the muscle bags were stepped from the holding potential of -35 mV to -25 mV and then in steps of 5 mV up to 20 mV. The calcium currents were isolated from the potassium currents by using 5 mM 4-aminopyridine in the perfusion solution and equimolar amounts (1.5 M) of potassium and cesium acetates in the recording micropipettes and not making large depolarizations (Verma *et al*., 2009). There was no need to block voltage-activated sodium currents in isolating the calcium currents because nematodes lack voltage-activated sodium currents. Calcium substitution experiments were performed by replacing calcium in the low-potassium APF-ringer solution with equimolar cobalt.

The currents were leak-subtracted using pCLAMP 8.2 software. All drugs were initially applied in current clamp and the effects on the voltage-activated currents investigated in voltage-clamp with the drugs still perfusing. Control measurements of membrane potential and potassium currents were made before drug applications, then at 10 min intervals. Unless otherwise stated, all drugs used to study the mechanisms of action of emodepside were applied for 10 min before co-application for 10 min with emodepside and effects on membrane potential and K current compared to the control at 0 min. The preparation was then washed in drug- free solutions and the wash (post-emodepside) effect measured following a 20 min time period. Our subsequent account is based on recordings from more than 130 muscle cells, each from a separate *A. suum* preparation. The membrane potentials of the selected cells recorded from were all more negative than -25 mV with stable input conductance < 4.0 µS.

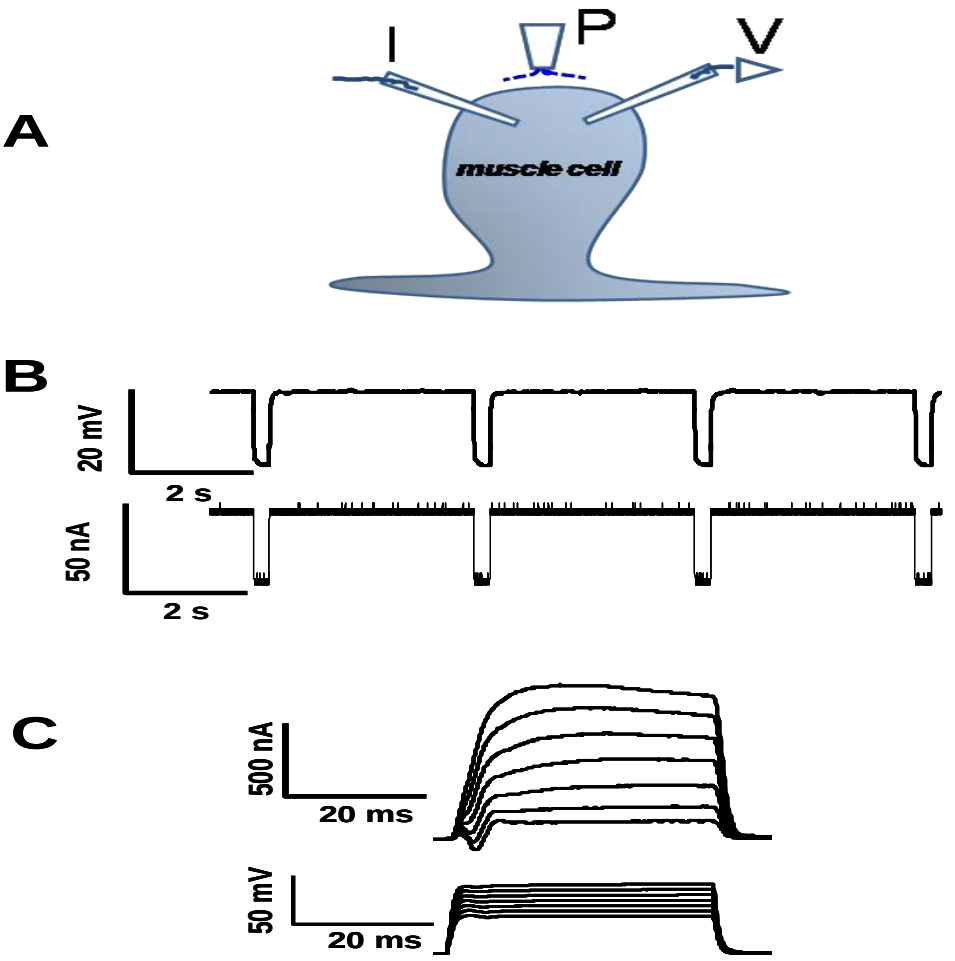

Figure 3.0 Electrophysiological techniques for recording from *Ascaris suum*.

(A) *A. suum* muscle bag showing the current (I) and voltage (V) micropipettes in the bag and the perfusion needle (P). (B) Current-clamp protocol used: bottom trace shows the 40 nA currents injected for 500 ms at 0.30 Hz; top trace shows the resting membrane potential (straight line) and the membrane response to the injected current (downward deflections). (C) Voltage-clamp protocol: bottom trace shows the voltage steps from the holding potential of -

35 mV to 0 mV and in steps of 5 mV to 30 mV; top trace shows the K currents generated in response to the voltage steps.

3.3.5 Time control experiments to test the stability of effects of NO modulators, PKC modulators and iberiotoxin

We conducted separate time-control experiments, without emodepside, to determine the time-course and stability of effects of the NO and PKC modulators on membrane potential and voltage-activated potassium currents. We found that 1 mM sodium nitroprusside (n = 4), 1 µM staurosporine (n =3) and 100 µM N-Nitro L-arginine (n = 6) had no significant effect ($p > 0.05$) on membrane potentials or voltage-activated potassium currents when tested at 10, 20 and 30 min during their application. Phorbol 12-myristate 13-acetate produced an increase in voltage-activated potassium currents and a small hyperpolarization within 5 min of application and did not show further change. We also found that 10 nM iberiotoxin had no effect at 10, 20 and 30 min on membrane potential but iberiotoxin (by 10 min) reduced (n = 3) voltage-activated potassium currents and this effect was not significantly ($p > 0.05$) changed at 20 and 30 min.

3.3.6 Data analysis

All acquired data were displayed on a Pentium IV desktop computer. GraphPad Prism software (version 5.0, San Diego, CA, USA) and Clampfit 9.2 (Molecular Devices, Sunnyvale, CA, USA) were used for the analysis. We observed the biggest effect of

emodepside on the late phase potassium currents (L_K: we measured the average current during the period 30 – 40 ms after the step potential start) at a step potential of 0 mV. The reversal potential was calculated for voltage-activated potassium current experiments. To obtain the activation curves, we calculated the conductance changes from the outward potassium currents and the driving force, E_{rev}-V. The activation curves were then fitted by the Boltzmann equation:

$$G = G_{max} / [1+\exp \{(V_{50}-V)/K_{slope}\}],$$

where G = conductance, G_{max} = maximal conductance change, V_{50} = half-maximal voltage, K_{slope} = slope factor.

The current was expressed as percent control and plotted against voltage to determine how the currents changed with each voltage step. For experiments on the same preparation, one-tailed paired t-test statistical analysis was used to estimate statistical significance, set at $P < 0.05$. For comparison between effects on different preparations an unpaired t-test was used. We quote mean ± s.e. values throughout the text.

To measure the emodepside-sensitive current as a proportion of the 4-aminopyridine sensitive current (at 0 mV) we first measured the control L_K current, then the L_K current at 10 min application of 1 μM emodepside: the difference was the current activated by emodepside. Next, we applied 5 mM 4-aminopyridine for 5 min and again measured the L_K current: the difference between the L_K current in the presence of 4-aminopyridine and the L_K current at 10 min 1 μM emodepside was the 4-aminopyridine-sensitive current. The proportion was then determined and expressed as a %

3.3.7 Materials

Emodepside was generously provided by Achim Harder (Bayer HealthCare AG, Germany). Emodepside stocks of 2 mM and 10 mM in 100 % DMSO were prepared every two weeks. The working emodepside concentrations of 1 and 10 µM were prepared so that the final DMSO concentration was 0.1 %. PF1 (SDPNFLRFamide, EZBiolab, Westfield, IN) stocks of 1 mM were prepared in distilled water every week. Ryanodine, staurosporine, iberiotoxin and phorbol 12-myristate 13-acetate (PMA) were obtained from Tocris Biosciences (Ellisville, MO, USA); 2 mM stock ryanodine was made every week. All stock concentrations were kept at -12^{o}C, thawed and used once. Glucose, 4-aminopyridine, sodium nitroprusside dihydrate (SNP) and N-Nitro L-Arginine (NNLA) were obtained from Sigma-Aldrich® (St. Louis, MO USA). HEPES was obtained from Calbiochem, EMD Biosciences Inc. (La Jolla, CA, USA). All other chemicals were obtained from Fisher Scientific®, Fair Lawn (NJ, USA).

3.4 Results

3.4.1 *slo-1* and *lat-1* homologous genes from *A. suum* are expressed at the adult stage

Using *C. elegans slo-1* and *lat-1* deduced amino-acid sequences for query, databank searches revealed homologous *A. suum* sequences for both genes. The alignment of *C. elegans* SLO-1 and LAT-1 sequences with their respective *A. suum* counterparts is presented in Figure 3.1. *A. suum* SLO-1 cDNA sequence (Genbank accession n° ACC68842.1) encodes a putative, 1117 amino-acid protein, sharing 78% identity and 87% similarity with the Cel-SLO-1

sequence. SLO-1 sequences from both nematode species possess seven transmembrane-spanning domains (S0 – S6), a P-loop, four hydrophobic intracellular segments, S7 – S10 and a "Ca^{2+} bowl" that typifies a large conductance calcium-sensitive potassium channel, SLO-1 (Wallner *et al*., 1996; Wei *et al*., 1996; Schreiber and Salkoff, 1997; Lim *et al*., 1999; Ghatta *et al*., 2006).

The predicted cDNA sequence for *A. suum*-LAT-1 encodes 986 amino-acids (Figure 3.1 B) which has 38% identity and 54% similarity to the Cel-LAT-1 sequence. Despite this limited conservation at the amino-acid level, the LAT-1 sequences from both nematode species share critical sequence features: the seven transmembrane regions, a galactose-binding lectin domain (PFAM Gal_Lectine: PF02140), a hormone receptor domain (SMART HormR: SM 00008) and two G-protein coupled protein domains (SMART GPS: SM00303 and PFAM 7Tm_2: PF00002).

In order to provide further evidence for the expression of *slo-1*- and *lat-1*-like genes in the muscle flaps of *A. suum*, we performed a set of RT-PCR experiments using gene specific primers (Supplementary Table S3.0) designed for *Asu-slo-1* and *Asu-lat-1* cDNA sequences respectively. For both candidates, a single amplification product at the expected size was obtained (Supplementary Figure S3.0). Sequencing reactions showed that the amplicons corresponded to *Asu–slo-1* and *Asu-lat-1* respectively, and confirmed their expression in the muscle flaps of adult *A. suum*. Evidence for the presence of these two genes encouraged electrophysiological investigation of effects of emodepside.

A

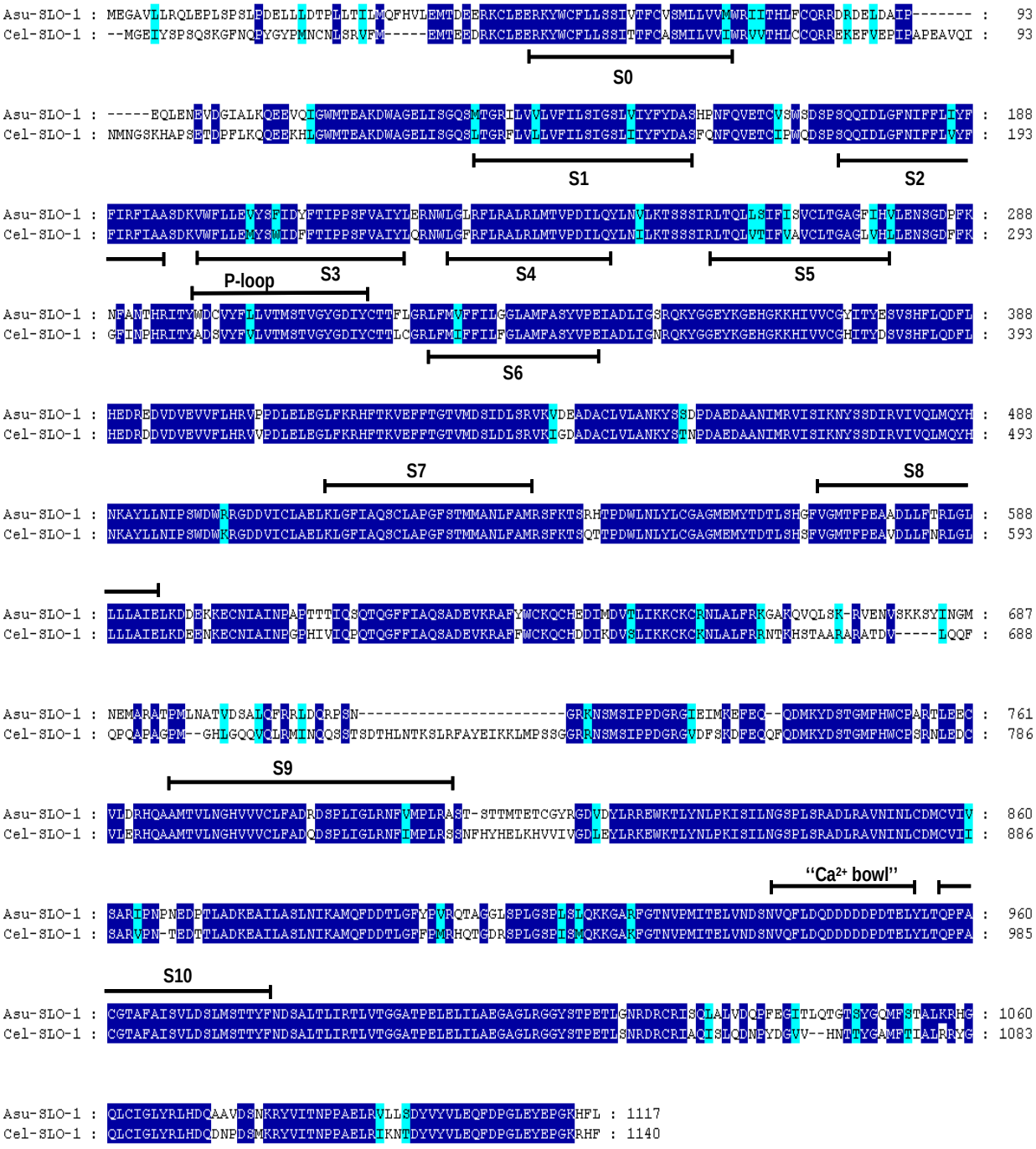

B

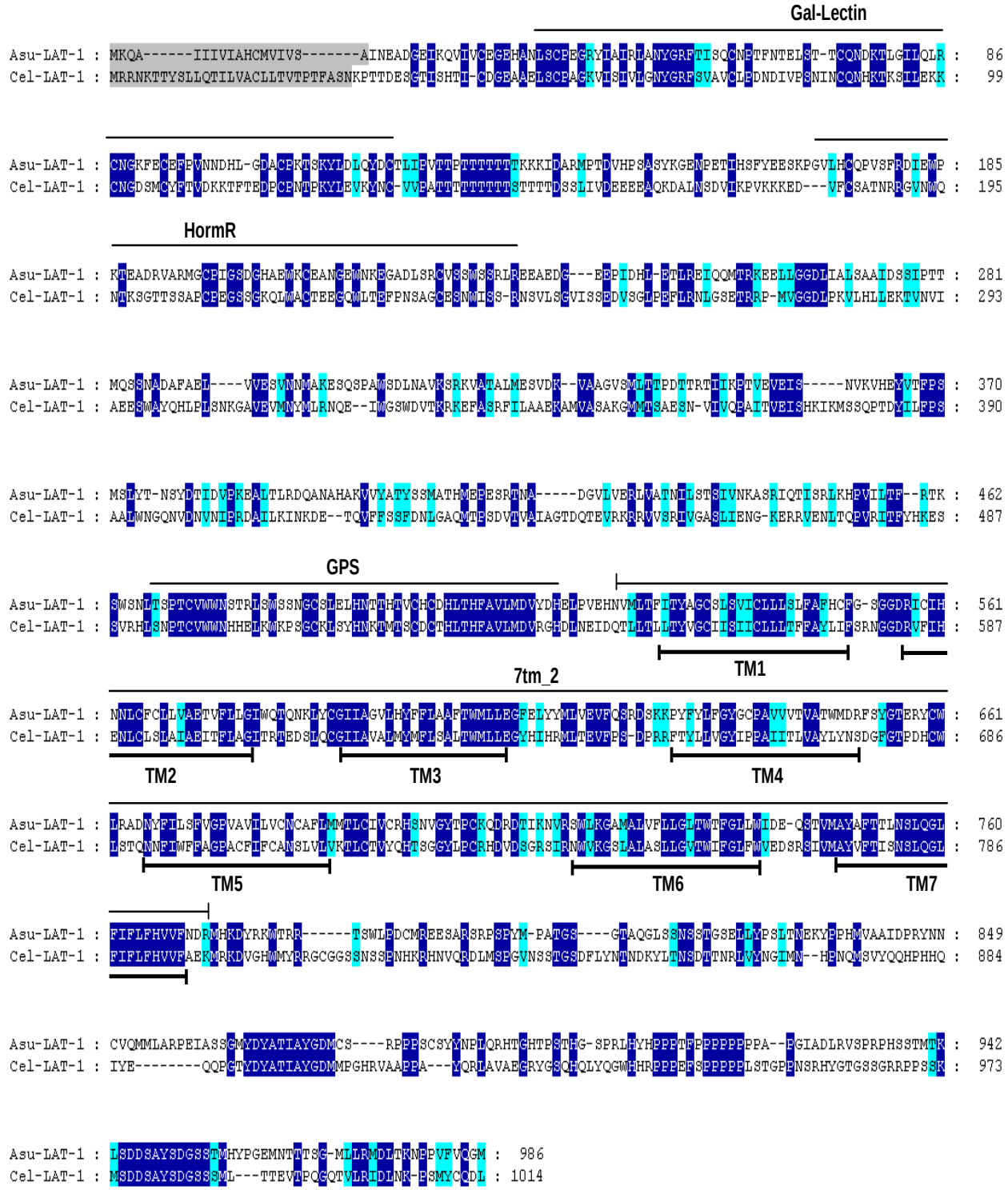

Figure 3.1 Conservation of SLO-1 and LAT-1 sequences in *C. elegans* and *A. suum*. Alignments of deduced amino-acid sequences were constructed using the MUSCLE algorithm (Edgar, 2004) and further processed using GeneDoc program (http://www.nrbsc.org/gfx/genedoc/index.html). Identical amino-acids between *C. elegans* and *A. suum* sequences are shaded in dark blue and distinct amino-acids sharing similar physic-chemical properties are shaded in light blue. Predicted signal peptide sequences are shaded in grey. The transmembrane domains (TM) are noted below the sequences. (A) Comparison of *Asu*-SLO-1(GenBank accession n^{o} ACC68842.1) and *Cel*-SLO-1 (GenBank accession n^{o} NP_001024259.1) showing the 7 TM domains (S0-S6), P-loop, S7-S10 intracellular domains and 'Ca^{2+} bowl'. Domain annotation corresponds to *A. suum* SLO-1. (B) Comparison of *Asu*-LAT-1 (GenBank accession n^{o} ADY40714.1) and *Cel*-LAT-1 (GenBank accession n^{o} NP_495894.1). Domain annotations correspond to *A. suum* LAT-1.

3.4.2 Emodepside has an inhibitory effect on spiking

Initially, we examined the effects of emodepside on muscle spiking under current-clamp as a way of discerning inhibitory actions of emodepside. We activated spiking by applying 1 µM ryanodine (Puttachary *et al.*, 2010) and compared effects of emodepside with the neuropeptide PF1 because emodepside has been suggested to act by stimulating release of inhibitory neuropeptides like PF1.

1 µM ryanodine produced a slow time-dependent increase in the spike frequency and comparison between the 20 and 35 minute period (Figure 3.2B) shows a significant increase of 15 spikes min^{-1} ($p < 0.05$, $n = 7$) in spike frequency. Figure 3.2A shows a representative

trace of the inhibitory effect of emodepside on the ryanodine-induced spiking. Emodepside significantly inhibited the ryanodine increase in spike frequency during the 20 and 35 minute period (Figure 3.2C) by 9.8 spikes min^{-1} ($p < 0.05$, $n = 5$). We also tested the effect of PF1 on ryanodine spiking and found that it was more potent and faster acting than emodepside: 1 µM PF1 decreased the ryanodine spike frequency by 46 spikes min^{-1} in a shorter time of 10 min ($p < 0.01$, $n = 5$, Figure 3.2D).

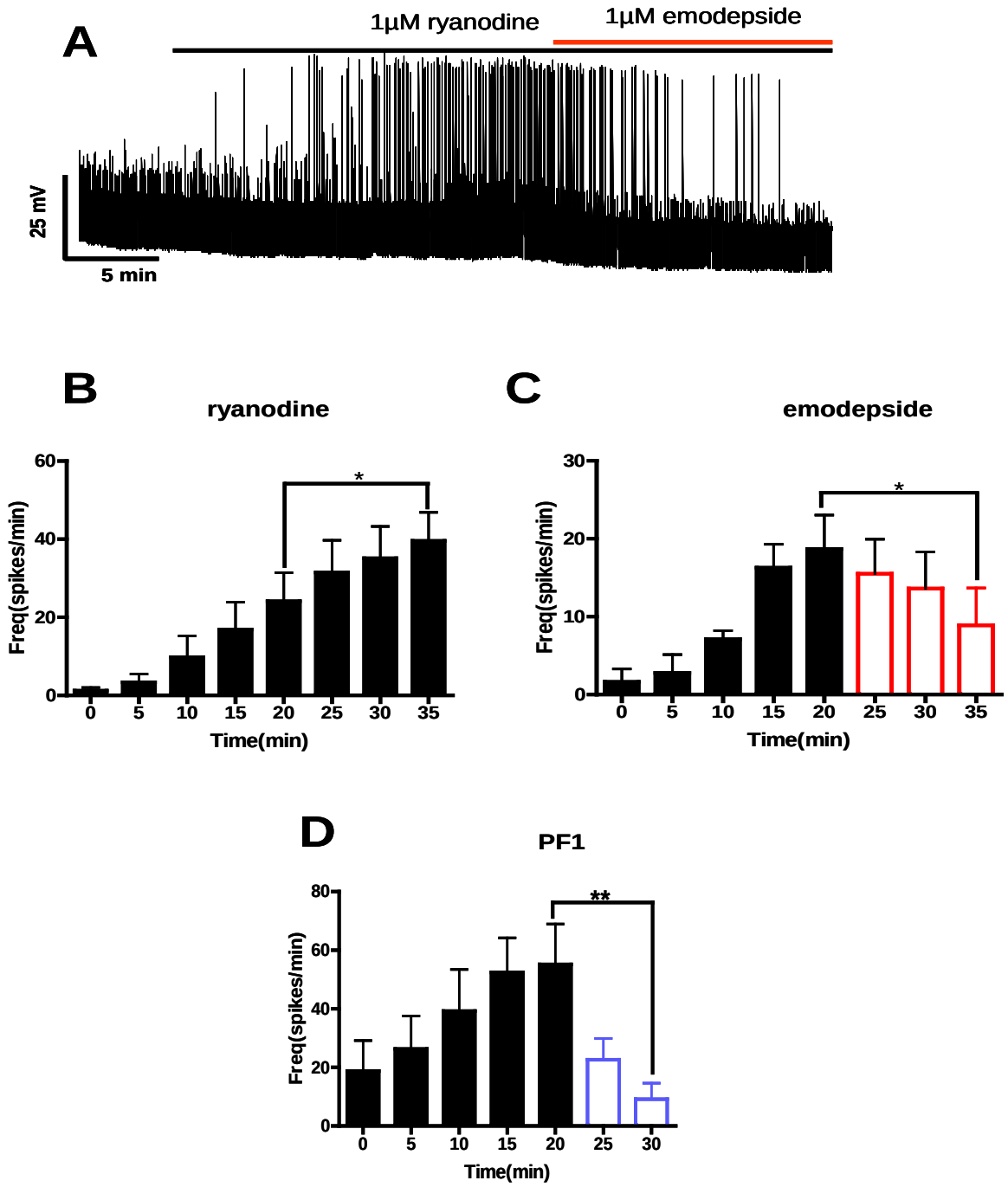

Figure 3.2 Effect of emodepside (1 μM) on membrane spiking.

(A) Representative current-clamp trace showing the spiking induced by ryanodine (1 μM) and the inhibitory effect of emodepside on the spikes. (B) Bar chart (mean ± SEM) of the effects of ryanodine on the frequency of spikes. Ryanodine caused a time-dependent increase

in the spike frequency; comparison was made between 20 min and 35 min of ryanodine application (*P < 0.05, n = 7, paired t-test).* (C) Bar chart (mean ± SEM) of the effects of emodepside on the frequency of ryanodine-induced spikes. Emodepside abolished the increase in spike frequency; comparison was made between 20 min of ryanodine application and 15 min (35 min) of emodepside + ryanodine application (*P < 0.05, n = 5, paired t-test).* (D) Bar chart (mean ± SEM) of the effects of PF1 (1 µM) on the ryanodine-induced spike frequency. After just 10 min application, PF1 caused a decrease in spike frequency (*P < 0.01, n = 5, paired t-test*).

3.4.3 Effect of emodepside on membrane potential and input conductance

Figure 3.3A shows a representative recording of the membrane potential before, during and after application of 1 µM emodepside. Perfusion of 1 µM emodepside for 10 min produced a slowly developing -5.2 mV hyperpolarization, which continued to increase during drug application; the resting input conductance was 3.5 µS before drug application and was not changed significantly by emodepside. We observed that the onset of membrane hyperpolarization produced by emodepside varied between 30 sec to 3 min. The mean hyperpolarization at 10 min was -5.1 ± 0.75 mV ($p < 0.001$, n = 10, Figure 3.3B). The hyperpolarization was not reversible but continued to increase gradually despite washing. At a higher concentration of 10 µM emodepside at 10 min, the hyperpolarization was -7.7 ± 1.2 mV ($p < 0.001$, n = 6, Figure 3.3B) but there was still no significant change in input conductance. Comparison of the hyperpolarization caused by 1 and 10 µM emodepside showed that the hyperpolarization was concentration-dependent; the difference, -2.6 ± 1.3 mV, was significant ($p < 0.05$, n = 16). The membrane potentials of some of the muscle cells

showed spontaneous small depolarizing potentials which were reduced or completely abolished by the emodepside.

To test if the membrane hyperpolarization caused by emodepside was mediated by opening of potassium channels, we used the potassium channel blocker, 5 mM 4-aminopyridine, in the perfusion solution throughout the experiment. Thus, there was a constant perfusion of low-K^+ APF containing 5 mM 4-aminopyridine. In the presence of 4-aminopyridine, the mean resting membrane potential was unchanged but the hyperpolarizing effect of 1 µM emodepside was significantly reduced at 10 min to -1.8 ± 0.23 mV ($p < 0.01$, $n = 8$, Figure 3.3B).

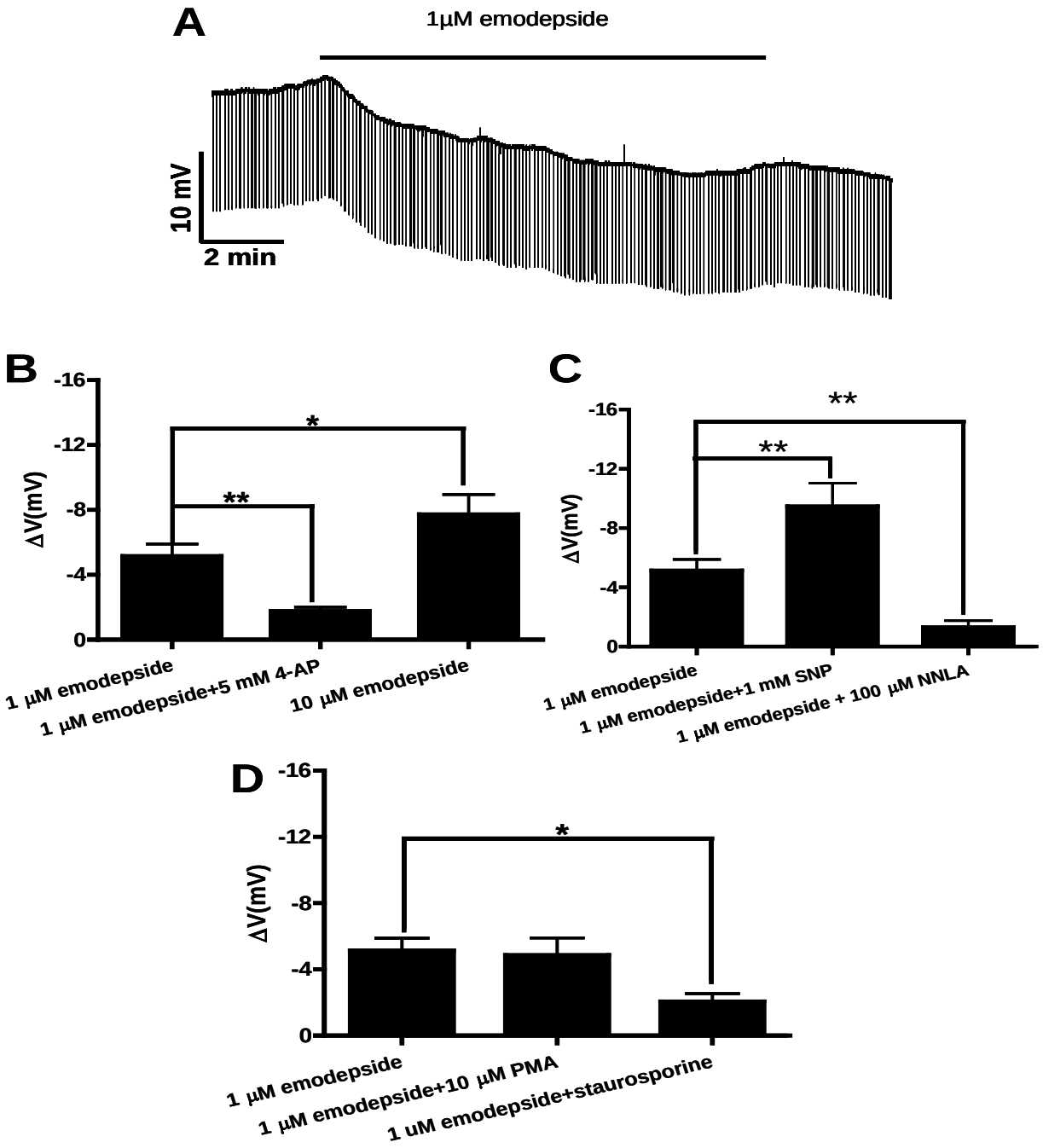

Figure 3.3 Effect of emodepside (1 μM) on membrane potential.

(A) Representative current-clamp trace showing the membrane potential before, during and after 10 min application of 1 μM emodepside. (B) Bar chart (mean ± SEM) of the effects of emodepside on the membrane potential. Comparison was made between membrane potential

before and during emodepside application. Emodepside caused a significant membrane hyperpolarization (*P < 0.001, n = 10, paired t-test*) which was reduced in the presence of 4-aminopyridine (5 mM) (*P < 0.05, unpaired t-test*). (C) Bar chart (mean ± SEM) of the effects of NO on emodepside-induced hyperpolarization. In the presence of 1 mM SNP, emodepside (1 µM) caused an increased hyperpolarization (*P < 0.01, n = 4, paired t-test*). NNLA (100 µM) decreased the hyperpolarization caused by emodepside (*P < 0.01, unpaired t-test*). (D) Bar chart (mean ± SEM) of the effects of protein kinase modulators on emodepside-induced hyperpolarization. PMA (10 µM) had no significant effects on the hyperpolarization caused by emodepside. However, staurosporine (1 µM) decreased the hyperpolarization caused by emodepside (*P < 0.05, unpaired t-test*).

3.4.4 Emodepside effect on membrane potential: role of NO and PKC

The slow hyperpolarizing effect of emodepside and sensitivity to 4-aminopyridine has similarities to the effect of the neuropeptide PF1 in *A. suum* and effects of PF1 are mediated by nitric oxide synthase (Bowman *et al*., 1995; 2002; Verma *et al*., 2009). We therefore tested the effects of N-Nitro-L-Arginine (NNLA), an inhibitor of inducible nitric oxide synthase (iNOS) and sodium nitroprusside (SNP), an NO releasing agent on the actions of emodepside.

In the presence of 100 µM NNLA, the emodepside hyperpolarization was significantly reduced to -1.3 ± 0.44 mV ($p < 0.01$, n = 6, Figure 3.3C). In contrast, in the presence of 1

mM SNP, emodepside caused a significantly increased hyperpolarization of -9.5 ± 1.6 mV ($p < 0.01$, $n = 4$, Figure 3.3C). Both of these observations suggest a role for NO in the mediation of the emodepside effects. In time control experiments, NNLA and SNP had no significant effect by themselves on the membrane potential.

We further investigated the role of protein kinase C (PKC) in mediating the effects of emodepside since emodepside has been suggested to bind to latrophilin-like receptors in *C. elegans* which can signal through Gq proteins and PKC in other preparations. 1 µM staurosporine, a broad-spectrum protein kinase inhibitor, significantly reduced the hyperpolarization produced by 1 µM emodepside to -2.1 ± 0.48 mV ($p < 0.05$, $n = 4$, Figure 3.3D). Staurosporine, by itself, had no significant effects on the membrane potential. The protein kinase C activator, PMA (10 µM), produced a small but significant hyperpolarization (-2.1 ± 0.3 mV, $p < 0.05$, $n = 5$). However, in the presence of the 10 µM PMA, 1 µM emodepside produced an additional membrane hyperpolarization of -4.9 ± 1.0 mV ($p < 0.01$, $n = 5$, Figure 3.3D). The effects of PMA and staurosporine are consistent with a role for PKC in the emodepside signaling pathway.

3.4.5 Effect of emodepside (1 µM) on voltage-activated K^+ currents

We investigated the effects of 1 µM emodepside on the voltage-activated K currents. Given the slow onset of emodepside effects on spiking and membrane potential, we investigated the time-dependent effects of 1 µM emodepside on the K currents, Figure 3.4. In control recordings, we tested and observed no significant change in the voltage-activated K currents at 10, 20, 30 and 40 min. We applied the emodepside for 30 min and examined the effect on

the K currents at 10 min intervals. Figure 3.4A shows representative K current traces of the control and 1 µM emodepside effects at 10, 20 and 30 min where it produced time-dependent increases in the currents. The maximum % increase in the late phase K currents (L_k) was observed at the 0 mV voltage step; at the higher voltage steps, 1 µM emodepside produced smaller % changes with no effect at +30 mV. In the sample plot of Figure 3.4B, 1 µM emodepside increased L_k at 0 mV to 130 %, 146 % and 167 % at 10 min, 20 min and 30 min, respectively. A similar trend was observed in all recordings (0 mV, Figure 3.4C, n = 4) where 1 µM emodepside significantly increased the currents at 10 min, 20 min and 30 min by means of 25 % ($p < 0.01$), 41 % ($p < 0.01$) and 73 % ($p < 0.05$) respectively. We tested the effects of 1 µM emodepside on the K current activation curves and were only able to see small changes in the kinetic parameters V_{50} and G_{max} throughout the application of emodepside.

When we applied emodepside for 10 min and then washed for 20 min we observed a continued increase in the K current following the onset of washing, Figure 3.4D, E & F. We termed the wash observations at 20 min, the post-emodepside period. In the sample plot in Figure 3.4E, L_K increased to 133% after 10 min exposure to 1 µM emodepside and to 186% following a further period of 20 minutes washing. We observed a similar trend in all 9 recordings: on average, 1 µM emodepside increased L_K by 28 % ($p < 0.001$, Figure 3.4F) at 10 min and by 59 % ($p < 0.01$, Figure 3.4F) at the 20 min post-emodepside period.

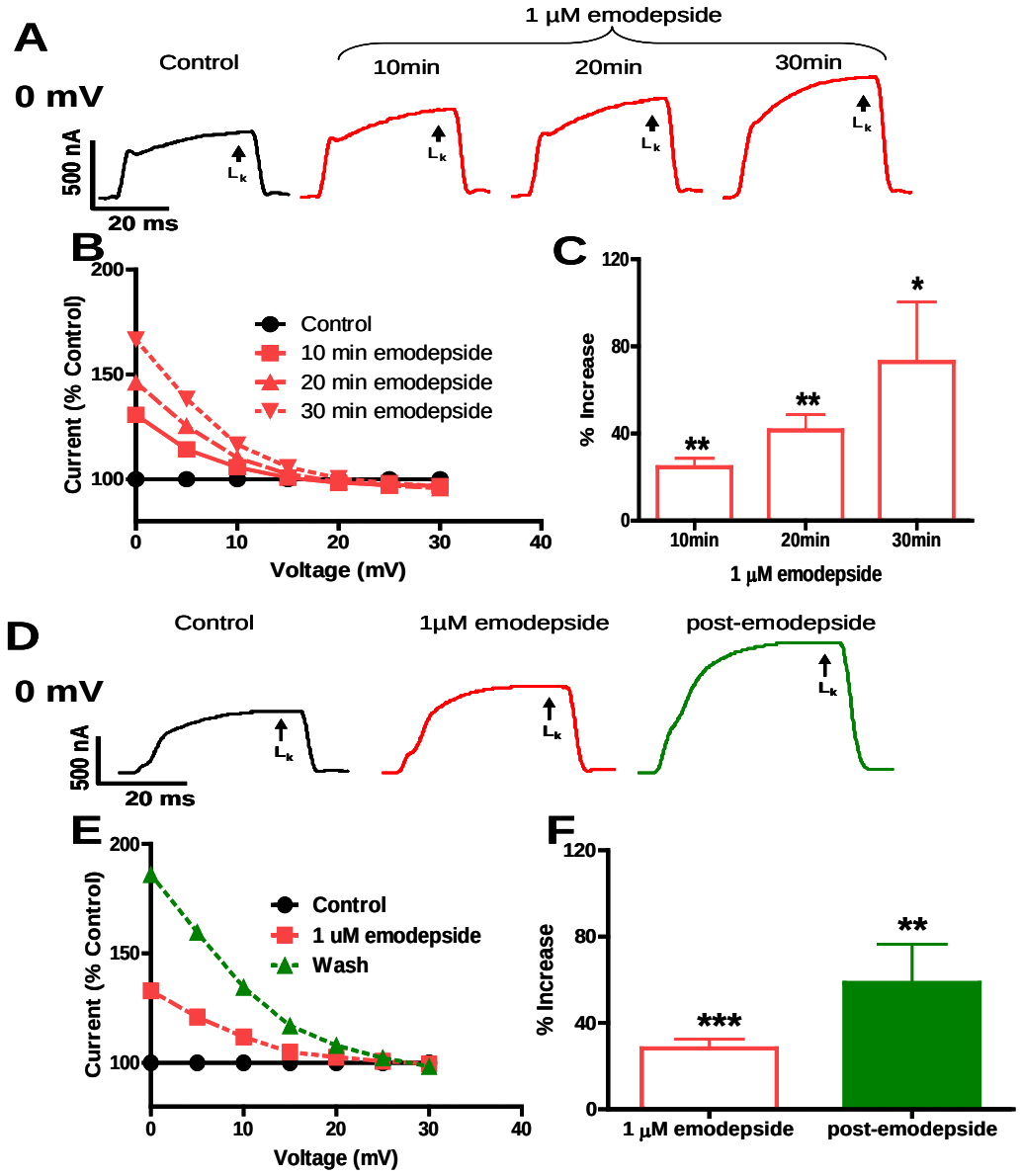

Figure 3.4 Effect of emodepside (1 µM) on voltage-activated L_K currents.

(A) Representative voltage-clamp traces of control K^+ current and the time-dependent effects of emodepside on the K^+ currents, all at 0 mV. (B) Sample plot of current (% control) against voltage showing the voltage-dependence of the K^+ currents increased by emodepside at different time points. (C) Bar chart (mean ± SEM) of the effects of emodepside on L_K currents. Comparison was made between control 0 mV step current at 30 – 40 ms and the

corresponding current increased by emodepside at 10, 20 and 30 min. Emodepside increased L_K currents at 10 min ($P < 0.01$, $n = 4$, *paired t-test*), 20 min ($P < 0.01$, $n = 4$, *paired t-test*) and 30 min ($P < 0.05$, $n = 4$, *paired t-test*). (D) Representative voltage-clamp traces of control L_K current, the effects of emodepside on the L_K current and the L_K currents after 20 min wash (post-emodepside). (E) Sample current (% control) versus voltage plot showing how the L_K currents change with voltage. Emodepside increased the current after 10 min and the increase was sustained at the post-emodepside period. (F) Bar chart (mean ± SEM) of the effects of emodepside on the L_K currents. After 10 min perfusion, emodepside increased the L_K currents ($P < 0.001$, $n = 9$) and the increase was sustained during the post-emodepside period ($P < 0.01$, $n = 9$).

3.4.6 Effect of emodepside (10 µM) on voltage-activated K^+ currents

We increased the concentration of emodepside to 10 µM in order to resolve effects on the kinetic parameters of the K current activation curves. Figure 3.5A shows representative traces. Figure 3.5B shows the average effect of 10 µM emodepside on the L_K currents. In the 6 recordings, 10 µM emodepside increased the L_K current by an average of 29 % ($p < 0.05$, Figure 3.5B) and 87 % during the post-emodepside period ($p < 0.05$, Figure 3.5B). The activation curve, Figure 3.5C, shows that 10 µM emodepside shifted V_{50} by 2.7 mV in the hyperpolarizing direction and by 6.4 mV during the post-emodepside period; there was no change in the G_{max}. Similar hyperpolarizing shifts without changes in G_{max} were observed in

all 6 experiments: 2.9 ± 0.3 mV ($p < 0.05$) in 10 μM emodepside and 6.6 ± 1.0 mV ($p < 0.01$) in the post-emodepside period. In control experiments we found that the conductance-voltage plots showed little or no change in V_{50} throughout a 40 minute recording period: specifically, at 20 min it was 0.28 ± 0.10 mV, n= 6; at 30 min it was 0.50 ± 0.20 mV, n= 6. The shape of the conductance activation curve with an increase in V_{50}, can explain why the emodepside K current is greater at 0 mV with little change near +30 mV: emodepside is not altering the maximum opening of channels but their voltage-sensitivity.

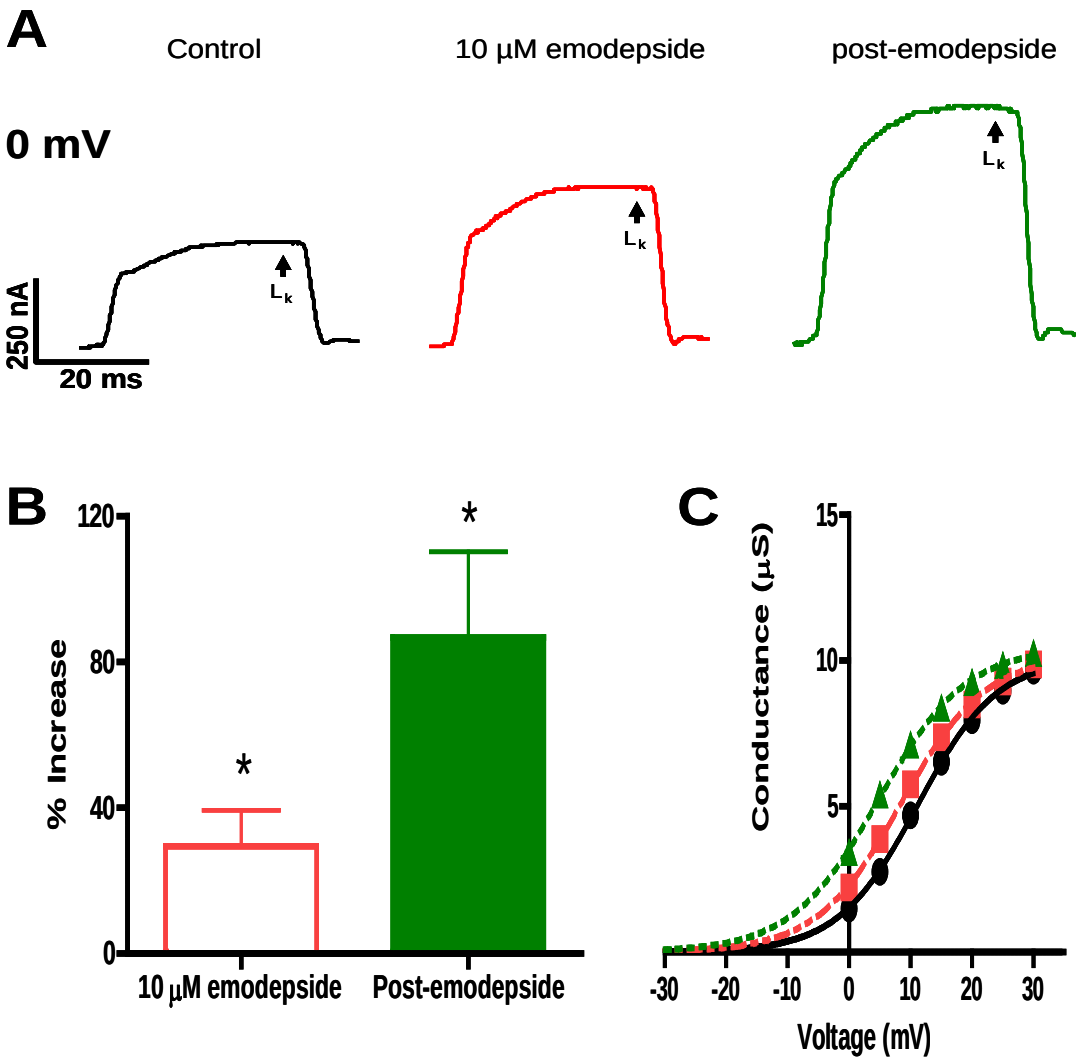

Figure 3.5 Effect of emodepside (10 µM) on the voltage-activated L_K currents.

(A) Representative traces of the control L_K current, the effects of emodepside on the current and the post-emodepside L_K current at 0 mV. (B) Bar chart (mean ± SEM) of % increase in L_K currents produced by emodepside ($P < 0.05$, $n = 6$, *paired t-test*) and the continued increase at the post-emodepside period ($P < 0.05$, $n = 6$, *paired t-test*). (C) Sample activation curve of the L_K currents; conductance-voltage plots were fitted to the Boltzmann equation.

Emodepside shifted the V_{50} in the hyperpolarization direction and the shift was sustained during the post-emodepside period. Essentially no change in G_{max} was observed.

3.4.7 Ca^{2+} is required for effects of emodepside on K^+ currents

We replaced extracellular Ca^{2+} with equimolar Co^{2+} to determine the Ca^{2+} requirement for the action of emodepside on K currents. In the absence of Ca^{2+} the effect of 1 µM emodepside was reduced; we observed only a 12.0 ± 5.0 % increase in L_K at 10 min and a 33.0 ± 17.0 % increase post-emodepside. The increases were not significantly different from the control L_k ($p > 0.05$, n = 10). These observations show that Ca^{2+} was required for effects of emodepside on the L_K current and because I_a– and I_K–like K currents are present in *A. suum* in Ca^{2+} free condition (Martin *et al*., 1992) the experiments suggest that emodepside does not act directly on I_a– or I_K–like K currents.

3.4.8 Emodepside effects on K^+ currents: role of NO and PKC

We investigated the role of NO on the effects of emodepside on the K^+ currents using SNP as an NO donor and NNLA as an iNOS inhibitor. 1 mM SNP by itself does not cause a significant change in the L_k currents even after 30 min ($p > 0.05$, n = 4). Figure 3.6A shows representative K^+ current traces with control, effects of 1 mM SNP, and 1 µM emodepside + 1 mM SNP and post emodepside L_K currents. In 6 preparations, 1 µM emodepside, in the presence of 1 mM SNP, caused a mean increase of 32 % in the L_K currents at 10 min which

was statistically significant ($p < 0.05$, n = 5, Figure 3.6D) and a mean increase of 98 % ($p < 0.05$, n = 4) at the post emodepside period. The activation curve, Figure 3.6C, shows that in the presence of SNP, emodepside shifted the V_{50} in the hyperpolarization direction by 2.9 mV and during the post-emodepside period, the shift was increased to 4.6 mV. The mean shift in the V_{50} at 10 min was 2.4 mV ($p < 0.05$, n = 6) and 6.2 mV ($p < 0.01$, n = 6) post-emodepside.

100 µM NNLA had no significant effect on K currents or membrane potential in control experiments ($p > 0.05$, n=3) but NNLA inhibited the effect of emodepside on K currents. In the presence of 100 µM of NNLA, there was little effect (1.9 ± 1.0 % increase, $p > 0.05$, n = 6) of 1 µM emodepside on the L_k currents at 10 min and the effect at the 20 min post-emodepside period was reduced to 26.0 ± 11.0 % ($p < 0.05$, n = 5), data not illustrated. Thus NNLA reduced the effects of emodepside on the K currents. The effects of both SNP and NNLA together indicate a role for NO during the action of emodepside.

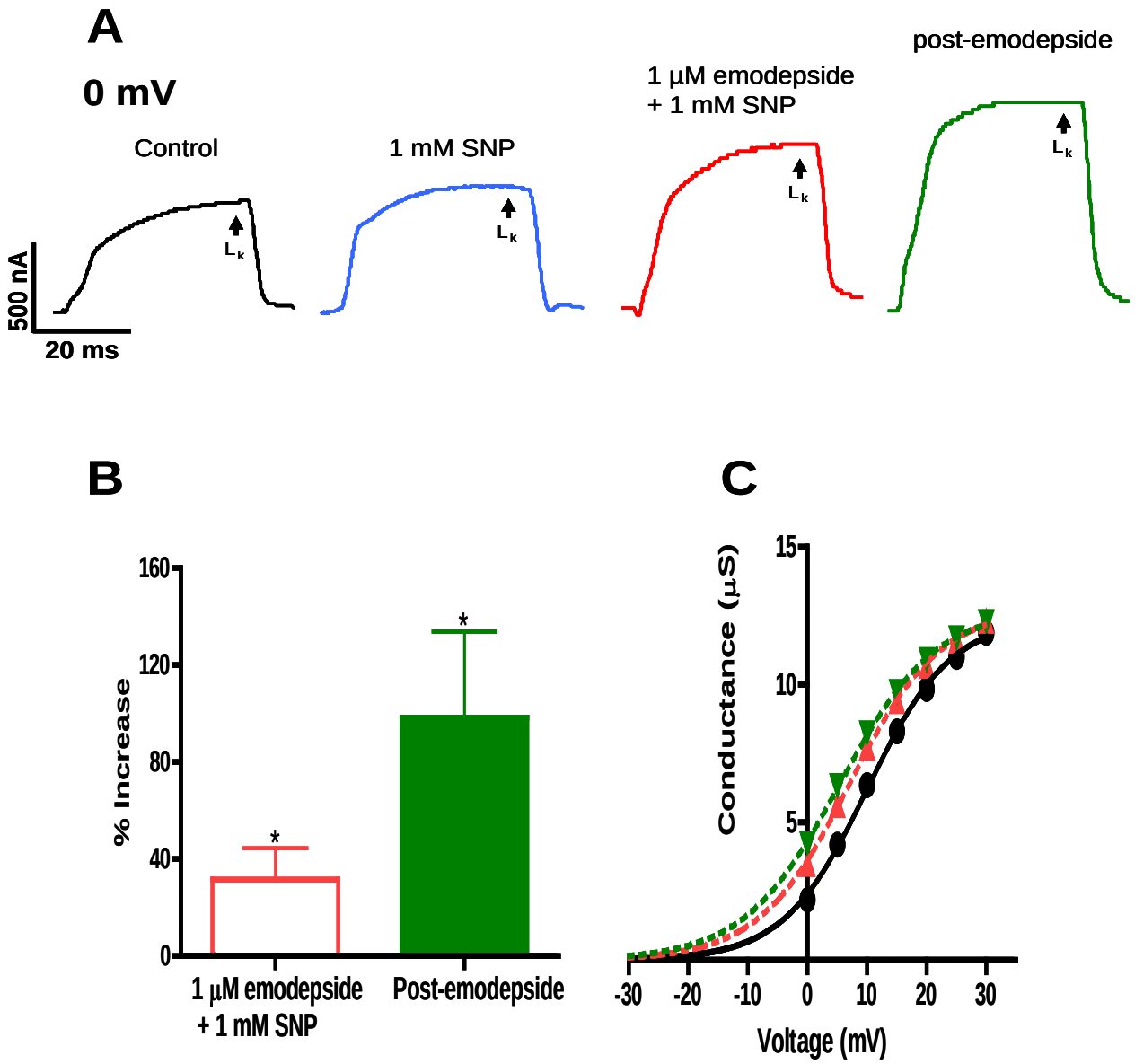

Figure 3.6 Effect of emodepside (1 µM) and SNP (1 mM) on the voltage-activated L_K currents.

(A) Representative traces of control L_K current, the effects of emodepside + SNP on the L_K current and the post-emodepside L_K current, all at 0 mV. (B) Bar chart (mean ± SEM) of % increase in L_K current produced by emodepside in the presence of SNP ($P < 0.05$, $n = 5$, *paired t-test*) and the continued increase in the post-emodepside period ($P < 0.05$, $n = 4$,

paired t-test). (C) Sample activation curve of the L_K currents; conductance-voltage plots were fitted to the Boltzmann equation. In the presence of SNP, emodepside shifted the V_{50} in the hyperpolarization direction. Essentially no change in G_{max} was observed.

We investigated the role of PKC in emodepside effects on the K currents using PMA as a PKC activator and staurosporine as a kinase inhibitor. PMA, by itself produces a small stable but significant increase in the K currents and small hyperpolarization. Figure 3.7A shows representative traces of the control L_K current, effect of 10 µM PMA on the L_K current, 1 µM emodepside + 10 µM PMA effect on the L_K current and the post-emodepside L_K current. In all 5 recordings, PMA caused a mean increase to 131 % of the control ($p < 0.05$) in the L_K currents and 1 µM emodepside, in the presence of the PMA, caused a further increase to 145% ($p < 0.01$) in L_K currents. During the post-emodepside period, the mean increase in the L_K current was to 191% ($p < 0.05$). In the representative activation curve in Figure 3.7C, PMA caused a 1.6 mV shift in the V_{50} in the hyperpolarization direction, whilst emodepside + PMA caused a further hyperpolarizing 2.4 mV shift in the V_{50}; during the post-emodepside period, there was a further additional hyperpolarizing shift 4.5 mV in V_{50}. There was no change in G_{max}. On average, PMA shifted V_{50} by 1.9 mV ($p < 0.05$, $n = 5$) and emodepside + PMA shifted it by 2.8 mV ($p < 0.01$, $n = 5$). PMA by itself increases the K currents and shifts the L_K current activation curve; we can see from these observations PMA mimics some of the effects of emodepside.

When we tested the effect of 1 µM staurosporine by itself on the K currents in control experiments, we found that it had no significant effect (at 30 min mean decrease 4.4 ± 4.0%, $p > 0.05$, $n = 3$). We found however, that staurosporine inhibited the action of 1 µM emodepside. Figure 3.7 shows effects on representative K currents. Figure 3.7E shows summary bar-charts and that 1 µM staurosporine, at 10 min, had no effect on the L_k current. The effect of 1 µM emodepside was no-longer activating but was inhibitory with a mean decrease of 10 % ($p < 0.05$, $n = 4$**,** Figure 3.7E). The effects of PMA mimicking emodepside, and the loss of emodepside activation when pretreated with staurosporine, together indicate a role for PKC during the action of emodepside. The inhibitory action of emodepside following staurosporine suggests additional actions of emodepside but these were not explored further.

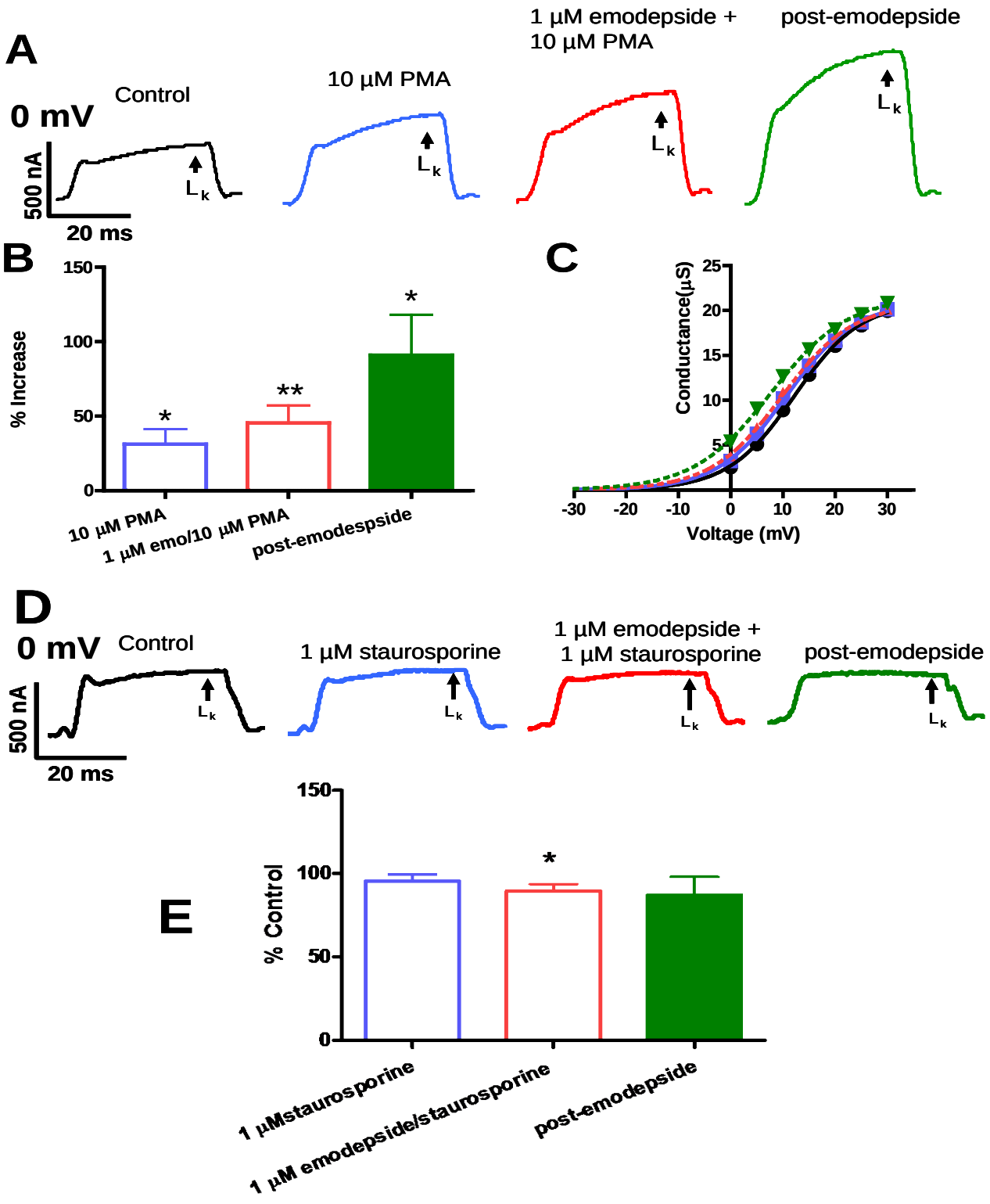

Figure 3.7 Effects of emodepside (1 μM) + PKC modulators on the voltage-activated L_K currents.

(A) Representative traces of control L_K current, the effects of PMA (10 μM) alone, emodepside + PMA and the post-emodepside period on the L_K current. (B) Bar chart (mean ± SEM) of the % increases in L_K currents caused by PMA ($P < 0.05$, $n = 5$, *paired t-test*), emodepside + PMA ($P < 0.01$, $n = 5$, *paired t-test*) and post-emodepside ($P < 0.05$, $n = 3$, *paired t-test*). Comparison was made with the % control L_K current. (C) Conductance-voltage plots were fitted to the Boltzmann equation. In the activation curves shown, PMA and emodepside + PMA shifted the V_{50} in the hyperpolarization direction. Essentially no change in G_{max} was observed. (D) Representative traces showing the effects of emodepside (1 μM) + staurosporine (1 μM) on the L_K current. (E) Bar chart (mean ± SEM) of % change in currents caused by emodepside + staurosporine. Comparison was made with the % control L_K current. In the presence of staurosporine, emodepside decreased the L_K ($P < 0.05$, $n = 4$, *paired t-test*) and the decrease was sustained during the post-emodepside period.

3.4.9 The 4-aminopyridine-sensitive K^+ current includes I_a as well as the emodepside-activated current

We found that in the presence of 5 mM 4-aminopyridine, 1 μM emodepside had no detectable effect on K^+ currents ($p > 0.05$, $n = 8$). When we applied 4-aminopyridine after the

emodepside, and measured the emodepside-activated K current as a proportion of the total 4-aminopyridine-sensitive K^+ current, it was only 50 ± 16 % (n = 6). Martin *et al*. (1992) have shown that 5 mM 4-aminopyridine selectively inhibits I_a–like K^+ currents but not I_K–like K^+ currents in *A. suum* under Ca^{2+} free conditions. The sensitivity of the emodepside K^+ currents to 4-aminopyridine shows that emodepside does not activate I_K currents. The presence of Ca^{2+} here, allows K^+ currents to be activated by emodepside. We found that the total 4-aminopyridine-sensitive current was bigger than the emodepside-activated current, indicating that 4-aminopyridine was not selective and inhibits the emodepside K^+ current as well as the I_a–like K^+ current.

3.4.10 Effect of iberiotoxin

We examined the effects of iberiotoxin; a selective inhibitor of high conductance Ca^{2+}-activated K^+ (SLO-1) channels with IC_{50}s often in the sub-nanomolar ranges (Galvez *et al*., 1990; Candia *et al*., 1992; Gruhn *et al*., 2002). 10 nM iberiotoxin was used to minimize effects on other channels (Sones *et al*., 2009). Iberiotoxin produced a significant decrease (-23.7%, $p < 0.05$, n = 4) in the control L_K currents, Figure 3.8, without a detectable change in membrane potential, indicating the presence of iberiotoxin-sensitive SLO-1-like K^+ channels in *A. suum*. The application of 1 µM emodepside was able to counter some of the effects of 10 nM iberiotoxin, producing hyperpolarization (-4.1 ± 0.2 mV, $p < 0.05$, n = 4) and a return of the L_K currents towards control levels, Figure 3.8, but emodepside no-longer increased the K^+ current above the control ($p > 0.05$). Thus iberiotoxin reduced (but did not entirely block) effects of emodepside indicating that iberiotoxin-sensitive SLO-1-like channels are involved.

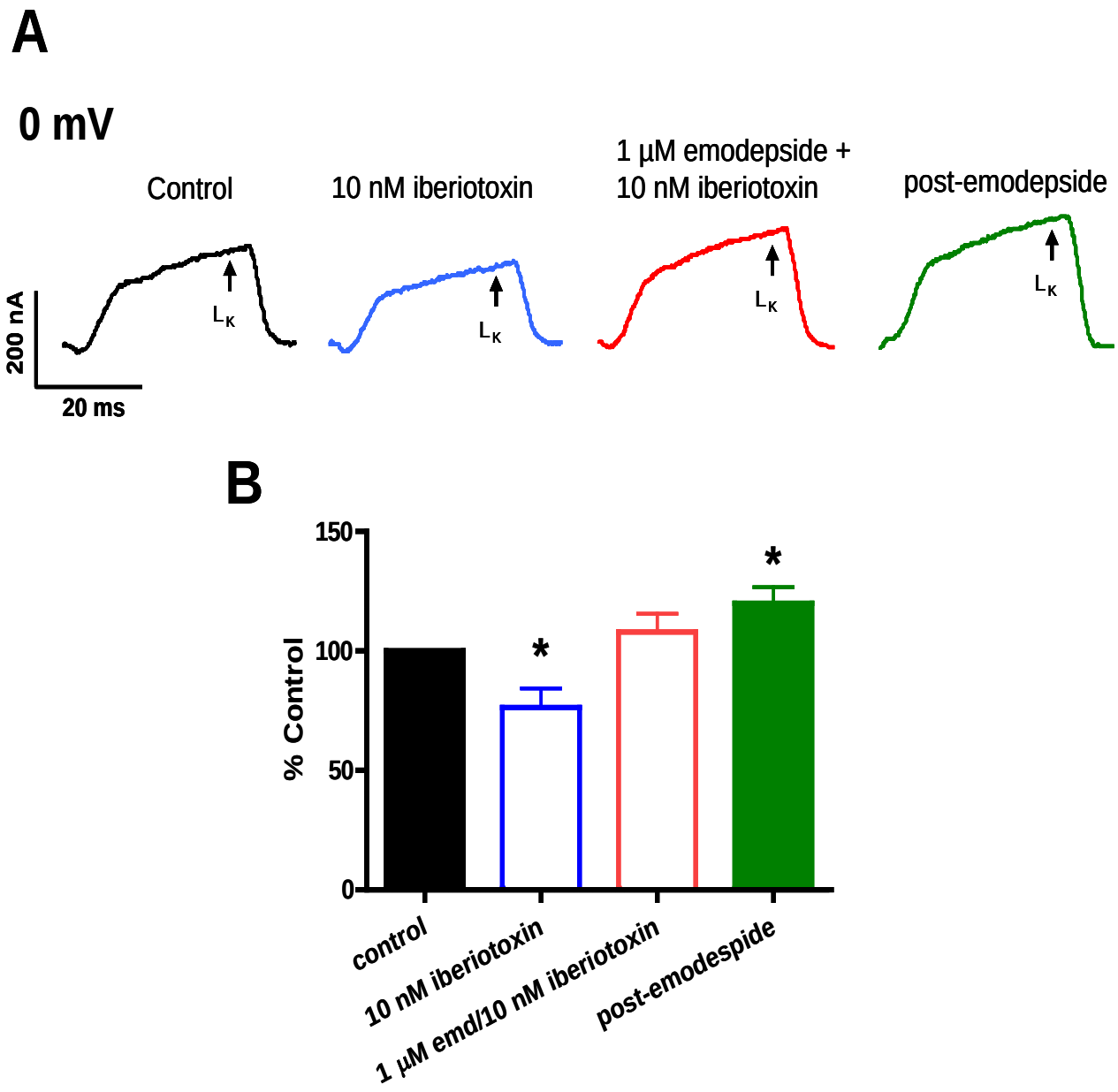

Figure 3.8 Effects of emodepside (1 µM) and iberiotoxin (10 nM) on the voltage-activated L_K currents.

(A) Representative traces of control L_K current, 10 nM iberiotoxin effect on the L_K currents, emodepside + iberiotoxin effect on the L_K currents and the post-emodepside L_K currents. (B)

Current, expressed as % control, at 0 mV showing the inhibitory effect of iberiotoxin and emodepside on the L_K currents.

3.4.11 Emodepside effects on voltage-activated Ca^{2+} currents

We investigated the effects of 1 µM emodepside on the voltage-activated Ca^{2+} currents. The inhibitory neuropeptide PF1, which has been suggested to be mimicked by emodepside, has been shown to significantly inhibit the voltage-activated Ca^{2+} currents in *A. suum* (Verma et al., 2009). In all 9 recordings, we observed no significant effect of 1 µM emodepside on the Ca^{2+} currents (Figure 3.9).

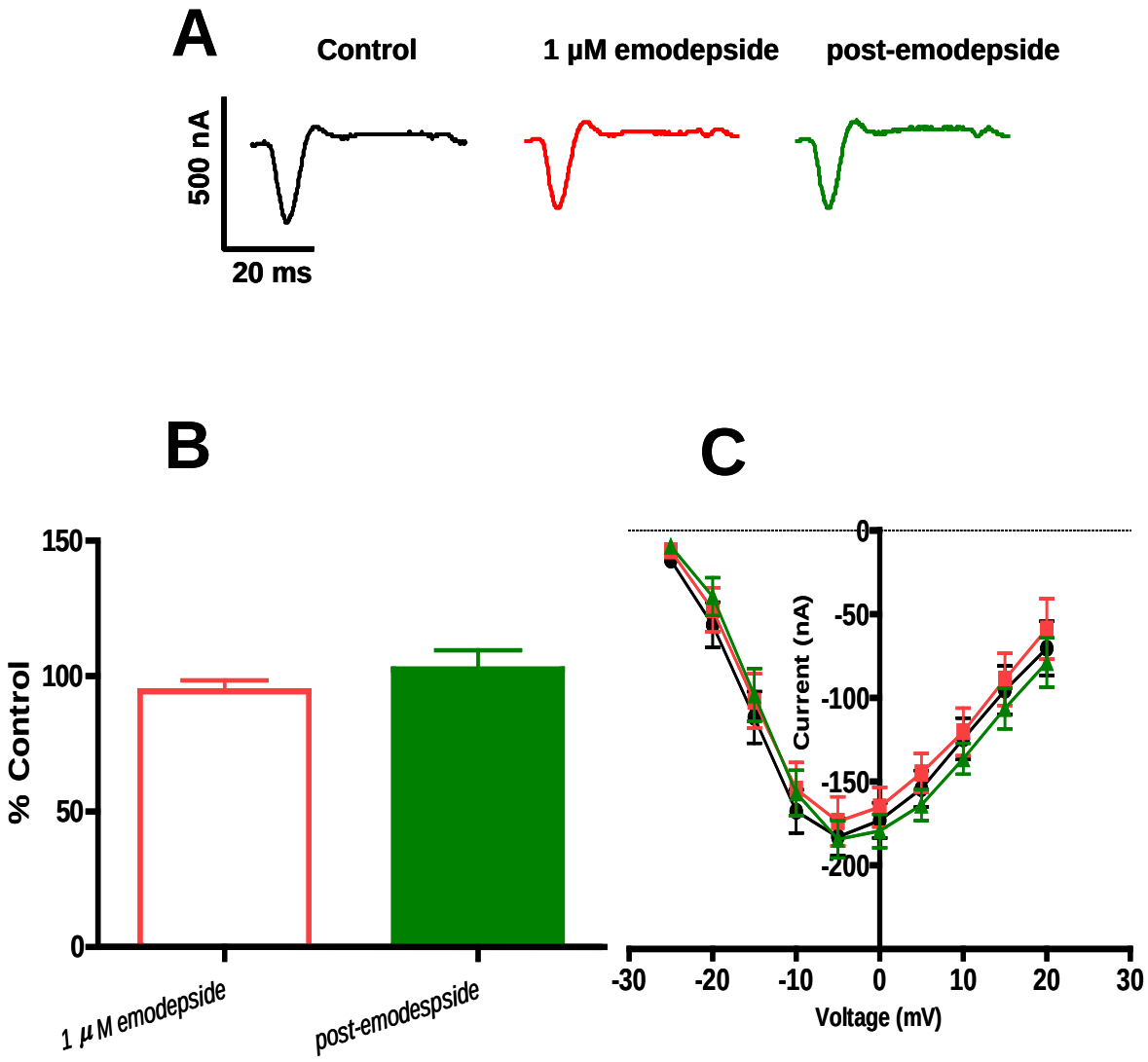

Figure 3.9 Effects of emodepside (1 μM) on the voltage-activated Ca^{2+} currents.

(A) Representative inward Ca^{2+} current traces of control, 1 μM emodepside and the post-emodepside currents. (B) Bar chart (mean ± SEM) of the effects of emodepside on the inward Ca^{2+} currents (green: 20 min post-emodepside). Emodepside has essentially no effect on the voltage-activated inward Ca^{2+} currents (*P > 0.05, n = 9, paired t-test*). (C) Current-voltage plot showing no effect of emodepside on the inward Ca^{2+} currents at the different voltage steps.

3.5 Discussion

3.5.1 Different mode of action

Emodepside is a cyclooctadepsipeptide anthelmintic that selectively inhibits muscle contraction of nematodes (Willson *et al*., 2003). It is effective against nematode isolates that have developed resistance to drugs from the other major classes of anthelmintic (Samson-Himmelstjerna von *et al*., 2005): ivermectin (an allosteric modulator of GluCl channels (Pemberton *et al*., 2001)), levamisole (a nematode selective nAChR agonist) and febantel (a selective ligand for nematode β-tubulin (Miro *et al*., 2006). Because emodepside retains its efficacy against these resistant isolates, it implies that emodepside has a different mode of action. In this paper we have examined effects of emodepside on the electrophysiology of *A. suum* muscle using two micropipette current- and voltage-clamp techniques with a view to determining its mechanism of action.

3.5.2 Emodepside is not a GABA receptor agonist

The earliest studies on the mechanisms of action of the cyclooctadepsipeptides used PF1022A. PF1022A seemed to exert its anthelmintic action on the nerves or muscle rather than affecting energy metabolism because low concentrations of PF1022A (<1 μM) depressed the motility of the nematode parasite, *Angiostrongylus cantonensis* (Terada, 1992). Chen *et al*. (1996) reported that PF1022A bound to GABA receptors of *Ascaris suum* muscle suggesting a direct effect on nematode GABA receptors. However, direct electrophysiological recording from *Ascaris suum* muscle found that PF1022A did not act

like GABA, nor did it act as a cholinergic antagonist (Martin *et al*., 1996a). Emodepside does not produce an increase in the muscle membrane conductance like GABA or piperazine (Martin, 1982) again showing that these compounds do not act as GABA agonists.

GeBner *et al.* (1996) reported that the depsipeptides PF1022A, PF1022-001 (antipode of PF1022A), valinomycin, enniatin A_1 and beauvericin have ionophore activities, increasing the bilayer conductivity to monovalent ions like Na^+, Li^+, K^+ and Cs^+. However, they reported that only PF1022A exerts high paralytic effect on *A. suum*, suggesting that the anthelmintic effects of the cyclooctadepsipeptides are not attributable to ion-carrier activity.

3.5.3 K^+-dependent hyperpolarization by releasing inhibitory neuropeptides (PF1/PF2)

Willson *et al*. (2003) tested the effects of emodepside on *Ascaris suum* muscle contraction and electrophysiology. They observed that 10 µM emodepside had a much slower inhibitory action on muscle contraction than GABA and produced a slow hyperpolarization with no detectable change in input conductance. The inhibitory neuropeptide, PF2, was also reported to cause slow inhibition of contraction of *A. suum* muscle, similar to emodepside (Fellowes *et al*., 2000; Willson *et al*., 2003). In this study we have observed similar, but concentration-dependent, effects with emodepside. Willson *et al*., (2003) showed that the K channel blocker 4-aminopyridine inhibited the effect of emodepside on membrane potential and suggested that emodepside may stimulate the release of inhibitory neuropeptides like PF1 or PF2 to produce its effects. PF1 causes slow, non-reversible, concentration-dependent membrane hyperpolarization that is significantly blocked by 4-aminopyridine (Franks *et al*., 1994; Verma *et al*., 2009). Here we have also observed similar effects of emodepside on the

membrane potential. Despite the similarity in PF1 and emodepside effects on the membrane potential, we have demonstrated clear differences in their mode of action. Unlike PF1 that has been reported to significantly inhibit voltage-activated Ca^{2+} currents (Verma *et al.*, 2009), we observed no effects of emodepside on the voltage-activated Ca^{2+} currents. We also observed that emodepside inhibited the ryanodine-induced spiking more slowly than PF1, probably because of the lack of emodepside effect on the voltage-activated Ca^{2+} currents. Though there are similarities in the effects of emodepside and the inhibitory neuropeptides PF1 and PF2, our body of evidence does not support the hypothesis that emodepside stimulates the release of a PF1-like neuropeptide.

3.5.4 Latrophilin Receptors

In 2004, Willson *et al.* described observations on the *C. elegans* pharynx with emodepside (100 nM) acting as an agonist to stimulate exocytosis and elicit pharyngeal paralysis. The paralysis of the pharynx produced by emodepside depended on the presence of LAT-1 with emodepside resistance appearing in *lat-1* null mutants. We observed evidence of expression of *Asc-lat-1* in adult muscle flaps and PKC & NO signaling pathways suggesting activation of G-protein receptor(s) by emodepside. Muhlfeld *et al.* (2009) used surface plasmon resonance to show that the neuropeptides AF1, AF10 and PF2 bind, albeit with low affinities, to HC110-R, implying that these neuropeptides may be putative natural ligands of the latrophilin-like receptor. They observed no reasonable binding characteristics with PF1 and other neuropeptides. Our observations, however, do not rule out a possible direct effect of emodepside on K channels.

3.5.5 SLO-1 as a target for emodepside in *C. elegans*

Guest *et al*. (2007) described use of a mutagenesis screen to generate alleles of *slo-1* that encodes for a calcium-activated K channel in *C. elegans*. They observed that *slo*-1 but not *slo-2* null mutants were more resistant to the inhibitory effects of emodepside than *lat-1* and *lat-2* (latrophilin receptor) double mutants. Guest *et al.* (2007) proposed that emodepside either directly or indirectly activates SLO-1 that is present in body wall muscle and motor neurons to produce its inhibitory effects in nematodes. Interestingly when *slo*-1 was selectively expressed in the pharyngeal muscle of *slo-1* null mutants, there was no effect of emodepside on the frequency of pharyngeal pumping contrary to what might be expected if emodepside exerts a direct effect on SLO-1. However, *slo-1* may regulate other features of the pharyngeal activity such as pump duration and pump interval and the effect of emodepside on these parameters remains to be investigated.

3.5.6 SLO-1 as a target for emodepside in *Ascaris suum*

We have observed expression of *Asc-slo-1*, an evolutionary conserved homolog of the *slo-1* gene in adult *A. suum* body muscle flaps; and have also observed a high conductance 250 pS K channel present in the *A. suum* bag membrane (unpublished single-channel observations). There is a Ca^{2+}-dependent and voltage-activated K channel present in *A. suum* muscle which is affected by the inhibitory neuropeptide PF1 (Verma *et al*., 2009). Our studies here indicate that the target of emodepside includes SLO-1-like K channels. We have observed: a Ca^{2+}-dependent and voltage-activated K current activated by emodepside; the inhibitory effects of

5 mM 4-aminopyridine on this current (which also blocks Ca^{2+}-independent I_a- but not Ca^{2+}-independent I_K-like K currents in *A. suum,* (Martin *et al*., 1992)); inhibitory effects of 10 nM iberiotoxin (which has selective effects on SLO-1 K currents, (Galvez *et al*., 1990; Candia *et al*., 1992; Gruhn *et al*., 2002). Not all of the emodepside K current was blocked by iberiotoxin which may be due to different types of β-subunits present with the SLO-1 α-subunits that effect iberiotoxin sensitivity (Meera et al., 2000b) or effects on K channels other than SLO-1, I_a or I_k.

We observed that the effect of emodepside was very slow in onset and increased over a period of more than 10 minutes. For example in our ryanodine-induced spiking experiments, we observed the speed of onset of the inhibitory action of emodepside was slower that the onset of PF1. The slowly developing effect of emodepside may be due to the highly lipophilic nature of this compound and a membrane partitioning effect. Indeed, the potency of a similarly lipophilic anthelmintic, ivermectin also follows a slow time-course in electrophysiological experiments in *A. suum* (Kass *et al*., 1980). Alternatively the slow time-course and persistence may be because emodepside does not directly activate the K channels but acts though a signaling cascade. We found that the emodepside effect was potentiated by a NO donor and a PKC activator, while antagonism of iNOS and inhibition of protein kinase with staurosporine inhibited the effects of emodepside. Interestingly, these signaling molecules are known activators of SLO-1 in other cells (Bolotina *et al*., 1994; Mistry and Garland, 1998; Wang *et al*., 1999b; Holden-Dye *et al*., 2007) and therefore emodepside may act through either or both of these signaling cascades and the signaling cascades may be in series or parallel. A number of studies on the mammalian orthologues of SLO-1 show that they are directly and alternately regulated by complex, multiple signaling cascades, involving

NO and diacylglyerol or Ca^{2+}-dependent PKC activation (Ghatta *et al*., 2006; Salkoff *et al*., 2006). Although emodepside is lipophilic, and this is consistent with the observed lack of a washout effect (Willson *et al*., 2003; Schurmann *et al*., 2007), we observed that the effect of emodepside on voltage-activated K currents continued to increase following washout. This is similar to PF1 (Verma *et al*., 2009) and therefore an additional, or alternative, explanation may be the involvement of a second messenger(s) signaling cascade.

To conclude, *Asu-slo-1* and *Asu-lat-1* are expressed in body flaps of the nematode parasite *A. suum.* Emodepside produces a 4-aminopyridine-sensitive hyperpolarization of the muscle membrane potential and potentiates voltage- & calcium-dependent, 4-aminopyridine- & iberiotoxin-sensitive, SLO-1-like channel currents that were affected by modulators of NO and PKC signaling pathways. Emodepside had no effect on voltage-activated calcium currents. The effects are consistent with a model in which NO, PKC and emodepside signaling pathways converge on the K channels, and/or a model in which emodepside activates the K channels through an NO or a PKC signaling cascade. Further experiments on heterologous expression systems are required to distinguish between these modes of action.

3.6 Acknowledgements

The research project culminating in this paper was funded by National Institute of Allergy and Infectious Diseases (NIH) grant R 01 A1 047194 to RJM, the Iowa Center for Advanced Neurotoxicity (ICAN) seed grant to APR and INRA (the French national institute for

Agricultural Research) to CLC and CN. We are grateful to Professor Dr Achim Harder (Bayer HealthCare AG, Animal Health, R & D-Parasiticides, Building 6700, 40789 Monheim, Germany) for generously providing the emodepside. We are grateful to Professor Robert J Walker and Dr Lindy Holden-Dye, University of Southampton, UK for critical reading of the manuscript.

3.7 Supplementary information

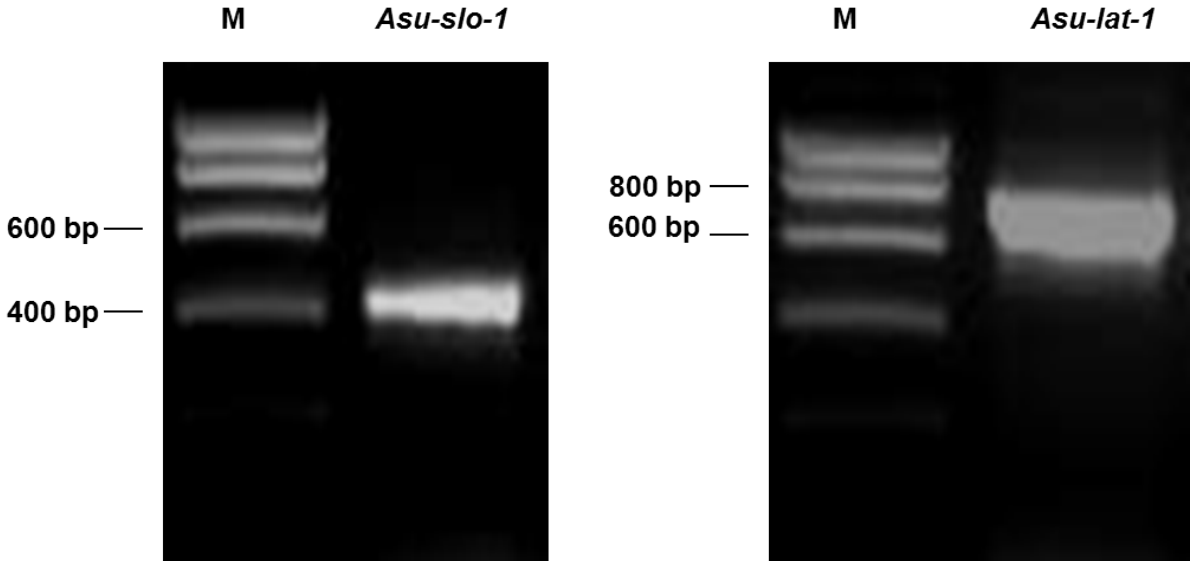

Supplementary Figure S3.0 Ethidium bromide stained agarose gel showing patterns revealed by RT-PCR for transcription of *Asu-slo-1* and *Asu-lat-1* from adult stage muscle flap.

M: Molecular marker

Table 4 Primer sequences used for *Asu-slo-1* and *Asu-lat-1* RT-PCR experiments

Gene name	Primer name	Primer sequence
Asu-slo-1	*Asu-slo-1F1*	ATGAGTGATGTGTATCACTCG
Asu-slo-1	*Asu-slo-1F2*	TTTACCGGCACAGTTATGGAT
Asu-slo-1	*Asu-slo-1R1*	ATCGAACTGCTCCAGTACGTA
Asu-slo-14	*Asu-slo-1R2*	ATAGGGTATCTGTGTACATTT
Asu-lat-1	*Asu-lat-1F1*	ATGAAGCAAGCAATTATCATT

Asu-lat-1	*Asu-lat-1F2*	CATTTCGCAGTCCTAATGGAT
Asu-lat-1	*Asu-lat-1R1*	CATATCACCATATGCTATCGT
Asu-lat-1	*Asu-lat-1R2*	GAACGCGTAGGCCATCACTGT

3.7.1 Diethylcarbamazine (DEC) potentiates emodepside effect on membrane potential and voltage-activated K^+ currents

We tested the effect of the anthelmintic diethylcarbamazine (DEC) on emodepside-induced hyperpolarization and increase in voltage-activated K^+ currents. DEC is used in the treatment of filarial diseases in humans, and heartworm disease (*Dirofilaria imitis*) in dogs. For example, a 6 mg/kg DEC plus 400 mg albendazole is used in the treatment of *Wuchereria bancrofti* and *Brugia malayi* in a mass drug administration (MDA) campaign in Thailand (Bhumiratana *et al*., 2010). The effect of DEC on *Brugia malayi* have been shown to be dependent on the inducible NOS and the cyclooxygenase pathways (McGarry, 2005).

Emodepside effect on the membrane potential was potentiated by DEC. 1 µM emodepside plus 100 µM DEC caused a significant hyperpolarization of 10.0 ± 2.0 mV ($p < 0.01$, $n = 5$, *paired t-test*, fig S3.1A) without significantly changing the input conductance. 100 µM DEC by itself caused a small, insignificant hyperpolarization.

Next, we investigated the effect of 100 µM DEC on the emodepside-induced increase in the SLO-1-like K^+ currents. We measured the change in the early phase K^+ currents (E_K), as opposed to the late phase currents (L_K). We elected to measure the E_K currents here because we observed that DEC and emodepside increased this phase of the K^+ currents more than

they increased the L_K K^+ currents. DEC alone significantly increased the E_K SLO-1-like K^+ currents by 20 % (*$p < 0.01$, $n = 4$, paired t-test*, fig S3.1C). When we applied 1 µM emodepside + 100 µM DEC, there was a 47 % increase in the E_K SLO-1-like K^+ currents (*$p < 0.01$, $n = 4$, paired t-test*, fig S3.1C) which continued to increase to 72 % during the post-emodepside period (*$p < 0.01$, $n = 4$, paired t-test*, fig S3.1C). In the change in half-maximal voltage bar chart in figure S3.1D, DEC shifted the average V_{50} by 1.4 mV (*$p < 0.001$, $n = 5$, paired t-test*) in the hyperpolarization direction and in the presence of emodepside + DEC, there was a further 3.2 mV (*$p < 0.01$, $n = 5$, paired t-test*) shift in the V_{50}. During the post-emodepside period, the shift in the hyperpolarization direction of the V_{50} continued to 4.7 mV (*$p < 0.01$, $n = 4$, paired t-test*). DEC and emodepside therefore lowers the voltage threshold for activation of the voltage-activated K^+ channel currents. DEC and emodepside had modest effects on the maximum conductance, G_{max}. Whereas DEC decreased G_{max} by 0.94 µS (*$p < 0.01$, $n = 5$, paired t-test*), emodepside + DEC decreased G_{max} by 1.2 (*$p < 0.05$, $n = 5$, paired t-test*).

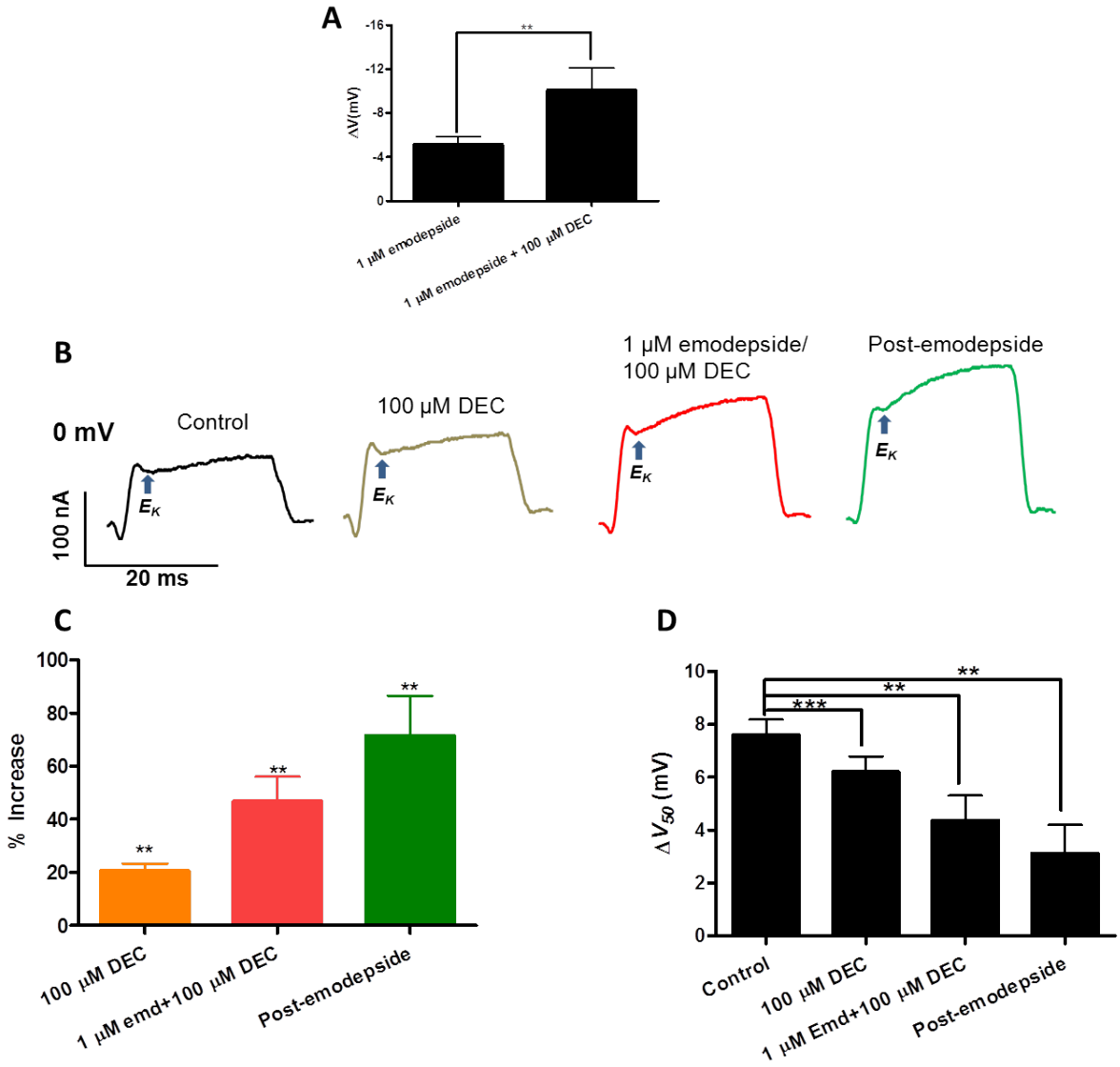

Supplementary figure S3.1 Effect of diethylcarbamazine (DEC) and emodepside on the membrane potential and voltage-activated K^+ currents in *A. suum*.

(A) Bar chart (Mean ± SEM) of the effect of 1 µM emodepside + 100 µM DEC on the membrane potential. 1 µM emodepside caused a significant hyperpolarization (*P < 0.001, n = 10, paired t-test*) which was significantly potentiated by 100 µM DEC (*P < 0.01, n = 5, paired t-test*). (B) Representative traces of control E_K current, 100 µM DEC effect on the E_K currents, emodepside + DEC effect on the E_K currents and the post-emodepside E_K currents.

(C) Bar chart (mean ± SEM) of the % increases in E_K currents caused by DEC (*P < 0.01, n = 4, paired t-test*), emodepside + DEC (*P < 0.01, n = 4, paired t-test*) and post-emodepside (*P < 0.05, n = 4, paired t-test*). Comparison was made with the % control E_K current. (D) Bar chart (mean ± SEM) of the change in half-maximal voltage, V_{50}, caused by DEC (*P < 0.001, n = 5, paired t-test*), emodepside + DEC (*P < 0.01, n = 5, paired t-test*) and post-emodepside (*P < 0.01, n = 4, paired t-test*).

Chapter 4 Levamisole-sensitive acetylcholine receptors of *Oesophagostomum dentatum*: diversity revealed by functional expression in *Xenopus* oocytes

A paper to be submitted to *PLoS Pathogens* 2012

Samuel K. Buxton[1, 2], Claude L. Charvet[2, 3], Cedric Neveu[2], Jacques Cabaret[2], Jacques Cortet[2], Alan P. Robertson[2], Richard J. Martin[2, 4*]

4.1 Abstract

More than 1.5 billion people are infected with parasitic nematodes. Parasitic nematode infections of animals have significant economic value. *Oesophagostomum dentatum* is a pig nodular worm that belongs to the same clade as *Caenorhabditis elegans* and *Haemonchus contortus*. The acetylcholine receptors in *O. dentatum* and other parasitic nematodes are targets for anthelmintics like levamisole and pyrantel. The *C. elegans* and *H. contortus* levamisole-sensitive receptors have been characterized in *Xenopus* oocytes, revealing important differences between the receptors in these nematodes. We have cloned four acetylcholine receptor subunits from *O. dentatum* (*Ode-unc-29, Ode-acr-8, Ode-unc-38, Ode-unc-63*) which are more identical to the homologs of *H. contortus* than *C. elegans*. By employing the *H. contortus* ancillary factors, RIC-3, UNC-50 and UNC-74, we demonstrate that these four *O. dentatum* subunits reconstitute four pharmacologically different levamisole receptor subtypes. Unlike in the *C. elegans* levamisole receptor, all four *O. dentatum* receptor subtypes responded to nicotine. When *Ode-unc-29* and *Ode-unc-63* were injected into the oocytes, a receptor that responded to pyrantel as the most potent agonist was formed (Pyr-nAChR subtype). When the subunit mix *Ode-*(*unc-29: unc-63: unc-38*) was injected, a receptor that responded to pyrantel and tribendimidine as the most potent agonists was

formed (Pyr/Tbd-nAChR subtype). These two receptor subtypes did not respond to bephenium and thenium. Injecting the subunit mix *Ode*-(*unc-29: unc-63: acr-8*) formed a receptor with ACh as the most potent agonist (nAChR subtype) and responses to bephenium and thenium. Last but not least, a receptor with levamisole as the most potent agonist (Lev-nAChR subtype) was formed when all four subunits were injected. The anthelmintic derquantel distinguished levamisole and pyrantel responses in the Lev-nAChR subtype, with pA2 values of 6.8 and 8.4 respectively, demonstrating the formation of more than one receptor subtype when all four subunits were injected. The calcium permeability (P_{Ca}/P_{Na}) of the Pyr/Tbd-nAChR, nAChR and Lev-nAChR subtypes differed; P_{Ca}/P_{Na} of 0.38, 0.38 and 10.3 were respectively measured for the three receptor subtypes. These results demonstrate the plasticity in parasitic nematode acetylcholine receptors.

---

[1] Graduate student and primary researcher
[2] Contributed to writing the manuscript
[3] Supervised and performed some of the molecular biology
[4] Corresponding author and Professor, Dept. Biomedical Sciences, Iowa State University.

4.2 Author Summary

Parasitic nematode infections of humans remain a public health concern in Latin America, Asia, and Africa. The drugs used in the treatment and prophylaxis of human nematode infections were first developed for use in animals. Although the anthelmintic levamisole is currently rarely used in humans, it nonetheless remains a relevant drug for treating parasitic nematode infections of animals in certain parts of the world. Levamisole targets the acetylcholine receptor in nematode somatic muscles, causing sustained depolarization and paralysis of the nematode which is actively removed from the hosts' GI tract. Although five

receptor subunits are required to reconstitute a levamisole receptor of *C. elegans*, we have demonstrated that a minimum of two subunits can reconstitute a levamisole receptor of *O. dentatum*. Although there are some similarities between the *C. elegans* levamisole receptor and that of *O. dentatum*, we demonstrate important differences in the sensitivity to nicotine, the number of subunits that forms a functional receptor, the number of levamisole receptor subtypes and the calcium permeability of *O. dentatum* levamisole receptors. This demonstrates the plasticity of *O. dentatum* receptors and has implications for use of other AChR agonist/antagonist anthelmintics in levamisole resistant parasites.

4.3 Introduction

Soil transmitted helminth infections are a public health concern in the tropic and subtropic regions of Africa, South America, Caribbean and Asia where over a billion people are infected (Hotez *et al*., 2007; Hotez *et al*., 2008). These helminthes also affect plants, livestock and domestic animals, causing economic losses in billions of dollars per year (Brown *et al*., 2006). Anthelmintics are used in the prophylaxis of soil transmitted helminth infections but the growing problem of anthelmintic resistance poses a major threat to human health and global livestock productions (Prichard, 1999; Kaplan, 2004). These anthelmintics include the benzimidazoles which act on beta-tubulins, the macrocyclic lactones which act on glutamate-gated chloride channels, the cholinomimetics which act on nicotinic acetylcholine receptors, and the cyclooctadepsipeptide emodepside which acts on SLO-1 channels (Martin, 1997; Wolstenholme and Rogers, 2005; Guest *et al*., 2007; Buxton *et al*., 2011). Cholinomimetic anthelmintics like levamisole and pyrantel act on nicotinic acetylcholine receptors located on the somatic muscle of parasitic nematodes, causing depolarization and

spastic paralysis of the worm (Aceves *et al*., 1970; Martin *et al*., 2005; Martin and Robertson, 2007).

Nicotinic acetylcholine receptors (nAChR) are prototypical members of the cys-loop ligand gated ion channel (LGIC) superfamily. Available evidence indicates that these receptors in parasitic nematodes are heterogeneous. In *Ascaris suum*, there are three subtypes of nAChR, *N*-, *L*- and *B*-subtypes (Robertson *et al*., 2002; Martin *et al*., 2004; Levandoski *et al*., 2005; Qian *et al*., 2006) and in *Oesophagostomum dentatum*, single channel recordings suggests the presence of four nAChR subtypes with the conductance states, G25, G35, G40 and G45 (Robertson *et al*., 1999). G25, G35, G40 and G45 conductance states are present in the levamisole-sensitive (SENS) isolate of the parasite but in the levamisole-resistant (LEVR) isolate, the G35 subtype is absent. In pyrantel-resistant *O. dentatum*, all four channel subtypes are present but the overall numbers of these channels are reduced (Robertson *et al*., 2000).

Three essential subunit genes, *unc-29, unc-38, unc-63* and two non-essential subunit genes, *lev-1* and *lev-8* make up the levamisole-sensitive nAChR in *Caenorhabditis elegans* (Lewis *et al*., 1980; Fleming *et al*., 1997; Richmond and Jorgensen, 1999; Culetto *et al*., 2004; Towers *et al*., 2005). The genes *unc-50, unc-74* and *ric-3* encode ancillary proteins required for AChR processing and assembly (Ben-Ami *et al*., 2005b; Haugstetter *et al*., 2005; Lansdell *et al*., 2005; Eimer *et al*., 2007; Millar, 2008). Boulin *et al.* (2008) reported that the 5 subunit genes and 3 ancillary factors are required for the robust expression of functional Lev-nAChR in *Xenopus* oocytes. Furthermore, Boulin *et al.* (2011) reconstituted two pharmacological subtypes of *Haemonchus contortus* nAChR, a Pyr-nAChR and a Lev-nAChR, with homologs of the *C. elegans* genes *unc-29, acr-8, unc-38, unc-63, ric-3, unc-50*

and *unc-74*. In contrast, Williamson *et al.* (2009) could reconstitute functional *A. suum* nAChR with only *Asu-unc-29* and *Asu-unc-38* without the requirement for any ancillary factors. These results suggest that there are differences in nAChRs between nematodes in different clades or in the same clade. Indeed, 11 distinct paralogous sequences of the *unc-29* gene have been discovered in the trichostrongylid parasites *Haemonchus contortus, Teladorsagia circumcincta* and *Trichostrongylus colubriformis*, showing the diversity in some parasitic nematode nAChR gene families (Neveu *et al*., 2010).

In the present study, we used candidate gene approach and the *Xenopus* oocyte expression system to characterize the *O. dentatum* L-nAChR. We report reconstitution of four pharmacologically different receptor subtypes, suggesting these receptors in *O. dentatum* are more plastic than in *C. elegans*. Three of the receptors bound levamisole with low affinity but the receptor that bound levamisole with high affinity was most permeable to calcium.

4.4 Materials and Methods

4.4.1 Ethical Concerns

All animal care and experimental procedures in this study were in strict accordance with guidelines of good animal practice defined by the Center France-Limousin ethical committee (France). Pig studies were performed under experimental agreement 6623 approved by the Veterinary Services (Direction des Services Vétérinaires) of Indre et Loire (France).

4.4.2 Accession numbers

The accession numbers for cDNA and protein sequences mentioned in this article are *C. elegans*: UNC-29 NM_059998, UNC-38 NM_059071, UNC-63 NM_059132, ACR-8 JF416644; *H. contortus*: *Hco-unc-29.1* GU060980, *Hco-unc-38* GU060984, *Hco-unc-63a* GU060985, *Hco-acr-8* EU006785, *Hco-unc-50* HQ116822, *Hco-unc-74* HQ116821, *Hco-ric-3.1* HQ116823; *O. dentatum*: *Ode-unc-29* not annotated yet, *Ode-unc-38* GU256648, *Ode-unc-63* HQ162136, *Ode-acr-8* not annotated yet.

4.4.3 Nematode Isolates

These studies were carried out on the levamisole-sensitive (SENS) and levamisole-resistant (LEVR) isolates of *O. dentatum* as previously described (Varady *et al*., 1997). Large pigs were experimentally infected with 1000 infective larvae (L3s) and infection was monitored 40 days later by fecal egg counts every 3 days. Levamisole susceptibility or resistance status of all isolates used in this study were checked in pairs of infected pigs, one treated with LEV at 7.5 mg/Kg and the other remaining untreated. The pigs were slaughtered after 80 days at the French National Institute for Agricultural Research (Nouzilly) abattoir and adult nematodes (males and females) of each isolate were collected from the large intestine and stored in RNA later (Qiagen®) at -80^{o}C.

4.4.4 Molecular Biology

Preparation of total RNA, cDNA clonings and cRNA synthesis was carried out as previously described (Boulin *et al*., 2011). cRNA samples were subjected to electrophoresis on ethidium

bromide-stained 1 % denaturing gel to assess their purity and integrity before storing at -80^{o}C.

4.4.5 Electrophysiological studies in oocytes

Xenopus laevis ovaries were obtained from NASCO (Fort Atkinson, Wisconsin, USA) and defolliculated using 1 – 2 mg/ml collagenase type II and Ca^{2+}-free OR2 (mM: NaCl 100, KCl 2.5, HEPES 5, pH 7.5 with NaOH). Alternatively, defolliculated oocytes were purchased from Ecocyte Bioscience (Austin, Texas, USA). Oocyte microinjection was carried out as described in (Boulin *et al*., 2008). Equal amounts of the *H. contortus* ancillary factors *ric-3, unc-50* and *unc-74* were added to each mix. Microinjected oocytes were incubated at 19^{o}C for 2 – 5 days. The oocytes were incubated in 200 µL of 100 µM BAPTA-AM for ~3 hours prior to recordings, unless stated otherwise. Recording and incubation solutions used are reported in (Boulin *et al*., 2008). Incubation solution was supplemented with Na pyruvate 2.5 mM, penicillin 100 U/mL and streptomycin 100 µg/ml. Oocytes were voltage-clamped at -60 mV with an Axoclamp 2B amplifier; all data were acquired on a desktop computer with Clampex 9.2.

4.4.6 Data analysis

Acquired data were analyzed with Clampfit 9.2 (Molecular Devices, Sunnyvale, CA, USA) and Graphpad Prism 5.0 software (San Diego, CA, USA). The response to 100 µM ACh was normalized to 100 % and the responses to the other agonists normalized to that of ACh. For

all dose-response relationships, the mean ± s.e of the responses is plotted. Dose-response data points were fitted with the Hill equation as described previously (Boulin *et al*., 2008).

4.5 Results

4.5.1 Identification of *unc-29, acr-8, unc-38* and *unc-63* homologs from *O. dentatum*

We have identified four full-length cDNAs from *O. dentatum* that encode genes homologous to *C. elegans unc-63, unc-38, unc-29* and *acr-8*. We cloned each subunit from both SENS (levamisole susceptible) and LEVR (levamisole resistant) strains of the parasite. The different AChR subunit sequences, accession numbers, characteristics and closest homologues in *C.elegans* and *H. contortus* are presented in Table 5.0. The *O. dentatum* AChR subunits cloned here are more closely related to the *H. contortus* homologues than the *C. elegans* homologues. The phylogenetic tree (Supplementary figure 4.6) shows the clustering of *O. dentatum unc-29, acr-8, unc-38* and *unc-63* with the *C. elegans* and *H. contortus* homologues.

Table 5 Comparison of *O. dentatum* AChR subunits with the homologs of *C. elegans* and *H. contortus*

Gene name	**Accession number**	**Full-length cDNA size (bp)**	**Deduced protein seq. length**	**% nucleotide identity**		**% amino acid identity/similarity**	
				C. elegans	***H. contortus***	***C. elegans***	***H. contortus***

Ode-unc-29	Yyyyy	1637	497	66	73	78/87	85/90
Ode-unc-38	GU256648	1681	507	66	70	72/77	83/87
Ode-unc-63	HQ162136	2265	507	67	80	77/84	92/95
Ode-acr-8	Zzzzzzz	1851	538	62	77	66/93	80/97

4.5.2 Four receptor subtypes reconstituted with four AChR subunit genes

To express *O. dentatum* receptors in *Xenopus* oocytes, we started by investigating the minimum number of subunits required to reconstitute a functional receptor. We injected cRNAs of the *O. dentatum* AChR subunits *unc-29, unc-38, unc-63* and *acr-8* in 1:1 ratio of different two-subunit combinations. We added the *H. contortus* ancillary factors *ric-3, unc-50* and *unc-74* to each mix. The oocytes injected with the 1:1 ratio of *unc-29* : *unc-63* responded to ACh, pyrantel (Pyr), tribendimidine (Tbd), nicotine (Nic) and levamisole (Lev). None of the oocytes injected with the other two-subunit combinations responded to any of the agonists we tested. Even at 30 µM, pyrantel had the most potent agonist effects on this receptor subtype compared to 100 µM ACh (Fig. 4.1B). We therefore termed this receptor *Ode*-(*29 – 63*) pyrantel-sensitive nAChR (Pyr-nAChR). We tested the effect of each subunit on the receptor by adding one subunit cRNA at a time to this receptor mix. The effect of AChR subunit on altering receptor pharmacology has been demonstrated in both vertebrate neuronal AChRs (Luetje and Patrick, 1991) and nematode AChRs (Williamson *et al*., 2009; Boulin *et al*., 2011).

Next, we injected a mix of *Ode*-(*unc-29 – unc-38 - unc-63*) plus the three ancillary factors. Oocytes injected with this new mix responded to all the agonists we tested except bephenium and thenium (Fig. 4.1D – F). Similar to the Pyr-nAChR *Ode-(29 – 63)* above, pyrantel was

the most potent agonist here. However in this mix, pyrantel and tribendimidine were equipotent at 30 µM. We termed this receptor *Ode*-(*29 – 38 – 63*) Pyr- and Tbd-sensitive receptor.

When we added *Ode-acr-8* to the *Ode*-(*unc-29 – unc-63*) receptor mix and injected this into the oocytes, we observed responses to all the agonists we tested including bephenium and thenium. This suggests that *Ode-acr-8* introduces bephenium and thenium binding site(s). At the concentrations tested, ACh was more potent than the other agonists in this receptor subtype (Fig. 4.2A – C). We termed this receptor *Ode*-(*29 – 8 – 63*) nAChR.

Last but not least, we injected all our subunits in a mix of *Ode*-(*unc-29 – acr-8 – unc-38 – unc-63*) plus the *H. contortus* ancillary factors. These reconstituted a receptor with levamisole as the most potent agonist (Fig. 4.2D – F). We termed this receptor *Ode*-(*29 – 8 – 38 – 63*) Lev-nAChR.

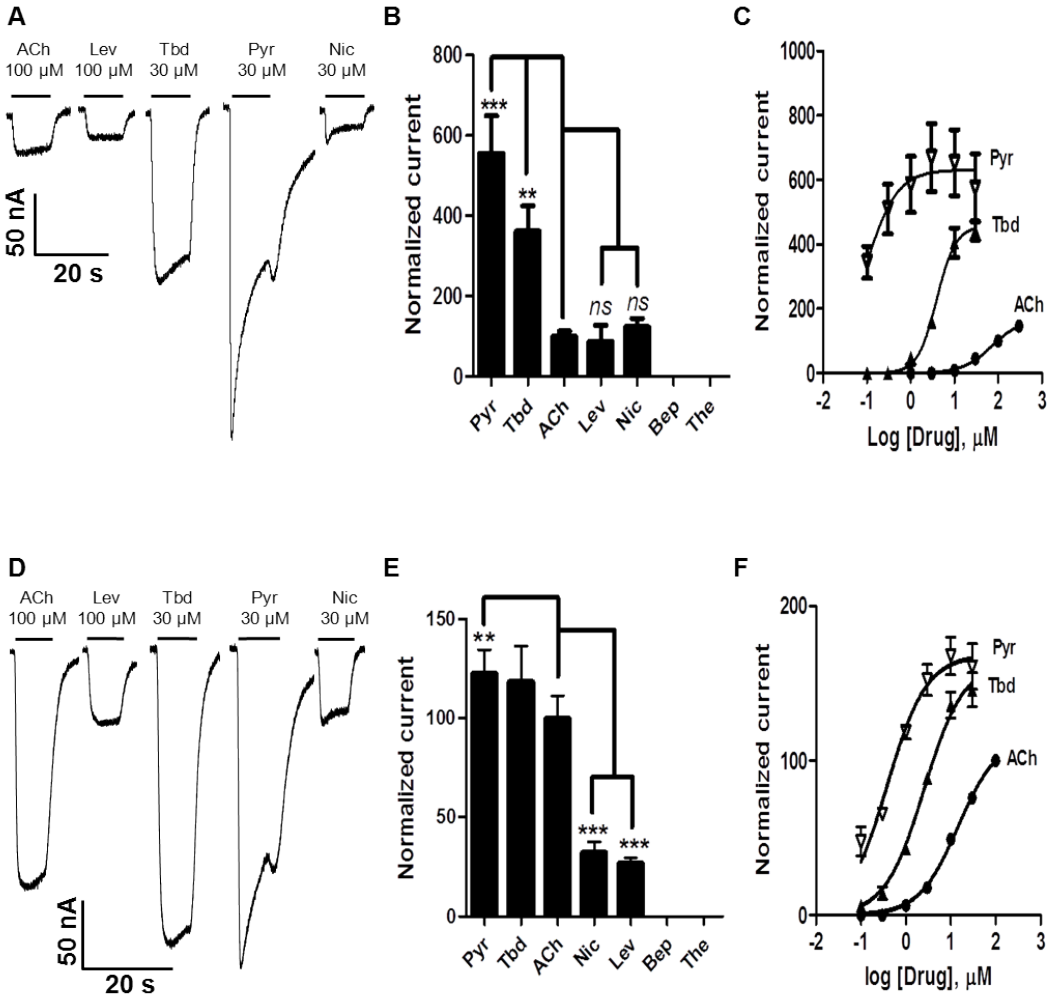

Figure 4.1 Voltage-clamp of oocytes injected with *O. dentatum* nAChR subunit genes.

(A) Representative traces showing the inward currents in oocytes injected with 1:1 *Ode-unc-29* and *Ode-unc-63*. We termed this receptor *Ode*-(*29 - 63*) Pyr-nAChR (B) Bar chart (mean ± se) of agonists-elicited currents in the *Ode*-(*29 - 63*) Pyr-nAChR, (p*aired t-test*, **p < 0.01, ***p < 0.001). (C) Dose-response relationships for Pyr (◊, n = 6), Tbd (▲, n = 5) and ACh (●, n = 6) in the *Ode*-(*29 - 63*) Pyr-nAChR, (n = number of oocytes). (D) Representative current responses to ACh, Lev, Tbd, Pyr and Nic in oocytes injected with 1:1:1 *Ode-unc-29.y, Ode-unc-38* and *Ode-unc-63*. Pyr/Tbd were the most potent agonists in this *Ode*-(*29 – 38 - 63*) Pyr/Tbd-nAChR (E) Bar chart (mean ± s.e) of the currents elicited by the different

agonists in the *Ode*-(*29 - 38 - 63*) Pyr/Tbd-nAChR (p*aired t-test, **p < 0.01, ***p < 0.001).* (F) Dose-response relationships for Pyr (◊, n = 6), Tbd (▲, n = 6) and ACh (●, n = 5) in the *Ode*-(*29 - 38 - 63*) Pyr/Tbd-nAChR.

4.5.3 The receptor subtypes are pharmacologically different

We further characterized each of these four receptor subtypes with the cholinergic anthelmintics levamisole, bephenium, thenium, tribendimidine and the agonists ACh and nicotine. It is noteworthy to state here that all the receptor subtypes responded to nicotine, thus our decision to rightly call them nAChR. In contrast, the levamisole-sensitive AChR in *C. elegans* do not respond to nicotine; the nicotine-sensitive receptor is a homopentamer of ACR-16 (Touroutine *et al*., 2005). Contrary to the observations in *H. contortus* (Boulin *et al*., 2011), the nicotine response in all four *O. dentatum* receptor subtypes is not insignificant; the smallest response was ~14.0 % of ACh response. In the *Ode*-(*29 – 63*) Pyr-nAChR, average pyrantel current amplitudes were >100 nA but <200 nA, although we occasionally recorded currents ~250 nA. Pyrantel currents were ~556 % of ACh currents ($p < 0.001$, $n = 9$, Fig. 4.1A-B). We initially applied 100 µM pyrantel to the injected oocytes but we observed a prominent open channel block effect. We thus lowered the pyrantel concentration to 30 µM although we still observed an open channel block effect at this concentration. Pyrantel is known to cause open channel block at high concentrations (Harrow and Gration, 1985a). Tribendimidine, the cholinergic anthelmintic approved for human use in China, was the second potent agonist with average currents <100 nA ($p < 0.01$, $n = 9$, Fig. 1B). Levamisole, nicotine and ACh were the least potent agonists and we observed no response to bephenium or thenium. Thus, the order of agonist potency for this *Ode*-(*29 – 63*) Pyr-nAChR subtype was Pyr > Tbd > Nic ≈ ACh ≈ Lev. The EC_{50} for pyrantel, tribendimidine and ACh were 0.09 µM, 3.9 µM and 72.4 µM respectively, indicating the relative potency of pyrantel over tribendimidine on this *Ode-(29 – 63)* receptor subtype.

The high and low affinities of AChRs to different agonists are due to the interaction between the α- and non-α-subunits (Arias, 1997), such that addition of another subunit(s) to the *Ode-(29 – 63)* mix above may change the affinity to some of the agonists. We observed that in the *Ode*-(*29 – 38 – 63*) Pyr-/Tbd-nAChR, pyrantel and tribendimidine were equally potent at 30 µM. The average pyrantel and tribendimidine currents were ~200 nA, 23 % ($p < 0.01$, n = 43, Fig. 4.1E) and 19 % ($p > 0.05$, n = 25, Fig. 4.1E) more than the response to ACh respectively. The nicotine and the levamisole currents were respectively 84 % ($p < 0.001$, n = 30, Fig. 4.1E) and 75 % ($p < 0.001$, n = 41, Fig. 4.1E) less than the ACh currents. The order of agonist potency for this receptor subtype was altered to Pyr ≈ Tbd > ACh > Nic ≈ Lev. The dose-response curves in Fig. 4.1F shows that pyrantel was more potent than tribendimidine at lower doses (0.1 – 10 µM) but at 30 µM both were approximately equipotent. The EC_{50} for pyrantel, tribendimidine and ACh were 0.4 µM (n = 6), 2.2 µM (n = 6) and 13.2 µM (n = 5) respectively. This receptor subtype suggests that tribendimidine could be used in cases where *O. dentatum* are resistant to levamisole.

In the *Ode*-(*29 – 8 – 63*) nAChR, the most potent agonist ACh elicited currents of ~800 nA or sometimes >1 µA. Tribendimidine, levamisole and pyrantel currents were respectively 25 % ($p < 0.05$, n = 24, Fig. 4.2B), 30 % ($n < 0.01$, n = 34, Fig. 4.2B) and 40 % ($p < 0.001$, n = 36, Fig. 4.2B) less than the ACh-induced currents. Here, the least potent agonists were nicotine, bephenium and thenium with average currents < 20 % of the ACh currents ($p < 0.001$, n = 27, Fig. 4.2B). The dose-response curves (Fig. 4.2C) suggest that levamisole and tribendimidine were partial agonists on this receptor subtype when compared with ACh. The EC_{50} for ACh, levamisole and tribendimidine were 3.5 µM, 2.2 µM and 0.8 µM respectively. Tribendimidine was more potent than ACh and levamisole at lower doses (0.1 – 3 µM) but

the top of the dose-response curves for tribendimidine and levamisole was below that of ACh. It is worth noting here that we used 30 µM tribendimidine as opposed to 100 µM levamisole. The pyrantel dose-response curve indicates that open channel block started after 3 µM pyrantel before the full agonist effect around 30 µM. Here, the altered agonist potency series was ACh > Lev ≈ Tbd > Pyr >Nic ≈ The ≈ Bep.

In the *Ode*-(*29 – 8 – 38 – 63*) Lev-nAChR, the current amplitudes of all the agonists were bigger than in the other three receptor subtypes. Average levamisole currents here were >1.5 µA, ~30 % more than the currents produced by ACh ($p < 0.001$, $n = 42$, Fig. 4.2E). The second and third most potent agonists were ACh and tribendimidine, respectively. Tribendimidine currents were >0.6 µA, ~1/2 of the ACh currents ($p < 0.001$, $n = 27$, Fig. 4.2E). The currents produced by bephenium, thenium and pyrantel were 23 % ($p < 0.001$, $n = 31$, Fig. 4.2E), 22 % ($p < 0.001$, $n = 25$, Fig. 4.2E) and 19 % ($p < 0.001$, $n = 21$, Fig. 4.2E) of the ACh currents respectively. The agonist potency series here was Lev > ACh > Tbd > Bep ≈ The ≈ Pyr > Nic. The EC_{50} values were 0.3, 3.1 and 4.2 µM for tribendimidine, levamisole and ACh respectively (Fig. 4.2F). Here, just as in the *Ode*-(*29 – 8 – 63*) nAChR, tribendimidine was more potent at the lower doses.

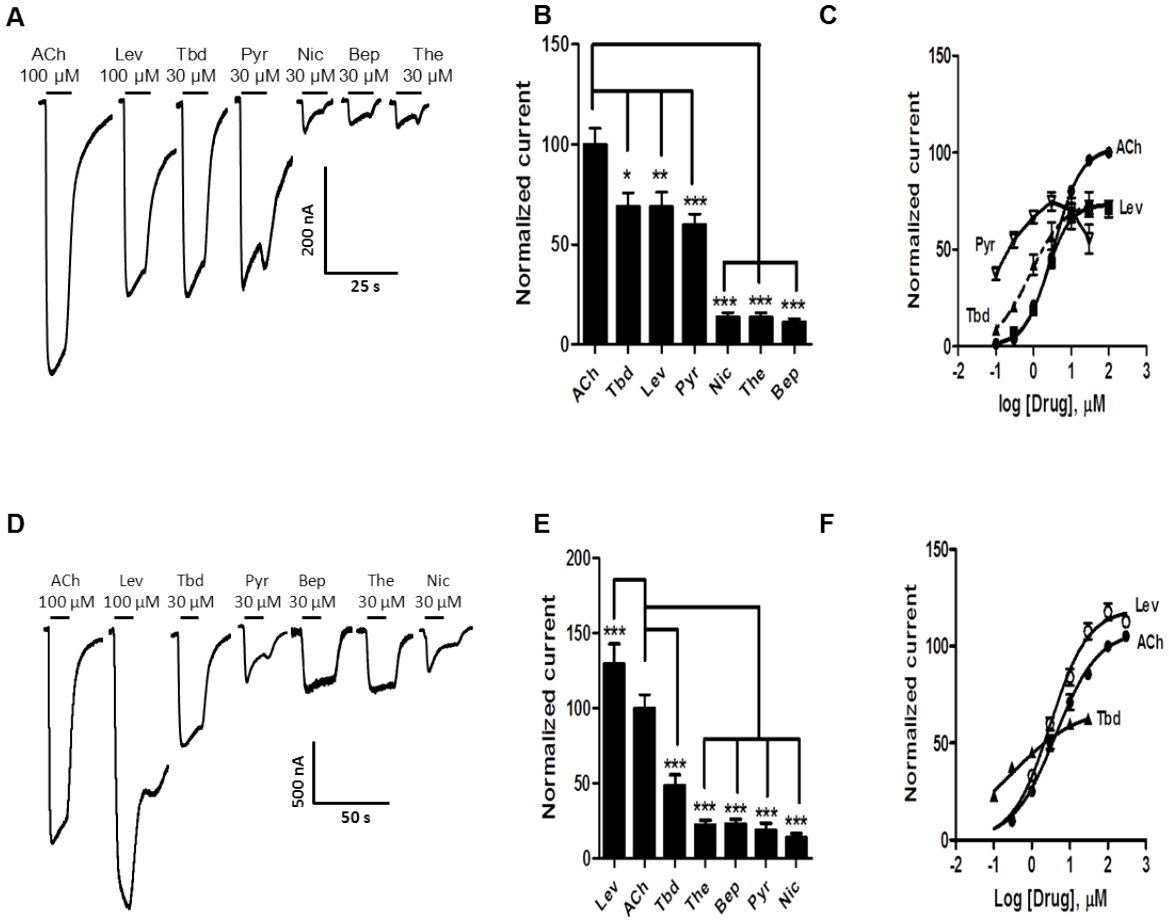

Figure 4.2 Voltage-clamp of oocytes injected with *O. dentatum* nAChR subunit genes.

(A) Representative currents elicited by ACh, Lev, Tbd, Pyr, Nic, Bep and The in the oocytes injected with *Ode-unc-29, Ode-acr-8* and *Ode- unc-63*. In this *Ode*-(*29 – 8 – 63*) nAChR, ACh was the most potent agonist. (B) Bar chart (mean ± se) of currents produced by the different agonists in the *Ode*-(*29 – 8 – 63*) nAChR, *(paired t-test, *p < 0.05, **p < 0.01, ***p < 0.001)*. (C) Dose-response relationships for ACh (●, n = 6), Lev (o, n = 6), Tbd (▲, n = 6) and Pyr (◊, n = 6) in the *Ode*-(*29 – 8 – 63*) nAChR. (D) Representative agonists-elicited currents in oocytes injected with *Ode-unc-29, Ode-acr-8, Ode-unc-38* and *Ode-unc-63*. Here, levamisole was the most potent agonist. Therefore, we termed this receptor *Ode*-(*29 – 8 – 38*

– *63*) Lev-nAChR. (E) Bar chart (mean ± se) of the normalized currents in the *Ode*-(*29 – 8 – 38 – 63*) Lev-nAChR, (p*aired t-test,* ***$p < 0.001$). (F) Dose-response relationships of Lev (o, n = 11), ACh (●, n = 18) and Tbd (▲, n = 6) in the *Ode*-(*29 – 8 – 38 – 63*) Lev-nAChR.

4.5.4 Pharmacological consequence of changing ratio of *Ode-*(*29 – 63*)

We injected 5:1 and 1:5 ratios of *Ode-unc-29 : Ode-unc-63* to find out if that alters the pharmacological profile of this receptor. We did not alter the amount of ancillary factors injected. Williamson *et al.* (2010) observed that changing the ratio of *Asu-unc-29* and *unc-38* injected into oocytes changed the pharmacology of the *A. suum* receptors.

In both 1:5 and 5:1 *Ode-29* : *Ode-63* injected oocytes, pyrantel remained the most potent agonist, followed by tribendimidine. In the 1:5 *Ode-29* : *Ode-63* injected oocytes, pyrantel current amplitudes were increased by >6-fold (~653 nA, $p < 0.001$, $n = 17$, data not displayed). The tribendimidine currents were also increased by ~6.6-fold (447 nA, $p < 0.01$, $n = 17$, data not displayed). Here, ACh was slightly more potent than nicotine and levamisole but the differences were not statistically significant. The agonist potency when we injected 5 times more *unc-63* than *unc-29* was therefore Pyr > Tbd > ACh ≈ Nic ≈ Lev. The increase in current amplitude with this ratio of subunits is less likely to be due to variations in current amplitudes in different batches of oocytes. When we injected the 1:1 and 1:5 *Ode-unc-29 : Ode-unc-63* in the same batch of oocytes, we still recorded currents of larger amplitude in the oocytes with a higher (5x) ratio of *Ode-unc-63*.

In the 5:1 *Ode-29* : *Ode-63*, nicotine and levamisole were slightly but significantly more potent than ACh ($p < 0.05$, data not displayed). The agonist potency series was slightly altered to Pyr > Tbd > Nic ≈ Lev > ACh. The current amplitudes in the 5:1 *Ode-29* : *Ode-63* were increased by not more than 1.5-fold. In heteropentameric nicotinic receptors, agonist binding sites are formed between an α-subunit and a non-α-subunit (Arias, 1997, 2000). We therefore predicted that pyrantel-preferred binding site(s) may be formed between *Ode-unc-29* and *Ode-unc-63* subunits with possible combinations of $(Ode\text{-}unc\text{-}29)_2(Ode\text{-}unc\text{-}63)_3$ and

(*Ode-unc-29*)$_3$(*Ode-unc-63*)$_2$. The (*Ode-unc-29*)$_2$(*Ode-unc-63*)$_3$ combination may predominate because we recorded currents of bigger amplitude in the 1:5 *Ode-unc-29 : Ode-unc-63* oocytes.

4.5.5 ACh response differs among the receptor subtypes

All four receptor subtypes we reconstituted responded to ACh but the current amplitudes differed among the subtypes. ACh is the main excitatory neurotransmitter in these nematodes. It is therefore expected that the receptor subtypes with bigger ACh current amplitudes may be physiologically relevant to the parasite. The *Ode*-(*29 – 63*) Pyr-nAChR gave the smallest response to 100 µM ACh, with average currents <50 nA. When we added *Ode-unc-38* to the above mix, the currents elicited by ACh in the *Ode*-(*29 – 38 – 63*) Pyr-/Tbd-nAChR increased ~10-fold. However, the currents elicited by pyrantel and tribendimidine in this subtype were increased by not more than ~2-fold. Further, we recorded ACh currents of ~800 nA or sometimes over 1 µA in the *Ode*-(*29 – 8 – 63*) nAChR subtype, after introducing *Ode-acr-8* to the two-subunits mix. We therefore hypothesized that *Ode-unc-38* (α-subunit) or *Ode-acr-8* (α-subunit) may interact with *Ode-unc-29* (non-α-subunit) to introduce additional binding site(s) that binds ACh with a higher affinity and/or these subunits may interact with *Ode-unc-63* (α-subunit) to increase ACh binding affinity at the *Ode-unc-29 – unc-63* binding site.

We recorded the biggest ACh currents in the mix containing all four receptor subunits. In this *Ode*-(*29 – 8 – 38 – 63*) Lev-nAChR, ACh elicited average currents >1.2 µA. Based purely on

the ACh current amplitudes, we speculate that the latter three receptor subtypes may be more physiologically relevant to the worm than the first receptor subtype.

4.5.6 Calcium permeability of the receptor subtypes differ

We measured the calcium permeability of three of the receptor subtypes, *Ode*-(*29 – 38 – 63*) Pyr-/Tbd-nAChR, *Ode*-(*29 – 8 – 63*) nAChR and *Ode*-(*29 – 8 – 38 – 63*) Lev-nAChR in BAPTA pre-soaked oocytes. The calcium permeabilities of different vertebrate neuronal and muscle AChRs have been well characterized, and these have an implication for the physiological function of the receptors. Generally, neuronal AChRs are more permeable to Ca^{2+} than muscle AChRs. Ca^{2+} entry through these receptors mediate a number of Ca^{2+}-dependent cellular processes, such as neurotransmitter release and synaptic plasticity (Fucile, 2004).

ACh-evoked currents in the three receptor subtypes were potentiated by increasing the external Ca^{2+} from 1 mM to 10 mM (Fig. 4.3A – C); this effect was voltage-dependent. Increasing or adding Ca^{2+} in the external solution should result in a positive shift in the reversal potential if Ca^{2+} is a permeant ion (Vernino *et al*., 1992). We observed a shift to the right in the reversal potential with the increase in external Ca^{2+} for the three receptor subtypes, suggesting that Ca^{2+} is a current-carrier in these receptor subtypes. The voltage-dependent increase in ACh-elicited currents with increasing external Ca^{2+} was more prominent in the *Ode*-(*29 – 8 – 38 – 63*) Lev-nAChR than in the other two receptor subtypes. In this receptor subtype the reversal potential shift was bigger, from -12.99 to 2.97 (Fig. 4.3A insert). Using the Goldman Hodgkin Katz constant field assumptions, we calculated this

change in reversal potential to correspond to Ca^{2+} permeability ratio P_{Ca}/P_{Na} of 10.26. The reversal potential shifts in the other two receptor subtypes were smaller. In *Ode*-(*29 – 38 – 63*) Pyr-/Tbd-nAChR the reversal potential shifted from 8.81 to 10.07, corresponding to permeability ratio P_{Ca}/P_{Na} of 0.38. A reversal potential shift from -4.35 to -2.63 was recorded in *Ode*-(*29 – 8 – 63*) nAChR, which corresponds to a permeability ratio P_{Ca}/P_{Na} of 0.38. The *Ode*-(*29 – 8 – 38 – 63*) Lev-nAChR appears to be more permeable to Ca^{2+} than the other two receptor subtypes and may play a more prominent role in modulating intracellular Ca^{2+} levels.

In addition to Ca^{2+} being a permeant ion in vertebrate neuronal nicotinic receptors, Ca^{2+} binds to the external side of the receptors and exerts a positive allosteric effect (Mulle et al., 1992b; Vernino et al., 1992). It is also possible that a positive allosteric site for Ca^{2+} exists in the *Ode*-(*29 – 8 – 38 – 63*) Lev-nAChR that is lacking in the other two receptor subtypes.

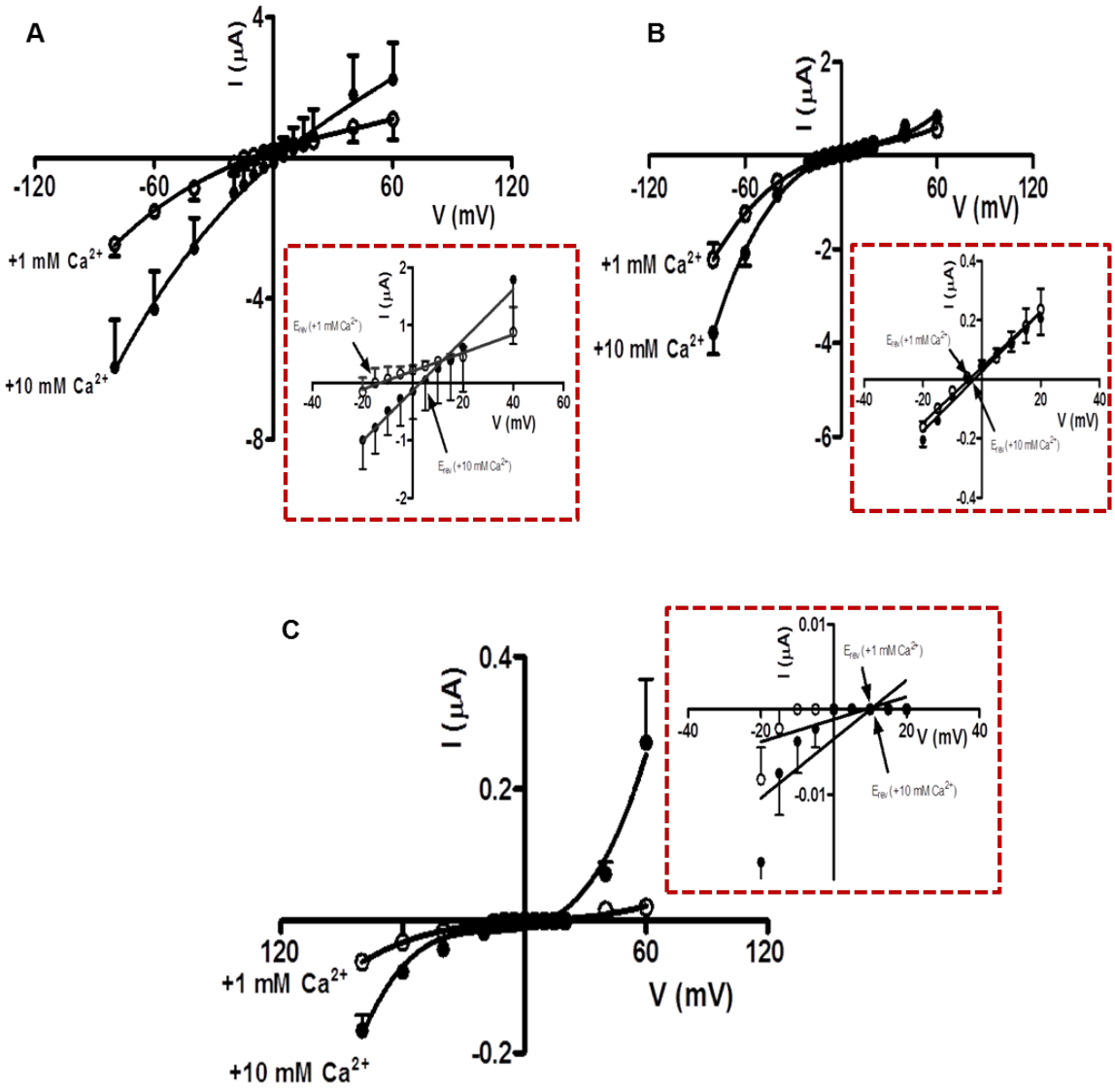

Figure 4.3 Ca^{2+}-permeability of three of the *O. dentatum* receptor subtypes

(A) Current-Voltage plot for oocytes injected with *Ode*-(*29 – 8 – 38 – 63*) in 1 mM and 10 mM Ca^{2+} recording solutions. *Insert:* Magnified view of current-voltage plot from -20 mV to +40 mV showing the E_{rev} in 1 mM and 10 mM extracellular Ca^{2+}. (B) Current-Voltage plot for oocytes injected with *Ode*-(*29 – 8 – 63*), showing the change in current with voltage in 1 mM and 10 mM Ca^{2+} recording solutions. *Insert:* Magnified view of current-voltage plot

from -20 mV to +40 mV showing the E_{rev} in 1 mM and 10 mM extracellular Ca^{2+}. (C) Current-Voltage plot for oocytes injected with *Ode*-(*29 – 38 – 63*) showing the current changes in 1 mM and 10 mM Ca^{2+} recording solution under different voltages. *Insert:* Magnified view of current-voltage plot from -20 mV to +40 mV showing the E_{rev} in 1 mM and 10 mM extracellular Ca^{2+}.

4.5.7 Derquantel distinguishes receptor subtypes in *Ode-(29 – 8 – 38 – 63)* Lev-nAChR

We hypothesized that when cRNA corresponding to the four nAChR subunit genes were injected to form the *Ode*-(*29 – 8 – 38 – 63*) Lev-nAChR, other receptor subtypes or combinations may also be formed. To test this hypothesis, we used 100 µM levamisole and 30 µM pyrantel to elicit inward currents in oocytes injected with a mix of the four receptor subunits and three ancillary factors. Derquantel was used to antagonize the responses produced by these two agonists (Fig. 4.4). Derquantel, or 2-deoxy-paraherquamide, is a semisynthetic derivative of paraherquamide. It has recently been marketed as Startect®, a combination of derquantel and abamectin. We then analyzed the antagonism produced by derquantel using the simple competitive model and nonlinear regression to estimate the pA_2 of levamisole and pyrantel (Martin *et al*., 2003). If levamisole and pyrantel acted on one and the same receptor subtype, then their pA_2 values will not differ. The pA_2 for levamisole was 6.8, different from the pyrantel pA_2 value of 8.4. The different pA_2 values indicate that the antagonism of levamisole by derquantel is different from the antagonism of pyrantel by derquantel. These suggest there is more than one receptor subtype formed in the *Ode*-(*29 – 8 – 38 – 63*) Lev-nAChR, and that levamisole and pyrantel have selective actions on the different receptor subtypes.

4.5.8 Requirement for the three ancillary factors is not absolute

According to Boulin *et al.* (2008, 2011), the ancillary factors RIC-3, UNC-50 and UNC-74 were absolutely required to reconstitute *C. elegans* and *H. contortus* receptors in oocytes. Removal of any or all of these factors either significantly decreased the amplitude or

completely abolished the reconstituted receptors. We tested the requirement for these ancillary proteins by sequentially removing each ancillary protein cRNA from the *Ode*-(*29 – 8 – 38 – 63*) Lev-nAChR mix.

When we injected this mix without the UNC-74 cRNA, the oocytes responded robustly to levamisole and ACh with currents greater than 1 µA. However, the levamisole current was reduced to just 6 % more than the ACh current (n = 11). We still observed responses to the other agonists, although the current amplitudes were reduced. UNC-74 appears to be required for the functional expression of Lev-AChRs. Its removal therefore reduced the Lev current amplitudes to near ACh current amplitudes. ACh currents here were ~91 % (Supplementary Fig. 4.7) of the ACh currents obtained with all the cRNAs, suggesting that robust functional receptors could be reconstituted without UNC-74. RIC-3 is an endoplasmic reticulum resident protein that acts as a chaperone for nAChR receptor maturation. RIC-3 enhances functional expression of some AChRs whilst inhibiting expression of other AChRs expressed in mammalian cell lines or *Xenopus* oocytes (Lansdell *et al*., 2005; Millar, 2008; Ben-Ami *et al*., 2009b). RIC-3 stabilizes receptor intermediates and promotes maturation of receptors through nAChR subunit-specific interactions (Ben-Ami *et al*., 2005b). When we removed RIC-3 cRNA from the mix, the levamisole and ACh currents were reduced by < 60 % of the corresponding currents obtained with all the cRNAs. Here, the ACh currents were ~42 % of the ACh currents obtained with the complete set of cRNAs (Supplementary Fig. 4.7).

The most striking decrease in current amplitudes was obtained when UNC-50 cRNA was removed from the mix. The ACh current amplitude obtained here was <20 % of the ACh current amplitude obtained with the complete set of cRNAs (Supplementary Fig. 4.7). UNC-50 is a Golgi resident protein that is required to prevent some AChR types from being

trafficked to and degraded by the lysosomal system (Eimer *et al*., 2007). In the absence of injected UNC-50 cRNA, it is reasonable to postulate that only a few synthesized receptors make it to the cell membrane. Removal of all the ancillary factors did not yield any measurable currents, demonstrating the requirement for at least one of these ancillary proteins to reconstitute robust functional receptors. We have showed therefore that unlike in *C. elegans*, robust functional *O. dentatum* receptors can be reconstituted when one of these three ancillary factors is omitted.

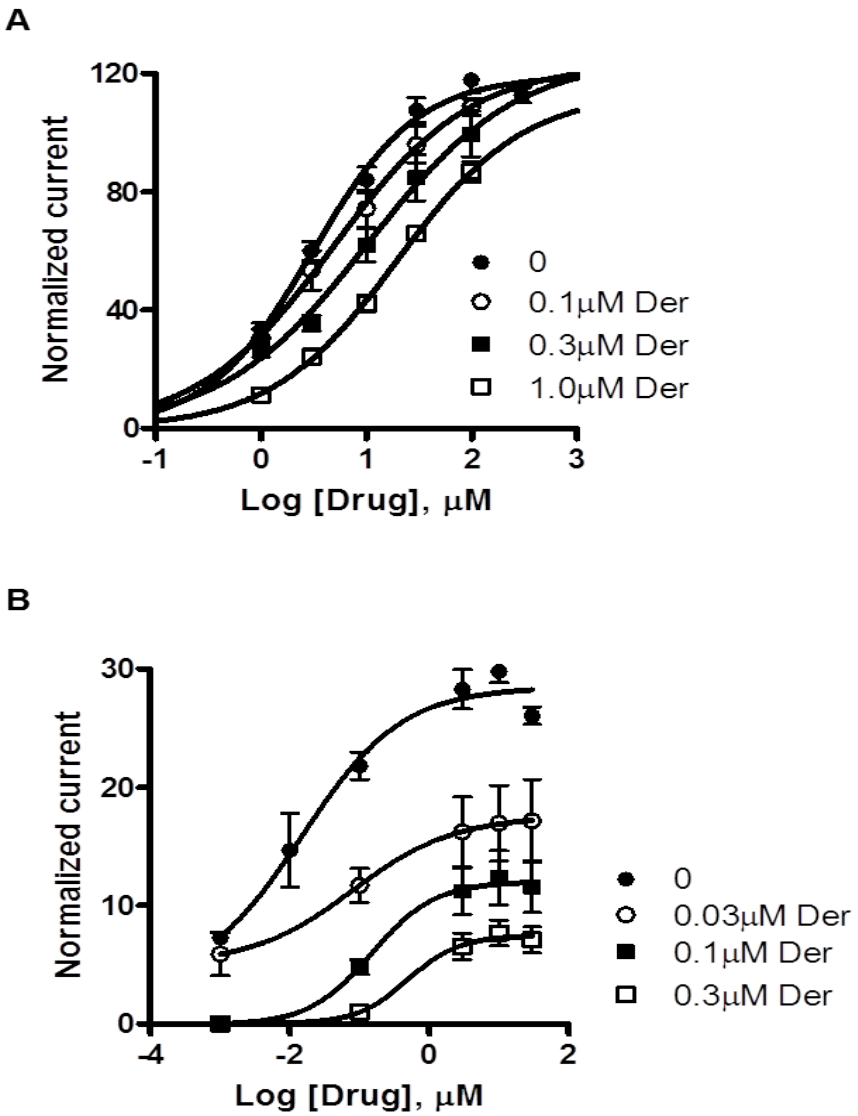

Figure 4.4 Derquantel as an antagonist of levamisole and pyrantel currents in *Ode*-(*29 – 8 – 38 – 63*) Lev-nAChR

(A) Antagonism of 100 µM levamisole responses by 0.1 – 1.0 µM derquantel. Note that derquantel produces dose-dependent effects but the top of the curves remain essentially unchanged, suggesting competitive antagonism. (B) Antagonism of 30 µM pyrantel responses by 0.03 – 0.3 µM derquantel. Note that the concentrations of derquantel here are lower but the antagonism is noncompetitive.

4.6 Discussion

4.6.1 Heterogeneity in parasitic nematode acetylcholine receptors

We have reported here the reconstitution of four subtypes of levamisole-sensitive AChR in oocytes using just four *O. dentatum* AChR subunits. The receptors differed in their pharmacology, subunit composition and calcium permeability. Interestingly, single channel recordings in the worm demonstrate levamisole- and pyrantel-activated receptors with four conductance states (Martin *et al*., 1997; Robertson *et al*., 1999, 2000). Single channel recordings and reconstitution studies in parasitic nematodes have demonstrated a heterogenous population of levamisole-sensitive AChRs (Robertson and Martin, 1993b; Qian et al., 2006; Williamson et al., 2009; Boulin et al., 2011). Williamson *et al* (2010) observed that by changing the ratio of just two *A. suum* AChR subunits injected into *Xenopus* oocytes, the pharmacology of the reconstituted receptors could be altered.

The heterogeneity of *O. dentatum* nicotinic acetylcholine receptors expressed in *Xenopus* oocytes or recorded directly from the worm is reminiscent of the heterogeneity of mammalian neuronal nicotinic acetylcholine receptors in sympathetic neurons (Mathie *et al*., 1991) or expressed in *Xenopus* oocytes (Papke and Heinemann, 1991; Zwart and Vijverberg, 1998). Mammalian α4β2 neuronal receptors expressed in oocytes at varying ratios of both subunits revealed four pharmacologically distinct receptor subtypes with stoichiometries not restricted to 2α:3β (Zwart and Vijverberg, 1998). Furthermore, replacing β4 with β2 in α3β4 injected into oocytes gave rise to channels with different conductance states, shorter open times and reduced tendency to re-open after closing (Papke and Heinemann, 1991), emphasizing the influence of different subunits on the pharmacology and

electrophysiological properties of these receptors. We have demonstrated here that just two subunits can form functional receptors in *Xenopus* oocytes, and addition of other subunits changes the pharmacology of these receptors. These heterogeneous, functional *O. dentatum* AChRs reconstituted in oocytes suggests that differential association of α and β-subunit is a mechanism by which multiple receptors are formed. The developmental regulation of the properties and distribution of AChRs (Schuetze and Role, 1987) may also account for the pharmacologically different receptor subtypes reconstituted here.

4.6.2 *O. dentatum* Lev-AChR differ from the *C. elegans* Lev-AChR

In *C. elegans*, five AChR subunit genes plus three ancillary factors were required to reconstitute a levamisole-sensitive AChR (Boulin *et al*., 2008). ACh was more potent than levamisole on this receptor type and most importantly, this Lev-AChR did not respond to nicotine. The *C. elegans* nicotine-sensitive receptor (N-AChR) is a homopentamer of ACR-16 subunits.

We were able to reconstitute functional *O. dentatum* AChRs with just two AChR subunit genes and the 3 ancillary factors. All four *O. dentatum* AChR subtypes we reconstituted responded to nicotine as well as levamisole. In 3 of the 4 receptor subtypes, ACh was more potent than levamisole but in the fourth receptor subtype with all 4 *Ode*-AChR subunits, levamisole was the most potent agonist. Unlike in the *C. elegans* Lev-AChR, we reconstituted two receptor subtypes with pyrantel as the most potent agonist.

According to Boulin *et al.* (Boulin *et al*., 2008), removal of the ancillary factors UNC-50 or UNC-74 from the mix resulted in over 90 % reduction of ACh currents when compared with

the mix containing all 3 ancillary factors. Removal of RIC-3 gave ACh currents that were slightly larger and more variable, although the ACh currents here were <40% of the currents obtained with all 3 ancillary factors. In contrast, the reduction in ACh currents when UNC-74 was removed from the *O. dentatum* receptor mix was <10% when compared to the mix containing the UNC-74 cRNA. Removal of UNC-74 from the *O. dentatum* mix however reduced the levamisole current amplitudes to just ~6% greater than the ACh current amplitudes, in agreement with UNC-74 requirement for Lev-AChR reconstitution. Furthermore, removal of RIC-3 gave ACh currents that were ~42 % of the currents obtained with all cRNAs. These results strongly demonstrate some differences in the requirement for ancillary proteins.

4.6.3 Physiological function of the *O. dentatum* receptor subtypes

Cholinergic receptors are permeable to and modulated by calcium. Neuronal nicotinic acetylcholine receptors have been shown to be more permeable to calcium than muscle receptors (Vernino *et al*., 1992). Changes in extracellular Ca^{2+} modulate neuronal nAChR in a dose-dependent manner. Ca^{2+} permeability through nAChRs modulates the excitability of neurons, participates in second-messenger cascades (Vijayaraghavan *et al*., 1995; Khiroug *et al*., 1998), controls neurotransmitter release from presynaptic terminals (Guo *et al*., 1998; Li *et al*., 1998), and regulates coexpressed postsynaptic receptors (Mulle *et al*., 1992a). Ca^{2+} entry through synaptic nAChRs could activate Ca^{2+}-dependent channels, such as Ca^{2+}-dependent K^{+} channel, leading to modulation of neuronal excitability (Tokimasa and North, 1984; Vernino *et al*., 1992).

We have demonstrated here that the levamisole-sensitive acetylcholine receptors of *O. dentatum* are permeable to Ca^{2+}. The *Ode*-(*29 – 8 –38 – 63*) Lev-nAChR subtype was the most permeable to Ca^{2+}, with P_{Ca}/P_{Na} of 10.3. This high Ca^{2+} permeability is comparable to that of chick α-bungarotoxin-sensitive α7 (P_{Ca}/P_{Na} = 10)(Bertrand *et al*., 1993), and rat α-bungarotoxin-sensitive α9 (P_{Ca}/P_{Na} ~ 9)(Katz *et al*., 2000) or α9α10 (P_{Ca}/P_{Na} = 9)(Weisstaub *et al*., 2002) expressed in oocytes; it is significantly higher than the P_{Ca}/P_{Na} recorded for *C. elegans* levamisole receptor (Boulin *et al*., 2008). In terms of Ca^{2+}-permeability, this *Ode*-(*29 – 8 –38 – 63*) Lev-nAChR channel subtype resembles a neuronal nAChR. Both *Ode*-(*29 – 38 - 63*) Pyr/Tbd-nAChR and *Ode*-(*29 – 8 – 63*) nAChR channel subtypes had Ca^{2+} permeabilities (P_{Ca}/P_{Na} = 0.38) slightly lower than that of *C. elegans* muscle levamisole receptor expressed in oocytes (P_{Ca}/P_{Na} = 0.6)(Boulin *et al*., 2008) and lower than the *Ode*-(*29 – 8 –38 – 63*) Lev-nAChR channel subtype.

Ca^{2+} is known to modulate acetylcholine receptors by acting as permeant ions and/or binding to an allosteric site on the extracellular face of the channel (Chang and Neumann, 1976; Vernino *et al*., 1992). Chelation of intracellular Ca^{2+} by BAPTA makes it less likely that Ca^{2+} is modulating the *O. dentatum* levamisole receptor channels from an intracellular side. However, second-messenger cascades closely associated with the intracellular side of the levamisole receptor channels cannot be precluded as a possible mechanism of modulating these channels. The subunits that make up these receptors are also known to affect their Ca^{2+} permeability. For example in muscle nAChRs, expression of the epsilon (ε) subunit increases the relative Ca^{2+}-permeability (Cens *et al*., 1997). Perhaps the high Ca2+-permeability of the *Ode*-(*29 – 8 –38 – 63*) Lev-nAChR channel subtype is due to the presence of an additional α-

subunit that is absent in either *Ode*-(*29 – 38 - 63*) Pyr/Tbd-nAChR or *Ode*-(*29 – 8 – 63*) nAChR channel subtypes.

4.7 Conclusion

We have demonstrated the plasticity of levamisole-sensitive acetylcholine receptors in *Oesophagostomum dentatum*. Four receptor subtypes with different pharmacological properties were reconstituted with four subunits. The calcium permeability of three of the four receptor subtypes has an implication for the physiological function of these receptors.

4.8 Acknowledgements

The authors will like to thank the funding partners, NIH RO1 AI047194 to RJM, Chateaubriand Fellowship from the French Embassy in USA to SB and INRA, Tours support to CN, CLC, and JC.

4.9 Supplementary information

4.9.1 Truncated *Ode-acr-8* from LEVR isolate

In addition to the *Ode-acr-8* that we cloned from both SENS and LEVR isolates of *O. dentatum*, we also cloned a truncated *Ode-acr-8* from the LEVR isolate. This truncated *acr-8, Ode-acr-8R,* is missing about ten amino acids in the transmembrane domain 1 (TM1) and all the amino acids in transmembrane domain 2 (TM2). Figure 4.5 below illustrates the amino acids lost in the TM1 and TM2 domains.

4.9.2 *Ode-acr-8R* reconstitutes Pyr/Tbd-nAChR

Because the truncated *Ode-acr-8R* is missing all the amino acids in the pore-lining TM2 domain, it is predicted here that it may not form part of the mature, functional receptor and it may affect the pharmacology of the receptor. TM2 from each subunit is predicted to form the lining of the ion channel pore (Hung *et al*., 2005; Bafna *et al*., 2008). If that was true, then replacing the full-length *acr-8* with the truncated form is predicted to reconstitute a receptor that is preferentially more sensitive to pyrantel and tribendimidine, similar to the receptor reconstituted without the full-length *acr-8S*. We tested this hypothesis by injecting this truncated *acr-8R* in the mix *Ode-unc-29 – unc-38 – acr-8R – unc-63* into oocytes. This receptor responded to ACh, pyrantel, tribendimidine, levamisole and nicotine but did not respond to bephenium or thenium. Similar to the *Ode*-(*unc-29 – unc-38 – unc-63*) Pyr/Tbd-nAChR described above, pyrantel and tribendimidine were the most potent agonists. However, the average pyrantel and tribendimidine currents were increased about 3-fold in this receptor. The average pyrantel and tribendimidine currents were respectively 637 nA and 636 nA (data not displayed). Also, the pyrantel and tribendimidine currents were both 54.0 % more than the ACh currents (for Pyr, $p < 0.05$, $n = 16$; for Tbd, $p < 0.001$, $n = 16$). Replacing the full-length *acr-8S* with the truncated form therefore reconstitutes a Pyr- and Tbd-sensitive receptor. This receptor type may likely exist in the LEVR *O. dentatum* parasites. Furthermore, the current responses to ACh, nicotine and levamisole were increased by 2.5-fold, 4.0-fold and 3.4-fold respectively when compared with the *Ode*-(*unc-29 – unc-38 – unc-63*) receptor above.

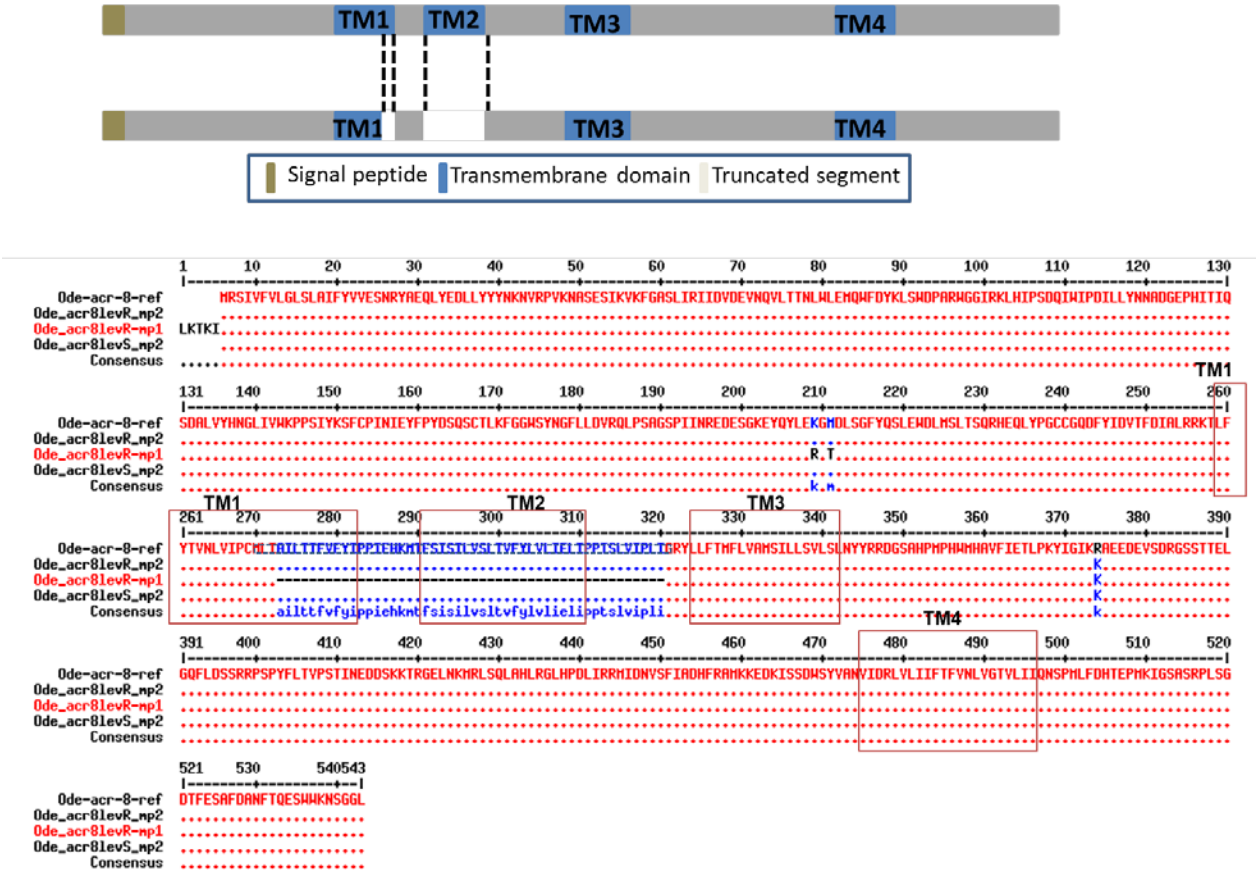

Figure 4.5 *Ode-acr-8R* showing the truncation in TM1 and TM2 domains.

All the amino acids that make up the TM2 domain are truncated, in addition to the last ~10 amino acids in the TM1. TM2 is predicted to line the pore of the ion channel receptor.

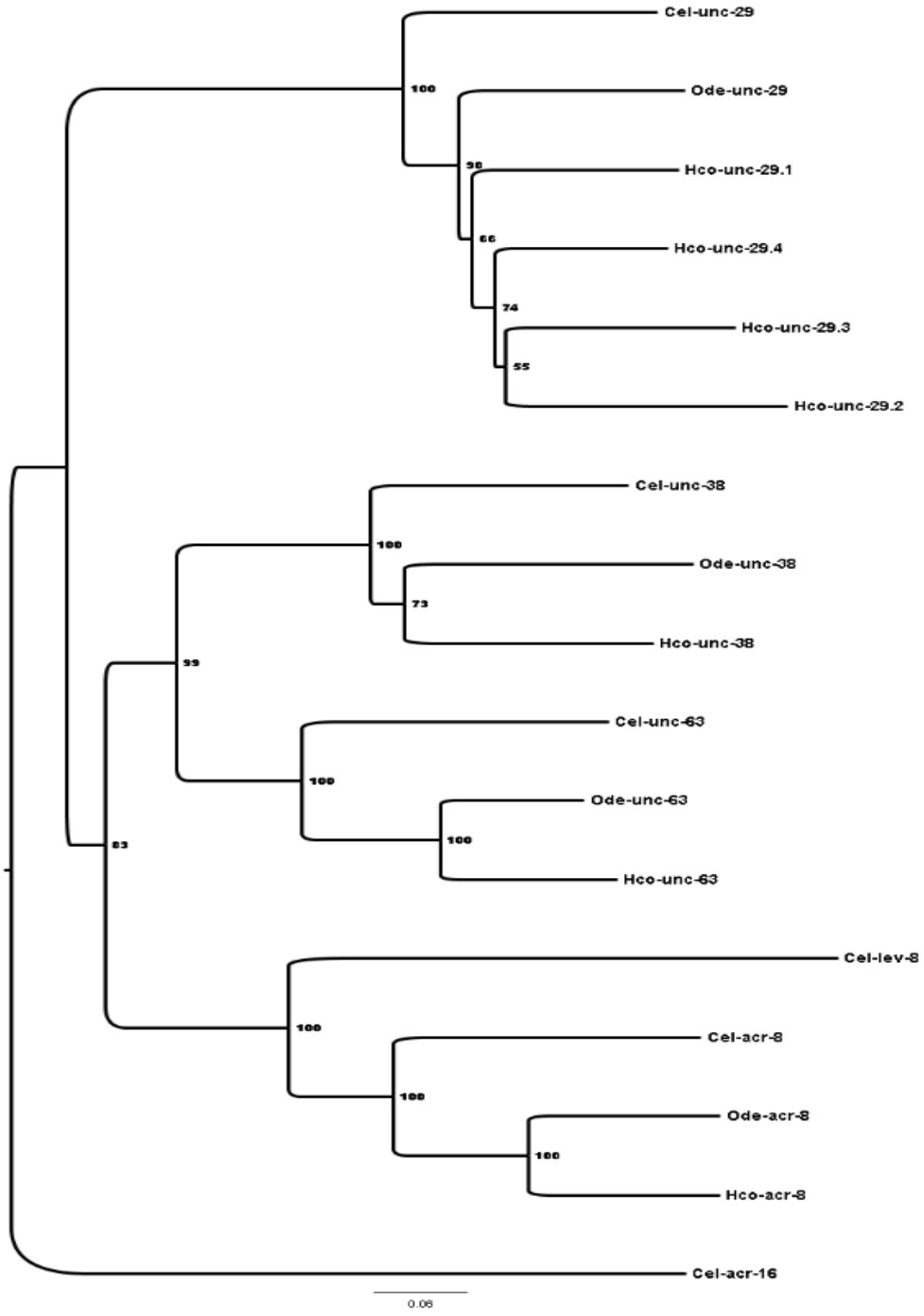

Figure 4.6 Phylogenetic comparisons of the *O. dentatum* AChR subunits with the *H. contortus* & *C. elegans* homologues. Neighbour joining (NJ), HKY substitution model were used in constructing the tree.

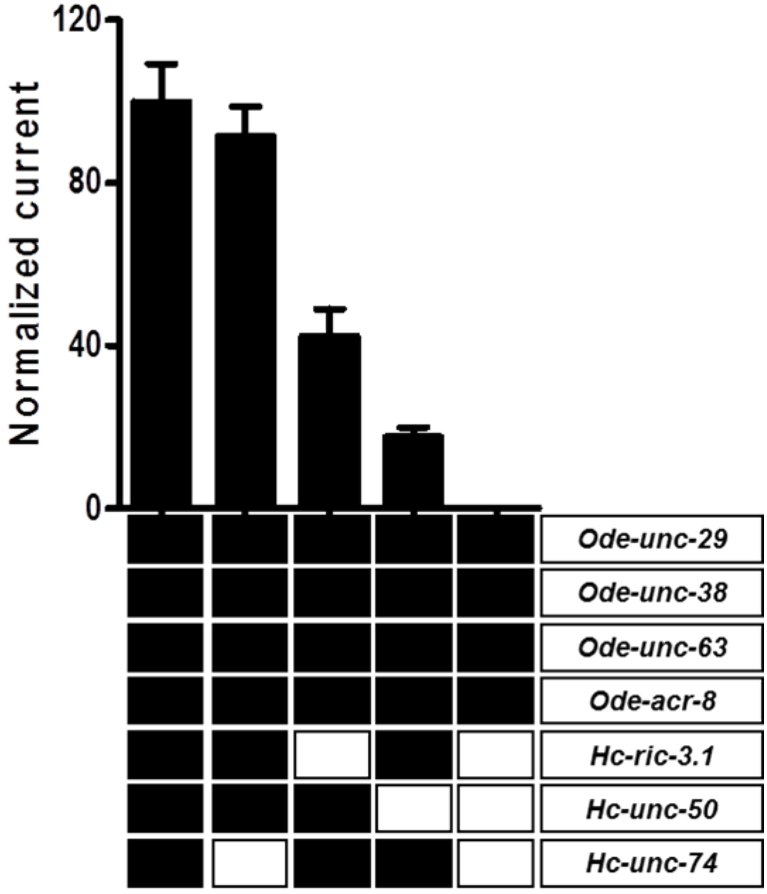

Figure 4.7 Effect of the *H. contortus* ancillary factors on ACh current responses in the *Ode-*(*29 – 8 – 38 – 63*) Lev-nAChR

4.9.3 Ca^{2+}-permeability measurements

For these set of experiments, we increased external Ca^{2+} in the recording solution from 1 mM to 10 mM without changing the concentration of the other ions. We used the GHK equation to calculate the permeability ratio, P_{Ca}/P_{Na}. Due to BAPTA treatment before recordings, we assumed the internal [Ca^{2+}] to be negligible; we also assumed permeability to Na and K, P_{Na} and P_K, are equal.

Table 6.0 Primers used for the PCR and cloning of *O. dentatum* AChR subunits

Gene name	**Primer name**	**Primer sequence**
Ode-unc-29	F-Hind3	AAAAAGCTTATGCGTCTCGAACCGTTACTTC
	R-Apa1	TTTGGGCCCTAAACCCGTACAGTCATAAAACAAT
Ode-unc-38	F-Xho1	AAACTCGAGATAGCTGGTTGCAAGTGCGTATT
	R-Apa1	TTTGGGCCCTCTCAACAAAATTGGCCTAATATAC
Ode-unc-63	F-Xho1	AAACTCGAGATGCTGACGCGACAAGTGTTC
	R-Apa1	TTTGGGCCCTACCCAGCCGGCTGCTCGC
Ode-acr-8	F-Hind3	AAACTCGAGCTTGGCTAGCTTAAAACTAAGATT
	R-Apa1	TTTGGGCCCAACCATAATACTATACATATCTCAGA

CHAPTER 5 GENERAL DISCUSSION

Most of the anthelmintics used in the prophylaxis of parasitic nematode infections act on nematode ion channels. These include the cholinergic agonists/antagonists, the avermectins and the milbemycins. The mainstay anthelmintics include the benzimidazoles (BZs), cholinergic agonists/antagonists, and the macrocyclic lactones. However, there are reports of resistance to some of the mainstay anthelmintics and this has increased the need to understand the mechanisms of resistance and in order to design better drugs that have 'resistance-busting' properties.

Emodepside is a member of the cyclooctadepsipeptide family that has a novel mechanism of action. Both emodepside and the parent compound, PF1022A, are effective against parasitic nematodes that are resistant to some of the mainstay anthelmintics. Earlier studies using the free-living non-parasitic nematode, *C. elegans* implicated the voltage-activated, calcium-dependent potassium channel, SLO-1 (also known as BK or maxi-K channel) and the latrophilin-like receptor, LAT-1/LAT-2 as emodepside/PF1022A target sites. We have showed for the first time the effects of emodepside on voltage-activated currents in a parasitic nematode, *A. suum*. We have demonstrated the potentiating effect of emodepside on voltage-activated, calcium-dependent K channels. This effect of emodepside is mediated by NO and/or protein kinases (PKC). We have also demonstrated that SLO-1 and LAT-1 are expressed in *A. suum* muscle flap. Emodepside has selective action on the parasites SLO-1; it is ~100 times less selective for the vertebrate receptor, KCNMA/KCNMB (Welz *et al*., 2011). There is reason to propose that emodepside may be effective against filarial worms, such as *Onchocerca volvulus* that causes river blindness in most parts of Africa and Asia (Boussinesq, 2008). In fact, according to the World Health Organization (WHO) African

Programme for Onchocerciasis Control (APOC), emodepside and monepantel are two potential drugs that will be evaluated for control of these parasites (WHO, 2009).

Recents reports have resurrected the hypothesis that one of the target sites for emodepside is the GABA receptor in *C. elegans* (2011 WAAVP conference communication). An earlier report by Chen *et al.* (1996) suggested that the parent compound of emodepside, PF1022A, bound to the GABA receptor in *Ascaris*. However, subsequent researchers observed that emodepside action on *Ascaris suum* membrane potential does not mimick that of GABA, raising doubts about the GABA receptor contributing to emodepside effects (Willson *et al*., 2003). What is presently not in doubt is the fact that SLO-1 is a major target receptor for emodepside.

On the other hand, levamisole is an old but still 'relevant' anthelmintic with well-documented reports of resistance in different parasitic nematodes. Levamisole remains 'relevant' because in countries (for example, Argentina and Uruguay) where there is resistance to ivermectin and benzimidazoles, it is an affordable anthelmintic alternative. In addition, levamisole has increased our understanding of the acetylcholine receptors in nematodes. Mutagenesis screens in *C. elegans* that uncovered levamisole-resistant genes (Lewis *et al*., 1980; Lewis *et al*., 1987) and subsequent reconstitution experiments (Fleming *et al*., 1997; Culetto *et al*., 2004; Boulin *et al*., 2008), as well as single-channel recordings have tremendously impacted our knowledge about levamisole receptors of nematodes. We have demonstrated here that in the pig nodular worm *Oesophagostomum dentatum,* four functional levamisole-sensitive receptor subtypes can be reconstituted in *Xenopus* oocytes with four subunit genes. Coincidentally, single-channel recordings with levamisole and pyrantel in the nodular worm demonstrate the presence of four conductance states of the

nicotinic receptors (Robertson *et al*., 1999, 2000). We have characterized the receptors and showed their pharmacological differences, as well as different calcium permeabilities. Our results indicate that there are some AChR receptor subtypes in parasitic nematodes that remain to be explored as targets for anthelmintic drugs. The receptor subtypes we have reconstituted here suggest that there may be tissue-specific expression of nicotinic receptors in nematodes, as well as life-stage-specific expression of some of these receptors. In fact, there is precedence for both tissue-specific expression and developmental regulation of nicotinic receptors in vertebrates (Schuetze and Role, 1987; Millar, 2003) and nematodes (Fleming *et al*., 1997; Culetto *et al*., 2004; Towers *et al*., 2005).

This PhD research demonstrates that there are attractive targets for new anthelmintics in parasitic nematodes that are underexplored/underutilized (voltage-activated K+ channels). Even for some nematode ion channels that are targeted by existing anthelmintics, there are subtypes that can be explored to increase the efficacy of these anthelmintics. Resistance to anthelmintics is thus not an insurmountable problem in parasitic nematodes.

Future directions

There are a number of experiments that can still be done to increase our understanding of the mechanism of action of emodepside in parasitic nematodes and to characterize the *O. dentatum* levamisole receptors. First, the cloning, expression and characterization of *Asu-slo-1* and/or *Asu-lat-1* with emodepside and other pharmacological compounds will be a great way to show whether or not emodepside has a direct effect on these ion channels. To show if intracellular NO is affected in any way be emodepside, the Greiss test can be used to measure

$[NO]_i$ in *A. suum* muscle flap in response to ACh. A similar assay can be used to check for the role of protein kinases, especially PKC in the effect of emodepside, for example, by measuring diacylglyerol (DAG) in *A. suum* by using fluorescent assays.

Although the three ancillary proteins, RIC-3, UNC-50 and UNC-74 are evolutionarily conserved, there are species dependent effects of these ancillary factors. In place of the *H. contortus* ancillary factors, one can clone the homologs of *O. dentatum* to see their effect on the pharmacology of the levamisole receptors. Although LEV-1 cloned from the trichostrongylid parasites appears to lack a signal peptide (Neveu *et al*., 2010; Boulin *et al*., 2011), raising questions about their involvement in forming part of the levamisole receptor in these parasites, *Cel-lev-1* forms part of the levamisole receptor. Cloning the *Ode-lev-1* and adding it to the receptor mixes will show the effect of this levamisole receptor subunit on the pharmacology of the receptor subtypes.

APPENDIX A Emodepside and SLO-1 potassium channels: A review

From paper published in *Experimental Parasitology* (2011)

RJ Martin[2, 3], SK Buxton[3], C Neveu[3], CL Charvet[3], AP Robertson[3]

A1.0 Abstract

Nematode parasites infect humans and domestic animals; treatment and prophylaxis require anthelmintic drugs because vaccination and sanitation is limited. Emodepside is a more recently introduced cyclooctadepsipeptide drug that has actions against GI nematodes, lungworm, and microfilaria. It has a novel mode of action which breaks resistance to the classical anthelmintics (benzimidazoles, macrocyclic lactones and cholinergic agonists). Here we review studies on its mode of action which suggest that it acts to inhibit neuronal and muscle activity of nematodes by increasing the opening of calcium-activated potassium (SLO-1) channels.

---

[1] Reprinted with permission of *Experimental Biology* (2011), **doi:10.1016/j.exppara.2011.08.012**

[2] Corresponding author and Professor, Dept. Biomedical Sciences, Iowa State University

[3] Contributed in writing the manuscript

A2.0 Introduction

Parasitic nematode infections place a heavy burden on both humans and animals. It is estimated that the global prevalence of parasitic nematode infections in humans is over two billion (de Silva *et al*., 2003). These infections are debilitating, produce lost productivity, mental impairment, and poor growth and contribute to poverty. The incidence of human helminthiasis is higher in warmer, wetter areas where poor sanitation makes the spread of

nematode parasite infections all too easy. In hot dry or very cold climates, the spread of the helminth infection is much slower even if sanitation is limited, because the free living intermediate stages do not survive well. In domestic animals, nematode parasites cause production loss, welfare issues and reduce the food supply. In the absence of effective vaccines and good sanitation to prevent the spread of these parasitic infections, anthelmintic drugs are used for both treatment and prophylaxis in humans and animals. Disturbingly, there are reports of growing resistance to the main groups of anthelmintic drugs in both man and animals. There is evidence of resistance to the benzimidazoles (albendazole), nicotinic agonists (levamisole/pyrantel) and macrocyclic lactones (ivermectin) in domestic animals (Wolstenholme *et al*., 2004) and concerns in humans (Geary *et al*., 2009). Recently, novel 'resistance- busting' anthelmintics (emodepside, a cyclooctadepsipeptide; monepantel, an amino-acetonitrile derivative, and derquantel, a paraherquamide derivative) have been developed. The need for these new anthelmintics and ways to combat resistance to the currently available anthelmintics is urgent. Here we review recent information on the mode of action of emodepside with the intention that this information will facilitate understanding and development of the drug, and perhaps development of additional compounds.

A3.0 Spectrum of action

Sasaki *et al*. (1992) described the isolation of the cyclooctadepsipeptide PF1022A from cultured Mycelia sterilia, a fungus found on leaves of a flowering shrub (Camellia japonica). Emodepside (Fig. 5.0A) is a semisynthetic analogue of PF1022A that is produced by adding two morpholine rings to the para-position of the two D-phenyllactic acids (Harder *et al*.,

2005) in order to enhance pharmacokinetic properties. Emodepside or PF1022A are effective against: gastro-intestinal nematodes of mice, rats, chickens, sheep, cattle, horse, dogs and cats and Trichonella spiralis (Martin *et al*., 1996a; Harder *et al*., 2003); and pre-adult stages of the filariae, *Acanthocheilonema viteae, Brugia malayi,* and *Litomosoides sigmodontis*. The effects against the adult stages of filaria are species dependent; there is little effect of emodepside against adult *B. malayi* (Harder *et al*., 2003).

A3.1 Different mode of Action

Emodepside selectively inhibits body muscle contraction of nematodes (Terada, 1992; Willson *et al*., 2003). Emodepside is effective against nematode isolates that have developed resistance to drugs from the major classes of anthelmintic (Samson-Himmelstjerna von *et al*., 2005), namely: ivermectin (an allosteric modulator of GluCl channels, (Pemberton *et al*., 2001)), levamisole (a nematode selective nAChR agonist, Qian *et al*., 2006; Qian *et al*., 2008) and febantel (a selective ligand for nematode b-tubulin, (Miro *et al*., 2006)). Because emodepside remains effective against resistant isolates, it suggests that emodepside has a different mode of action.

A3.2 Does not act as a GABA agonist or nicotinic antagonist

The earliest studies on the mechanisms of action of the cyclooctadepsipeptides used PF1022A. PF1022A seemed to exert its anthelmintic action on either nematode nerve or muscle rather than on its energy metabolism; low concentrations of PF1022A (<1 µM) inhibited the motility of the nematode parasite, Angiostrongylus cantonensis (Terada, 1992).

Although it was reported (Chen *et al*., 1996) that PF1022A bound to GABA receptors of *Ascaris suum* muscle, suggesting a direct effect on nematode GABA receptors, direct electrophysiological recording from *A. suum* muscle found that PF1022A did not act like GABA, nor did it act as a cholinergic antagonist (Martin *et al*., 1996). Emodepside does not produce an increase in the muscle membrane conductance like GABA or piperazine (Martin, 1982) again showing that these compounds do not act as GABA agonists. Another possibility (GeBner *et al*., 1996) was that PF1022A is an ionophore because PF1022, PF1022-001 (antipode of PF1022A), valinomycin, enniatin A1 and beauvericin all have ionophore activities, and may increase bilayer conductivity to monovalent ions (Na^+, Li^+, K^+ and Cs^+). However, only PF1022A not PF1022-001 (the antipode), had a potent paralytic effect on *A. suum*, suggesting that the selective anthelmintic effects of PF1022A was not due to any ion-carrier activity.

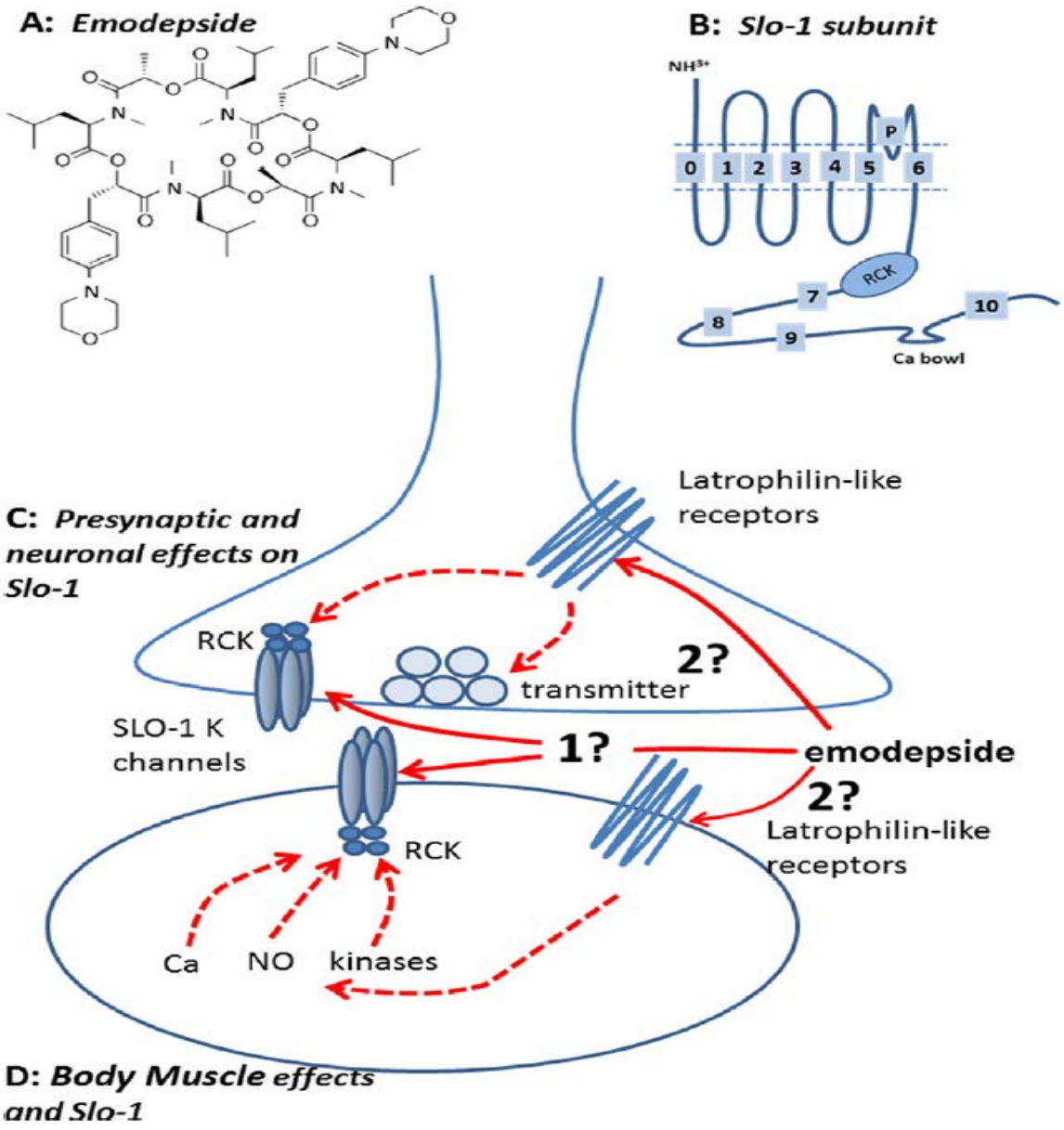

Figure 5.0 Summary diagram of emodepside structure, *Slo-1* subunit and a model of the mode of action of emodepside on nematode body muscle.

(A) Emodepside (molecular formula $C_{60}H_{90}N_6O_{14}$ molecular weight 1119.4). (B) Diagram of transmembrane structure of one *Slo-1* subunit; each *Slo-1* K^+ channel is made up of 4 of these subunits. Emodepside may act in part presynaptically on neurons (C) and in part on body

muscle (D). Emodepside may act directly on SLO-1 K^+ channels in the muscle or neurons (1) or indirectly by stimulating latrophilin-like receptors and signaling cascades that may involve NO, protein kinase C and/or calcium. The release of transmitters may also be affected by the activation of neuronal SLO-1 K^+ channels. It is unlikely that emodepside acts at the extracellular surface of the SLO-1 K^+ channel because of the slow time course of its action. It is very lipophilic and could act in the lipid membrane phase on the SLO-1 K^+ channel or move into the cytoplasm and act intracellularly. A SLO-1 K^+ subunit (B) and channel (C & D) is shown composed of 4 subunits along with the 'RCK' cytoplasmic regulatory region of the channel.

A3.3 K-dependent hyperpolarization by releasing inhibitory neuropeptides (PF1/PF2)

Willson *et al.* (2003) tested further effects of emodepside on *Ascaris suum* muscle contraction and electrophysiology. They observed that 10 µM emodepside had a slower inhibitory action on muscle contraction than GABA and produced a slow hyperpolarization without a detectable change in conductance. The inhibitory neuropeptides, PF1 & PF2, also produce a slow inhibition of contraction of *A. suum* muscle, similar to emodepside (Fellowes *et al*., 2000; Willson *et al*., 2003). PF1 causes a slow, non-reversible, concentration-dependent membrane hyperpolarization that is significantly blocked by 4-aminopyridine (Franks *et al*., 1994; Verma *et al*., 2009). When Willson *et al*. (2003) found that the K channel blocker 4-aminopyridine inhibited the effect of emodepside on membrane potential they reasoned that emodepside may mimic effects of PF1 & PF2 by stimulating the release of

inhibitory neuropeptides like PF1 or PF2 which then produce a K-dependent hyperpolarization. Although there is a similarity between effects of PF1 and emodepside effects on the membrane potential their effects are not identical. PF1 and emodepside both increase calciumdependent voltage-activated K^+ currents in A. suum, but the effects on calcium currents are different: PF1 inhibits voltage-activated Ca^{2+} currents (Verma *et al*., 2009); but emodepside has no effect on voltage-activated Ca^{2+} currents (Buxton *et al*., 2011). The effects of emodepside are also slower in onset: emodepside inhibits ryanodine-induced spiking more slowly than PF1, probably because of the lack of emodepside effect on the voltage-activated Ca^{2+} currents (Buxton *et al*., 2011). Thus although there may be some similarities in the effects of emodepside and the inhibitory neuropeptides, the evidence suggests that emodepside does not act by releasing PF1-like neuropeptides.

A3.4 Latrophilin receptors

Immunoscreening with an antibody to PF1022A of an Haemonchus contortus cDNA library revealed a G protein receptor that is latrophilin-like, now designated HC110R, and which has been expressed in HEK293 cells where it lead to PF1022A-dependent gating of calcium (Saeger *et al*., 2001). The homology of HC110R to mammalian latrophilin receptors which trigger neurotransmitter release, raises the hypothesis that emodepside may act (in part) by stimulating neurotransmitter release producing inhibition of muscle activity. Muhlfeld *et al.* (2009) used surface plasmon resonance to show that the neuropeptides AF1, AF10 and PF2 bind, with low affinities, to HC110-R, implying that these neuropeptides may be putative natural ligands of the latrophilin-like receptor. They did not observe any high affinity binding

characteristics with PF1. *Caenorhabditis elegans* is sensitive to effects of emodepside (Bull *et al*., 2007). The effects are: inhibition of movement, inhibition of pharyngeal pumping and inhibition of egg-laying. In 2004, Willson *et al*. described effects of emodepside (100 nM) on the *C. elegans* pharynx with the effects of emodepside stimulating exocytosis and eliciting pharyngeal paralysis. The paralysis of the pharynx produced by emodepside depended on the presence of the latrophilin (LAT-1) receptor with emodepside resistance appearing in *lat-1* null mutants. Two genes were recognized that encode latrophilin receptors in *C. elegans*, l*at-1* and *lat-2*. The role of LAT-1 and LAT-2 in mediating effects of emodepside on feeding and locomotion were investigated with RNAi and null-mutants *(Willson et al., 2004; Bull et al*., 2007; Guest *et al*., 2007). The pharyngeal system of *lat-1* null-mutants had reduced emodepside sensitivity, but the sensitivity of locomotion to emodepside was unchanged (Guest *et al*., 2007), suggesting that emodepside has both LAT-1 dependent effects on the pharynx and LAT-independent effects on locomotion.

A3.5 SLO-1 as a target for emodepside in *C. elegans*

Guest *et al*. (2007) used a mutagenesis screen of *C. elegans* and found mutant alleles of *slo-1* that encode a Ca^{2+}-dependent K channel in *C. elegans* that were resistant to the effects of emodepside on locomotion. They observed that *slo-1* but not *slo-2* null-mutants were more resistant to the inhibitory effects of emodepside than *lat-1* and *lat-2* (latrophilin receptor) double mutants. Guest *et al*. (2007) proposed that emodepside either directly or indirectly activates SLO-1 that is present in body wall muscle and motor neurons to produce its inhibitory effects in nematodes. Initial *slo-1* pharyngeal expression experiments in *slo-1* null-

mutants did not detect effects of emodepside on the frequency of pharyngeal pumping. However, Crisford *et al.* (2011) subsequently described how ectopic over-expression of SLO-1a in *C. elegans* pharyngeal muscle did, in fact, give rise to sensitivity of the pharyngeal muscle to emodepside. Crisford *et al.* (2011) also described transgenic experiments in which the *C. elegans* SLO-1a channel was swapped for KCNMA1, the human orthologue. Interestingly, the sensitivity to emodepside in the rescues depended upon origin of the SLO-1 channel: the human KCNMA1 channel was 10–100 times less sensitive to emodepside than the rescues expressing *C. elegans* SLO-1α channel. In addition to the heterologous expression of the human KCNMA1 BK channel, expression of the SLO-1 K channels of the nematode parasites, *Ancylostomum caninum* and *Cooperia oncophora* in the *C. elegans slo-1* loss of function mutant, NM1968, found that expression restored emodepside sensitivity (Welz *et al*., 2011). Restoration of the full emodepside sensitivity was also found to depend on the nature of the promoter used: the parasite *slo-1* promoter produced only partial recovery of sensitivity compared to full recovery produced by the *C. elegans slo-1* promoter. One explanation for this effect of the promoters on emodepside sensitivity suggests that the parasite promoter is less efficient in *C. elegans*; another explanation is that the parasite promoters used for *slo-1* expression might be truncated, thus driving only partial expression activity. A proposed model for the mode of action of emodepside in *C. elegans* (Welz *et al*., 2011) is that: emodepside acts directly or indirectly to activate the SLO-1 K channel; the effect on pharyngeal pumping involves latrophilin receptors and SLO-1 on pharyngeal neurons; and the effect on body wall muscle involves SLO-1 in the muscle but not latrophilin receptors.

A4.0 Properties of SLO-1 K channels

Two similar, SLO-1 and SLO-2 types of K channel (Lim *et al*., 1999; Wang *et al*., 2001; Jospin *et al*., 2002) have been identified in *C. elegans*. Although the proteins of these channels have some similar motif sequences, the channels are very different in their regulation by intracellular ions. SLO-2 is regulated by intracellular Na^+ as well as Cl^- ; SLO-1 is regulated primarily by intracellular Ca^{2+} (Jospin *et al*., 2002). We focus here more on the SLO-1 ion channels, as it is the putative site of action of emodepside. The SLO-1 K channels have large (200 pS) conductances and are sometimes called 'big' potassium (Dworetzky *et al*., 1996) channels, maxi-K channels or SLO family channels. The SLO-1 K channel of vertebrates is composed of 4 α-subunits; homologous subunits of *C. elegans* and *A. suum* are found and like vertebrate SLO-1 α-subunits have seven (S0–S6) transmembrane regions, a P-loop between S5 and S6, a large intracellular domain (S7–S10) and a well conserved 'calcium bowl' between domains S9 and S10 (see Fig. 5.0B–D and 5.1). In addition, the regulator of the K channel conductance domains (S7, S8) contains high and low affinity calcium binding sites.

The SLO-1 α-subunits show alternative splicing, producing channels with different calcium sensitivities; in *C. elegans* there are at least 3 splice variants (SLO-1a, SLO-1b and SLO-1c; (Wang *et al*., 2001)). Each α-subunit of the channel has at least two high affinity calcium binding sites and one low calcium/magnesium binding sites. The channel also combines with secondary, regulatory β-subunits (Knaus *et al*., 1994c) in vertebrates but these subunits have not yet been identified in *C. elegans*. However, BKIP-1 has been identified in *Caenorhabditis elegans* as a Slo-1 channel auxiliary subunit of physiological importance (Chen *et al*., 2010). The suggested function of the SLO-1 K channels is that they adjust the

resting membrane potential of electrically excitable cells and adjust the level of excitability, up or down, and so affect the response to other inputs. In addition to opening of the channel being regulated (Fig. 5.0 C and D) by membrane potential and calcium, magnesium, NO, CO, arachidonic acid, prostaglandins and phosphorylation by cAMP-dependent protein kinase A, diacylgycerol/ Ca^{2+}-dependent protein kinase C, and cyclic GMP-dependent protein kinase G can affect channel opening (Ghatta *et al*., 2006; Salkoff *et al*., 2006). These kinases allow SLO-1 to be coupled to multiple and quite diverse signaling cascades permitting different ways of adjusting the excitability of the cells. The effect of different nematode neuropeptides which can affect cAMP and cGMP levels, (e.g. AF1, AP2, PF1 & PF2) could then affect SLO-1 channels (Verma *et al*., 2007, 2009).

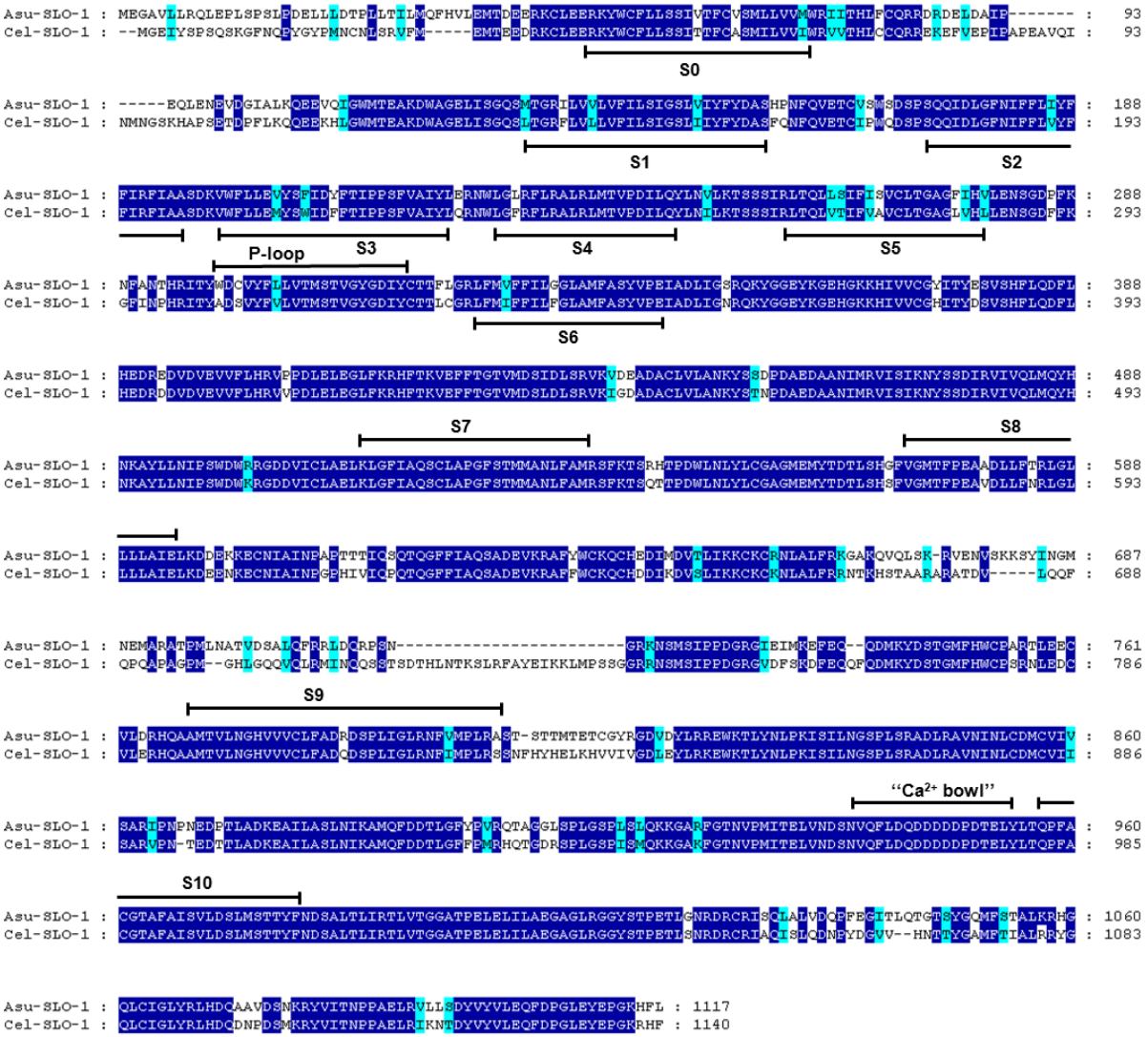

Figure 5.1 SLO-1 of *A. suum* and *C. elegans* alignments of deduced amino-acid sequences. Identical amino-acids between *C. elegans* and *A. suum* sequences are shaded in dark blue and distinct amino-acids sharing similar physico-chemical properties are shaded in light blue. Predicted signal peptide sequences are shaded in grey. The transmembrane domains (TM) are noted below the sequences. Comparison of *Asu*-SLO-1 (Genbank accession no ACC68842.1) and *Cel*-SLO-1 (Genbank accession no NP_001024259.1) showing the 7 TM domains (S0-

S6), P-loop, S7-S10 intracellular domains and "Ca^{2+} bowl". Domain annotation corresponds to *A. suum* SLO-1. Figure modified from Buxton *et al.*, 2011.

A4.1 SLO-1 as a target for emodepside in *A. suum*

Willson *et al*. (2003) described the muscle relaxation and inhibitor effect of emodepside on *A. suum* body muscle and that emodepside produced a Ca^{2+}-dependent hyperpolarization. It was suggested that emodepside may act at the neuromuscular junction to stimulate release of an inhibitory neuropeptide similar in action to PF1 or PF2. Voltage-clamp experiments have now allowed the effect of PF1, increasing the opening of Ca^{2+}-dependent voltage-activated K channels and decreasing the calcium currents present in *A. suum* muscle to be observed (Verma *et al*., 2009). Buxton *et al*. (2011) found *Asc-lat-1* and *Asu-slo-1*, evolutionarily conserved homologues of the *lat-1* and *slo-1* genes, to be expressed in adult *A. suum* body muscle flaps. They showed, using the same voltage-clamp techniques, that emodepside activates SLO-1-like K channels like PF1 (Fig. 5.2) but unlike PF1, emodepside does not decrease calcium currents. These voltage-activated K channels were Ca^{2+}-dependent and inhibited by 5 mM 4-aminopyridine. The membrane hyperpolarization and increase in voltage-activated K current produced by emodepside (Fig. 5.2) are very slow in onset and increase over a period of more than 10 min (Buxton *et al*., 2011); the speed of onset is slower than the onset of the effect of the inhibitory action of PF1. The slow onset effect of emodepside might be due to the very lipophilic nature of emodepside and a membrane

partitioning effect. It may also be because the effects of emodepside are indirect and produced by activation of a slow signaling cascade. The effect of emodepside is potentiated by sodium nitroprusside (a NO donor) and PMA (a protein kinase C activator), antagonized by iNOS inhibitors (with NNLA) and antagonized by inhibition of protein kinase C (staurosporine, Buxton *et al*., 2011). Interestingly, these signaling molecules are known activators of SLO-1 in other cells (Bolotina *et al*., 1994; Mistry and Garland, 1998; Wang *et al*., 1999a; Holden-Dye *et al*., 2007) and therefore encourage the view that emodepside could act through either or both of these signaling cascades and the signaling cascades may be in series or parallel (Fig. 5.0 C and D). A number of studies on the mammalian orthologues of SLO-1 show that they are directly and alternately regulated by complex, multiple signaling cascades, involving NO and diacylglyerol or PKC activation (Ghatta *et al*., 2006; Salkoff *et al*., 2006). Fig. 5.1 shows alignments of *C. elegans* and *A. suum* SLO-1 (Genbank accession no ACC68842.1). The *Asu*-SLO-1 sequence encodes a protein of 1117 amino-acids that has 78% identity and 87% similarity to the *Cel*-SLO-1 sequence. The SLO-1 sequences have seven transmembrane-spanning domains (S0–S6), a P-loop, four hydrophobic intracellular segments, (S7–S10) and a ‘‘Ca^{2+} bowl’’ that typifies a large conductance calcium-sensitive potassium channels, (Wallner *et al*., 1996; Wei *et al*., 1996; Schreiber and Salkoff, 1997; Lim *et al*., 1999; Ghatta *et al*., 2006).

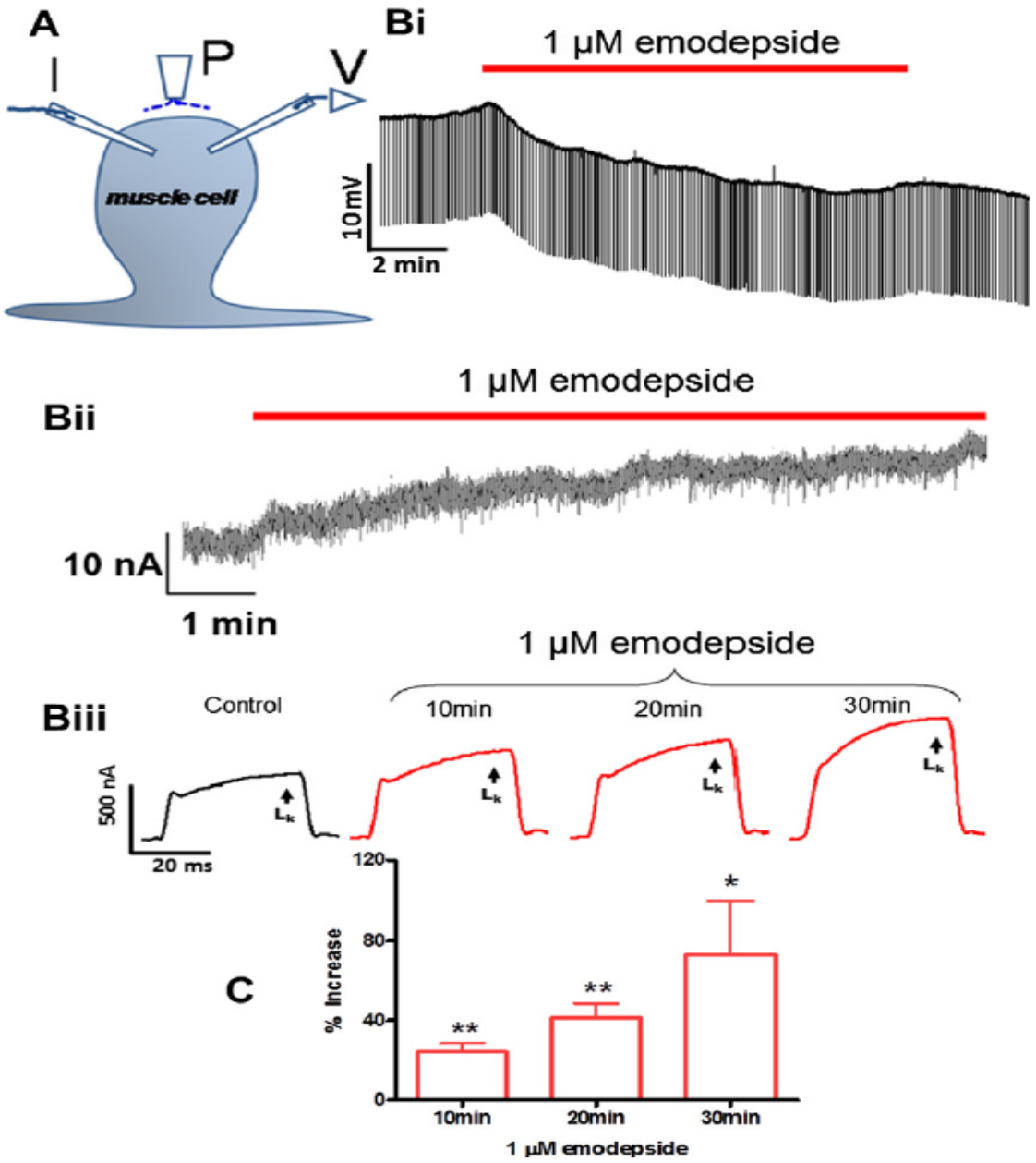

Figure 5.2 Electrophysiological techniques (two micropipette current-clamp and voltage-clamps) for recording from *Ascaris suum*.

(A) *A. suum* muscle bag showing the current (I) and voltage (V) micropipettes in the bag, and the perfusion needle (P). (Bi) Representative current-clamp traces showing the slow

hyperpolarizing membrane potential during and after 10 min application of 1 µM emodepside. Note that the trace does not get thinner because the membrane resistance does not change detectably. (Bii) Outward current response to 1 µM emodepside at higher time resolution. Holding potential -35 mV. Notice that emodepside produces a gradually increasing current after a delay of some 30 s. The response does not plateau in the time period of this recording. (Biii) Voltage-clamp traces of control K current and the time-dependent effect of 1 µM emodepside on the K currents, all to a step potential of 0 mV from a holding potential of -35 mV. (C) Bar chart (mean ± se) of 1 µM emodepside effect on steady state (L_K) currents. Comparison was made between the control 0 mV step current at 30 – 40 ms and the corresponding current increased by emodepside at 10, 20 and 30 min. Emodepside increased L_K currents at 10 min ($p < 0.01$, n = 4, *paired t-test*), 20 min ($p < 0.01$, n = 4, *paired t-test*) and 30 min ($p < 0.05$, n = 4, *paired t-test*). Fig modified from Buxton *et al.* (2011).

A5.0 Conclusion

Emodepside is a broad spectrum anthelmintic that has a mode of action different from the other classical groups of anthelmintic and is not expected to show cross-resistance with them. It has an inhibitory effect on motility, pharyngeal pumping and egg laying of nematodes and its mode of action involves increased opening of a SLO-1 K channel. In rescue experiments done by Crisford *et al*. (2011), there is evidence of direct action of emodepside on the SLO-1 K channel. The very slow time-dependent effect (Buxton *et al*., 2011) suggests that the site of

action is not an extracellular domain of the SLO-1 K channel. The slow time course is consistent with a site of action within the membrane or intracellular domain.

A6.0 Acknowledgments

The research project culminating in this paper was funded by National Institute of Allergy and Infectious Diseases (NIH) grant 2R56AI047194-11 RJM, the Iowa Center for Advanced Neurotoxicity (ICAN) seed grant to APR and by the French National Institute for Agricultural Research to CLC, CN and JC. SKB is the grateful recipient of a scientific Chateaubriand doctoral fellowship granted by the Office for Science and Technology of the Embassy of France in the USA and from the ‘‘Santé, Sciences, Technologies’’ doctoral school Tours University. CLC held a 2011 Fellowship award from the OECD’s Co-operative Research Programme ‘‘Biological Resource Management for Sustainable Agricultural Systems’’. The content is solely the responsibility of the authors and does not necessarily represent the official views of the National Institute of Allergy and Infectious Diseases of the National Institutes of Health or other funding bodies.

APPENDIX B Electrophysiological recording from parasitic nematode muscle

From paper published in *Invertebrate Neuroscience* (2008)

Alan P. Robertson[2, 3], Sreekanth Puttachary[3], Samuel K Buxton[3], Richard J Martin[3]

B1.0 Abstract

Infection of man and animals with parasitic nematodes is recognized as a significant global problem (McLeod, 1994; Hotez *et al*., 2007). At present control of these infections relies primarily on chemotherapy. There are a limited number of classes of anthelmintic compounds and the majority of these acts on ion-channels of the parasite (Martin *et al*., 1996b). In this report, we describe electrophysiological recording techniques as applied to parasitic nematodes. The aim of this report is: (1) to promote the study of ion channels in nematodes to help further the understanding of antinematodal drug action; (2) to describe our recording equipment and experimental protocols; and (3) provide some examples of the information to be gleaned from this approach and how it can increase our understanding of these important pathogens.

---

[1] Reprinted with permission of *Invert Neurosci* (2011), **8**: 167-175

[2] Corresponding author and Assoc. Professor, Dept. Biomedical Sciences, Iowa State University

[3] Contributed in writing the manuscript

B2.0 Introduction

Nematode infections are a significant problem in both human (Hotez *et al.,* 2007) and veterinary medicine (McLeod, 1994). Chemotherapy is widely used for treating these

infections. The range of drugs available for treatment is limited and repeated large scale use has led to the development of drug resistance in numerous parasite species (Kaplan, 2004). It is anticipated that the problem of drug resistance will get worse particularly since only one new class of anthelmintic has come to market recently (emodepside). A Consortium on Anthelmintic Resistance SNPS (CARS) has been set up to monitor drug resistance and advance molecular methods for detecting resistance (http:// consortium.mine.nu/cars/pmwiki.php/Main/HomePage).

The majority of anthelmintic compounds act on the neuromuscular system of the worm, for review see Robertson and Martin (2007). As with any excitable system, ion-channels are central to nematode neuromuscular signaling and function. Here we review the methods we have used to study ion-channels on nematode muscle that are either potential or actual target sites of new and existing compounds. The current anthelmintics that act on nematode ion-channels include: the avermectins/milbemycins which act on glutamate-gated chloride channels and/or GABA channels; the nicotinic anthelmintics (pyrantel, etc.) gate non-selective cation channels (nicotinic acetylcholine receptors). However, our understanding of the receptors activated during the therapeutic response is incomplete. In addition, there are many other ion-channels (peptide-gated, potassium and calcium selective channels) that may have critical roles for neuromuscular function in the nematode. Here we describe the electrophysiological methods we have used to examine nematode ion channels. These techniques are widely used by biologists to study channels in almost every living system and are not specific to our approach. We give details of methods of how we use them to study parasitic nematode ion channels. Our aim is to encourage others to study this important but overlooked field. This report is not intended as an introduction to electrophysiology. It is

intended to highlight the small alterations in methodology required to adapt these classical electrophysiological techniques to study currents and channels in parasitic nematodes.

B3.0 Methods

B3.1 Nematode tissue

Successful electrophysiological studies require a regular supply of live, viable parasite tissue (Fig. 1). This, in itself, is a common limiting experimental step: many parasitic species cannot easily be maintained for long periods *in vitro*. We have found *Ascaris suum* can be obtained from the local abattoir, although the ease of collection (related to the incidence of infection in the local swine population) appears to be somewhat seasonal. Adult worms remain viable for 4–7 days when kept at 30–35_C in Locke's solution (mM): NaCl 155; KCl 5; CaCl2 2; NaHCO3 1.5; D-glucose 5. It is possible, though significantly more labor and cost intensive, to maintain experimental infections of different parasite species; the *Oesophagostomum dentatum* life-cycle can be successfully maintained by passage through pigs (the native host) and will also yield useful adult worms on euthanasia of the hog. An additional benefit of using laboratory infections is the possibility of maintaining specific isolates, e.g. drug resistant isolates that have less genetic diversity than sampling the wild population. Obtaining viable material from other parasite species (e.g. human pathogens) can be more problematic and may necessitate the studies to be carried out on non-adult life cycle stages or even expression of the ion channel of interest in a heterologous system, e.g. *Xenopus laevis* oocytes.

B3.2 Dissection

Ascaris are large worms and the dissection needed to expose the muscle cells for recording is simple. A ~1 cm section of the worm is cut from the anterior region of the parasite. The resulting tube is then cut along one of the lateral lines and pinned onto a sylgard lined recording chamber cuticle side down. The gut is easily removed using fine forceps to expose muscle bags. With smaller nematodes the same approach can be applied but this time using the whole length of the worm. For adult *O. dentatum*, the entire worm (~1 cm) is pinned into the chamber (head and tail only) and then cut along a lateral line using a scalpel. The gut and reproductive tissue can then be removed and the preparation pinned out further to reveal the somatic muscle cells. A similar approach has been developed for electrophysiological recording from the muscle cells in *Caenorhabditis elegans* (Richmond and Jorgensen, 1999). For *C. elegans*, the small size of the worms means that the pins have been replaced by cyanoacrylate glue, but the principles of sticking the worm down, cutting it open, removing the gut and reproductive tissue and producing a ‘‘flap’’ or ‘‘filleted worm’’ remain the same. Thus, electrophysiological techniques have been applied to worms from ~30 cm to less than 1 mm in size. It should be noted, however, that as the worm size decreases the technical difficulty of the dissection increases substantially.

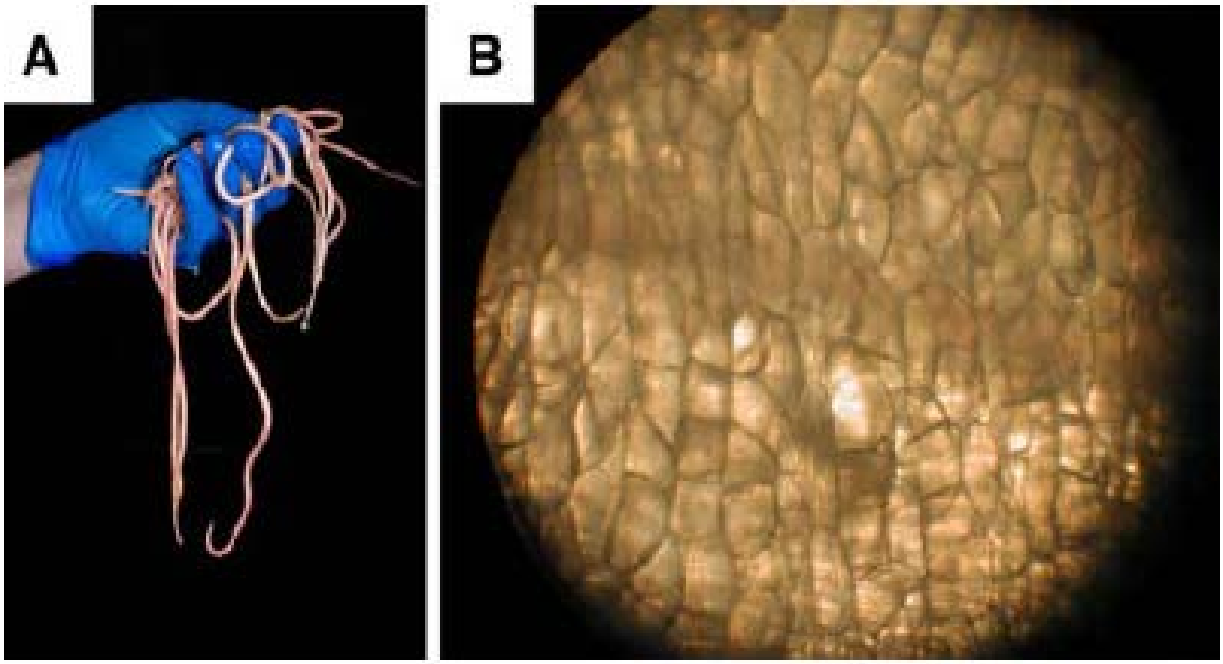

Figure 6.0 *Ascaris suum* used for the electrophysiology recordings.

(A) Photograph of adult *Ascaris suum*; (B) photograph of muscle flap preparation showing muscle cell bags (~200 µlm diameter) suitable for two-electrode recording techniques.

The faint horizontal line is the ventral nerve cord in this preparation.

B3.3 Two electrode current-clamp

The large size of many nematode cells makes them amenable for study using classical two-electrode recording techniques. The electrophysiology ‘‘rig’’ used for both current-clamp and voltage-clamp experiments is essentially identical (Fig. 6.1). The electronic components are: a current/voltage amplifier (Axoclamp 2A or 2B); a digitizer to convert the amplified signals from analog to digital format (digidata 1320A/1322A) and a computer for running the data acquisition software. The computer software (Clampex v8 or v9, Axon Instruments) not only acquires the data but can be used to control the perfusion system and command the

amplifier to inject current or voltage through either electrode. The tissue is perfused by a system controlled by six valves, a computer and a Warner VC-6 valve controller. The incoming perfusate is warmed to the desired temperature by a Warner SH-27B inline heater controlled by a Warner TC-324B heater controller. The preparation is viewed using a Stereo zoom dissecting microscope (Bausch & Lomb) and a fiber optic light source. The tissue is mounted in a sylgard lined Perspex chamber (custom made) surrounded by a water jacket to maintain temperature. The water jacket is perfused with warm water using a heated water pump (Isotemp 301b, Fisher Scientific). Microelectrodes are mounted on the amplifier headstages and maneuvered into position using a Leica micromanipulator.

For current-clamp experiments we pull microelectrodes using standard walled borosilicate glass with filament, o.d. 1.5 mm, i.d. 0.86 mm (G150F-6, Warner Instruments). Microelectrodes are fabricated using a Flaming/Brown horizontal electrode puller (Model P-97, Sutter Instruments) and are typically pulled to a resistance of 20–30 MΩ. The filament allows easy backfilling of the electrodes with the relevant solution, typically for current-clamp this is 3 M potassium acetate. The recording chamber is mounted on a nitrogen supported anti-vibration table (TMC Corp.) to minimize mechanical noise. A Faraday cage (TMC Corp.) surrounds the recording chamber to reduce electrical noise. Microelectrodes are positioned directly over the cell to be recorded from. The muscle cell is carefully impaled with both electrodes. Typically resting membrane potentials are in the range -25 to -40 mV for somatic muscle cells in *Ascaris*. The current injecting protocol is then applied through one microelectrode (I_m, Fig. 6.1D); our standard protocol is 0.5 s pulses of -40 nA current at a frequency of 0.25 Hz. Another microelectrode (V_m, Fig. 6.1D) can then be used to monitor the membrane potential and also the input conductance of the cell (typically 1–3 µS). The

signal is filtered at 0.3 kHz, digitized and stored on the computer hard drive for later analysis. The effect of perfused drugs can then be monitored. It is possible to record for ~1 h from a single cell in a healthy preparation. Our basic recording solution, *Ascaris* Perienteric Fluid (APF) consists of NaCl (23 mM), Na-acetate (110 mM), KCl (24 mM), CaCl2 (6 mM), MgCl2 (5 mM), glucose (11 mM), HEPES (5 mM), pH 7.6, adjusted with NaOH, and can be modified when necessary to determine the ionic basis of drug effects.

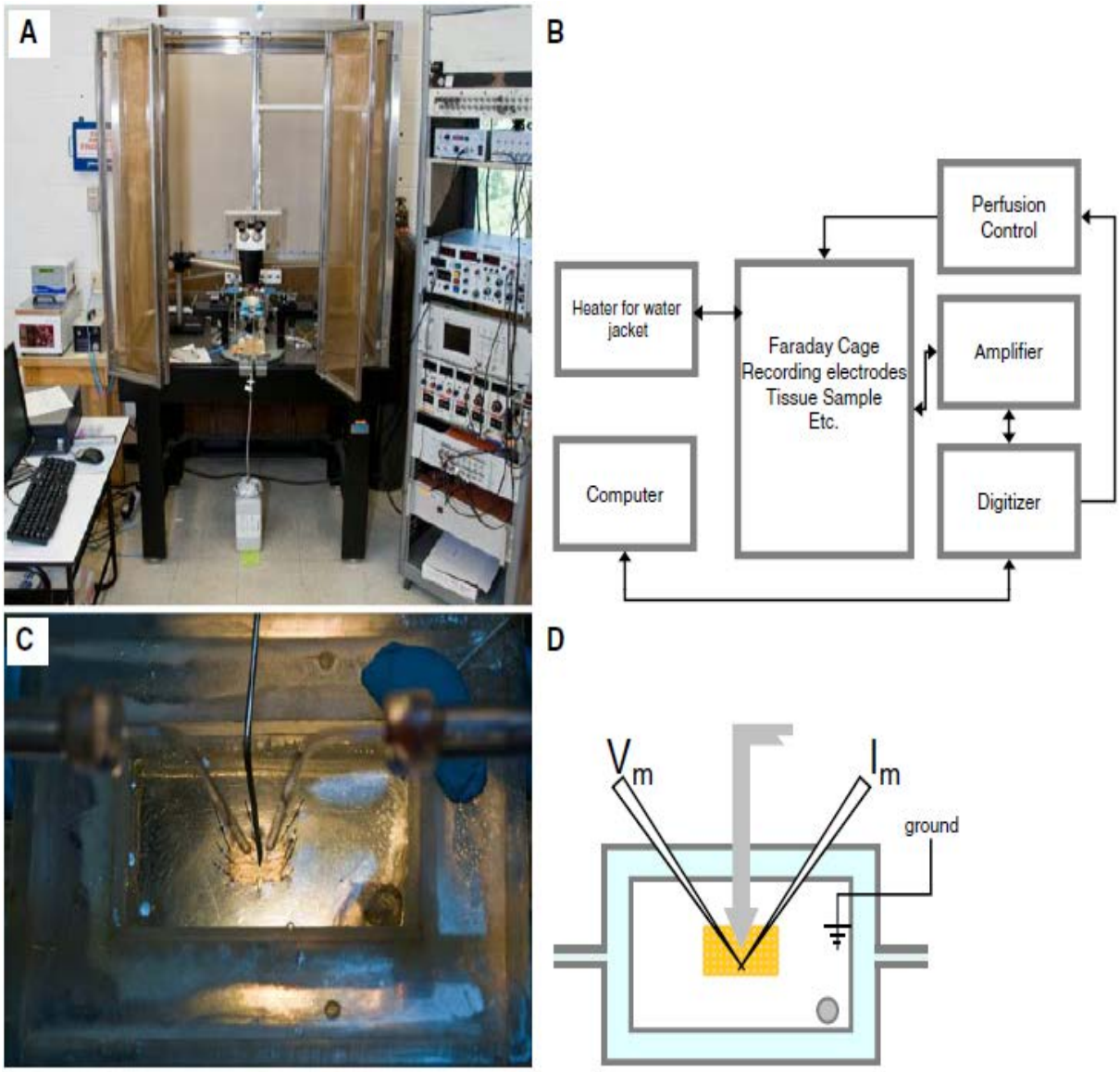

Figure 6.1 Current-clamp electrophysiology set-ups.

(A) Photograph; (B) diagram of two electrode current-clamp ‘‘rig’’; (C) photograph and (D) diagram of the recording chamber for current-clamp experiments. The muscle flap is clearly seen with both microelectrodes visible. The perfusate is applied via a 20-gauge needle (gray arrow in diagram) and excess removed by gravity through the outflow on the bottom right of the photograph and diagram (gray circle)

B3.4 Two electrode voltage-clamp

The electrophysiology ‘‘rig’’ for two-electrode voltage clamp is identical to that used for current-clamp experiments. However, there are some small but significant changes required to perform successful voltage-clamp experiments. Firstly, in electrode manufacture, the large size of the *Ascaris* muscle cell means that space clamp is quite poor. The injection of the large currents required to effect the desired voltage change requires a lower resistance current injecting electrode. Typically for voltage-clamp experiments we use a current injecting electrode (I_m) with a resistance of 2–5 MX. This is easily achieved by carefully breaking the tip of a standard current-clamp electrode using a piece of tissue paper. The voltage sensing electrode (V_m) is a standard current-clamp electrode.

Secondly, in voltage-clamp experiments, it is desirable to investigate the current flow through specific ion channel types or currents carried by individual ion species, e.g. outward K currents or inward Ca currents. To this end it is desirable to eliminate, as much as possible, currents carried by other ions and channels. Traditionally, this is achieved by either elimination/substitution of ions (other than the ion of interest) from recording solutions or by pharmacological block of other channel types present. For example, to record voltage activated inward calcium currents we have added cesium to the pipette filling solution (intracellular Cs blocks potassium currents, electrode fill solution is 1.5 M Cesium acetate + 1.5 M potassium acetate) and 4-amino pyridine (4-AP) to the bathing solution (4-AP is a selective blocker of K channels). Conversely, we have found that voltage-activated outward potassium currents are more easily studied when calcium is substituted for magnesium in the bathing medium, thus eliminating voltage activated inward calcium currents. It is also possible to isolate a current of interest by varying the voltage changes applied to the cell.

Isolating and optimizing the current to be studied is often the most demanding and time consuming aspect of these experiments. Unfortunately, parasitic nematodes are not the most widely studied group of organisms and drugs that affect ion channels in other preparations have been found to be inactive or significantly less active on *Ascaris* muscle cells. For example, the calcium channel blocker verapamil is frequently used to eliminate certain types of calcium current in vertebrate preparations, thus facilitating the study of other current types. Unfortunately, in *Ascaris* verapamil has no significant effect on voltage gated inward currents.

B3.5 Single-channel patch-clamp

The majority of parasitic nematode cell types we have worked with are too large to render whole cell patch-clamp recording a viable option; so we use two-electrode techniques. Whole cell patch recording has been successfully developed for investigating the muscle cells of *C. elegans* (Richmond and Jorgensen 1999) and is not described further here. It should be noted, however, that this approach may be suitable for the study of smaller nematode cells where impalement with two sharp electrodes is not possible. It is possible to use the patch-clamp technique to measure the properties of individual ion channel molecules. This ‘‘single-channel’’ patch recording technique is relatively straightforward using parasitic nematode muscle cells. The principle of this technique is the electrical isolation of a small ‘‘patch’’ of membrane containing one (or very few) ion channel molecules. Then conventional voltage protocols are applied to the membrane patch and the opening and closing of the single channel molecule can be measured.

The principles behind this technique are straightforward but in practice this is probably the most technically demanding compared to the other approaches outlined in this review. For single-channel recording from nematode muscle we use an anti-vibration table and Faraday cage (TMC Corp.) as in the current-clamp ‘‘rigs’’. The amplifier is an Axopatch 200B (Axon Instruments) connected to a PC (Lansdell et al.) via a digitizer (Digidata 1320A/1322A) and controlled by Clampex (v8 or v9) data acquisition software (Axon Instruments). Nematode muscle cells or muscle cell derived vesicles are held in a recording chamber (Warner Instruments) and viewed through a Nikon TE2000 inverted light microscope at 9400 magnification. Vesicles are easily viewed under normal light but small *C. elegans* muscle cells are best viewed using DIC optics. The amplifier headstage and microelectrode are positioned using a Narishige (MHW-3, Narishige Inc.) hydraulic micromanipulator.

Microelectrodes for patch clamp studies are pulled from thin walled glass capillaries, o.d. 1.5 mm, i.d. 1.16 mm with no filament (G85150T-3, Warner Instruments) using a two stage vertical electrode puller (models PP-830 or PC-10, Narishige Inc.). Electrodes are coated close to the tip with Sylgard to improve frequency responses and fire polished (MF-900 micro-forge, Narashige Instruments) to the desired resistance, typically 2–5 MX.

A major requirement for successful patch-clamp experiments is the formation of a high resistance seal (>1 GΩ, a giga seal) between the glass microelectrode and the cell membrane. Giga seal formation requires clean debris free membranes, which are reasonably common in cells in tissue culture but less so in intact tissue. *Ascaris* and other nematodes have a large amount of collagen overlying the muscle cell preventing giga seal formation. This must be removed by enzyme treatment using collagenase (type 1A, Sigma). Collagenase treatment removes the collagen matrix and allows access of the patch pipette to clean muscle cell

membranes. One result of collagenase treatment is the ‘‘budding’’ off of clean membrane vesicles from the bag region of the muscle cells. By applying the patch clamp technique Martin *et al*. (1990) discovered that these membrane vesicles contain functional ion-channels. We have successfully applied this method to record ion channels from vesicles originating from *O. dentatum* muscle cells (Robertson *et al*., 1999). Details of vesicle preparation and recording protocols are given below.

Ascaris were dissected and a muscle flap was prepared and pinned cuticle side down onto a plastic dish lined with Sylgard. The muscle flap preparation was washed with maintenance solution to remove fragments of the gut. Maintenance solution is (in mM): 35 NaCl, 105 sodium acetate, 2.0 KCl, 2.0 $MgCl_2$, 10 HEPES, 3.0 D-glucose, 2.0 ascorbic acid, 1.0 EGTA, pH 7.2 with NaOH. The maintenance solution was then replaced with collagenase solution. Collagenase solution is maintenance solution without EGTA and with 1 mg/ml collagenase Type 1A added (Sigma). After collagenase treatment for 4–8 min at 37^{o}C, the muscle preparation was washed (5–10 times) and incubated in maintenance solution at 37^{o}C for 20–40 min. Small membranous vesicles, 10–50 lm in diameter, grew out from the membrane of the muscle cells. These membranous vesicles are transferred to a recording chamber using a glass Pasteur pipette. For *O. dentatum* the vesicle preparation protocol is unchanged, however, the yield of vesicles is significantly less due to the smaller size of the parasite. We have found that vesicle yield and quality can vary significantly between batches of worms and worms of different size. As a guide, smaller worms require less collagenase treatment than larger ones. Prolonged collagenase treatment yields an abundance of vesicles but they are more fragile and rapidly become unusable. Shorter collagenase treatment yields fewer vesicles but they are generally more robust. For worms as small as *C. elegans* the collagen

matrix is significantly less of a problem and collagenase treatments of 0.5 mg/ml for 5–10 s are adequate to clean the muscle cell membrane and allow seal formation directly from the body wall muscle cells. Finally, we have found that collagenase from different suppliers or even different batches from the same supplier can affect the quality of vesicles produced.

Vesicles are placed in the recording chamber and patch experiments are carried out in the isolated inside out patch configuration. Achieving the outside-out patch configuration is considerably more difficult when using membrane vesicles as they tend to implode when rupturing the patch membrane. The recording conditions for studying nAChR channels are given below. Voltage protocols and solution recipes can be altered depending on the ion-channel to be studied.

The pipette was filled with pipette solution containing (mM): CsCl, 140; $MgCl_2$, 2; HEPES, 10; EGTA, 1; pH 7.2 with CsOH. The pipette solution also contained the agonist (levamisole, acetylcholine, etc.) at the desired concentration. The bathing solution was (mM): CsCl, 35; Cs acetate, 105; $MgCl_2$, 2; HEPES, 10; EGTA, 1; pH 7.2 with CsOH. As in other voltage clamp experiments, it is desirable to isolate the specific ion-channel of interest. To this end the bathing solutions contained symmetrical Cs as it permeates the nAChR but blocks potassium channels. The chloride concentration was asymmetrical to identify contaminating chloride channels by their non-zero reversal potentials on later analysis. Calcium is absent from the solutions to prevent contamination of the recordings with Ca-dependent chloride channel openings. Typically for ligand-gated ion channels we record for approximately 1 min at several different holding potentials between -100 and +100 mV (normally, -100, -75, -50, +50, +75 and +100 mV). Membrane breakdown is common at both -100 and +100 mV. In some preparations, we have found that addition of 0.5 mM dithiothreitol helps to stabilize the

membrane at more extreme potentials (Robertson *et al*. 1999). Recordings are viewed in real time by filtering at 2.5 kHz (8-pole Besel filter, custom made) and viewing on a digital storage oscilloscope (Hitachi VC-6025). The recordings are also filtered by the amplifier (5 KHz, Besel filter) digitized and stored on the PC for later analysis.

As with all recordings made using the above methods the data generated is suitable for analysis using standard methods. In the case of nAChR single-channel currents we normally calculate the single-channel conductance, mean open-time, mean closed-times and the probability of the channel being in the open state (P_{open}). Other more complex single-channel analysis is possible but beyond the scope of this manuscript.

B4.0 Results

Examples of the type of data available from each of our experimental approaches are given below. The data in this section was obtained from *Ascaris* somatic muscle.

B4.1 Illustrative results using two electrode current-clamp

Figure 6.2 is a current-clamp recording from *Ascaris* somatic muscle. Figure 6.2A is a low time resolution display covering approximately 30 min. The blue arrow (dark gray) indicates the resting membrane potential of the cell (-37 mV in this experiment). The red arrow (light gray) shows the voltage response to the -40 nA injected current pulses. The size of the voltage response is inversely related to the input conductance of the cell. The size of the response increases as the conductance decreases (when ion channels close) and vice versa. Figure 6.2A clearly demonstrates that levamisole application induces a rapid depolarization.

When the trace is examined in more detail (Fig. 6.2B, C) the effect on the cell's conductance also becomes apparent. In Fig. 6.2B, C, the red arrow (light gray) again represents the response to injected current and the blue arrow (dark gray) this time represents the depolarization induced by levamisole. In Fig. 6.2B the depolarization induced by levamisole (blue arrow, dark gray) is clearly seen. Levamisole is an agonist of the nicotinic acetylcholine receptor (nAChR) ion channel; application of the drug causes these channels to open and cations to enter the cell thus causing the depolarization. The opening of the ion channels causes an increase in input conductance during the depolarization. The red arrow highlights the voltage response to injected current and at the peak of the depolarization this response is reduced, reflecting the conductance increase due to nAChR opening. Figure 6.2B is the levamisole response after a 2 min application of the neuropeptide AF2 (1 μM). It is apparent that both the levamisole induced depolarization (blue arrow) and conductance change are substantially increased by treatment with this peptide. Figure 6.2A also demonstrates that AF2 treatment prolongs the recovery time after levamisole treatment.

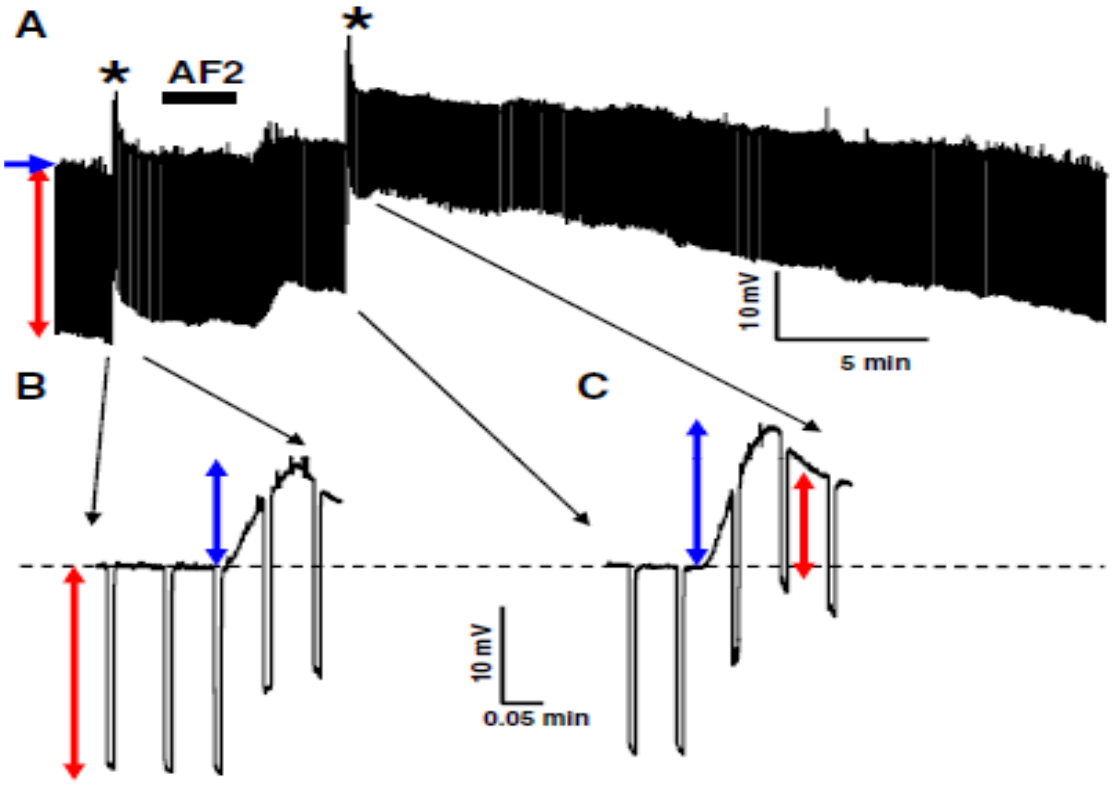

Figure 6.2 Representative current-clamp results.

(A) Low time resolution current-clamp trace illustrating the effects of 20 s applications (asterisk) of 1 µM levamisole (4 ml/min flow rate) before and after treatment of the muscle flap with 1 µM AF2 (a nematode FMRF-related neuropeptide). Blue arrow illustrates the resting membrane potential while the red arrow illustrates the size of the voltage response to -40 nA injected current. Levamisole induces an obvious depolarization of the cell; B, C higher time resolution view of sections of the recording in (A). Red arrow (light gray) illustrates the voltage response to injected current and blue arrow (dark gray) illustrates the amplitude of levamisole induced depolarization. It can be clearly seen that both the depolarization and conductance change in response to levamisole are larger after AF2 treatment (C) than before (B).

B4.2 Illustrative results using two electrode voltage-clamp

A sample experiment using two electrode voltage-clamp recording on *Ascaris* muscle is shown in Fig. 6.3. In this experiment, we have isolated the voltage gated potassium currents and examined the effects of the potassium channel blocker 4-amino pyridine (4-AP). To study the potassium currents in isolation we have replaced calcium (a permeant ion) in our recording solutions with the same concentration of magnesium (an impermeant ion) to remove the voltage activated inward currents carried by calcium. Figure 6.3A are the outward currents carried by potassium in response to 40 ms step voltage changes in the holding potential of the cell. In this instance, the cell was held at -35 mV and stepped to -25, -20, -15, -10, -5, 0, 5, 10, 15, and 20 mV. The same voltage step protocol was applied in the presence of 5 mM 4-AP (Fig. 6.3B) which substantially reduced the amplitude of the outward potassium currents.

After a 30-min wash period the currents had partially recovered (Fig. 6.3C). The maximum current at each voltage step was plotted (Fig. 6.3D) and clearly shows the inhibitory effect of 4-AP and this effect was partially reversible.

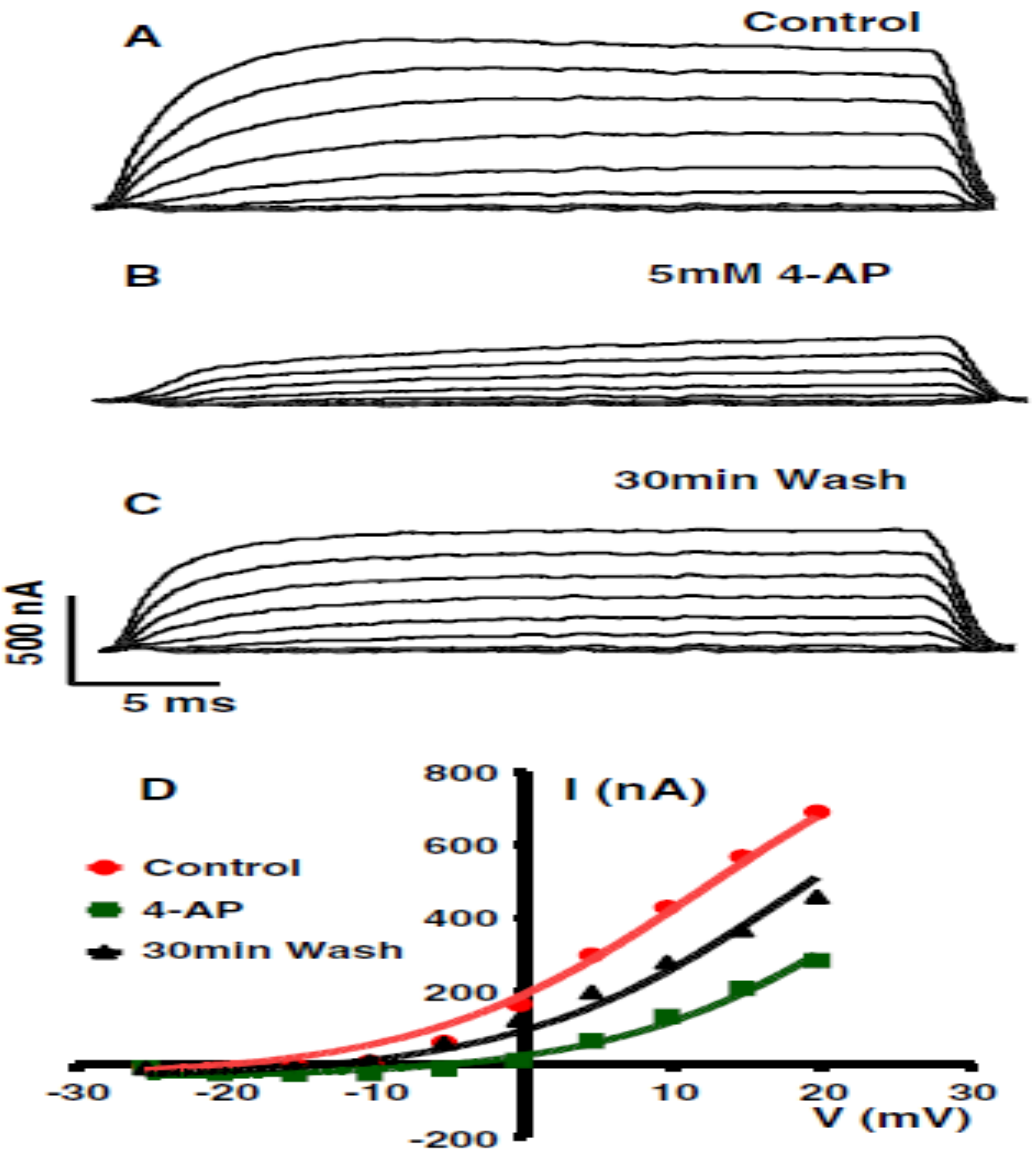

Figure 6.3 Illustrative results obtained with voltage-clamp technique.

Voltage activated potassium currents from *Ascaris* muscle bags recorded under two electrode voltage-clamp; (A) under control conditions (Ca free APF solution); (B) during application of 5 mM 4-amino pyridine (4-AP); and (C) after 30 min wash in calcium free APF solution; (D) current–voltage relationship for the recordings in A–C clearly showing the inhibitory effect of 4-AP and that it is partially reversed on washing.

B4.3 Illustrative results using single-channel patch-clamp

A sample of a recording from an Ascaris muscle derived vesicle is shown in Fig. 6.4A. The isolated inside-out patch was held at +75 mV and the patch pipette contained 30 µM levamisole. Rectangular channel openings are clearly visible ranging from ~2 to 4 pA in size and ~0.3 to 10 ms in duration. In this experiment, there are openings to more than one level indicating the presence of multiple subtypes of nAChR present in this isolated patch of membrane. In Fig. 6.4B, we plotted an amplitude histogram of all openings in the recording and fitted with Gaussian distributions to calculate the mean amplitude for each of the three peaks. By using multiple agonists, concentrations and antagonists we have been able to characterize three subtypes of nAChR on Ascaris muscle cells that have different single-channel and pharmacological properties. Figure 6.5 is a summary diagram of these findings where N-type refers to nicotine preferring subtype of nAChR, L-type refers to a levamisole preferring subtype of nAChR and B-type refers to a bephenium preferring subtype of nAChR.

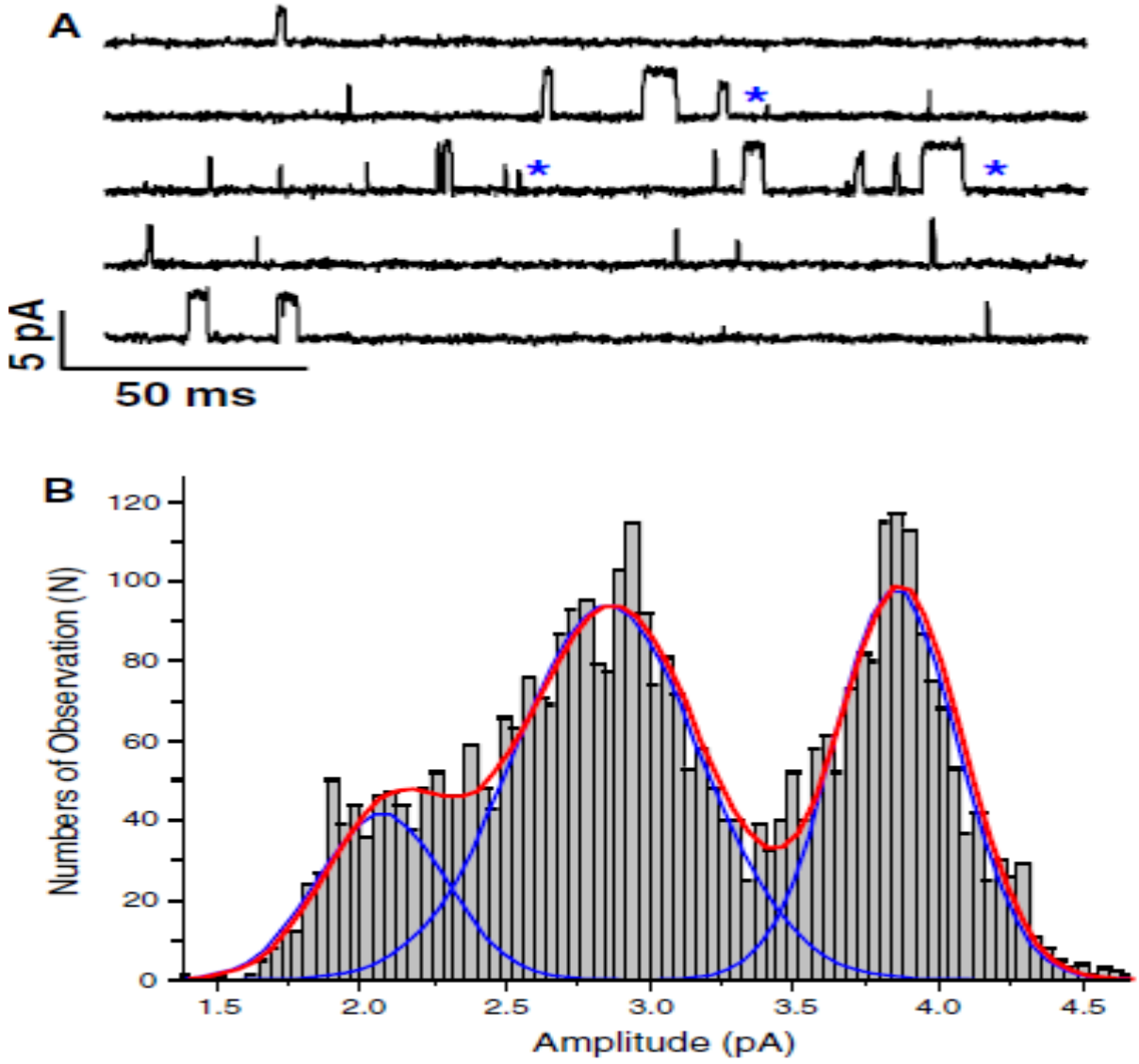

Figure 6.4 Illustrative single-channel recordings from *A. suum* muscle vesicle.

(A) Sample of a single-channel recording from a membrane patch of *Ascaris* muscle vesicle held at +75 mV. Discrete single-channel openings are visible as rectangular current pulses of ~2 – 4 pA. Blue asterisk highlight the presence of three separable open levels and therefore three different ion channel molecules in this membrane patch; (B) histogram of all channel openings from the recording illustrated in (A). Three separable peaks are obvious and have

been fitted using Gaussian distributions to determine the amplitude of channel opening at +75 mV for each channel type.

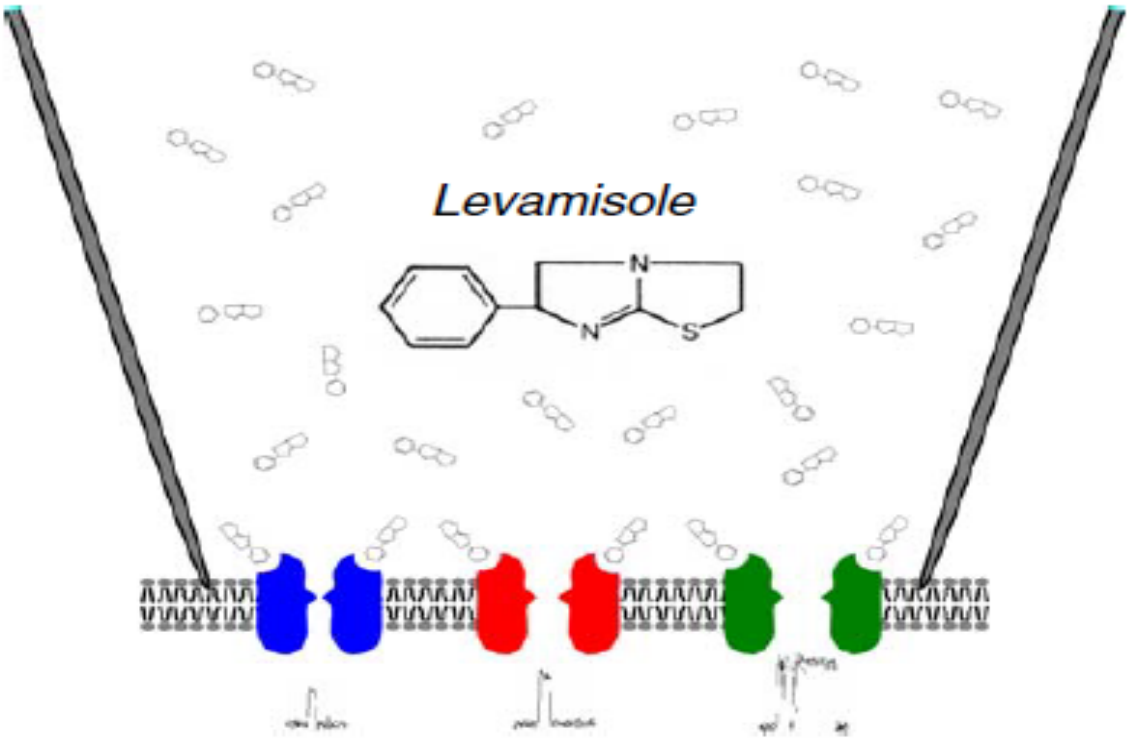

	G25	G35		G45
Pharmacological type	N-type	L-type		B-type
Conductance (pS)	(24.2±0.6)	(34.6±0.5)		(44.5±0.7)
Tau (ms)	0.6 ± 0.1	0.8 ± 0.1		1.2 ± 0.1
PHQ sensitive	No	Yes	≈	Yes
2DPHQ sensitive		Yes	<	Yes

Figure 6.5 Summary diagram representing a membrane patch containing the three nAChR subtypes present on *Ascaris* muscle with some of their single-channel and pharmacological properties illustrated.

B5.0 Discussion

The development of electrophysiological methods has taken ~50 years to mature. Early studies concentrated on large easily observable cells that were easy to impale, e.g. the squid giant axon. Interestingly, *Ascaris suum* muscle cells were investigated as early as the 1950s (Jarman, 1959). As the techniques were refined the need for large cells decreased. Additionally, Brading and Caldwell (1971) found that *Ascaris* had different properties to other more typical cell types. These developments possibly led to the conclusion that *Ascaris* was not necessarily a good model for general electrophysiology studies of cells and have thus restricted the amount of research carried out on this and other parasitic nematodes using electrophysiological techniques.

We have described some of the electrophysiological methods that can be used to study ion-channels in *Ascaris* and other nematodes. Included in the methods section are additional details that we have found important for successful studies, details that are seldom discussed at length in other publications due to space constraints. The aim of this report is to provide detailed information to facilitate the study of ion channels in parasitic nematodes by any interested researchers.

The importance of studying these parasite ion-channels is readily apparent. There are a number of groups of anthelmintic compound that act on channels in parasites. These include: the cholinomimetics (pyrantel, etc.) that act as agonists of nAChRs on muscle (Harrow and Gration, 1985); the avermectins are allosteric activators of glutamate-gated chloride channels in the pharynx (Wolstenholme and Rogers, 2005) and/or GABA-gated chloride channels on muscle; piperazine an agonist of GABA-gated chloride channels on muscle (Martin, 1982); emodepside is proposed to have an effect on potassium currents (Guest *et al*., 2007); and

recently the amino acetonitrile derivatives (AADs) are proposed to be nAChR antagonists (Kaminsky *et al*., 2008).

We have detailed our approaches on nematode muscle. Several other groups have successfully used electrophysiological techniques in a variety of preparations including the musculature (Holden-Dye and Walker, 1990) to examine ion-channel properties, drug action and more basic biological questions. The pharynx of *Ascaris* has been investigated using whole cell current-clamp (Martin, 1996) and voltage-clamp (Byerly and Masuda, 1979), while Adelsberger *et al*. (1997) successfully developed vesicle production from the pharynx to make patch recordings of glutamate-gated chloride channels. The electrophysiological properties of parasite nerve cells have also been investigated in detail (Davis and Stretton, 1996). While more recent work on *C. elegans* has developed techniques for recording whole cell currents from body wall muscle (Richmond and Jorgensen, 1999), single-channel recording of nAChRs from body wall muscle (Qian *et al.*, 2008) and even electrical recording of pharyngeal activity (Cook *et al*., 2006).

B6.0 Acknowledgments

A.P.R., S.P., S.B. and R.J.M. are funded by an NIH RO1 grant (AI04719406A1). The authors would like to thank Kim Adams for photographic services.

APPENDIX C Levamisole receptors: a second awakening

From a review paper published in *Trends in Parasitology, 2012*

Richard J Martin[1, 2], Alan P. Robertson[3], Samuel K Buxton[3], Robin N Beech[3], Claude L Charvet[3], Cedric Neveu[3]

C1.0 Abstract

Levamisole and pyrantel are old (1965) but useful anthelmintics that selectively activate nematode acetylcholine ion channel receptors; they are used to treat roundworm infections in humans and animals. Interest in their actions has surged, giving rise to new knowledge and technical advances, including an ability to reconstitute receptors that reveal more details of modes of action/resistance. We now know that the receptors are plastic and may form diverse species-dependent subtypes of receptor with different sensitivities to individual cholinergic anthelmintics. Understanding the biology of the levamisole receptors is expected to inform other studies on anthelmintics (ivermectin and emodepside) that act on ion channels.

---

[1] Reprinted with permission of *Invert Neurosci* (2011), **8**: 167-175

[2] Corresponding author and Professor, Dept. Biomedical Sciences, Iowa State University

[3] Contributed in writing the manuscript

C2.0 Levamisole and pyrantel: interest and new knowledge

One-third of the human population of the world is at risk of helminth infection, and infection is also very common in animals. Regrettably, there are still no effective vaccines for controlling these infections, so that both treatment and prophylaxis rely on anthelmintic drugs. The continued use of these drugs has given rise to concerns over levels of resistance

and promoted the search for new knowledge and understanding that might slow its progress. The cholinergic anthelmintics (see Glossary), which include levamisole and pyrantel, are an important group of anthelmintics that target parasite ion-channels, a property they share with other major anthelmintics such as ivermectin and emodepside. Levamisole selectively opens a restricted subgroup of nematode acetylcholine receptor (AChR) ion channels in nematode nerve and muscle. Opening of AChR channels produces depolarization (Puttachary *et al*., 2010), entry of calcium through the opened channels, and an increase in sarcoplasmic calcium, producing spastic muscle contraction (Robertson *et al*., 2010); the parasite is then unable to maintain its location (often in the intestine) and is then swept away, effecting the cure. Interest in this class of anthelmintic has increased recently because application of new methods has demonstrated the presence of diverse receptor subtypes and different cholinergic anthelmintic subtype selectivities. It has also allowed better mechanistic explanations of resistance and the development of exciting novel compounds such as monepantel and derquantel. This review describes new knowledge and insights that have increased our understanding of the biology of these receptors.

Glossary

Cholinergic anthelmintic: antinematodal drugs which interact with acetylcholine receptors.

Cholinomimetics: drugs which mimic the actions of acetylcholine and activate acetylcholine receptors.

Conductance subtypes: a classification of receptor ion channels based on conductance groupings; G25 (nAChRs with conductances near 25 pS); G35 (nAChRs with conductances near 35 pS); G40 (nAChRs with conductances near 40 pS); G45 (nAChRs with conductances near 45 pS).

Hco-lev-1, Tci-lev-1, Tco-1, Cel-acr-8: Identification of genes. The first letter of the genus and the first two of the species name identify the organism and this is followed by three letters and a number unique for each gene. Genes in the other species take the name of the ortholog in *C. elegans*. The ortholog of the *C. elegans lev-1* gene in *H. contortus* is *Hco-lev-1*, in *Teladorsagia circumcincta* is *Tci-lev-1* and *Trichostrongylus colubriformis* is *Tco-lev-1*.

IC_{50}: the dose of a drug that inhibits 50% of the response.

LD_{50}: the dose of a drug that kills 50% of the population under test.

Null mutants: defective gene mutants where the genes are nonfunctional.

Patch clamp technique: an electrophysiological technique for recording the very small currents that flow through single ion channels.

Phylogenetic clade: a subgroup within a phylogenetic tree that all trace back to a common point.

C3.0 Levamisole-sensitive AChRs show pharmacological- and species-dependent diversity

The very small currents (1 pA = 1 x 10^{-12} A) that flow through single receptor channels activated by levamisole or pyrantel have been recorded from muscle of the parasitic nematodes *Ascaris suum* (Robertson and Martin, 1993), *Oesophagostomum dentatum* (Robertson *et al*., 1999) and *Brugia malayi* (Robertson *et al*., 2011) using the patch clamp technique (Figure 7.0). In *A. suum* there is the L-type (G35 pS) that is preferentially activated by levamisole, the N-type (G25 pS) that is preferentially activated by nicotine and the B-type (G45 pS) that is preferentially activated by bephenium (Qian *et al*., 2006).

At the single channel level, high concentrations of levamisole activated all three AChR subtypes (Box 1). In the strongyle species, *O. dentatum*, that belongs to the same phylogenetic clade as *Haemonchus contortus* and *Caenorhabditis elegans*, a fourth levamisole-activated AChR subtype with a conductance of 40 pS has also been observed (Figure 7.0d) (Robertson *et al*., 1999). We point out that in the free-living nematode, *C. elegans*, that levamisole activates only one conductance subtype of 30 pS, which is not activated by nicotine and is pharmacologically different from some of the parasite levamisole receptors that can be activated by nicotine (Qian *et al*., 2008). Together, these observations show that levamisole activates a diverse range of receptor subtypes which are separated by their detailed pharmacology, channel conductances and species. This diversity emphasizes a need for molecular and functional characterization of these receptors in different parasitic nematode species as well as in *C. elegans*.

Box 1. Levamisole AChRs of nematodes *in vivo* are composed of diverse species-dependent subtypes

The levamisole AChR subtypes have different channel conductances and the subtypes may be separated pharmacologically (Table I).

Table I. Main muscle nAChR channel conductances opened by different anthelmintic in nematodes[a]

Species	Clades	Drugs	Conductances (pS)[e]				Refs.
A. suum	III	ACh	25–35	–	40–50		[48]
		Lev	23	33	43		[6]
		Nic	26	36	–		[47]
		Pyr	22	–	41		[49]
		Beph	–	36	43		[6]
***C. elegans lev-10* mutant**[b]	V	ACh	30				[7]
		Lev	29.3				[7]
***lev-10;lev-1* mutant**[c]		Lev	26.9				[7]
***lev-10;lev-8* mutant**[d]		ACh	27.4				[7]
		Lev	30				[7]
O. dentatum	V	Lev	22	35	40	45	[4,41]

Abbreviations: ACh, acetylcholine; Lev, levamisole; Nic, nicotine; Pyr, pyrantel; Beph, bephenium.

[a] In *C. elegans* only one was separated (approx. 30 pS), in *A. suum* up to three subtypes (approx. G25 pS, G35 pS, and G45 pS) were separated, and in *O. dentatum* four were separated (approx. G25 pS, G35 pS, G40 pS and G45 pS).

[b] *C. elegans lev-10* mutant.

[c] *lev-1* mutant.

[d] *lev-8* mutant.

[e] Conductances.

C4.0 The *C. elegans* model of the levamisole receptor

Although levamisole was developed for treatment of parasitic nematodes, the intensive study of the effects of levamisole in the *C. elegans* model nematode has given us tremendous insight into what may be happening in parasitic nematodes. Starting from the early days of Sydney Brenner (Brenner, 1974), levamisole (tetramisole) has been used in genetic studies of *C. elegans*, so that we now have a better understanding of the molecular mechanisms associated with levamisole AChR signaling. Each AChR is composed of five subunits formed in a ring in the membrane with the channel pore in the center (Figure I in Box 2); the subunits are either α subunits with two vicinal cysteines present or β (non-α) subunits that lack these cysteines (Corringer *et al*., 1998; Changeux and Edelstein, 2005). There are at least 27 genes for AChR subunits in *C. elegans*. The levamisole receptor channel was found to be composed of five different subunits (Jones and Sattelle, 2004). Each subunit is approximately 500 amino acids in length and harbors four transmembrane regions (M1, M2, M3, and M4). The M2 region forms the lining of the ion channel pore. In *C. elegans* (Box 2; Figure 7.1), three separate genes code for the levamisole α subunits: *unc-63, unc-38, lev-8*, and two genes code for the β subunits, *unc-29* and *lev-1* (Fleming *et al*., 1997; Culetto *et al*., 2004; Towers *et al*., 2005; Boulin *et al*., 2008). The canonical agonist binding sites are assumed to be between the positive face of the α subunit and the negative face of the adjacent β subunit; the adjacent pairs of subunits are not identical, so the agonist binding sites are not equivalent (Figure I in Box 2). Evidence from other preparations leads us to believe that at least two agonist molecules need to bind to open the receptor channel effectively. In addition to the canonical sites, anthelmintics may also bind to noncanonical sites formed between the positive face of the β subunit and the negative face of an α subunit and increase opening of

the ion channel (Evans and Martin, 1996; Wu *et al*., 2008; Seo *et al*., 2009). Thus, the site of action and the potency of a cholinergic anthelmintic will depend upon the channel subunit composition.

In addition to the requirement for the subunits, full function of the levamisole channel is associated with proteins derived from at least seven other genes: *lev-9, lev-10, tpa-1, tax-6, soc-1, nra-1,* and *oig-4* (Figure 7.1) (Fleming *et al*., 1996; Gally *et al*., 2004; Martin and Robertson, 2007); it is anticipated that other associated proteins will be recognized in the future. Null mutants of these genes can produce a degree of levamisole resistance. The gene *unc-68,* which encodes a ryanodine receptor (Maryon *et al*., 1996), is associated with amplifying the calcium signal following opening of the levamisole receptor, and two other genes, *unc-22* and *lev-11* (Fleming *et al*., 1997), are associated with contractile elements of muscle and produce levamisole resistance by reducing the muscle response to the drug. In addition to these genes, other null mutants of genes that can produce levamisole resistance are involved in processing and assembly of the subunits; these genes are *nra-2, nra-4, ric-3, unc-74,* and *unc-50* (Gottschalk *et al*., 2005; Eimer *et al*., 2007; Almedom *et al*., 2009). RIC-3 is a small transmembrane protein, which is a chaperone promoting nAChR folding in the endoplasmic reticulum (Halevi *et al*., 2002). The gene *unc-74* encodes a thioredoxin protein required for the expression of levamisole AChR subunits (Haugstetter *et al*., 2005). The gene *unc-50* encodes a transmembrane protein in the Golgi apparatus (Eimer *et al*., 2007). In *unc-50* mutants, levamisole AChR subunits are directed to lysosomes for degradation. These three ancillary proteins have been widely conserved through evolution from nematodes to humans and have been used for the expression of levamisole receptors in *Xenopus* oocytes. In addition to these proteins, microRNAs (miRNAs) are also involved in regulation of

receptor subunit expression; miR-1 is one specific miRNA that binds to the mRNA of UNC-63 and UNC-29 but not LEV-1 or LEV-8 (Simon *et al*., 2008). A null mutant of miR-1 leads to reduced sensitivity to levamisole; although the mechanism for this is unclear, it is suggested to involve a change in receptor expression (Simon *et al*., 2008).

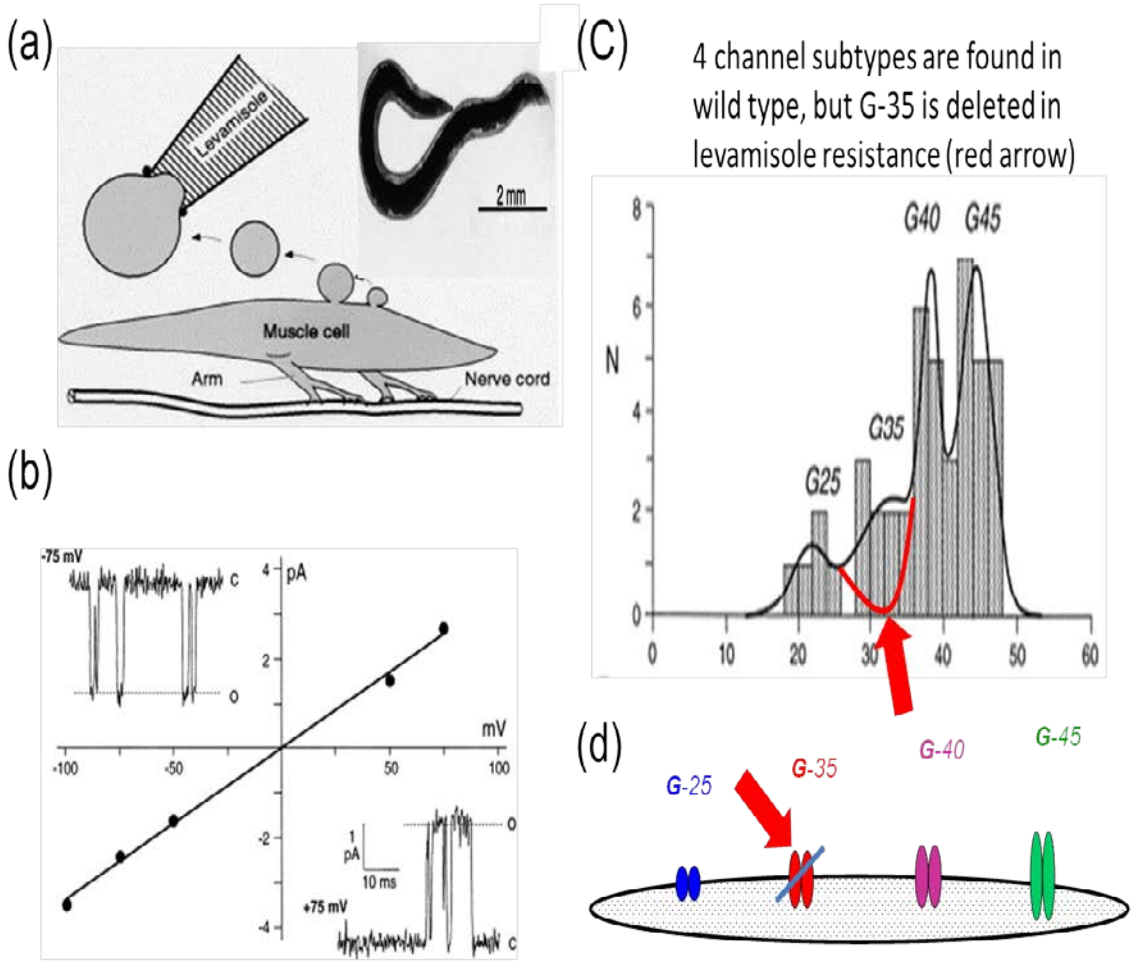

Figure 7.0 Acetylcholine receptor (AChR) single channel currents from *Oesophagostomum dentatum* using the patch clamp technique (Robertson *et al*., 1999, 2000)

(a) Diagram of the production of the membrane vesicles and patch pipette used to record the levamisole-activated AChR channel currents; (inset) adult female *O. dentatum*. (b) Examples of levamisole-activated channel currents recorded at -75 mV and +75 mV patch potentials and the current voltage plot showing a linear relationship, zero reversal potential, and slope giving a channel conductance of 42 pS. (c) Channel conductance distribution for the anthelmintic sensitive isolate (wild type) showing the four peaks (fitted using the sum of four

normal distributions). The peaks illustrate the presence of four subtypes: G25 pS, G35 pS, G40 pS, and G45 pS. In the levamisole-resistant (LEVR) isolate, there were only three subtypes present because the G35 pS subtype was missing. In the pyrantel-resistant isolate, the four G subtypes were present and included the G35 pS subtype, but there were fewer channels present in the muscle compared with the anthelmintic sensitive (wild) isolate. (d) Diagram of the different channel subtypes detected and presented by size on a basis of the conductances in O. dentatum; G35 pS is not present in levamisole-resistant isolates, but present in pyrantel isolates.

Box 2. Levamisole AChR channels and models of subunit structure

Levamisole AChR channels

Levamisole and pyrantel are nematode selective cholinergic (acetylcholine) agonists that open nonselective cation ion channel receptors (AChRs) present on nematode body muscle. The drugs bind to canonical and/or noncanonical binding sites on the receptors (Figures I and II). Opening of these channels produces depolarization, entry of calcium, and muscle contraction; the nematode parasite becomes paralyzed and is ejected from its location, effecting a cure. The ligand binding sites are between adjacent subunits of the receptor and include canonical and noncanonical binding sites.

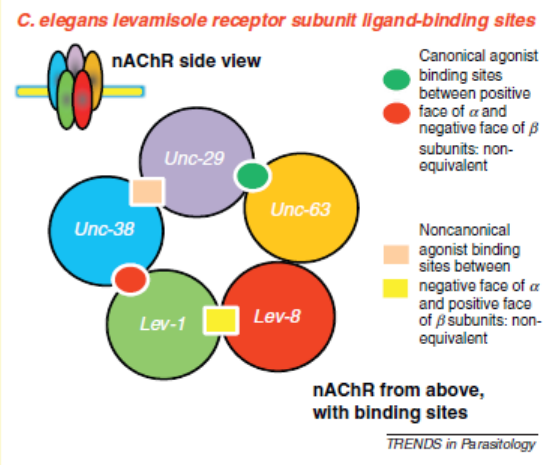

Figure I. Possible canonical and noncanonical ligand binding sites. The sites are based on the *C. elegans* levamisole AChR consensus structure. These AChRs are composed of five heterologous subunits; each may be an α or β subunit, approximately 500 amino acids in length. In *C. elegans* there are five genes coding for the levamisole AChR channel: *unc-38, unc-29, unc-63, lev-1,* and *lev-8*. The canonical agonist binding sites are formed at the interface of two subunits, between the positive surface of the subunit that contributes the principle agonist binding surface and the negative surface of the adjacent β subunit that provides the complimentary agonist binding surface. Thus, the receptor subunit composition and arrangements affect the binding sites and pharmacology of the receptor. The canonical binding sites for acetylcholine or other agonists are not identical (nonsynonymous) if either of the adjacent subunits forming the binding sites is different. There may also be noncanonical binding sites on the negative face of the subunits [47].

Modeling ligand binding and the levamisole AChR channel

The structure of the nematode levamisole AChR channel and subunits is predictable because the structure of ligand-gated ion channel subunits is conserved (Figure II).

These structures can predict those of other ion channels by providing an initial approximate configuration for energy minimization techniques that yield optimal predicted structures [50,51]. The predictions are used in docking studies where configurations of a ligand are evaluated to find the most probable pose identified as that with the lowest energy. The intrinsic flexibility of ion channels is essential to their function but creates problems for docking studies *in silico*. This can be seen by the dramatic change is position of the c-loop between the closed channel configuration (Figure IIa) and the open form (Figure IIb). Presence of the ligand stabilizes the c-loop around the ligand. This change is followed by a series of other structural changes that ultimately results in rotation of the M2 transmembrane that opens the channel.

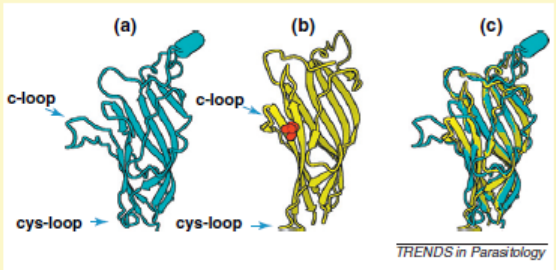

Figure II. Open and closed channel configurations. **(a)** The *Torpedo* fish acetylcholine receptor (2BG9) and **(b)** the bacterial proton gated channel (3EAM) is separated by more than 2 billion years of sequence change and yet the structures remain remarkably similar. Only the extracellular ligand binding domain is shown in the illustration, viewed parallel to the plasma membrane; the transmembrane domains extend from the bottom of each structure but are not shown. The characteristic cys-loop is labeled and the ligand binding pocket, indicated in red in the center, is enclosed by the c-loop. A majority of the ligand binding domain is present as two curved β-sheets that can be seen in almost identical positions when the two structures are superimposed **(c)**. The looped regions of both structures also occupy very similar configurations between the two.

C5.0 Molecular diversity: levamisole AChR subunits in parasitic nematodes

Molecular cloning and bioinformatic searches in parasitic nematode genomes and transcriptome databanks have identified homologs of *unc-29*, *unc-38*, and *unc-63* all across the phylum Nematoda (Williamson *et al*., 2007; Neveu *et al*., 2010). The conservation of these genes in distantly related nematode species may reflect the common and important role they play in the function of the levamisole AChR. It is noteworthy that in the trichostrongylid species, *H. contortus* and *Teladorsagia circumcincta*, that there are four distinct *unc-29* paralogs which have been identified (Neveu *et al*., 2010). Unlike the *unc-29, unc-38*, and *unc-63* genes, orthologs of the *lev-1* gene have only been identified in Clade V nematode species (*C. elegans* and trichostrongylids). There is currently no evidence for *lev-1* orthologs in nematodes of Clade III species (*A. suum* or *B. malayi*) nor in Clades I, II, or IV. Intriguingly, lev-1 homologs from *H. contortus, T. circumcincta*, and *Trichostrongylus colubriformis* lack a signal peptide raising questions about the contribution of LEV-1 to the function of levamisole AChRs (Neveu *et al*., 2010). Because AChR subunit oligomerization takes place within the endoplasmic reticulum, the absence of a signal peptide for *Hco*-LEV-1, *Tci*- LEV-1, and *Tco*-LEV-1 suggests that the subunit is processed differently; perhaps it is not involved in levamisole AChR construction, or it could associate with other levamisole AChR subunits using a molecular pathway that remains to be identified. Finally, there is also no evidence to date for a gene orthologous to *lev-8* in the trichostrongylids, despite intensive laboratory and bioinformatics searches (Williamson *et al*., 2007; Neveu *et al*., 2010). However, homologs of the *acr-8* gene that are closely related to *lev-8* appear to be well conserved in parasitic nematode species (Boulin *et al*., 2011). The similarity between *H. contortus, T. circumcincta*, and *T. colubriformis* ACR-8 homologs and the *C. elegans*

sequence is spread over the length of the primary amino acid sequence. However, the motif, YxxCC, which is part of the ligand binding site is conserved for trichostrongylid ACR-8 and *C. elegans* LEV-8 (YPGCC versus YAGCC for *Cel*-ACR-8), suggesting that conservation of these residues is associated with specific agonist-binding properties. It has been hypothesized that the *lev-8* and *acr-8* genes arose from a duplication that occurred after the divergence between strongyloidea and rhabditoidea (Boulin *et al*., 2011). Alternatively, a common ancestor that had both *lev-8* and *acr-8* may have occurred with the *lev-8* being lost in the trichostrongylids. Another persuasive observation for ACR-8 being a subunit of levamisole AChR subtypes in parasitic nematodes is that levamisole resistance in *H. contortus* has been associated with the presence of truncated ACR-8 subunits (Fauvin *et al*., 2010) (Box 3).

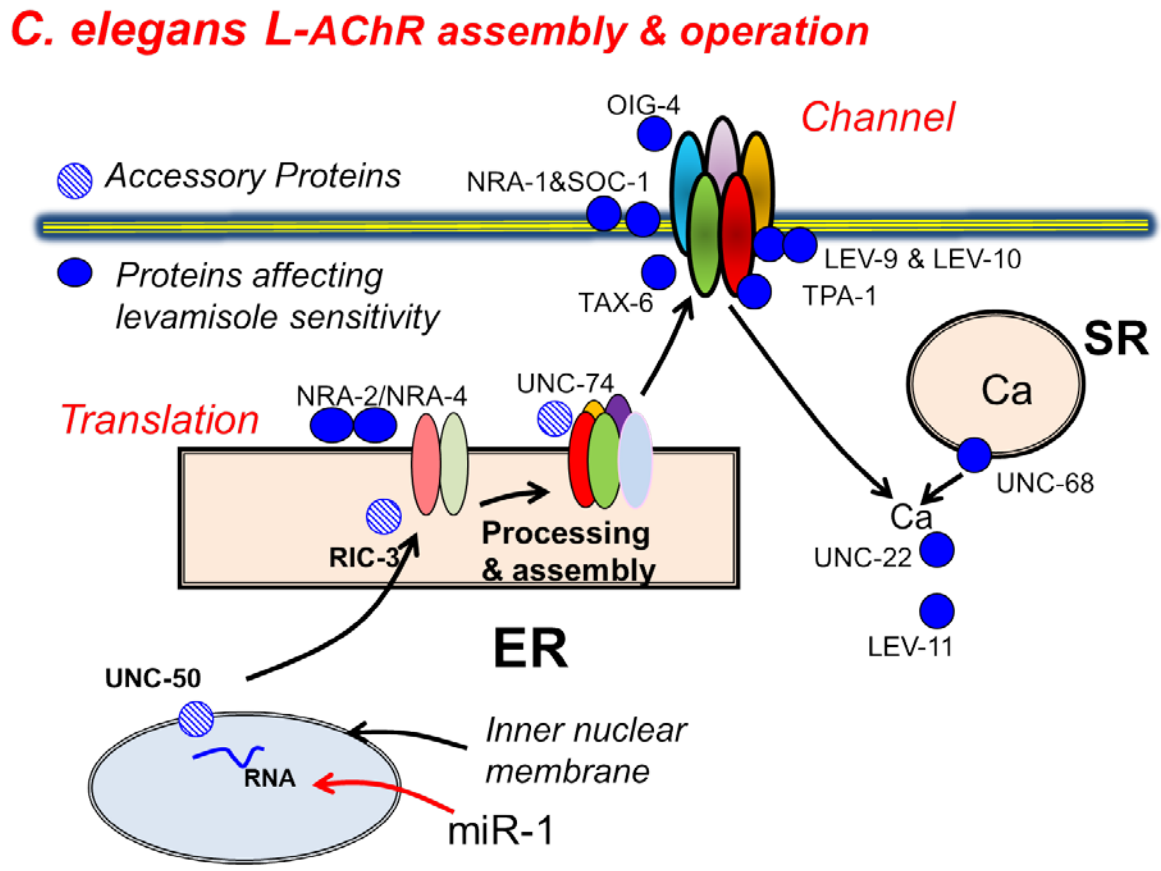

Figure 7.1 Assembly and function of levamisole receptors.

Caenorhabditis elegans levamisole-sensitive AChR channels in the muscle membrane are formed by five subunits (UNC-38, blue; UNC-29, purple; UNC-63, yellow; LEV-1, green; and LEV-8, red) with normal function being supported by OIG-4, NRA-1, NRA-2, NRA-4, SOC-1, TAX-6, TPA-1, LEV-9, and LEV-10 proteins. Once the levamisole AChR channel opens, calcium enters and its signal is amplified by the ryanodine receptor (UNC-68); the increased calcium then initiates contraction, requiring the proteins UNC-22 and LEV-11. The expression of the levamisole receptor subunits requires RNAs encoding the five subunits together with three C. elegans ancillary proteins involved in AChR assembly (RIC-3), folding (UNC-74), and trafficking (UNC-50) (Halevi *et al.*, 2002; Haugstetter *et al.*, 2005;

Eimer *et al*., 2007). miRNA (miR-1) is also known to regulate and modulate the expression of subunit RNA.

Abbreviations: ER, endoplasmic reticulum; SR, sarcoplasmic reticulum.

Box 3. Levamisole resistance

***C. elegans* levamisole resistance**

The degree of our understanding of the mechanisms of levamisole resistance depends on species of nematode studied. Levamisole resistance in *C. elegans* has been associated with null mutants of 21 genes [12–15,21–28]. Five of the genes are: *unc-38, unc-29, unc-63, lev-1,* and *lev-8,* which code for subunits of the levamisole AChR channel; seven of the genes: *oig-4, nra-1, soc-1, tax-6, tpa-1, lev-9,* and *lev-10* are associated with the proper distribution and maintaining the normal opening of the receptor channel. Three genes associated with calcium release or calcium-sensitive contraction are: *unc-68, unc-22,* and *lev-11.* Three genes, known as accessory proteins are: *unc-50, ric-3,* and *unc-74.* These accessory proteins along with *nra-2* and *nra-4* are associated with the processing, assembly, and delivery of the ion channel receptor to the membrane.

Resistance in nematode parasites

In *O. dentatum,* levamisole resistance has been associated with a reduced number of receptor channels at the muscle surface and a loss of the G35 pS conductance subtypes of levamisole AChR channel [4], whereas pyrantel resistance was associated with a reduced number of all conductance subtypes [41]. In *A. caninum,* pyrantel resistance has been associated with reduced expression levels of UNC-38, UNC-63, UNC-29 but not ACR-8. No functional change was detected in the amino acid sequence of either of these proteins or in the bases coding for the genes (single nucleotide polymorphism, SNP). In *H. contortus,* levamisole resistance has been associated with truncated forms of UNC-63. With loss of or truncation of ACR-8, the isolate is expected to be less sensitive to levamisole but still sensitive to pyrantel. Thus, it is suggested that loss of ACR-8 subunits may lead to a selective loss of sensitivity to levamisole but not pyrantel. Loss of UNC-63, however, is predicted to lead to a loss of sensitivity to both levamisole and pyrantel. The role of the other *C. elegans* genes in resistance to levamisole in parasitic nematodes remains to be investigated.

Transcriptomic approach for identifying resistance genes

In addition to the candidate gene strategy, based on *C. elegans,* a global comparative transcriptomic approach is another useful tool for identification of novel parasitic genes involved in levamisole resistance. This non-hypothesis driven approach using an amplified restriction fragment technique (cDNA-AFLP) has been used to identify genes differentially expressed in levamisole-resistant and susceptible isolates of *H. contortus* [30]. More than 17 000 transcript-derived fragments (TDFs) were amplified and 26 TDFs displayed differential expression including 11 TDFs specifically present in resistant isolates. Among those candidates, HAX was specifically expressed in the two resistant isolates and presented strong homology with the *acr-8* gene. HAX corresponded to a truncated *H. contortus acr-8* mRNA isoform (*Hco-acr-8b*) containing the two first exons and a part of intron 2. The specific expression of *Hco-acr-8b* was confirmed in other *H. contortus* levamisole-resistant isolates, highlighting its interest as a potent marker for levamisole resistance [32,45].

C6.0 Functional diversity: *Xenopus* expression of different levamisole AChR subtypes

After cloning *C. elegans* levamisole receptor subunits, it became possible to express the receptor in *Xenopus* oocytes. Robust expression of the levamisole receptor from *C. elegans* required injection of cRNA of five subunits (UNC-38, UNC-63, LEV-8, UNC-29, and LEV-1) (Figure 7.2a) and three ancillary proteins (UNC-74, RIC-3, and UNC-50) (Boulin *et al*., 2011). The maximum response to acetylcholine is much greater than the response to levamisole with no nicotine response with this expressed *C. elegans* levamisole AChR; the lack of response to nicotine demonstrates that the *C. elegans* receptor is pharmacologically different from the levamisole receptors of some parasitic nematodes. Expression of an acetylcholine- and nicotine-sensitive *C. elegans* muscle homomeric receptor was achieved by injecting ACR-16 cRNA (Figure 7.2b) (Raymond *et al*., 2000; Boulin *et al*., 2008). Two levamisole-sensitive AChR subtypes from *A. suum* required only two subunits (UNC-38 and UNC-29) and did not require the accessory proteins (Williamson *et al*., 2009). Two types of receptor were produced: (i) one type, more sensitive to levamisole and pyrantel than nicotine, was observed when more UNC-29 than UNC-38 cRNA was injected (Figure 7.2c; Box 1); (ii) the other type that was more sensitive to oxantel and nicotine than levamisole was observed when more UNC-38 than UNC-29 cRNA was injected (Figure 7.2d). It is suggested that two types of levamisole receptor are produced by different stoichiometric combinations of UNC-38 and UNC-29: the levamisole/pyrantel receptor by $(UNC\text{-}38)_2$:$(UNC\text{-}29)_3$ and the nicotine, oxantel receptor by $(UNC\text{-}38)_3$:$(UNC\text{-}29)_2$. These observations illustrate that the levamisole AChR subunit structure and anthelmintic sensitivity can vary and is plastic.

Expression of the receptor subunits derived from *H. contortus*, which is more phylogenetically related to *C. elegans*, was also different. Expression of a functional receptor

highly responsive to levamisole required the presence of four subunits (UNC-63, UNC-29, UNC-38, and ACR-8) and the three ancillary proteins (Figure 7.2e) (Boulin *et al*., 2011). This receptor, referred to as *Hco*-L-AChR1, is more sensitive to levamisole than acetylcholine and is poorly responsive to pyrantel and nicotine (Figure 7.2f). When the cRNA for ACR-8 is omitted, the UNC-63, UNC-29, UNC- 38 subunit combination gave rise to a second, pharmacologically different levamisole AChR referred to as *Hco*-LAChR2 (Figure 7.2f). The Hco-L-AChR2 was more sensitive to pyrantel and acetylcholine than levamisole. Therefore, two distinct subtypes of recombinant *H. contortus* levamisole AChR could be distinguished, possibly mirroring some of the levamisole AChR diversity revealed with single channel recording experiments performed on the closely related species *O. dentatum* (Figure 1). The crucial role for the ACR-8 subunit in levamisole sensitivity is highlighted by the fact that the *Hco*-L-AChR1 and *Hco*-L-AChR2 only differ by the presence or absence of *Hco*-ACR-8. In *C. elegans*, the functional expression of the *C. elegans* levamisole AChR did not require ACR-8 subunits (Boulin *et al*., 2008). Of interest in parasitic nematodes is the potential role that ACR-8 plays in levamisole resistance, as absence of ACR-8 in the expressed receptors (Figure 7.2f) gives rise to the *Hco*-L-AChR2 receptor, which is less sensitive to levamisole but highly responsive to pyrantel. Thus, an acr-8 null mutant parasitic nematode isolate may be sensitive to pyrantel but not levamisole.

C7.0 Modeling the levamisole receptor

The family of ligand gated ion channels is present in nearly all animal groups and has also been found in bacteria, predating eukaryotes (Chen *et al*., 1999). The subunit genes of this

family may be extremely divergent in sequence but retain a highly conserved structure and specific functional motifs (Box 2). This allows the use of known crystal structures to serve as templates for the prediction of related ion channel structures and identification of acetylcholine and nicotine within the ligand binding pocket of the AChR (Brejc *et al*., 2001; Le Novere *et al*., 2002). The models identify potentially important hydrogen bonds formed upon ligand binding and are able to discriminate between compounds with high and low experimentally determined LD50 values. In the future, we could use this approach to examine levamisole and pyrantel binding to the various levamisole-sensitive AChRs of identified parasitic nematodes. The next challenge is for *in silico* prediction of ligand receptor interaction for novel compounds. The example of cytisinoid derivatives and their affinity for acetylcholine binding protein demonstrates that it is possible to achieve a good correlation over a wide range of predicted binding energy and IC50 values (Abin-Carriquiry *et al*., 2010).

The neurotransmitter binding pocket lies between two adjacent subunits of the channel pentamer (Box 2), formed from three loops of the positive subunit (known as the A, B, and C loops) and three β-strands of the negative subunit (loops D, E, and F). The closed, unbound form of the *Torpedo* fish AChR is an asymmetric pentamer that becomes symmetrical in the presence of acetylcholine (Unwin, 1995). Comparison of a refined version of this structure and that of the channel produced in the open channel configuration shows that the c-loop closes around the bound neurotransmitter, a movement of perhaps 8 A°, accompanied by significant changes in the β-sheet regions of the ligand binding domain and rotation of the transmembrane domain, opening a path for the flow of cations (Unwin, 1995; Brejc *et al*., 2001). Modeling interactions of such flexible structures is still being developed and

simulation of the ligand–receptor interaction will require either an ensemble of receptors in different physical states, or use of molecular dynamics to produce time simulations of the ligand bound structure. Snapshots can be evaluated to determine the stability of ligand binding and changes in flexibility of residues that interact with the ligand (Brandsdal *et al*., 2003). Although still at the limits of protein modeling, these techniques will help us to understand details of nAChR function and their interaction with levamisole and other anthelmintic compounds.

C8.0 Resistance: mechanisms of resistance for parasites *in vivo*

In sensitive *O. dentatum* parasites, levamisole readily activates and opens the receptor channels (Figure 7.0b) frequently. In the levamisole and pyrantel resistant isolates, the channels open infrequently and there are fewer receptor channels present in the muscle membrane (Robertson *et al*., 1999, 2000). A histogram of single channel conductances from the anthelmintic sensitive isolate of *O. dentatum* (Robertson *et al*., 1999, 2000) shows the presence of four separate channel conductance subtypes: G25 pS, G35 pS, G40 pS, G45 pS (Figure 7.0c,d). Interestingly, in the levamisole-resistant isolate the G35 pS peak is missing, but in the pyrantel-resistant isolate this peak is still present (Robertson *et al*., 1999, 2000). These observations suggest that resistance is associated with an overall reduction in the number of receptors, that levamisole resistance may be associated specifically with loss of the G 35 pS subtype but that pyrantel resistance may be different and is not associated with a loss of a specific subtype. We might expect that the changes associated with resistance may lead to subtle changes in motility without compromising the ability of the parasite to

complete its life cycle. The changes in motility have been detected by detailed phenotyping (Carr *et al*., 2011; Chen *et al*., 2011).

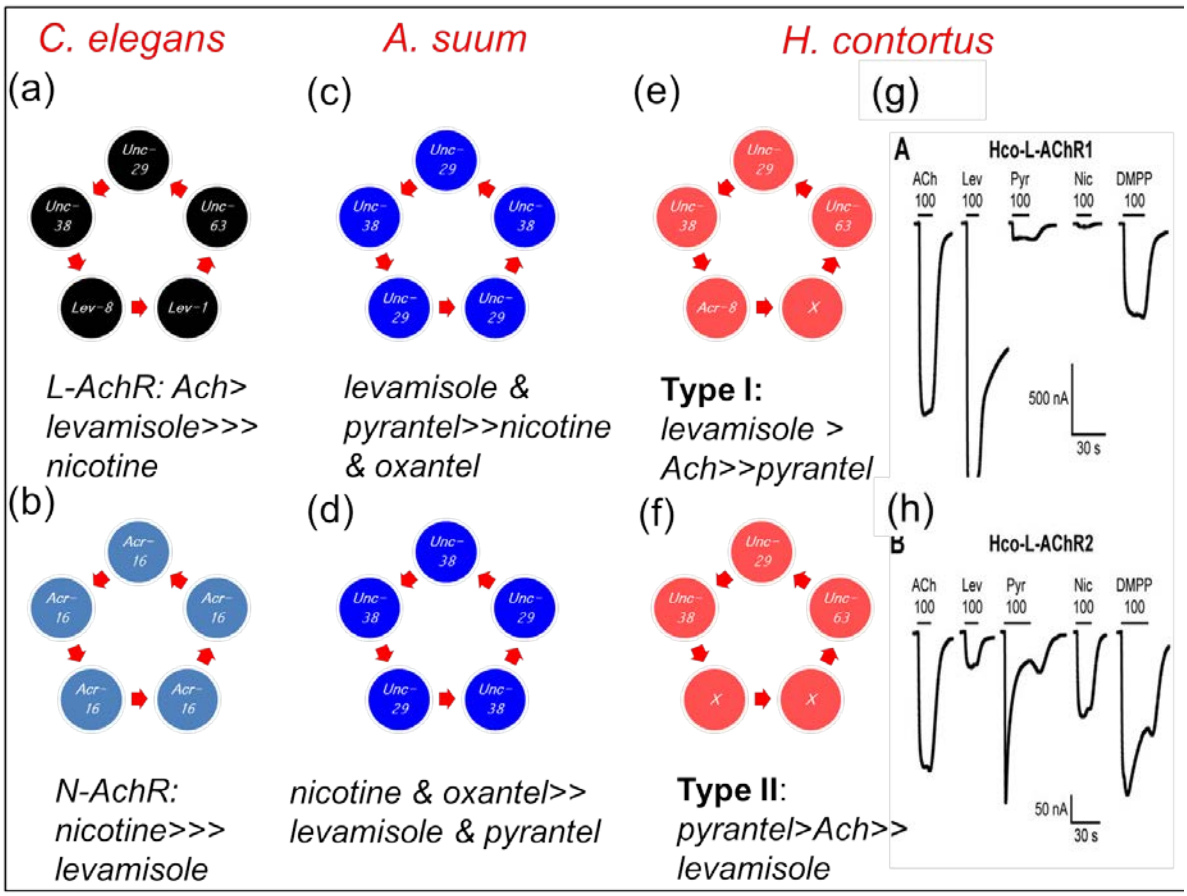

Figure 7.2 Diagram of possible stoichiometric arrangements of some different acetylcholine receptors (AChRs) from *Caenorhabditis elegans*, *Ascaris suum*, and *Haemonchus contortus* and the relative potencies of anthelmintic agonists

(a) The *C. elegans* levamisole AChR. (b) The *C. elegans* muscle nicotine AChR. (c) The *A. suum* AChR where levamisole is more potent than nicotine when more cRNA for UNC-29 than UNC-38 is injected. (d) The *A. suum* AChR where nicotine is more potent than levamisole when more cRNA for UNC-38 than UNC-29 is injected into the *Xenopus* oocytes for expression. (e) The *H. contortus* L-AChR 1 receptor, which is most sensitive to

levamisole. (f) The *H. contortus* L-AChR2, which is most sensitive to pyrantel (Boulin *et al*., 2011). (g) Currents recorded from the *Xenopus* oocyte expressing *H. contortus* Hco-L-AChR1 receptor when 100 mM acetylcholine (ACh), 100 mM levamisole (Lev), 100 mM pyrantel (Pyr), 100 mM nicotine (Nic), or 100 mM dimethylphenylpiperazinium (DMPP) are applied. Levamisole is the most potent agonist. (h) Currents recorded from the *Xenopus* oocyte expressing *H. contortus Hco*-L-AChR2 receptor when 100 mM ACh, 100 mM Lev, 100 mM Pyr, 100 mM Nic, or 100 mM DMPP are applied. Pyrantel produces the biggest peak response.

C9.0 Phenotyping sensitive and resistant isolates: microfluidics

We have seen above that there are a range of different levamisole receptor subtypes suggesting some redundancy and that there may be differences between sensitive and resistant isolates. It is now possible to screen and observe effects of drugs such as levamisole affecting motion of L3 larvae of parasitic nematodes with greater resolution using computer tracking and microfluidic technology (Carr *et al*., 2011; Chen *et al*., 2011). These multiparameter microfluidic bioassays were developed to observe the innate locomotory properties of larval movement along with transient and real time responses to the application of anthelmintics within a single experiment.

An electrical field is used in the platform to guide the movement of the larvae (electrotaxis) into and out of the drug wells. Video recording of the experiment along with automatic worm tracking software reveals important information about changes in the locomotion of the worm during entry exposure and exit periods from the drug. The tracking software used can measure subtle locomotion changes in the microfluidic device in the presence or in the absence of drugs. The approach allows quantification of transient drug effects and measurement of locomotory parameters such as the sinusoidal properties of the larval movement (velocity, wavelength, frequency, and amplitude). The more precise measurements of locomotion can detect levamisole resistance in the absence of drugs from changes in the parameters of locomotion, as well as changes associated with application of anthelmintics (Carr *et al*., 2011; Chen *et al*., 2011). This new method of quantitative phenotyping offers a new way to detect and investigate anthelmintic resistance and anthelmintic interactions that affect the phenotype of locomotion associated with subtle changes in receptor subtypes.

C10.0 Investigating levamisole resistance at the molecular level in parasitic nematodes

Four sets of proteins have been found to contribute to levamisole resistance in *C. elegans*. The four sets are: (i) levamisole-sensitive AChR subunits; (ii) proteins involved in processing and assembly of levamisole AChR channel subunits; (iii) proteins involved in regulating the levamisole AChR channel; and (iv) proteins involved in the calcium contraction signaling cascade (Figure 7.1; Box 3). In parasitic nematodes, searches for expression or sequence polymorphisms associated with levamisole resistance mainly focused on levamisole AChR subunits. In the strongylid parasite, *Ancylostoma caninum* (dog hookworm), genes orthologous to *unc-38*, *unc-63*, and *unc-29* have reduced expression in a highly pyrantel-resistant isolate when compared with a low pyrantel-resistant isolate (Kopp *et al*., 2007). By contrast, in the trichostrongylid species *H. contortus*, *T. circumcincta*, and *T. colubriformis*, expression of complete coding mRNAs corresponding to *unc-38*, *unc-63*, *unc-29*, and *lev-1* homologs were found to be similar in both levamisole-susceptible and -resistant isolates. However, in addition to full-length coding mRNAs corresponding to *unc-63* orthologs, abbreviated isoforms (*unc-63b*) were found to be specifically expressed in some levamisole-resistant isolates from the three nematode species, suggesting a possible role of the truncated UNC-63 subunit in levamisole resistance (Neveu *et al*., 2010). Transcript levels may also change with resistance (Williamson *et al*., 2011). Recent progress with the functional expression of nematode levamisole AChRs in *Xenopus* oocytes has provided a unique opportunity to test the role of truncated subunits in levamisole resistance (Boulin *et al*., 2011).

The truncated *Hco-unc-63b* transcript in a *H. contortus* isolate encoded a protein of 343 amino acids that has two transmembrane domains (TM1 and TM2). In *Xenopus* oocytes, expression of the truncated *Hco*-UNC-63b along with the full-length *Hco-unc-63a*, *Hco-unc-29.1, Hco-unc-38,* and *Hco-acr-8* cRNA produced a dose-dependent inhibition of the *Hco*-L-AChR1 expression (Boulin *et al*., 2011). The results show that the truncated *Hco-unc-63b* is dominant negative, inhibiting the wild type *Hco*-UNC-63 subunits and therefore could induce a levamisole-resistant phenotype in parasites expressing this mutant form. Expression of the truncated UNC-63b is predicted to reduce expression of both the *Hco*-L-AChR1 and *Hco*-L-AChR2 receptors. Hence, if such a dominant negative effect also occurs *in vivo*, a cross-resistance to levamisole and pyrantel could be expected in the *H. contortus* isolates expressing *Hco*-UNC-63b. The role of truncated ACR-8, which is associated with levamisole resistance, (Fauvin *et al*., 2010) remains to be tested in expression experiments.

C11.0 Concluding remarks

Better molecular and functional platforms have allowed a tremendous increase in our understanding of: (i) the biology of the levamisole AChR channel; (ii) how there are several diverse pharmacological subtypes; (iii) how the subunit structure is plastic and affects drug sensitivity; and (iv) how subunit truncation (UNC-63 or ACR-8) or reduced subunit expression may play a role in levamisole resistance. There is optimism that the understanding of the molecular and pharmacological mechanism (or mechanisms) of resistance will allow molecular diagnostic tests for resistance and better pharmacological therapies to be used, including combination drug therapy. The current advances in levamisole receptor molecular

biology have bridged the gap between genes and the physiological expression of anthelmintic sensitivity. Further examination of the various receptor subtypes in important parasites such as filaria, hookworm, and whipworm, the range of nematode parasite AChR channels in muscle receptors and other tissues, and the changes brought about by resistance and altered subunit composition will provide a deeper understanding of AChR functions and the mechanisms that control the evolution of their diversity. In the future, new approaches that include novel methods to measure small changes in phenotype such as microfluidics, the development of molecular techniques to manipulate parasites *in vivo*, and computer simulation of the ligand receptor interaction will usher in a new awakening for receptor research. Over the next 10 years we should expect to see a more detailed map of AChR function as well as new anthelmintics that target these receptors.

C12.0 Conflict of interest

The authors declare no conflict of interest.

C13.0 Acknowledgements

The authors acknowledge support from all of our colleagues in parasitology, and specifically for this work from the Institut National de la Recherche Agronomique (INRA) to C.L.C. and C.N, the Chateaubriand fellowship from the Embassy of France in the US, grants R56 AI047194-11 to R.J.M and R21AI092185-01 to A.P.R from the National Institute of Allergy and Infectious Diseases. The content is solely the responsibility of the authors and does not

necessarily represent the official views of the National Institute of Allergy and Infectious Diseases of the National Institutes of Health.

REFERENCES

Abin-Carriquiry, J., Zunini, M., Cassels, B., Wonnacott, S., Dajas, F., 2010. In silico characterization of cytisinoids docked into an acetylcholine binding protein. Bioorg Med Chem Lett 20(12), 3683-3687.

Aceves, J., Erlij, D., Martinez-Maranon, R., 1970. The mechanism of the paralysing action of tetramisole on *Ascaris* somatic muscle. Br J Pharmacol 38, 602-607.

Adelsberger, H., Scheuer, T., Dudel, J., 1997. A patch clamp study of a glutammatergic chloride channel on pharyngeal muscle of the nematode *Ascaris suum*. Neurosci Lett 230, 183-186.

Almedom, R., Liewald, J., Hernando, G., Schultheis, C., Rayes, D., Pan, J., Schedletzky, T., Hutter, H., Bouzat, C., Gottschalk, A., 2009. An ER-resident membrane protein complex regulates nicotinic acetylcholine receptor subunit composition at the synapse. EMBO J 28(17), 2636-2649.

Altschul, S., Madden, T., Schaffer, A., Zhang, J., Zhang, Z., Miller, W., 1997. Gapped BLAST and PSI-BLAST: a new generation of protein database search programs. Nucleic Acids Res 25, 3389-3402.

Amoah, P., Drechsel, P., Henseler, M., Abaidoo, R., 2007. Irrigated urban vegetable production in Ghana: microbiological contamination in farms and markets and associated consumer risk groups. J Water Health 5(3), 455-466.

Anderson, R.C., 1992. Nematode Parasites of Vertebrates, their development and transmission. C.A.B International University Press, Cambridge ISBN 0 85198, 799.

Anderson, R.C., 2000. Nematode parasites of vertebrates: their development and transmission. Wallingford, Oxon, UK ; New York: CABI Pub.

Angstadt, J.D., Donmoyer, J.E., Stretton, A.O., 1989. Retrovesicular ganglion of the nematode Ascaris. J Comp Neurol 284, 374-388.

Arias, H.R., 1997. Topology of ligand binding sites on the nicotinic acetylcholine receptor. Brain Research Reviews 25, 133-191.

Arias, H.R., 2000. Localization of agonist and competitive antagonist binding sites on nicotinic acetylcholine receptors. Neurochemistry International 36, 595-645.

Bafna, P.A., Purohit, P.G., Auerbach, A., 2008. Gating at the Mouth of the Acetylcholine Receptor Channel: Energetic Consequences of Mutations in the alphaM2-Cap. PloS ONE 3, e2515.

Ballivet, M., Patrick, J., Lee, J., Heinemann, S., 1982. Molecular cloning of cDNA coding for the γ subunit of *Torpedo* acetylcholine receptor. Proc Natl Acad Sci U S A 79, 4466-4470.

Ballivet, M., Alliod, C., Bertrand, S., Bertrand, D., 1996. Nicotinic acetylcholine receptors in the nematode *Caenorhabditis elegans*. J Mol Biol 258(2), 261-269.

Baylis, H.A., Matsuda, K., Squire, M.D., Fleming, J.T., Harvey, R., Darlison, M., Barnard, E.A., Sattelle, D.B., 1997. ACR-3, a *Caenorhabditis elegans* nicotinic acetylcholine receptor subunit. Molecular cloning and functional expression. Receptors Channels 5(3-4), 149-158.

Ben-Ami, H., Yassin, L., Farah, H., Michaeli, A., Eshel, M., Treinin, M., 2005a. RIC-3 affects properties and quantity of nicotinic acetylcholine receptors via a mechanism that does not require the coiled-coil domains. J Biol Chem 280(30), 28053-28060.

Ben-Ami, H., Biala, Y., Farah, H., Elishevitz, E., Battat, E., Treinin, M., 2009a. Receptor and subunit specific interactions of RIC-3 with nicotinic acetylcholine receptors. Biochemistry 48(51), 12329-12336.

Ben-Ami, H.C., Yassin, L., Farah, H., Michaeli, A., Eshel, M., Treinin, M., 2005b. RIC-3 affects properties and quantity of nicotinic acetylcholine receptors via a mechanism that does not require the coiled-coil domains. The Journal of Biological Chemistry 280, 28053-28060.

Ben-Ami, H.C., Biala, Y., Farah, H., Elishevitz, E., Battat, E., Treinin, M., 2009b. Receptor and subunit specific interactions of RIC-3 with Nicotinic Acetylcholine Receptors. Biochemistry 48, 12329-12336.

Bendtsen, J., Nielsen, H., von Heijne, G., Brunak, S., 2004. Improved prediction of signal peptides: SignalP 3.0. J Mol Biol 340, 783-795.

Bertrand, D., Galzi, J., Devillers-Thiery, A., Bertrand, S., Changeux, J., 1993. Mutations at two distinct sites within the channel domain M2 alter calcium permeability of neuronal α7 nicotinic receptor. Proc. Natl. Acad. Sci. USA. 90, 6971-6975.

Bethony, J., Brooker, S., Albonico, M., Geiger, S.M., Loukas, A., Diemert, D., Hotez, P.J., 2006. Soil-transmitted helminth infections: ascariasis, trichuriasis, and hookworm. The Lancet 367, 1521-1532.

Bhumiratana, A., Pechgit, P., Koyadun, S., Siriaut, C., Yongyuth, P., 2010. Inported bancroftian filariasis: Diethylcarbamazine response and benzimidazole susceptibility of *Wuchereria bancrofti* in dynamic cross-border migrant population targeted by the National Program to Eliminate Lymphatic Filariasis in South Thailand. Acta Tropica 113, 121-128.

Bianchi, L., Driscoll, M., 2006. Heterologous expression of *C. elegans* ion channels in *Xenopus* oocytes. *WormBook,* ed. The *C. elegans* Research Community.

Blackhall, W., Pouliot, J., Prichard, R., Beech, R., 1998. *Haemonchus contortus*: selection at a glutamate-gated chloride channel gene in ivermectin- and moxidectin-selected strains. Exp Parasitol 90(1), 42-48.

Blaxter, M., 1998. *Caenorhabditis elegans* is a nematode. Science 282, 2041-2046.

Blount, P., Merlie, J., 1989. Molecular basis of the two nonequivalent ligand binding sites of the muscle nicotinic acetylcholine receptor. Neuron 3, 349-357.

Blount, P., Merlie, J., 1990. Mutational analysis of muscle nicotinic acetylcholine receptor subunit assembly. J Cell Biol 111(1), 2613-2622.

Blount, P., Merlie, J., 1991. BIP associates with newly synthesized subunits of the mouse muscle nicotinic receptor. J Cell Biol 113, 1125-1132.

Bolotina, V.M., Najibi, S., Palacino, J.J., Pagano, P.J., Cohen, R.A., 1994. Nitric oxide directly activates calcium-dependent potassium channels in vascular smooth muscle. Nature 368, 850-853.

Bossie, E., Centinaio, E., Moriondo, A., Peres, A., 1998. Ca^{2+}-dependence of the depolarization-inducible Na^{+} current of Xenopus oocytes. J Cell Physiol 174, 154-159.

Boulin, T., Gielen, M., Richmond, J.E., Williams, D.C., Paoletti, P., Bessereau, J.-L., 2008. Eight genes are required for functional reconstitution of the *Caenorhabditis elegans* levamisole-sensitive acetylcholine receptor. PNAS 105, 18590-18595.

Boulin, T., Fauvin, A., Charvet, C.L., Cortet, J., Cabaret, J., Bessereau, J.-L., Neveu, C., 2011. Functional reconstitution of *Haemonchus contortus* acetylcholine receptors in *Xenopus* oocytes provides mechanistic insights into levamisole resistance. Br J Pharmacol 164, 1421-1432.

Boussinesq, M., 2008. Onchocerciasis control: biological research is still needed. Parasite 15, 510-514.

Bowman, J.W., Winterrowd, C.A., Friedman, A.R., Thompson, D.P., Klein, R.D., Davis, J.P., Maule, A.G., Blair, K.L., Geary, T.G., 1995. Nitric Oxide Mediates the Inhibitory Effects of SDPNFLRFamide, a Nematode FMRFamide-Related Neuropeptide, in *Ascaris suum*. Journal of Neurophysiology 74, 1880-1888.

Bowman, J.W., Friedman, A.R., Thompson, D.P., Maule, A.G., Alexander-Bowman, S.J., Geary, T.G., 2002. Structure-activity relationships of an inhibitory nematode FMRFamide-related peptide, SDPNFLRFamide (PF1), on *Ascaris suum* muscle. International Journal for Parasitology 32, 1765-1771.

Brading, A.F., Caldwell, P.C., 1971. The resting membrane potential of the somatic muscle cells of *Ascaris lumbricoides*. J Physiol 217, 605-624.

Bradley, J., Jackson, J., 2004. Immunity, immunoregulation and the ecology of trichuriasis and ascariasis. Parasite Immunol 26, 429-441.

Brandsdal, B., Osterberg, F., Almlof, M., Feierberg, I., Luzhkov, V., Aqvist, J., 2003. Free energy calculations and ligand binding. Advances in Protein Chemistry 66, 123-158.

Brejc, K., van Dijk, W., Klaassen, R., Schuurmans, M., van der Oost, J., Smit, A., Sixma, T., 2001. Crystal structure of an ACh-binding protein reveals the ligand-binding domain of nicotinic receptors. Nature 411, 269-276.

Brenner, R., Jegla, T., Wickenden, A., Liu, Y., Aldrich, R., 2000. Cloning and functional characterization of novel large conductance calcium-activated potassium channel β-subunits, hKCNMB3 and hKCNMB4. J Biol Chem 275(9), 6453-6461.

Brenner, S., 1974. The genetics of *Caenorhabditis elegans*. Genetics 77, 71-94.

Brochiero, E., Coady, M., Klein, H., Laprade, R., Lapointe, J.-Y., 2001. Activation of an ATP-dependent K^{+} conductance in *Xenopus* oocytes by expression of adenylate kinase cloned from renal proximal tubules. Biochemica et Biophysica Acta 1510, 29-42.

Brown, L.A., Jones, A.K., Buckingham, S.D., Mee, C.J., Sattelle, D.B., 2006. Contributions from *Caenorhabditis elegans* functional genetics to antiparasitic drug target identification and validation: Nicotinic acetylcholine receptors, a case study. International Journal for Parasitology 36, 617-624.

Browne, C., Werner, W., 1984. Intercellular junctions between the follicle cells and oocytes of *Xenopus laevis*. J Exp Zool 230, 105-113.

Buckingham, S.D., Pym, L., Sattelle, D.B., 2006. Oocytes as an expression system for studying receptor/channel targets of drugs and pesticides. Methods in Molecular Biology 322, 331-345.

Bull, K., Cook, A., Hopper, N.A., Harder, A., Holden-Dye, L., Walker, R., 2007. Effects of the novel anthelmintic emodepside on the locomotion, egg-laying behaviour and development of *Caenorhabditis elegans*. International Journal for Parasitology 37, 627-636.

Buxton, S., Neveu, C., Charvet, C., Robertson, A.P., Martin, R.J., 2011. On the mode of action of emodepside: slow effects on membrane potential and voltage-activated currents in *Ascaris suum*. British Journal of Pharmacology 164, 453-470.

Byerly, L., Masuda, M., 1979. Voltage-clamp analysis of the potassium current that produces a negative-going action potential in *Ascaris* muscle. J Physiol 288, 263-284.

Caldwell, P.C., Ellory, J.C., 1968. Ion movements in the somatic muscle cells of *Ascaris lumbricoides*. J Physiol 197, 75P-76P.

Caldwell, P.C., 1974. Possible mechanisms for linkage of membrane potentials to metabolism by electrogenic transport processes with special reference to *Ascaris* muscle. Bioenergetics 4, 201-209.

Callamaras, N., Parker, I., 2000. Ca^{2+}-dependent activation of Cl^- currents in *Xenopus* oocytes is modulated by voltage. Am J Physiol Cell Physiol 278, C667-675.

Candia, S., Garcia, M.L., Latorre, R., 1992. Mode of action of iberiotoxin, a potent blocker of the large conductance Ca^{2+}-activated K^+ channel. Biophys. J 63, 583-590.

Carr, J., Parashar, A., Gibson, R., Robertson, A.P., Martin, R.J., Pandey, S., 2011. A microfluidic platform for high-sensitivity, real-time drug screening on *C. elegans* and parasitic nematodes. Lab Chip 11(14), 2385-2396.

Carre-Pierrat, M., Grisoni, K., Gieseler, K., Mariol, M., Martin, E., Jospin, M., Allard, B., Segalat, L., 2006. The SLO-1 BK channel of *Caenorhabditis elegans* is critical for muscle function and is involved in dystrophin-dependent muscle dystrophy. J Mol Biol 358(2), 387-395.

Carrera, E., Nesheim, M., Crompton, D., 1984. Lactose maldigestion in Ascaris-infected preschool children. Am J Clin Nutr 39, 255-264.

Castillo, M., Mulet, J., Gutierrez, L., Ortiz, J., Castelan, F., Gerber, S., Sala, S., Sala, F., Criado, M., 2005. Dual role of the RIC-3 protein in trafficking of serotonin and nicotinic acetylcholine receptors. J Biol Chem 280(29), 27062-27068.

Cens, T., Nargeot, J., Charnet, P., 1997. Ca^{2+}-permeability of muscle nicotinic acetylcholine receptor is increased by expression of the ε subunit. Receptors Channels 5(1), 29-40.

Chang, H., Neumann, E., 1976. Dynamic properties of isolated acetylcholine receptor proteins: release of calcium ions caused by ACh binding. Proc. Natl. Acad. Sci. USA. 73, 3364-3368.

Changeux, J., Edelstein, S., 2005. Allosteric mechanisms of signal transduction. Science 308, 1424-1428.

Chen, B., Qian, G., Xiano-Ming, X., Ping, P., Wang, S., Zhan, H., Eipper, B., Zhao-Wen, W., 2010. A novel auxiliary subunit critical to BK channel function in *Caenorhabditis elegans*. J Neurosci 20, 16651-16661.

Chen, B., Deutmeyer, A., Carr, J., Robertson, A.P., Martin, R.J., Pandey, S., 2011. Microfluidic bioassay to characterize parasitic nematode phenotype and anthelmintic resistance. Parasitology 138(1), 80-88.

Chen, C., Cui, C., Mayer, M., Gouaux, E., 1999. Functional characterization of a potassium-selective prokaryotic glutamate receptor. Nature 402(6763), 817-821.

Chen, W., Terada, M., Cheng, J.T., 1996. Characterization of subtypes of gamma-aminobutyric acid receptors in an *Ascaris* muscle preparation by binding assay and binding of PF1022A, a new anthelmintic, on the receptors. Parasitol Res 82, 97-101.

Cioli, D., Pica-Mattoccia, L., Archer, S., 1995. Antischistosomal drugs: Past, present...and future? Pharmacology & Therapeutics 68(1), 35-85.

Colquhoun, D., Ogden, D., Mathie, A., 1987. Nicotinic acetylcholine receptors of nerve and muscle: functional aspects. Trends in pharmacological sciences 8(12), 465-475.

Conder, G., Johnson, S., Nowakowski, D., Blake, T., Dutton, F., Nelson, S., Thomas, E., Davis, J.P., Thompson, D.P., 1995. Anthelmintic profile of the cyclodepsipeptide PF1022A in *in vitro* and *in vivo* models. Journal of Antibiotics 48, 820-823.

Cook, A., Franks, C., Holden-Dye, L., 2006. Electrophysiological recordings from the pharynx. WormBook 17, 1-7.

Corringer, J., Bertrand, S., Bohler, S., Edelstein, S., Changeux, J., Bertrand, D., 1998. Critical elements determining diversity in agonist binding and desensitization of neuronal nicotinic acetylcholine receptors. Neuroscience J 18(2), 648-657.

Corringer, P.-J., Le Novére, N., Changeux, J.-P., 2000. Nicotinic receptors at the amino acid level. Annu. Rev. Pharmacol. Toxicol. 40, 431-458.

Cox, F.E.G., 2002. History of Human Parasitology. Clinical Microbiology Reviews 15, 595-612.

Crisford, A., Murray, C., O'Connor, V., Edwards, R., Kruger, N., Welz, C., Von Samson-Himmelstjerna, G., Harder, A., Walker, R., Holden-Dye, L., 2011. Selective toxicity of the anthelmintic emodepside revealed by heterologous expression of human KCNMA1 in *Caenorhabditis elegans*. Mol Pharmacol 79(6), 1031-1043.

Cruz, E.L., Allanson, M., Kwa, B., Azizan, A., Izurieta, R., 2011. Morphological changes of *Ascaris spp.* eggs during their development outside the host. Journal of Parasitology In-Press.

Culetto, E., Baylis, H.A., Richmond, J.E., Jones, A.K., Fleming, J.T., Squire, M.D., Lewis, J.A., Sattelle, D.B., 2004. The *Caenorhabditis elegans unc-63* Gene

Encodes a Levamisole-sensitive Nicotinic Acetylcholine Receptor alpha Subunit. The Journal of Biological Chemistry 279, 42476-42483.

Cymes, G.D., Grosman, C., 2008. Pore-opening mechanisms of the nicotinic acetylcholine receptor evinced by proton transfer. Nature Structural & Molecular Biology 15, 389-396.

Davis, R.E., Stretton, A.O., 1989. Passive membrane properties of motorneurons and their role in long-distance signaling in the nematode *Ascaris*. J Neurosci 9, 403-414.

de Silva, N.R., Brooker, S., Hotez, P.J., Montresor, A., Engels, D., Savioli, L., 2003. Soil-transmitted helminth infections: updating the global picture. Trends in Parasitology 19, 547-551.

DeBell, J.T., del Castillo, J., Sanchez, V., 1963. Electrophysiology of the Somatic Muscle Cells of *Ascaris Lumbricoides*. J Cell Comp Physiol 62, 159-177.

del Castillo, J., Demello, W.C., Morales, T., 1964a. Influence of Some Ions on the Membrane Potential of *Ascaris* Muscle. J Gen Physiol 48, 129-140.

del Castillo, J., Rivera, A., Solorzano, S., Serrato, J., 1989. Some aspects of the neuromuscular system of *Ascaris*. Quarterly Journal of Experimental Physiology 74, 1071-1087.

Devillers-Thiery, A., Giraudat, J., Bentaboulet, M., Changeux, J.-P., 1983. Complete mRNA coding sequence of the acetylcholine binding alpha-subunit of *Torpedo marmorata* acetylcholine receptor: a model for the transmembrane organization of the polypeptide chain. Proc Natl Acad Sci U S A 80, 2067-2071.

Donnen, P., Brasseur, D., Dramaix, M., Vertongen, F., Zihindula, M., Muhamiriza, M., Hennart, P., 1998. Vitamine A supplementation but not deworming improves growth of malnourished preschool children in eastern Zaire. J Nutr 128, 1320-1327.

Drenan, R., Nashmi, R., Imoukhuede, P., Just, H., McKinney, S., Lester, H., 2008. Subcellular trafficking, pentameric assembly, and subunit stoichiometry of neuronal nicotinic acetylcholine receptors containing fluorescently labeled α6 and β3 subunits. Mol Pharmacol 73(1), 27-41.

Dumont, J., 1972. Oogenesis in *Xenopus laevis* (Daudin). Stages of oocyte development in laboratory-maintained animals. J. Morphol 136, 153-180.

Dworetzky, S., Boissard, C., Lum-Ragan, J., McKay, M., Post-Munson, D., Trojnacki, J., Chang, C., Gribkoff, V., 1996. Phenotypic alteration of a human BK (hSlo) channel by hSloβ subunit coexpression: changes in blocker sensitivity, activation/relaxation and inactivation kinetics, and protein kinase A modulation. J Neurosci 16(15), 4543-4550.

Edgar, R.C., 2004. MUSCLE: multiple sequence alignment with high accuracy and high throughput. . Nucleic Acids Res 32, 1792-1797.

Eimer, S., Gottschalk, A., Hengartner, M., Horvitz, H.R., Richmond, J., Schafer, W.R., Bessereau, J.-L., 2007. Regulation of nicotinic receptor trafficking by the transmembrane Golgi protein UNC-50. EMBO J 26, 4313-4323.

Elkins, T., Ganetzky, B., Wu, C.-F., 1986. A *Drosophila* mutation that eliminates a calcium-dependent potassium current. *Proc Natl Acad Sci. USA* 83, 8415-8419.

Evans, A., Martin, R.J., 1996. Activation and cooperative multiion block of single nicotinic-acetylcholine channel currents of *Ascaris* muscle by the tetrahydropyrimidine anthelmintic, morantel. Br J Pharmacol 118(5), 1127-1140.

Fauvin, A., Charvet, C., Issouf, M., Cortet, J., Cabaret, J., Neveu, C., 2010. cDNA-AFLP analysis in levamisole-resistant *Haemonchus contortus* reveals alternative splicing in a nicotinic acetylcholine receptor subunit. Mol Biochem Parasitol 170(2), 105-107.

Fellowes, R.A., Maule, A.G., Marks, N.J., Geary, T.G., Thompson, D.P., Halton, D.W., 2000. Nematode neuropeptide modulation of the vagina vera of *Ascaris suum*: *in vitro* effects of PF1, PF2, PF4, AF3 and AF4. Parasitology 120, 79-89.

Fleming, J.T., Baylis, H.A., Sattelle, D.B., Lewis, J.A., 1996. Molecular cloning and *in vitro* expression of *C. elegans* and parasitic nematode ionotropic receptors. Parasitology 113 S175-190.

Fleming, J.T., Squire, M.D., Barnes, T.M., Tornoe, C., Matsuda, K., Ahnn, J., Fire, A., Sulston, J.E., Barnard, E.A., Sattelle, D.B., Lewis, J.A., 1997. *Caenorhabditis elegans* levamisole resistance genes lev-1, unc-29 and unc-38 encode functional nicotinic acetylcholine receptor subunits. J Neurosci 17, 5843-5857.

Franks, C., Holden-Dye, L., Williams, R., Pang, F., Walker, R., 1994. A nematode FMRFamide-like peptide, SDPNFLRFamide (PF1), relaxes the dorsal muscle strip preparation of *Ascaris suum*. Parasitology 108, 229-236.

Froehner, S., Luetje, C., Scotland, P., Patrick, J., 1990. The postsynaptic 43K protein clusters muscle nicotinic acetylcholine receptors in *Xenopus* oocytes. Neuron 5(4), 403-410.

Fucile, S., 2004. Ca^{2+} permeability of nicotinic acetylcholine receptors. Cell Calcium 35, 1-8.

Gally, C., Eimer, S., Richmond, J.E., Bessereau, J.-L., 2004. A transmembrane protein required for acetylcholine receptor clustering in *Caenorhabditis elegans*. Nature 431, 578-582.

Galvez, A., Gimenez-Gallego, G., Reuben, J.P., Roy-Contancin, L., Feigenbaum, P., Kaczorowski, G.J., Garcia, M.L., 1990. Purification and characterization of a unique, potent, peptidyl probe for the high conductance calcium-activated potassium channel from venom of the scorpion *Buthus tamulus*. The Journal of Biological Chemistry 265, 11083-11090.

Galzi, J., Bertrand, D., Devillers-Thiery, A., Revah, F., Bertrand, S., Changeux, J., 1991. Functional signigicance of aromatic acids from three peptide loops of the alpha 7 neuronal nicotinic receptor site investigated by site-directed mutagenesis. FEBS Lett 294(3), 198-202.

Garcia-Calvo, M., Knaus, H., McManus, O., Giangiacomo, K., Kaczorowski, G., Garcia, M.L., 1994. Purification and reconstitution of the high-conductance,

calcium-activated potassium channel from tracheal smooth muscle. J Biol Chem 269, 676-682.

Gasser, R.B., Cottee, P., Nisbet, A.J., Ruttkowski, B., Ranganathan, S., Joachim, A., 2007. *Oesophagostomum dentatum* - Potential as a model for genomic studies of strongylid nematodes, with biotechnological prospects. Biotechnology Advances 25, 281-293.

Geary, T.G., Woo, K., McCarthy, J., Mackenzie, C., Horton, J., Prichard, R., De Silva, N.R., Olliaro, P., Lazdins-Helds, J., Engels, D.A., Bundy, D., 2009. Unresolved issues in anthelmintic pharmacology for helminthiasis of humans. International Journal for Parasitology 40, 1-13.

GeBner, G., Meder, S., Rink, T., Boheim, G., Harder, A., Jeschke, P., Scherkenbeck, J., Londershausen, M., 1996. Ionophore and Anthelmintic Activity of PF1022A, a Cyclooctadepsipeptide, are not related. Pestic Sci 48, 399-407.

Gelman, M., Chang, W., Thomas, D., Bergeron, J., Prives, J., 1995. Role of the endoplasmic reticulum chaperone calnexin in subunit folding and assembly of nicotinic acetylcholine receptors. J Biol Chem 270, 15085-15092.

Ghatta, S., Nimmagadda, D., Xu, X., O'Rourke, S.T., 2006. Large-conductance, calcium-activated potassium channels: Structural and functional implications. Pharmacology & Therapeutics 110, 103-116.

Ghiglietti, R., Rossi, P., Ramsan, M., Colombi, A., 1995. Viability of *Ascaris suum, Ascaris lumbricoides* and *Trichuris muris* eggs to alkaline pH and different temperatures. Parassitologia 37, 229-232.

Giraudat, J., Devillers-Thiery, A., Auffray, C., Rougeon, F., Changeux, J.-P., 1982. Identification of a cDNA clone coding for the acetylcholine binding subunit of *Torpedo marmorata* acetylcholine receptor. The EMBO Journal 1, 713-717.

Gomez-Hernandez, J.-M., Stuhmer, W., Parekh, A.B., 1997. Calcium dependence and distribution of calcium-activated chloride channels in *Xenopus* oocytes. Journal of Physiology 502.3, 569-574.

Gottschalk, A., Almedom, R., Schedletzky, T., Anderson, S., Yates III, J., Schafer, W.R., 2005. Identification and characterization of novel nicotinic receptor-associated proteins in *Caenorhabditis elegans*. EMBO J 24(14), 2566-2578.

Green, W., Claudio, T., 1993. Acetylcholine receptor assembly: subunit folding and oligomerization occur sequentially. Cell 74, 57-69.

Gruhn, N., Boesgaard, S., Eiberg, J., Bang, L., Thiis, J., Schroeder, T.V., Aldershvile, J., 2002. Effects of large conductance Ca^{2+}-activated K^{+} channels on nitroglyerin-mediated vasorelaxation in humans. European Journal of Pharmacology 446, 145-150.

Guest, M., Bull, K., Walker, R.J., Amliwala, K., O'Connor, V., Harder, A., Holden-Dye, L., Hopper, N.A., 2007. The calcium-activated potassium channel, SLO-1, is required for the action of the novel cyclo-octadepsipeptide anthelmintic, emodepside, in *Caenorhabditis elegans*. International Journal for Parasitology 37, 1577-1588.

Gundersen, C.B., Miledi, R., Parker, I., 1983. Serotonin receptors induced by exogenous messenger RNA in *Xenopus* oocytes. Proc. R. Soc. Lond. B. 219, 103-109.

Guo, J.-Z., Tredway, T., Chiappinelli, V., 1998. Glutamate and GABA release are enhanced by different subtypes of presynaptic nicotinic receptors in the lateral geniculate nucleus. J Neurosci 18, 1963-1969.

Gurdon, J.B., Lane, C.D., Woodland, H.R., Marbaix, G., 1971. Use of frog eggs and oocytes for the study of messenger RNA and its translation in living cells. Nature 233, 177-182.

Gurdon, J.B., 1973. The translation of messenger RNA injected in living oocytes of *Xenopus laevis*. Acta Endocrinol. Suppl. (Copenh) 180, 225-243.

Gurdon, J.B., Lingrel, J.B., Marbaix, G., 1973. Message stability in injected frog oocytes: long life of mammalian alpha and beta globin messages. J. Mol. Biol. 80, 539-551.

Gurdon, J.B., Woodland, H.R., Lingrel, J.B., 1974. The translation of mammalian globin mRNA injected into fertilized eggs of *Xenopus laevis* I. Message stability in development. Dev Biol 39, 125-133.

Gutierrez, Y., 2000. Diagnostic pathology of parasitic infections with clinical correlations. Oxford University Press.

Gutman, G.A., Chandy, K.G., Adelman, J.P., Aiyar, J., Bayliss, D.A., Clapham, D.E., Covarriubias, M., Desir, G.V., Furuichi, K., Ganetzky, B., Garcia, M.L., Grissmer, S., Jan, L.Y., Karschin, A., Kim, D., Kuperschmidt, S., Kurachi, Y., Lazdunski, M., Lesage, F., Lester, H.A., McKinnon, D., Nichols, C.G., O'Kelly, I., Robbins, J., Robertson, G.A., Rudy, B., Sanguinetti, M., Seino, S., Stuehmer, W., Tamkun, M.M., Vandenberg, C.A., Wei, A., Wulff, H., Wymore, R.S., 2003. International Union of Pharmacology. XLI. Compendium of voltage-gated ion channels: potassium channels. Pharmacol Rev 55(4), 583-586.

Gutman, G.A., Chandy, K.G., Grissmer, S., Lazdunski, M., McKinnon, D., Pardo, L.A., Robertson, G.A., Rudy, B., Sanguinetti, M.C., Stuhmer, W., Wang, X., 2005. International Union of Pharmacology. LIII. Nomenclature and molecular relationships of voltage-gated potassium channels. Pharmacol Rev 57, 473-508.

Ha, T., Heo, M., Park, C., 2004. Functional effects of auxiliary β4-subunit on rat large-conductance Ca^{2+}-activated K^{+} channel. Biophys J 86(5), 2871-2882.

Halevi, S., McKay, J., Palfreyman, M., Yassin, L., Margalit, E., Jorgensen, E., Treinin, M., 2002. The *C. elegans ric-3* gene is required for maturation of nicotinic acetylcholine receptors. EMBO J 21, 1012-1020.

Hanner, M., Vianna-Jorge, R., Kamassah, A., Schmalhofer, W., Knaus, H., Kaczorowski, G., Garcia, M.L., 1998. The β subunit of the high conductance calcium-activated potassium channel. Identification of residues involved in charybdotoxin binding. J Biol Chem 273(26), 16289-16296.

Harder, A., Schmitt-Wrede, H.-P., Krucken, J., Marinovski, P., Wunderlich, F., Willson, J., Amliwala, K., Holden-Dye, L., Walker, R., 2003. Cyclooctadepsipeptides-an anthelmintically active class of compounds

exhibiting a novel mode of action. International Journal of Antimicrobial Agents 22, 318-331.

Harder, A., Holden-Dye, L., Walker, R., Wunderlich, F., 2005. Mechanisms of action of emodepside. Parasitol Res 97, S1-S10.

Harrow, I., Gration, A., 1985a. Mode of action of the anthelmintics morantel, pyrantel and levamisole on muscle cell membrane of the nematode *Ascaris suum*. Pestic Sci 16, 662-672.

Harrow, I., Gration, K., 1985b. Mode of action of the anthelmintics morantel, pyrantel and levamisole on muscle cell membrane of the nematode *Ascaris suum*. Pesticide Science 16(6), 662-672.

Haugstetter, J., Blicher, T., Ellgaard, L., 2005. Identification and characterization of a novel thioredoxin-related transmembrane protein of the endoplasmic reticulum. The Journal of Biological Chemistry 280, 8371-8380.

Helwigh, A., Christensen, C., Roepstorff, A., Nansen, P., 1999. Concurrent *Ascaris suum* and *Oesophagostomum dentatum* infections in pigs. Vet Parasitol 82, 221-234.

Hobson, A., Stephenson, W., Beadle, L., 1952a. Studies on the physiology of *Ascaris lumbricoides* I. The relation of total osmotic pressure, conductivity and chloride content of the body fluid to that of the external environment. J Exp Biol 29, 1-21.

Holden-Dye, L., Walker, R., 1990. Avermectin and avermectin derivatives are antagonists at the gamma-aminobutyric acid (GABA) receptor on the somatic muscle cells *Ascaris*-is this the site of anthelmintic action? Parasitology 101, 265-271.

Holden-Dye, L., O'Connor, V., Hopper, N.A., Walker, R.J., Harder, A., Bull, K., Guest, M., 2007. SLO, SLO, quick, quick, slow: calcium-activated potassium channels as regulators of *Caenorhabditis elegans* behaviour and targets for anthelmintics. Invert Neurosci 7, 199-208.

Horrigan, F., Aldrich, R., 2002. Coupling between voltage sensor activation, Ca^{2+} binding and channel opening in large conductance (BK) potassium channels. J Gen Physiol 120(3), 267-305.

Hotez, P.J., Molyneux, D.H., Fenwick, A., Kumaresan, J., Sachs, S.E., Sachs, J.D., Savioli, L., 2007. Control of Neglected Tropical Diseases. The New England Journal of Medicine 357, 1018-1027.

Hotez, P.J., 2008. Forgotten people, forgotten diseases: the Neglected Tropical Diseases and their impact on global health and development. ASM Press, Washington Dc.

Hotez, P.J., Brindley, P.J., Bethony, J.M., King, C.H., Pearce, E.J., Jacobson, J., 2008. Helminth infections: the great neglected tropical diseases. The Journal of Clinical Investigation 118, 1311-1321.

Hotez, P.J., Kamath, A., 2009. Neglected Tropical Diseases in Sub-Saharan Africa: Review of their prevalence, distribution, and disease burden. PLoS Neglected Tropical Diseases 3, e412.

Hu, Y., Xiao, S., Aroian, R., 2009. The new anthelmintic tribendimidine is an L-type (levamisole and pyrantel) nicotinic acetylcholine receptor agonist. PLoS Neglected Tropical Diseases 3(8), e499.

Hudson, A., Nwaka, S., 2007. The concept paper on the helminth drug initiative. Onchocerciasis/lymphatic filariasis and schistosomiasis: opportunities and challenges for the discovery of new drugs/diagnostics. Expert Opinion on Drug Discovery 2, S3-7.

Hung, A., Tai, K., Sansom, M.S.P., 2005. Molecular Dynamics Simulation of the M2 Helices within the Nicotinic Acetylcholine Receptor Transmembrane Domain: Structure and Collective Motions. Biophysical Journal 88, 3321-3333.

James, C.E., Hudson, A.L., Davey, M.W., 2009. Drug resistance mechanisms in helminths: is it survival of the fittest? Trends in Parasitology 25, 328-335.

Jarman, M., 1959. Electrical activity in the muscle cells of *Ascaris lumbricoides*. Nature, London 184, 1244.

Johnson, C.D., Stretton, A.O., 1985. Localization of choline acetyltransferase within identified motoneurons of the nematode *Ascaris*. J Neurosci 5, 1984-1992.

Johnson, C.D., Stretton, A.O., 1987. GABA-immunoreactivity in inhibitory motor neurons of the nematode *Ascaris*. J Neurosci 7, 223-235.

Johnson, P., Dixon, R., Ross, A., 1998. An in-vitro test for assessing the viability of *Ascaris suum* eggs exposed to various sewage treatment processes. International Journal for Parasitology 28, 627-633.

Jones, A.K., Elgar, G., Sansom, M.S.P., 2003. The nicotinic acetylcholine receptor gene family of the pufferfish, *Fugu rubripes*. Genomics 82, 441-451.

Jones, A.K., Sattelle, D.B., 2004. Functional Genomics of the nicotinic acetylcholine receptor gene family of the nematode, *Caenorhabditis elegans*. Bioessays 26, 39-49.

Jones, A.K., Sattelle, D.B., 2010. Diversity of Insect Nicotinic Acetylcholine Receptor Subunits. In: Thany, S.H. (Ed.), Insect Nicotinic Acetylcholine Receptors, Landes Bioscience and Springer Science+Business Media, Austin, TX.

Jospin, M., Mariol, M., Segalat, L., Allard, B., 2002. Characterization of K+ currents using an *in situ* patch clamp technique in body wall muscle cells from *Caenorhabditis elegans*. J Physiol 544, 373-384.

Kaczorowski, G., Knaus, H., Leonard, R., McManus, O., Garcia, M.L., 1996. High-conductance calcium-activated potassium channels; structure, pharmacology, and function. J Bioenerg Biomembr 28(3), 255-267.

Kaminsky, R., Ducray, P., Jung, M., Clover, R., Rufener, L., Bouvier, J., Weber, S.S., Wenger, A., Wieland-Berghausen, S., Goebel, T., Gauvry, N., Pautrat, F., Skripsky, T., Froelich, O., Komoin-Oka, C., Westlund, B., Sluder, A., Maser, P., 2008. A new class of anthelmintics effective against drug-resistant nematodes. Nature 452, 176-180.

Kaplan, R.M., 2002. Anthelmintic resistance in nematodes of horses. Veterinary Research 33, 491-507.

Kaplan, R.M., 2004. Drug resistance in nematodes of veterinary importance: a status report. TRENDS in Parasitology 20, 477-481.

Karlin, A., 1980. Molecular properties of nicotinic acetylcholine receptors. . In: Cotman, C.W. (Ed.), The cell surface and neuronal function, North-Holland Pub Co., Amsterdam; New York, pp. 191-260.

Karlin, A., Cox, R., Kaldany, R.-R., Lobel, P., Holtzman, E., 1983. The arrangement and functions of the chains of the acetylcholine receptor of *Torpedo* electric tissue. *Cold spring Harb Symp Quant Biol* 48, 1-8.

Karlin, A., Akabas, M., 1995. Toward a structural basis for the function of nicotinic acetylcholine receptors and their cousins. Neuron 15(6), 1231-1244.

Karlin, A., 2002. Emerging structure of the Nicotinic Acetylcholine receptors. Nature Reviews Neuroscience 3, 102-114.

Kass, I.S., Wang, C.C., Walrond, J.P., Stretton, A.O.W., 1980. Avermectin B1a, a paralyzing anthelmintic that affects interneurons and inhibitory motorneurons in *Ascaris. Proc. Natl. Acad. Sci.* USA 77, 6211-6215.

Katz, E., Verbitsky, M., Rothlin, C., Vetter, D., Heinemann, S.F., Elgoyhen, A., 2000. High calcium permeability and calcium block of the α9 nicotinic acetylcholine receptor. Hear Res 141, 117-128.

Keller, S., Lindstrom, J., Yaylor, P., 1996. Involvement of the chaperone protein calnexin and the acetylcholine receptor β-subunit in the assembly and cell surface expression of the receptor. J Biol Chem 271, 22871-22877.

Keller, S., Taylor, P., 1998. Mechanisms regulating expression of nicotinic acetylcholine receptor subunits. Journal of Physiology-Paris 92(5), 446-447(442).

Keller, S., Taylor, P., 1999. Determinants responsible for assembly of the nicotinic acetylcholine receptor. J Gen Physiol 113, 171-176.

Kerboeuf, D., Blackhall, W., Kaminsky, R., von Samson-Himmelstjerna, G., 2003. P-glycoprotein in helminths: function and perspectives for anthelmintic treatment and reversal of resistance. Int J Antimicrob Agents 22(3), 332-346.

Khiroug, L., Sokolova, E., Giniatullin, R., Afzalov, R., Nistri, A., 1998. Recovery from desensitization of neuronal nicotinic acetylcholine receptors of rat chromaffin cells is modulated by intracellular calcium through distinct second messengers. Journal of Neuroscience 18(7), 2458-2466.

Khuroo, M., Zargar, S., Mahajan, R., 1990. Hepatobiliary and pancreatic ascariasis in India. Lancet 335, 1503-1506.

Kim, E., Day, T.A., Bennett, J.L., Pax, R.A., 1995. Cloning and functional expression of a Shaker-related voltage-gated potassium channel gene from Schistosoma mansoni (Trematoda: Digenea). Parasitology 110 (Pt 2), 171-180.

Kliks, M.M., 1990. Helminths as heirlooms and souvenirs: a review of new world paleoparasitology. Parasitology Today 6, 93-100.

Knaus, H., Eberhart, A., Kaczorowski, G., Garcia, M.L., 1994a. Covalent attachment of charybdotoxin to the β-subunit of the high conductance Ca^{2+}-activated K^{+} channel. Identification of the site of incorporation and implications for channel topology. J Biol Chem 269(37), 23336-23341.

Knaus, H., Folander, K., Garcia-Calvo, M., Garcia, M.L., Kaczorowski, G., Smith, M., Swanson, R., 1994b. Primary sequence and immunological characterization

of β-subunit of high conductance Ca^{2+}-activated K^{+} channel from smooth muscle. J Biol Chem 269(25), 17274-17278.

Knaus, H., Garcia-Calvo, M., Kaczorowski, G.J., Garcia, M.L., 1994c. Subunit composition of the high conductance calcium-activated potassium channel from smooth muscle, a representative of the mSlo and slowpoke family of potassium channels. J Biol Chem 269, 3921-3924.

Köhler, P., 2001. The biochemical basis of anthelmintic action and resistance. International Journal for Parasitology 31, 336-345.

Kopp, S., Kotze, A., McCarthy, J., Coleman, G., 2007. High-level pyrantel resistance in the hookworm *Ancylostoma caninum*. Vet Parasitol 143(3-4), 299-304.

Krafte, D., Volberg, W., 1992. Properties of endogenous voltage-dependent sodium currents in *Xenopus laevis* oocytes. Journal of Neuroscience Methods 43, 189-193.

Kreienkamp, H.-J., Maeda, R., Sine, S., Taylor, P., 1995. Intersubunit contacts governing assembly of the mammalian nicotinic acetylcholine receptor. Neuron 14, 635-644.

Kwa, M., Veenstra, J., Roos, M., 1994. Benzimidazole resistance in *Haemonchus contortus* is correlated with a conserved mutation at amino acid 200 in β-tubulin isotype 1. Mol Biochem Parasitol 63(2), 299-303.

Lafaire, A., Schwarz, W., 1986. Voltage dependence of the rheogenic Na+/K+ ATPase in the membrane of oocytes of *Xenopus laevis*. Journal of Membrane Biology 91, 43-51.

Lansdell, S.J., Gee, V.J., Harkness, P.C., Doward, A.I., Baker, E.R., Gibb, A.J., Millar, N.S., 2005. RIC-3 enhances functional expressioin of multiple nicotinic acetylcholine receptor subtypes in mammalian cells. Mol Pharmacol 68, 1431-1438.

Laskey, R.A., Gurdon, J.B., Crawford, L.V., 1972. Translation of encephalomyocarditis viral RNA in oocytes of *Xenopus laevis*. Proc. Natl. Acad. Sci. USA. 69, 3665-3669.

Laskey, R.A., Gurdon, J.B., 1973. Induction of polyoma DNA synthesis by injection into frog-egg cytoplasm. Eur J Biochem 37, 467-471.

Laskey, R.A., Gurdon, J.B., 1974. The translation of viral RNAs in frog oocytes. Hamatol Bluttransfus 14, 272-274.

Le Jambre, L., Gill, J., Lenane, I., Baker, P., 2000. Inheritance of avermectin resistance in *Haemonchus contortus*. Int J Parasitol 30(1), 105-111.

Le Novere, N., Grutter, T., Changuex, J., 2002. Models of the extracellular domain of the nicotinic receptors and of agonist- and Ca^{2+}-binding sites. PNAS 99(5), 3210-3215.

Leake, J., 2004. Myco-heterotroph/epiparasitic plant interactions with ectomycorrhizal and arbuscular mycorrhizal fungi. Curr Opin Plant Biol 7(4), 422-428.

Levandoski, M., Robertson, A.P., Kuiper, S., Qian, H., Martin, R.J., 2005. Single-channel properties of N- and L-subtypes of acetylcholine receptor in *Ascaris suum*. International Journal for Parasitology 35, 925-934.

Lewis, J.A., Wu, C.-H., Berg, H., Levine, J.H., 1980. The genetics of levamisole resistance in the nematode *Caenorhabditis elegans*. Neuroscience 5, 967-989.

Lewis, J.A., Elmer, J.S., Skimming, J., McLafferty, S., Fleming, J., McGee, T., 1987. Cholinergic receptor mutants of the nematode *Caenorhabditis elegans*. J Neurosci 7, 3059-3071.

Li, R., Gao, J., Wang, S., Pei, Y., Shen, J., Yan, P., Yin, G., 2011. Effect of oral administration of tribendimidine at different dosages against *Trichinella spiralis* encapsulated larvae in mice. Zhongguo Ji Sheng Chong Xue Yu Ji Sheng Chong Bing Za Zhi 29(2), 117-121.

Li, X., Rainnie, D., McCarley, R., Greene, R., 1998. Presynaptic nicotinic receptors facilitate monoaminergic transmission. J Neurosci 18, 1904-1912.

Liang, Y., Coles, G.C., Doenhoff, M., 2000. Detection of praziquantel resistance in schistosomes. Trop. Med. Int. Health 5, 72.

Lim, H.H., Park, B.J., Choi, H.S., Park, C.S., Eom, S.H., Ahnn, J., 1999. Identification and characterization of a putative *C. elegans* potassium channel gene (*Ce-slo-2*) distantly related to Ca^{2+}-activated K^{+} channels. Gene 240, 35-43.

Ling, S., Woronuk, G., Sy, L., Lev, S., Braun, A., 2000. Enhanced activity of a large conductance, calcium-sensitive K+ channel in the presence of Src tyrosine kinase. J Biol Chem 275(39), 30683-30689.

Lionel, N., Mirando, E., Nanayakkara, J., Soysa, P., 1969. Levamisole in the treatment of Ascariasis in children. British Medical J 4, 340-341.

Lu, L., Montrose-Rafizadeh, C., Hwang, T.-C., Guggino, W., 1990. A delayed rectifier potassium current in *Xenopus* oocytes. Biophysical Journal 57, 1117-1123.

Ludwig, A., Burckhardt, G., Burckhardt, B., 1999. NH^{4+} conductance in *Xenopus laevis* oocytes. European Journal of Physiology 437, 484-490.

Luetje, C., Patrick, J., 1991. Both α- and β-subunits contribute to the agonist sensitivity of neuronal nicotinic acetylcholine receptors. J Neurosci 11(3), 837-845.

Ma, Z., Lou, X., Horrigan, F., 2006. Role of charged residues in the S1-S4 voltage sensor of BK channels. J Gen Physiol 127(3), 309-328.

Magleby, K., 2003. Gating mechanism of BK (Slo1) channels: So near, yet so far. J Gen Physiol 121, 81-96.

Martin, R.E., Donahue, M.J., 1987. Correlation of myosin light chain phosphorylation and gamma aminobutyric acid receptors in *Ascaris suum* muscle. Comp Biochem Physiol C 87, 23-29.

Martin, R.J., 1982. Electrophysiological effects of piperazine and diethylcarbamazine on *Ascaris suum* somatic muscle. British Journal of Pharmacology 77, 255-265.

Martin, R.J., Kusel, J.R., Pennington, A.J., 1990. Surface properties of membrane vesicles prepared from muscle cells of Ascaris suum. J Parasitol 76, 340-348.

Martin, R.J., Pennington, A.J., Duittoz, A.H., Robertson, S., Kusel, J.R., 1991. The physiology and pharmacology of neuromuscular transmission in the nematode parasite, *Ascaris suum*. Parasitology 102, S41-58.

Martin, R.J., P, T., Gration, K.A.F., Harrow, I.D., 1992. Voltage-activated currents in somatic muscle of the nematode parasite *Ascaris suum*. J Exp Biol 173, 75-90.

Martin, R.J., Harder, A., Londershausen, M., Jeschke, P., 1996a. Anthelmintic Actions of the Cyclic Depsipeptide PF1022A and its Electrophysiological Effects on Muscle Cells of *Ascaris suum*. Pestic Sci 48, 343-349.

Martin, R.J., Valkanov, M., Dale, M., Robertson, A.P., Murray, I., 1996b. Electrophysiology of *Ascaris* muscle and anti-nematodal drug action. Parasitology 113, S137-156.

Martin, R.J., 1997. Modes of action of anthelmintic drugs. Veterinary Journal 154, 11-34.

Martin, R.J., Robertson, A.P., Bjorn, H., Sangster, N.C., 1997. Heterogeneous levamisole receptors: a single-channel study of nicotinic acetylcholine receptors from *Oesophagostomum dentatum*. European Journal of Pharmacology 322, 249-257.

Martin, R.J., Bai, G., Clark, C.L., Robertson, A.P., 2003. Methyridine (2-[2-methoxyethyl]-pyridine]) and levamisole activate different ACh receptor subtypes in nematode parasites: a new lead for levamisole-resistance. Br J Pharmacol 140, 1068-1076.

Martin, R.J., Clark, C.L., Trailovic, S.M., Robertson, A.P., 2004. Oxantel is an N-type (methyridine and nicotine) agonist not an L-type (levamisole and pyrantel) agonist: classification of cholinergic anthelmintics in *Ascaris*. International Journal for Parasitology 34, 1083-1090.

Martin, R.J., Verma, S., Levandoski, M., Clark, C.L., Qian, H., Stewart, M., Robertson, A.P., 2005. Drug resistance and neurotransmitter receptors of nematodes: recent studies on the mode of action of levamisole. Parasitology 131, S71-84.

Martin, R.J., Robertson, A.P., 2007. Mode of action of Levamisole and pyrantel, anthelmintic resistance, E153 and Q57. Parasitology 134, 1093-1104.

Maryon, E., Coronado, R., Anderson, P., 1996. *unc-68* encodes a ryanodine receptor involved in regulating *C. elegans* body-wall muscle contraction. Cell Biology J 134(4), 885-893.

Mathie, A., Cull-Candy, S.G., Colquhoun, D., 1991. Conductance and kinetic properties of single nicotinic acetylcholine receptor channels in rat sympathetic neurones. Journal of Physiology 439, 717-750.

McGarry, H.F., Plant, L. D. & Taylor, M. J., 2005. Diethylcarbamazine activity against *Brugia malayi* microfilariae is dependent on inducible nitric-oxide synthase and the cyclooxygenase pathway. Filaria Journal 4.

McLeod, R., 1994. Costs of major parasites to the Australian livestock industries. International Journal for Parasitology 25(11), 1363-1367.

McManus, O., Helms, L., Pallanck, L., Ganetzky, B., Swanson, R., Leonard, R., 1995. Functional role of the β subunit of high conductance calcium-activated potassium channels. Neuron 14(3), 645-650.

Meera, P., Wallner, M., Toro, L., 2000a. A neuronal β subunit (KCNMB4) makes the large conductance, voltage- and Ca^{2+}-activated K^+ channel resistant to charybdotoxin and iberiotoxin. Proc Natl Acad Sci. USA 97(10), 5562-5567.

Meera, P., Wallner, M., Toro, L., 2000b. A neuronal β subunit (KCNMB4) makes the large conductance, voltage- & Ca^{2+}-activated K^+ channel resistant to charybdotoxin and iberiotoxin. Proc Natl Acad Sci USA 97, 5562-5567.

Miledi, R., Parker, I., Sumikawa, K., 1982a. Properties of acetylcholine receptors translated by cat muscle mRNA in *Xenopus* oocytes. EMBO J 1, 1307-1312.

Miledi, R., Parker, I., Sumikawa, K., 1982b. Synthesis of chick brain GABA receptors by frog oocytes. Proc. R. Soc. Lond. B. Biol. Sci. 216, 509-515.

Miledi, R., Parker, I., Sumikawa, K., 1983. Recording of single gamma-amino-butyrate- and acetylcholine-activated receptor channels translated by exogenous mRNA in *Xenopus* oocytes. Proc. R. Soc. Lond. B. 218, 481-484.

Miledi, R., Woodland, H.R., 1989a. Effects of defolliculation on membrane current responses of *Xenopus* oocytes. Journal of Physiology 416, 601-621.

Miledi, R., Woodland, H.R., 1989b. Membrane currents elicited by prostaglandins, atrial natriuretic factor and oxytocin in follicle-enclosed *Xenopus* oocytes. Journal of Physiology 416, 623-643.

Millar, N.S., 2003. Assembly and subunit diversity of nicotinic acetylcholine receptors. Biochemical Society Transactions 31(4), 869-874.

Millar, N.S., 2008. RIC-3: a nicotinic acetylcholine receptor chaperone. British Journal of Pharmacology 153, S177-S183.

Miro, G., Mateo, M., Montoya, A., Vela, E., Calonge, R., 2006. Survey of intestinal parasites in stay dogs in the Madrid area and comparison of the efficacy of three anthelmintics in naturally infected dogs. Parasitol Res 100, 317-320.

Mistry, D.K., Garland, C.J., 1998. Nitric Oxide (NO)-induced activation of large conductance Ca^{2+}-dependent K^+ channels (BK_{Ca}) in smooth muscle cells isolated from the rat mesenteric artery. British Journal of Pharmacology 124, 1131-1140.

Miyazawa, A., Fujiyoshi, Y., Stowell, M., Unwin, N., 1999. Nicotinic acetylcholine receptor at 4.6 Å resolution: transverse tunnels in the channel wall. J. Mol Biol 288(4), 765-786.

Muhlfeld, S., Schmitt-Wrede, H.-P., Harder, A., Wunderlich, F., 2009. FMRFamide-like neuropeptides as putative ligands of the latrophilin-like HC110-R from *Haemonchus contortus*. Molecular & Biochemical Parasitology 164, 162-164.

Mulle, C., Choquet, D., Korn, H., Changeux, J., 1992a. Calcium influx through nicotinic receptor in rat central neurons: its relevance to cellular regulation. Neuron 8, 135-143.

Mulle, C., Lena, C., Changeux, J.P., 1992b. Potentiation of nicotinic receptor response by external calcium in rat central neurons. Neuron 8, 937-945.

Neveu, C., Charvet, C.L., Fauvin, A., Cortet, J., Beech, R.N., Cabaret, J., 2010. Genetic diversity of levamisole receptor subunits in parasitic nematode

species and abbreviated transcripts associated with resistance. Pharmacogenetics and Genomics 20, 414-425.
Noda, M., Takahashi, H., Tanabe, T., Toyosato, M., Furutani, Y., Hirose, T., Asai, M., Inayama, S., Miyata, T., Numa, S., 1982. Primary structure of alpha-subunit precursor of *Torpedo californica* acetylcholine receptor deduced from cDNA sequence. Nature 299 (5886), 793-797.
Noda, M., Takahashi, H., Tanabe, T., Toyosato, M., Kikyotani, S., Hirose, T., Asai, M., Takashima, H., Inayama, S., Miyata, T., Numa, S., 1983. Primary structures of beta- and delta-subunit precursors of *Torpedo californica* acetylcholine receptor deduced from cDNA sequences. Nature 301(5897), 251-255.
Papazian, D., Timpe, L., Jan, Y., Jan, L., 1991. Alteration of voltage-dependence of *Shaker* potassium channel by mutations in the S4 sequence. Nature 349, 305-310.
Papazian, D., Shao, X., Seoh, S., Mock, A., Huang, Y., Wainstock, D., 1995. Electrostatic interactions of S4 voltage sensor in Shaker K+ channel. Neuron 14(6), 1293-1301.
Papke, R.L., Heinemann, S.F., 1991. The role of the beta4-subunit in determining the kinetic properties of rat neuronal nicotinic acetylcholine alpha3-receptors. Journal of Physiology 440, 95-112.
Parker, I., Ivorra, I., 1990. A slowly inactivating potassium current in native oocytes of Xenopus laevis. Proceedings of the Royal Society of London 238, 369-381.
Paterson, D., Nordberg, A., 2000. Neuronal nicotinic receptors in the human brain. Progress in Neurobiology 61, 75-111.
Paulson, H., Ross, A., Green, W., Claudio, T., 1991. Analysis of early events in acetylcholine receptor assembly. J Cell Biol 113, 1371-1384.
Pemberton, D., Franks, C., Walker, R., Holden-Dye, L., 2001. Characterization of Glutamate-Gated Chloride Channels in the Pharynx of Wild-Type and Mutant Caenorhabditis elegans Delineates the Role of the Subunit GluCl-alpha2 in the Function of the Native Receptor. Molecular Pharmacology 59, 1037-1043.
Phillips, W., Kopta, C., Blount, P., Gardner, P., Steinbach, J., Merlie, J., 1991. ACh receptor-rich membrane domains organized in fibroblasts by recombinant 43-kilodalton protein. Science 251(4993), 568-570.
Pike, A.W., Biddle, M., 1966. Parasite eggs in medieval Winchester. Antiquity 40, 293-296.
Pit, D., Rijcken, F., Raspoort, E., Baeta, S., Polderman, A., 1999. Geographic distribution and epidemiology of *Oesophagostomum bifurcum* and hookworm infections in humans in Togo. Am J Trop Med Hyg 61, 951-955.
Prichard, R., Hall, C., Kelly, J., Martin, I., Donald, A., 1980. The problem of anthelmintic resistance in nematodes. Aust Vet J 56(5), 239-251.
Prichard, R., 1994. Anthelmintic resistance. Veterinary Parasitology 54, 259-268.
Prichard, R., 2001. Genetic variability following selection of *Haemonchus contortus* with anthelmintics. Trends Parasitol 17, 445-453.

Prichard, R.K., 1990. Anthelmintic resistance in nematodes: Extent, recent understanding and future directions for control and research. International Journal for Parasitology 20, 515-523.

Prichard, R.K., 1999. Drug resistance. International Journal for Parasitology 29, 137-138.

Puttachary, S., Robertson, A.P., Clark, C.L., Martin, R.J., 2010. Levamisole and ryanodine receptors (II): An electrophysiological study in *Ascaris suum*. Molecular & Biochemical Parasitology 171, 8-16.

Qian, H., Martin, R.J., Robertson, A.P., 2006. Pharmacology of *N*-, *L*-, and *B*-subtypes of nematode nAChR resolved at the single-channel level in *Ascaris suum*. The FASEB Journal 20, E2108-E2116.

Qian, H., Robertson, A.P., Powell-Coffman, J., Martin, R.J., 2008. Levamisole resistance resolved at the single-channel level in *Caenorhabditis elegans*. FASEB J 22, 3247-3254.

Rapti, G., Richmond, J., Bessereau, J.-L., 2011. A single immunoglobulin-domain protein required for clustering acetylcholine receptors in *C. elegans*. EMBO J 30, 706-718.

Raymond, V., Mongan, N., Sattelle, D.B., 2000. Anthelmintic actions on homomer-forming nicotinic acetylcholine receptor subunits: chicken α7 and ACR-16 from the nematode *Caenorhabditis elegans*. Neuroscience 101(3), 785-791.

Reynoldson, J., Behnke, J., Pallant, L., Macnish, M., Gilbert, F., Giles, S., Spargo, R., Thompson, R., 1997. Failure of pyrantel in treatment of human hookworm infections (*Ancylostoma duodenale*) in the Kimberley region of north west Australia. Acta Trop. 68, 301-312.

Richmond, J.E., Jorgensen, E.M., 1999. One GABA and two acetylcholine receptors function at the *C. elegans* neuromuscular junction. Nature Neuroscience 2, 791-797.

Robertson, A.P., Bjorn, H.E., Martin, R.J., 1999. Resistance to levamisole resolved at the single-channel level. The FASEB Journal 13, 749-760.

Robertson, A.P., Bjorn, H.E., Martin, R.J., 2000. Pyrantel resistance alters nematode nicotinic acetylcholine receptor single-channel properties. European Journal of Pharmacology 394, 1-8.

Robertson, A.P., Clark, C.L., Burns, T.A., Thompson, D.P., Geary, T.G., Trailovic, S.M., Martin, R.J., 2002. Paraherquamide and 2-Deoxy-paraherquamide Distinguish Cholinergic Receptor Subtypes in *Ascaris suum*. The Journal of Pharmacology & Experimental Therapeutics 302, 853-860.

Robertson, A.P., Clark, C.L., Martin, R.J., 2010. Levamisole and ryanodine receptors I: A contraction study in *Ascaris suum*. Mol Biochem Parasitol 171(1), 1-7.

Robertson, A.P., Puttachary, S., Martin, R.J., 2011. Single-channel recording from adult *Brugia malayi*. Invert Neurosci 11(1), 53-57.

Robertson, S.J., Martin, R.J., 1993a. Levamisole-activated single-channel currents from muscle of the nematode parasite *Ascaris suum*. Br J Pharmacol 108, 170-178.

Robertson, S.J., Martin, R.J., 1993b. Levamisole-activated single-channel currents from muscle of the nematode parasite *Ascaris suum*. Br J Pharmacol 108, 170-178.

Robertson, S.J., Pennington, A.J., Evans, A.M., Martin, R.J., 1994. The action of pyrantel as an agonist and an open channel blocker at acetylcholine receptors in isolated Ascaris suum muscle vesicles. Eur J Pharmacol 271, 273-282.

Roepstorff, A., Nansen, P., 1994. Epidemiology and control of helminth infections in pigs under intensive and non-intensive production systems. Vet Parasitol 54, 69-85.

Rosenbluth, J., 1965a. Ultrastructural organization of obliquely striated muscle fibers in *Ascaris lumbricoides*. J Cell Biol 25, 495-515.

Rosenbluth, J., 1965b. Ultrastructure of somatic muscle cells in *Ascaris lumbricoides*. II. Intermuscular junctions, neuromuscular junctions, and glycogen stores. J Cell Biol 26, 579-591.

Rosenbluth, J., 1967. Obliquely striated muscle. 3. Contraction mechanism of *Ascaris* body muscle. J Cell Biol 34, 15-33.

Rosenbluth, J., 1969. Ultrastructure of dyads in muscle fibers of *Ascaris lumbricoides*. J Cell Biol 42, 817-825.

Saeger, B., Schmitt-Wrede, H.-P., Dehnhardt, M., Benten, W.P.M., Krucken, J., Harder, A., Samson-Himmelstjerna von, G., Wiegand, H., Wunderlich, F., 2001. Latrophilin-like receptor from the parasitic nematode *Haemonchus contortus* as target for the anthelmintic depsipeptide PF1022A. FASEB J 15, 1332-1334.

Salkoff, L., Butler, A., Ferreira, G., Santi, C., Wei, A., 2006. High-conductance potassium channels of the SLO family. Nature Reviews Neuroscience 5, 921-931.

Samson-Himmelstjerna von, G., Harder, A., Sangster, N.C., Coles, G.C., 2005. Efficacy of two cyclooctadepsipeptides, PF1022A and emodepside, against anthelmintic-resistant nematodes in sheep and cattle. Parasitology 130, 343-347.

Sangster, N.C., Bannan, S., Weiss, A., Nulf, S., Klein, R.D., Geary, T.G., 1999. *Haemonchus contortus*: Sequence heterogeneity of internucleotide binding domains from P-glycoproteins and an association with avermectin/milbemycin resistance. Exp Parasitol 91(3), 250-257.

Sangster, N.C., Gill, J., 1999. Pharmacology of anthelmintic resistance. Parasitology Today 15, 141-146.

Sangster, N.C., 2001. Managing parasiticide resistance. Veterinary Parasitology 98, 89-109.

Sasaki, T., Takagi, M., Yaguchi, T., Miyadoh, S., Okada, T., Koyama, M., 1992. A new anthelmintic cyclodepsipeptide, PF1022A. J Antibiot 45, 692-697.

Savioli, L., Albonico, M., 2004. Global distribution and control status of soil-transmitted helminthiasis. Nature Reviews Microbiology 2, 618-619.

Saz, H., Weil, A., 1962. A pathway of formation of α-methyl valerate by *Ascaris lumbricoides*. J Biol Chem 237, 2053-2056.

Schneider, A., 1866. Monographie der Nematoden. Berlin.
Schreiber, M., Salkoff, L., 1997. A novel calcium-sensing domain in the BK channel. Biophys. J 73, 1355-1363.
Schubert, R., Nelson, M., 2001. Protein kinases: tuners of the BK_{Ca} channel in smooth muscle. Trends Pharmacol Sci 22(10), 505-512.
Schuetze, S., Role, L., 1987. Developmental regulation of nicotinic acetylcholine receptors. Ann Rev Neurosci 10, 403-457.
Schultz, J., Milpetz, F., Bork, P., Ponting, C., 1998. SMART, a simple modular architecture research tool: identification of signaling domains. Proc Natl Acad Sci USA 95, 5857-5864.
Schurmann, S., Harder, A., Schnieder, T., Samson-Himmelstjerna von, G., 2007. Effects of Emodepside on Egg Hatching, Larval Development and Larval Motility in Parasitic Nematodes. Parasitol Res 101, S45-S56.
Seidu, R., Heistad, A., Amoah, P., Drechsel, P., Jenssen, P., Stenström, T., 2008. Quantification of the health risk associated with wastewater reuse in Accra, Ghana: a contribution toward local guidelines. J Water Health 6(4), 461-471.
Seo, S., Henry, J., Lewis, A., Wang, N., Levandoski, M.M., 2009. The positive allosteric modulator morantel binds at noncanonical subunit interfaces of neuronal nicotinic acetylcholine receptors. J Neurosci 29(27), 8734-8742.
Seoh, S., Sigg, D., Papazian, D., Bezanilla, F., 1996. Voltage-sensing residues in the S2 and S4 segments of the shaker K+ channel. Neuron 16(6), 1159-1167.
Sigel, E., 1990. Use of *Xenopus* oocytes for the functional expression of plasma membrane proteins. Journal of Membrane Biology 117, 201-221.
Silvestre, A., Cabaret, J., 2002. Mutation in position 167 of isotype 1 β-tubulin gene of Trichostrongylid nematodes: role in benzimidazole resistance? Mol Biochem Parasitol 120, 297-300.
Simon, D., Madison, J., Conery, A., Thompson-Peer, K., Soskis, M., Ruvkun, G., Kaplan, J.M., Kim, J., 2008. The microRNA miR-1 regulates a MEF-2-dependent retrograde signal at neuromuscular junctions. Cell 133, 903-915.
Sine, S., Claudio, T., 1991. Gamma- and delta-subunits regulate the affinity and the cooperativity of ligand binding to the acetylcholine receptor. J Biol Chem 266, 19369-19377.
Sithigorngul, P., Cowden, C., Guastella, J., Stretton, A.O.W., 1989. Generation of monoclonal antibodies against a nematode peptide extract: another approach for identifying unknown neuropeptides. J Comp Neurol 284, 389-397.
Sones, W., Leblanc, N., Greenwood, I., 2009. Inhibition of vascular calcium-gated chloride currents by blockers of $Kca_{1.1}$, but not modulators of $Kca_{2.1}$ or $Kca_{2.3}$ channels. British Journal of Pharmacology 158.
Squire, M.D., Tornoe, C., Baylis, H.A., Fleming, J.T., Barnard, E.A., Sattelle, D.B., 1995. Molecular cloning and functional co-expression of a *Caenorhabditis elegans* nicotinic acetylcholine receptor subunit (acr-2). Receptors Channels 3(2), 107-115.
Sripa, B., Hong, S., 2011. Tribendimidine: an alternative anthelmintic for liver flukes? Lancet Infect Dis 11(2), 77-78.

Stefani, E., Ottolia, M., Noceti, F., Olcese, R., Wallner, M., Latorre, R., Toro, L., 1997. Voltage-controlled gating in a large conductance Ca^{2+}-sensitive K^{+} channel (hSlo). Proc Natl Acad Sci U S A 94(10), 5427-5431.

Steinbach, J., Ifune, C., 1989. How many kinds of nicotinic acetylcholine receptor are there? Trends Neurosci 12(1), 3-6.

Stephenson, L., Crompton, D., Latham, M., Schulpen, T., Nesheim, M., Jansen, A., 1980. Relationships between Ascaris infection and growth of malnourished preschool children in Kenya. Am J Clin Nutr 33, 1165-1172.

Stephenson, L., Latham, M., Kurz, K., Kinoti, S., Brigham, H., 1989. Treatment with a single dose of albendazole improves growth of Kenyan schoolchildren with hookworm, *Trichuris trichiura,* and *Ascaris lumbricoides* infections. Am J Trop Med Hyg 41, 78-87.

Stephenson, L., Latham, M., Adams, E., Kinoti, S., Pertet, A., 1993a. Physical fitness, growth and appetite of Kenyan school boys with hookworm, *Trichuris trichiura* and *Ascaris lumbricoides* infections are improved four months after a single dose of albendazole. J Nutr 123, 1036-1046.

Stephenson, L., Latham, M., Adams, E., Kinoti, S., Pertet, A., 1993b. Weight gain of Kenyan school children infected with hookworm, *Trichuris trichiura* and *Ascaris lumbricoides* is improved following once- or twice-yearly treatment with albendazole. J Nutr 123, 656-665.

Steward, T., Gasbarre, L., 1989. The veterinary importance of nodular worms (*Olesophagostomum spp*). Parasitol Today 5, 209-213.

Storey, P., Faile, G., Hewitt, E., Yelifari, L., Polderman, A., Magnussen, P., 2000. Clinical epidemiology and classification of human oesophagostomiasis. Trans R Soc Trop Med Hyg 94, 177-182.

Storey, P., Steenhard, N., van Lieshout, L., Anemana, S., Magnussen, P., Polderman, A., 2001. Natural progression of *Oesophagostomum bifurcum* pathology and infection in a rural community of northern Ghana. Trans R Soc Trop Med Hyg 95, 295-299.

Stretton, A.O., Fishpool, R.M., Southgate, E., Donmoyer, J.E., Walrond, J.P., Moses, J.E., Kass, I.S., 1978. Structure and physiological activity of the motoneurons of the nematode Ascaris. Proc Natl Acad Sci U S A 75, 3493-3497.

Stretton, A.O.W., 1976. Anatomy and development of the somatic musculature of the nematode *Ascaris*. J Exp Biol 64, 773-788.

Stretton, A.O.W., Davis, R.E., Angstadt, J.D., Donmoyer, J.E., Johnson, C.D., 1985. Neural control of behavior in *Ascaris*. Trends in Neurosciences 8, 294-300.

Stuhmer, W., Parekh, A.B., 1995. Electrophysiological recordings from *Xenopus* oocytes. In *Single-Channel Recording*, 2nd edition. Neher E & Sakmann B. Plenum Press, New York pp. 341-356.

Sumikawa, K., Houghton, M., Smith, J., Bell, L., Richards, B., Barnard, E., 1982. The molecular cloning and characterisation of cDNA coding for the alpha subunit of the acetylcholine receptor. Nucleic Acids Res. 10, 5809-5822.

Sumikawa, K., 1992. Sequences on the N-terminus of ACh receptor subunits regulate their assembly. Brain Res Mol Brain Res 13(4), 349-353.

Taren, D., Nesheim, M., Crompton, D., Holland, C., Barbeau, I., Rivera, G., Sanjur, D., Tiffany, J., Tucker, K., 1987. Contributions of ascariasis to poor nutritional status in children from Chiriqui Province, Republic of Panama. Parasitology 95, 603-613.

Tay, S., Twum, W., Abruquah, H., 2010. Epidemiological survey of soil-transmitted helminths in occupational risk groups and non school going children in the Kintampo North District of Ghana. Journal of the Ghana Science Association 12(2).

Terada, M., 1992. Neuropharmacological mechanism of action of PF1022A, an antinematode anthelmintic with a new structure of cyclic depsipeptide, on *Angiostrongylus cantonensis* and isolated frog rectus. Jpn J Parasitol 41, 108-107.

Thorn, P., Martin, R., 1987. A high-conductance calcium-dependent chloride channel in *Ascaris suum* muscle. Q J Exp Physiol 72, 31-49.

Tian, L., Coghill, L., MacDonald, S., Armstrong, D., Shipston, M., 2003. Leucine zipper domain targets cAMP-dependent protein kinase to mammalian BK channels. J Biol Chem 278(10), 8669-8677.

Tokimasa, T., North, R., 1984. Calcium entry through acetylcholine-channels can activate potassium conductance in bullfrog sympathetic neurons. Brain Res 295, 364-367.

Touroutine, D., Fox, R.M., Von Stetina, S.E., Burdina, A., Miller III, D.M., Richmond, J.E., 2005. ACR-16 encodes an essential subunit of the levamisole-resistant nicotinic receptor at the *C. elegans* neuromuscular junction. J Biol Chem 280(29), 27013-27021.

Towers, P.R., Edwards, B., Richmond, J.E., Sattelle, D.B., 2005. The *Caenorhabditis elegans* lev-8 gene encodes a novel type of nicotinic acetylcholine receptor alpha subunit. J Neurochem 93, 1-9.

Trailovic, S.M., Verma, S., Clark, C.L., Robertson, A.P., Martin, R.J., 2007. Effects of the muscarinic agonist, 5-methylfurmethiodide, on contraction and electrophysiology of Ascaris suum muscle. Int J Parasitol.

Treinin, M., Chalfie, M., 1995. A mutated acetylcholine receptor subunit causes neuronal degeneration in *C. elegans*. Neuron 14, 871-877.

Treinin, M., Gillo, B., Liebman, L., Chalfie, M., 1998. Two functionally dependent acetylcholine subunits are encoded in a single *Caenorhabditis elegans* operon. Proc. Natl. Acad. Sci. USA. 95, 15492-15495.

Treinin, M., 2008. RIC-3 and nicotinic acetylcholine receptors: biogenesis, properties, and diversity. Biotechnol J 3(12), 1539-1547.

Tritten, L., Nwosu, U., Vargas, M., Keiser, J., 2012. *In vitro* and *in vivo* efficacy of tribendimidine and its metabolites alone and in combination against the hookworms *Heligmosomoides bakeri* and *Ancylostoma ceylanicum*. Acta Trop 122(1), 101-107.

Tsang, V., Saz, H., 1973. Demonstration and function of 2-methyl-butyrate racemase in *Ascaris lumbricoides*. J Comp Bioch & Physiol 45B, 617-623.

Unwin, N., 1993. Neurotransmitter action: opening of ligand-gated ion channels. Cell 72, S31-41.

Unwin, N., 1995. Acetylcholine receptor channel imaged in the open state. Nature 373, 37-43.

Unwin, N., 2005. Refined structure of the nicotinic acetylcholine receptor at 4 Å resolution. J. Mol Biol 346, 967-989.

Varady, M., Bjorn, H., Craven, J., Nansen, P., 1997. *In vitro* characterization of lines of *Oesophagostomum dentatum* selected or not selected for resistance to pyrantel, levamisole and ivermectin. International Journal for Parasitology 27, 77-81.

Verma, S., Robertson, A.P., Martin, R.J., 2007. The nematode neuropeptide, AF2 (KHEYLRF-NH_2), increases voltage-activated calcium currents in *Ascaris suum* muscle. British Journal of Pharmacology 151, 888-899.

Verma, S., Robertson, A.P., Martin, R.J., 2009. Effects of SDPNFLRF-amide (PF1) on voltage-activated currents in *Ascaris suum* muscle. International Journal for Parasitology 39, 315-326.

Vernino, S., Amador, M., Luetje, C.W., Patrick, J., Dani, J.A., 1992. Calcium modulation and high calcium permeability of neuronal nicotinic acetylcholine receptors. Neuron 8, 127-134.

Vijayaraghavan, S., Huang, B., Blumenthal, E., Berg, D., 1995. Arachidonic acid as a possible negative feedback inhibitor of nicotinic acetylcholine receptors on neurons. Journal of Neuroscience 15(5), 3679-3687.

Villamizar, E., Mendez, M., Bonilla, E., Varon, H., de Onatra, S., 1996. Ascaris lumbricoides infestation as a cause of intestinal obstruction in children: experience with 87 cases. J Pediatr Surg 31, 201-204; discussion 204-205.

Wall, R., Shearer, D., 2001. Veterinary ectoparasites: Biology, Pathology & Control. 2nd Ed. Blackwell Science, Oxford.

Wallner, M., Meera, P., Ottolia, M., Kaczorowski, G., Latorre, R., Garcia, M.L., Stefani, E., Toro, L., 1995. Characterization of and modulation by a β-subunit of a human maxi-K_{Ca} channel cloned from myometrium. Receptors Channels 3(3), 185-199.

Wallner, M., Meera, P., Toro, L., 1996. Determinant for beta-subunit regulation in high-conductance voltage-activated and Ca^{2+}-sensitive K^+ channels: An additional transmembrane region at the N terminus. Proc Natl Acad Sci USA 93, 14922-14927.

Wallner, M., Meera, P., Toro, L., 1999. Molecular basis of fast inactivation in voltage and Ca^{2+}-activated K^+ channels: a transmembrane β-subunit homolog. Proc Natl Acad Sci. USA 96(7), 4137-4142.

Wang, J., Zhou, Y., Wen, H., Levitan, I., 1999a. Simultaneous binding of two protein kinases to a calcium-dependent potassium channel. J Neurosci 19, RC4.

Wang, J., Zhou, Y., Wen, H., Levitan, I.B., 1999b. Simultaneous binding of two protein kinases to a calcium-dependent potassium channel. J Neurosci 19, 1-7.

Wang, L.J., Cao, Y., Shi, H.N., 2008. Helminth infections and intestinal inflammation. World J Gastroenterol 14, 5125-5132.

Wang, Z., Saifee, O., Nonet, M., Salkoff, L., 2001. SLO-1 potassium channels control quantal content of neurotransmitter release at the *C. elegans* neuromuscular junction. Neuron 32(5), 867-881.

Weber, W.-M., 1999. Ion currents of *Xenopus laevis* oocytes: state of the art. Biochemica et Biophysica Acta 1421, 213-233.

Wei, A., Solaro, C., Lingle, C., Salkoff, L., 1994a. Calcium sensitivity of BK-type K_{Ca} channels determined by a separable domain. Neuron 13, 671-681.

Wei, A., Solaro, C., Lingle, C., Salkoff, L., 1994b. Calcium sensitivity of BK-type K_{Ca} channels determined by a separable domain. Neuron 13(3), 671-681.

Wei, A., Jegla, T., Salkoff, L., 1996. Eight potassium channel families revealed by the *C. elegans* genome project. Neuropharmacology 35, 805-829.

Weiger, T., Holmgvist, M., Levitan, I., Clark, F., Sprague, S., Huang, W., Ge, P., Wang, C., Lawson, D., Jurman, M., Glucksmann, M., Silos-Santiago, I., DiStefano, P., Curtis, R., 2000. A novel nervous system β subunit that downregulates human large conductance calcium-dependent potassium channels. J Neurosci 20(10), 3563-3570.

Weisblat, D.A., Byerly, L., Russell, R.L., 1976. Ionic mechanisms of electrical activity in somatic muscles of the nematode *Ascaris lumbricoides*. J Comp Physiol [A] 111, 93-113.

Weisblat, D.A., Russel, R.L., 1976. Propagation of electrical activity in the nerve cord and muscle syncytium of the nematode *Ascaris lumbricoides*. J. Comp. Physiol 107, 293-307.

Weisstaub, N., vetter, D., Elgoyhen, A., Katz, E., 2002. The α9α10 nicotinic acetylcholine receptor is permeable to and is modulated by divalent cations. Hear Res 167, 122-135.

Welz, C., Harder, A., Schnieder, T., Hoglund, J., Samson-Himmelstjerna von, G., 2005. Putative G protein-coupled receptors in parasitic nematodes-potential targets for the new anthelmintic class cyclooctadepsipeptides? Parasitol Res 97, S22-32.

Welz, C., Kruger, N., Schniederjans, M., Miltsch, S., Krucken, J., Guest, M., Holden-Dye, L., Harder, A., Von Samson-Himmelstjerna, G., 2011. SLO-1-channels of parasitic nematodes reconstitute locomotor behaviour and emodepside sensitivity in *Caenorhabditis elegans slo-1* loss of function mutants. PLoS Pathog 7(4), e1001330.

WHO, 2002. Prevention and control of schistosomiasis and soil-transmitted helminthiasis. WHO Technical Report Series 912. World Health Organization, Geneva.

WHO, 2004. Global Burden of Diseases: 2004 update. Deaths and DALYs 2004: Annex tables, Annex A. World Health Organization, 54-84.

WHO, 2009. African Programme for Onchocerciasis Control (APOC). In, Report of the twenty-ninth session of the technical consultative committee (TCC), Ouagadougou, pp. 1-107.

Williamson, S.M., Walsh, T., Wolstenholme, A.J., 2007. The cys-loop ligand-gated ion channel gene family of *Brugia malayi* and *Trichinella spiralis*: a comparison with *Caenorhabditis elegans*. Invert Neurosci 7(4), 219-226.

Williamson, S.M., Robertson, A.P., Brown, L., Williams, T., Woods, D.J., Martin, R.J., Sattelle, D.B., Wolstenholme, A.J., 2009. The Nicotinic Acetylcholine Receptors of the Parasitic Nematode *Ascaris suum*: Formation of Two Distinct Drug Targets by Varying the Relative Expression Levels of Two Subunits. PloS PATHOGENS 5, e1000517.

Williamson, S.M., Storey, B., Howell, S., Harper, K., Kaplan, R., Wolstenholme, A.J., 2011. Candidate anthelmintic resistance-associated gene expression and sequence polymorphisms in a triple-resistant field isolate of *Haemonchus contortus*. Mol Biochem Parasitol 180(2), 99-105.

Willson, J., Amliwala, K., Harder, A., Holden-Dye, L., Walker, R.J., 2003. The effect of the anthelmintic emodepside at the neuromuscular junction of the parasitic nematode *Ascaris suum*. Parasitology 126, 79-86.

Willson, J., Amliwala, K., Davis, A., Cook, A., Cuttle, M.F., Kriek, N., Hopper, N.A., O'Connor, V., Harder, A., Walker, R.J., Holden-Dye, L., 2004. Latrotoxin Receptor Signaling Engages the UNC-13-Dependent Vesicle-Priming Pathway in *C. elegans*. Current Biology 14, 1374-1379.

Wolstenholme, A., 2011. Ion channels and receptor as targets for the control of parasitic nematodes. Int J Parasitol: Drugs & Drug Resistance 1, 2-13.

Wolstenholme, A.J., Fairweather, I., Prichard, R., von Samson-Himmelstjerna, G., Sangster, N.C., 2004. Drug resistance in veterinary helminths. Trends Parasitol 20, 469-476.

Wolstenholme, A.J., Rogers, A., 2005. Glutamate-gated chloride channels and the mode of action of the avermectins/milbemycin anthelmintics. Parasitology 131 Suppl, S85-95.

Woodland, H.R., Gurdon, J.B., Lingrel, J.B., 1974. The translation of mammalian globin mRNA injected into fertilized eggs of *Xenopus laevis* II. The distributioin of globin synthesis in different tissues. Dev. Biol. 39, 134-140.

Wu, T., Smith, C., Sine, S., Levandoski, M., 2008. Morantel allosterically enhances channel gating of neuronal nicotinic acetylcholine alpha 3 beta 2 receptors. Mol Pharmacol 74(2), 466-475.

Xia, X., Ding, J., Lingle, C., 1999. Molecular basis for the inactivation of Ca^{2+}- and voltage-dependent BK channels in adrenal chromaffin cells and rat insulinoma tumor cells. J Neurosci 19(13), 5255-5264.

Xia, X., Zeng, X., Lingle, C., 2002. Multiple regulatory sites in large-conductance calcium-activated potassium channels. Nature 418(6900), 880-884.

Xiao, S., Hui-Ming, W., Tanner, M., Utzinger, J., Chong, W., 2005. Tribendimidine: a promising, safe and broad-spectrum anthelmintic agent from China. Acta Trop 94(1), 1-14.

Xu, M., Molento, M., Blackhall, W., Ribeiro, P., Beech, R., Prichard, R., 1998. Ivermectin resistance in nematodes may be caused by alteration of P-glycoprotein homolog. Mol Biochem Parasitol 91, 327-335.

Yassin, L., Gillo, B., Kahan, T., Halevi, S., Eshel, M., Treinin, M., 2001. Characterization of the DEG-3/DES-2 receptor: a nicotinic acetylcholine receptor that mutates to cause neuronal degeneration. Mol Cell Neurosci 17(3), 589-599.

Yelifari, L., Bloch, P., Magnussen, P., van Lieshout, L., Dery, G., Anemana, S., Agongo, E., Polderman, A., 2005. Distribution of human *Oesophagostomum bifurcum,* hookworm and *Strongyloides stercolaris* infections in northern Ghana. Trans R Soc Trop Med Hyg 99, 32-38.

Yellen, G., 2002. The voltage-gated potassium channels and their relatives. Nature 419, 35-42.

Yesilirmak, F., Sayers, Z., 2009. Heterologous expression of plant genes. International Journal of Plant Genomics 2009, Article ID 296482, 16 pages.

Yu, X., Hall, Z., 1991. Extracellular domains mediating epsilon subunit interactions of muscle acetylcholine receptor. Nature 352, 64-67.

Zhou, X., Arntz, C., Kamm, S., Motejlek, K., Sausbier, U., Wang, G., Ruth, P., Korth, M., 2001. A molecular switch for specific stimulation of the BK_{Ca} channel by cGMP and cAMP kinase. J Biol Chem 276(46), 43239-43245.

Ziem, J., Spannbrucker, N., Magnussen, P., Olsen, A., Amon-Kotey, D., Frenzel, K., Nang-beifubah, A., Westendorp, R., Polderman, A., 2005. *Oesophagostomum bifurcum*-induced nodular pathology in a highly endemic area of Northern Ghana. Trans R Soc Trop Med Hyg 99, 417-422.

Ziem, J., Olsen, A., Magnussen, P., Horton, J., Agongo, E., Geskus, R., Polderman, A., 2006. Distribution and clustering of *Oesophagostomum bifurcum* and hookworm infections in Northern Ghana. Parasitology 132, 525-534.

Zwart, R., Vijverberg, H.P.M., 1998. Four pharmacologically distinct subtypes of alpha4beta2 nicotinic acetylcholine receptor expressed in *Xenopus laevis* oocytes. Molecular Pharmacology 54, 1124-1131.